QUANTIFYING UNCERTAINTIES IN FRAGILITY FUNCTION PARAMETER ESTIMATION FOR STRUCTURAL MODELING UNCERTAINTIES

A THESIS SUBMITTED TO
THE GRADUATE SCHOOL OF NATURAL AND APPLIED SCIENCES
OF
MIDDLE EAST TECHNICAL UNIVERSITY

BY

BARIŞ ÜNAL

IN PARTIAL FULFILLMENT OF THE REQUIREMENTS
FOR
THE DEGREE OF DOCTOR OF PHILOSOPHY
IN
CIVIL ENGINEERING

MARCH 2024

Approval of the thesis:

QUANTIFYING UNCERTAINTIES IN FRAGILITY FUNCTION PARAMETER ESTIMATION FOR STRUCTURAL MODELING UNCERTAINTIES

submitted by **BARIŞ ÜNAL** in partial fulfillment of the requirements for the degree of **Doctor of Philosophy in Civil Engineering Department, Middle East Technical University** by,

Prof. Dr. Naci Emre Altun
Dean, Graduate School of **Natural and Applied Sciences** _____

Prof. Dr. Erdem Canbay
Head of Department, **Civil Engineering** _____

Prof. Dr. Ayşegül Askan Gündoğan
Supervisor, **Civil Engineering, METU** _____

Prof. Dr. Murat Altuğ Erberik
Co-supervisor, **Civil Engineering, METU** _____

Examining Committee Members:

Assoc. Prof. Dr. Mustafa Tolga Yılmaz
Engineering Sciences, METU _____

Prof. Dr. Ayşegül Askan Gündoğan
Civil Engineering, METU _____

Assoc. Prof. Dr. Özkan Kale
Civil Engineering, TED University _____

Assoc. Prof. Dr. Ozan Cem Çelik
Civil Engineering, METU _____

Assoc. Prof. Dr. Alper Aldemir
Civil Engineering, Hacettepe University _____

Date: 11.03.2024

I hereby declare that all information in this document has been obtained and presented in accordance with academic rules and ethical conduct. I also declare that, as required by these rules and conduct, I have fully cited and referenced all material and results that are not original to this work.

Name, Surname: Barış Ünal

Signature :

ABSTRACT

QUANTIFYING UNCERTAINTIES IN FRAGILITY FUNCTION PARAMETER ESTIMATION FOR STRUCTURAL MODELING UNCERTAINTIES

Ünal, Barış
Ph.D., Department of Civil Engineering
Supervisor: Prof. Dr. Ayşegül Askan Gündoğan
Co-Supervisor: Prof. Dr. Murat Altuğ Erberik

March 2024, 183 pages

Large-scale seismic risk assessments have a crucial role in disaster management planning. Ensuring the resilience of communities against seismic events necessitates the accurate assessment of structural vulnerabilities. In this study, the effects of uncertainties originating from diverse sources such as material properties, geometric complexities, and modeling assumptions on fragility curves are investigated for uncertainty quantification in fragility functions to improve the accuracy of loss assessment analyses. This research focuses on estimating fragility function parameters for selected code-compliant residential buildings consisting of reinforced concrete frames while considering various modeling uncertainties. Through rigorous simulations and sensitivity analyses, the study systematically examines the influence of these uncertainties on the fragility predictions. The Latin hypercube sampling technique is utilized to represent the probabilistic distribution of random variables in structural analyses. The seismic input is expressed through hazard analyses conducted for different soil conditions and hazard levels.

The study emphasizes the importance of accounting for structural variability in fragility calculations with comparative analysis between scenarios with and without modeling uncertainties and contributes to probabilistic structure response assessment by quantifying the impact of a wide range of structural input variables on the fragility calculations. This research contributes to probabilistic structure response assessment by offering insights into the influence of structural input variables on fragility, ultimately contributing to safer and more resilient civil infrastructure in seismic regions.

Keywords: Structural fragility, Modeling uncertainty, Uncertainty quantification, Parameter sensitivity

ÖZ

YAPISAL MODELLEME BELİRSİZLİKLERİ İÇİN KIRILGANLIK FONKSİYONU PARAMETRE TAHMİNİ BELİRSİZLİKLERİNİN ÖLÇÜLMESİ

Ünal, Barış
Doktora, İnşaat Mühendisliği Bölümü
Tez Yöneticisi: Prof. Dr. Ayşegül Askan Gündoğan
Ortak Tez Yöneticisi: Prof. Dr. Murat Altuğ Erberik

Mart 2024 , 183 sayfa

Büyük ölçekli sismik risk değerlendirmeleri afet yönetimi planlamasında çok önemli bir role sahiptir. Toplumların sismik olaylara karşı dayanıklılığının artması için yapısal kırılganlığın doğru değerlendirilmesini gerekmektedir. Bu çalışmada, kayıp değerlendirme analizlerinin doğruluğunu artırmak amacıyla, kırılganlık fonksiyonlarındaki belirsizliğin ölçülmesi için malzeme özellikleri, geometrik karmaşıklıklar, ve modelleme varsayımları gibi farklı kaynakları olan belirsizliklerin kırılganlık eğrileri üzerindeki etkileri araştırılmaktadır.

Bu araştırmada, çeşitli modelleme belirsizliklerini göz önünde bulundurarak, yönetmeliklere uygun betonarme konut binaları için kırılganlık fonksiyonu parametrelerinin tahmin edilmesi konusuna odaklanılmıştır. Bu çalışmada, simülasyonlar ve duyarlılık analizleri aracılığıyla bu belirsizliklerin kırılganlık tahminleri üzerindeki etkisi sistematik olarak incelenmiştir. Yapısal analizlerde rastgele değişkenlerin olasılıksal dağılımı Latin hiperküp örnekleme tekniği ile dikkate alınmıştır. Sismik girdiler,

farklı zemin koşulları ve tehlike seviyeleri için yürütülen tehlike analizleri aracılığıyla ifade edilmişlerdir.

Çalışmada, modelleme belirsizlikleri dahil edilen ve edilmeyen senaryoların karşılaştırmalı analizi ile kırılganlık hesaplamalarında yapısal parametrelerdeki değişkenliğin etkisinin önemi vurgulanmıştır. Çalışmada geniş kapsamlı değişken yapısal parametrelerinin kırılganlık hesaplamaları üzerindeki etkisi ölçülerek olasılıksal yapı tepki analizi alanına katkıda bulunulmaktadır. Bu araştırma, değişken yapısal parametrelerin kırılganlık üzerindeki etkisine yönelik bir bakış sağlayarak olasılıksal yapı tepkisi değerlendirmesine katkıda bulunmaktadır ve dolayısıyla sismik bölgelerdeki altyapının daha güvenli ve dayanıklı olması için katkı sağlamaktadır.

Anahtar Kelimeler: Yapısal kırılganlık, modelleme belirsizliği, Belirsizlik ölçümü, Parametre hassasiyeti

To my family

ACKNOWLEDGMENTS

I would like to express my gratitude to Prof. Dr. Ayşegül Askan Gündoğan. This study would not have been possible without her optimism and motivation. Her selfless efforts are truly appreciated.

I would like to thank Prof. Dr. Murat Altuğ Erberik for his patience and guidance. I am deeply grateful for his valuable suggestions and continuous support.

I would like to extend my gratitude to Assoc. Prof. Dr. Ozan Cem Çelik and Assoc. Prof. Dr. Özkan Kale. Their knowledge and valuable insights guided this study into the right path. I also thank Professor Kale for his invaluable contributions to the seismic hazard calculations and ground motion selection process.

I would like to express my appreciation to Koray Kadaş and Asst. Prof. Dr. Kaan Kaatsız for their input and suggestions in the structural modeling process.

I would like to thank Assoc. Prof. Dr. Mustafa Tolga Yılmaz and Assoc. Prof. Dr. Alper Aldemir for providing valuable feedback and encouraging me as the members of my thesis defense committee.

I would like to express my gratitude to my friends, for their compassion and fond memories.

Special thanks to Bahadır and Zeynep Bilgin, for their support and for offering their help anytime I needed it.

Finally, I would like to express my gratitude to my parents for their unconditional love and endless support.

TABLE OF CONTENTS

ABSTRACT v

ÖZ vii

ACKNOWLEDGMENTS x

TABLE OF CONTENTS xi

LIST OF TABLES xiv

LIST OF FIGURES xxi

LIST OF ABBREVIATIONS xxiv

CHAPTERS

1 INTRODUCTION 1

1.1 Motivation and Problem Definition 1

1.2 Literature Review on Uncertainty Quantification in Fragility Analysis 3

1.3 Proposed Methodology 4

1.4 Objective and Scope 7

2 SEISMIC HAZARD ANALYSIS AND GROUND MOTION SELECTION 9

2.1 Introduction 9

2.1.1 Study Region and the Site of Interest 10

2.2 Probabilistic Seismic Hazard Analysis 11

2.2.1 Seismic Source Models 14

2.2.2 Ground Motion Models 15
2.2.3 Target Spectra 16
2.3 Ground Motion Selection and Scaling 17
2.3.1 Basic Scaling 18
2.3.1.1 Estimation of the Specific Period Range 19
2.3.1.2 Initial scale factor determination 20
2.3.2 Ground motion suite selection 20
3 STRUCTURAL MODELING 25
3.1 Introduction 25
3.2 Reference Reinforced Concrete Frame Properties 25
3.3 Structural Parameters Used as Random Variables 26
3.3.1 Sampling Methodology 26
3.4 Analytical Models 28
3.4.1 Analysis Parameters and Convergence Control 40
4 ANALYSIS RESULTS AND UNCERTAINTY QUANTIFICATION 43
4.1 Introduction 43
4.2 Single Random Variable Analyses 46
4.3 Multi Random Variable Analyses 51
4.3.1 Maximum likelihood method 51
5 CONCLUSIONS 65
5.1 Summary 65
5.2 Conclusions 67
5.3 Recommendations for Future Work 69

REFERENCES 71

APPENDICES

A GROUND MOTION SUITE TABLES 81

B GROUND MOTION SUITE SPECTRA 155

C ANALYSIS INPUT PARAMETERS 169

VITA 182

LIST OF TABLES

TABLES

Table 2.1 Ground Motion Models and Logic Tree Weights 16

Table 2.2 Screening Parameters for Ground Motion Suite Selection 21

Table 2.3 Ground Motion Suite for F8S3B Building with 2% Probability of Exceedence in 50 Years for NEHRP Class D Site 24

Table 3.1 Dynamic Parameters of the Reference Structures 26

Table 3.2 Statistical Parameters of the Selected Random Variables 27

Table 3.3 F2S2B Reference Model Material Properties 32

Table 3.4 F2S2B Reference Model Section Properties 33

Table 3.5 F2S2B Reference Model Story Masses 33

Table 3.6 F5S4B Reference Model Material Properties 35

Table 3.7 F5S4B Reference Model Section Properties 36

Table 3.8 F5S4B Reference Model Story Masses 36

Table 3.9 F8S3B Reference Model Material Properties 38

Table 3.10 F8S3B Reference Model Section Properties 39

Table 3.11 F8S3B Reference Model Story Masses 40

Table 4.1 MIDR values associated with the limit states 44

Table 4.2 Uncertainties Included in Uncertainty Scenarios 51

Table A.1 Ground Motion Suite for F2S2B Building with 68% Probability of Exceedence in 50 Years for NEHRP Class D Site 82

Table A.2 Ground Motion Suite for F5S4B Building with 68% Probability of Exceedence in 50 Years for NEHRP Class D Site 83

Table A.3 Ground Motion Suite for F8S3B Building with 68% Probability of Exceedence in 50 Years for NEHRP Class D Site 84

Table A.4 Ground Motion Suite for F2S2B Building with 68% Probability of Exceedence in 50 Years for NEHRP Class C Site 85

Table A.5 Ground Motion Suite for F5S4B Building with 68% Probability of Exceedence in 50 Years for NEHRP Class C Site 86

Table A.6 Ground Motion Suite for F8S3B Building with 68% Probability of Exceedence in 50 Years for NEHRP Class C Site 87

Table A.7 Ground Motion Suite for F2S2B Building with 68% Probability of Exceedence in 50 Years for Generic Rock Site 88

Table A.8 Ground Motion Suite for F5S4B Building with 68% Probability of Exceedence in 50 Years for Generic Rock Site 89

Table A.9 Ground Motion Suite for F8S3B Building with 68% Probability of Exceedence in 50 Years for Generic Rock Site 90

Table A.10 Ground Motion Suite for F2S2B Building with 68% Probability of Exceedence in 50 Years for NEHRP Class B Site 91

Table A.11 Ground Motion Suite for F5S4B Building with 68% Probability of Exceedence in 50 Years for NEHRP Class B Site 92

Table A.12 Ground Motion Suite for F8S3B Building with 68% Probability of Exceedence in 50 Years for NEHRP Class B Site 93

Table A.13Ground Motion Suite for F2S2B Building with 50% Probability of Exceedence in 50 Years for NEHRP Class D Site 94

Table A.14Ground Motion Suite for F5S4B Building with 50% Probability of Exceedence in 50 Years for NEHRP Class D Site 95

Table A.15Ground Motion Suite for F8S3B Building with 50% Probability of Exceedence in 50 Years for NEHRP Class D Site 96

Table A.16Ground Motion Suite for F2S2B Building with 50% Probability of Exceedence in 50 Years for NEHRP Class C Site 97

Table A.17Ground Motion Suite for F5S4B Building with 50% Probability of Exceedence in 50 Years for NEHRP Class C Site 98

Table A.18Ground Motion Suite for F8S3B Building with 50% Probability of Exceedence in 50 Years for NEHRP Class C Site 99

Table A.19Ground Motion Suite for F2S2B Building with 50% Probability of Exceedence in 50 Years for Generic Rock Site 100

Table A.20Ground Motion Suite for F5S4B Building with 50% Probability of Exceedence in 50 Years for Generic Rock Site 101

Table A.21Ground Motion Suite for F8S3B Building with 50% Probability of Exceedence in 50 Years for Generic Rock Site 102

Table A.22Ground Motion Suite for F2S2B Building with 50% Probability of Exceedence in 50 Years for NEHRP Class B Site 103

Table A.23Ground Motion Suite for F5S4B Building with 50% Probability of Exceedence in 50 Years for NEHRP Class B Site 104

Table A.24Ground Motion Suite for F8S3B Building with 50% Probability of Exceedence in 50 Years for NEHRP Class B Site 105

Table A.25Ground Motion Suite for F2S2B Building with 10% Probability of Exceedence in 50 Years for NEHRP Class D Site 106

Table A.26Ground Motion Suite for F5S4B Building with 10% Probability of Exceedence in 50 Years for NEHRP Class D Site 107

Table A.27Ground Motion Suite for F8S3B Building with 10% Probability of Exceedence in 50 Years for NEHRP Class D Site 108

Table A.28Ground Motion Suite for F2S2B Building with 10% Probability of Exceedence in 50 Years for NEHRP Class C Site 109

Table A.29Ground Motion Suite for F5S4B Building with 10% Probability of Exceedence in 50 Years for NEHRP Class C Site 110

Table A.30Ground Motion Suite for F8S3B Building with 10% Probability of Exceedence in 50 Years for NEHRP Class C Site 111

Table A.31Ground Motion Suite for F2S2B Building with 10% Probability of Exceedence in 50 Years for Generic Rock Site 112

Table A.32Ground Motion Suite for F5S4B Building with 10% Probability of Exceedence in 50 Years for Generic Rock Site 113

Table A.33Ground Motion Suite for F8S3B Building with 10% Probability of Exceedence in 50 Years for Generic Rock Site 114

Table A.34Ground Motion Suite for F2S2B Building with 10% Probability of Exceedence in 50 Years for NEHRP Class B Site 115

Table A.35Ground Motion Suite for F5S4B Building with 10% Probability of Exceedence in 50 Years for NEHRP Class B Site 116

Table A.36Ground Motion Suite for F8S3B Building with 10% Probability of Exceedence in 50 Years for NEHRP Class B Site 117

Table A.37Ground Motion Suite for F2S2B Building with 5% Probability of Exceedence in 50 Years for NEHRP Class D Site 118

Table A.38Ground Motion Suite for F5S4B Building with 5% Probability of Exceedence in 50 Years for NEHRP Class D Site 119

Table A.39Ground Motion Suite for F8S3B Building with 5% Probability of Exceedence in 50 Years for NEHRP Class D Site 120

Table A.40Ground Motion Suite for F2S2B Building with 5% Probability of Exceedence in 50 Years for NEHRP Class C Site 121

Table A.41Ground Motion Suite for F5S4B Building with 5% Probability of Exceedence in 50 Years for NEHRP Class C Site 122

Table A.42Ground Motion Suite for F8S3B Building with 5% Probability of Exceedence in 50 Years for NEHRP Class C Site 123

Table A.43Ground Motion Suite for F2S2B Building with 5% Probability of Exceedence in 50 Years for Generic Rock Site 124

Table A.44Ground Motion Suite for F5S4B Building with 5% Probability of Exceedence in 50 Years for Generic Rock Site 125

Table A.45Ground Motion Suite for F8S3B Building with 5% Probability of Exceedence in 50 Years for Generic Rock Site 126

Table A.46Ground Motion Suite for F2S2B Building with 5% Probability of Exceedence in 50 Years for NEHRP Class B Site 127

Table A.47Ground Motion Suite for F5S4B Building with 5% Probability of Exceedence in 50 Years for NEHRP Class B Site 128

Table A.48Ground Motion Suite for F8S3B Building with 5% Probability of Exceedence in 50 Years for NEHRP Class B Site 129

Table A.49Ground Motion Suite for F2S2B Building with 2% Probability of Exceedence in 50 Years for NEHRP Class D Site 130

Table A.50Ground Motion Suite for F5S4B Building with 2% Probability of Exceedence in 50 Years for NEHRP Class D Site 131

Table A.51Ground Motion Suite for F8S3B Building with 2% Probability of Exceedence in 50 Years for NEHRP Class D Site 132

Table A.52Ground Motion Suite for F2S2B Building with 2% Probability of Exceedence in 50 Years for NEHRP Class C Site 133

Table A.53Ground Motion Suite for F5S4B Building with 2% Probability of Exceedence in 50 Years for NEHRP Class C Site 134

Table A.54Ground Motion Suite for F8S3B Building with 2% Probability of Exceedence in 50 Years for NEHRP Class C Site 135

Table A.55Ground Motion Suite for F2S2B Building with 2% Probability of Exceedence in 50 Years for Generic Rock Site 136

Table A.56Ground Motion Suite for F5S4B Building with 2% Probability of Exceedence in 50 Years for Generic Rock Site 137

Table A.57Ground Motion Suite for F8S3B Building with 2% Probability of Exceedence in 50 Years for Generic Rock Site 138

Table A.58Ground Motion Suite for F2S2B Building with 2% Probability of Exceedence in 50 Years for NEHRP Class B Site 139

Table A.59Ground Motion Suite for F5S4B Building with 2% Probability of Exceedence in 50 Years for NEHRP Class B Site 140

Table A.60Ground Motion Suite for F8S3B Building with 2% Probability of Exceedence in 50 Years for NEHRP Class B Site 141

Table A.61Ground Motion Suite for F2S2B Building with 1% Probability of Exceedence in 50 Years for NEHRP Class D Site 142

Table A.62Ground Motion Suite for F5S4B Building with 1% Probability of Exceedence in 50 Years for NEHRP Class D Site 143

Table A.63Ground Motion Suite for F8S3B Building with 1% Probability of Exceedence in 50 Years for NEHRP Class D Site 144

Table A.64Ground Motion Suite for F2S2B Building with 1% Probability of Exceedence in 50 Years for NEHRP Class C Site 145

Table A.65Ground Motion Suite for F5S4B Building with 1% Probability of Exceedence in 50 Years for NEHRP Class C Site 146

Table A.66Ground Motion Suite for F8S3B Building with 1% Probability of Exceedence in 50 Years for NEHRP Class C Site 147

Table A.67Ground Motion Suite for F2S2B Building with 1% Probability of Exceedence in 50 Years for Generic Rock Site 148

Table A.68Ground Motion Suite for F5S4B Building with 1% Probability of Exceedence in 50 Years for Generic Rock Site 149

Table A.69Ground Motion Suite for F8S3B Building with 1% Probability of Exceedence in 50 Years for Generic Rock Site 150

Table A.70Ground Motion Suite for F2S2B Building with 1% Probability of Exceedence in 50 Years for NEHRP Class B Site 151

Table A.71Ground Motion Suite for F5S4B Building with 1% Probability of Exceedence in 50 Years for NEHRP Class B Site 152

Table A.72Ground Motion Suite for F8S3B Building with 1% Probability of Exceedence in 50 Years for NEHRP Class B Site 153

Table C.1 Tornado Analysis Input Parameters of F2S2B 170

Table C.2 Tornado Analysis Input Parameters of F5S4B 171

Table C.3 Tornado Analysis Input Parameters of F8S3B 172

Table C.4 NLTHA Analysis Input Parameters of F2S2B 174

Table C.5 NLTHA Analysis Input Parameters of F5S4B 176

Table C.6 NLTHA Analysis Input Parameters of F8S3B 179

LIST OF FIGURES

FIGURES

Figure 1.1 Block of similar RC constructions in Adıyaman after the 2023 earthquakes: one collapsed, the others experienced various degrees of damage 2

Figure 1.2 Quantification of Fragility Function Parameter Uncertainty Flowchart 5

Figure 2.1 Tectonic map of Türkiye 11

Figure 2.2 Active fault map of the Western Türkiye region 12

Figure 2.3 Basic 4 steps of PSHA: Source identification, source characterization, GMM selection, and computation of probability of exceedance of the ground motion parameter 13

Figure 2.4 Target Uniform Hazard Spectra for Different Hazard Levels and for Different Site Conditions 17

Figure 2.5 Ground Motion Suite Spectra for F8S3B Building with 2% Probability of Exceedence in 50 Years for NEHRP Class D Site 23

Figure 3.1 Example LHS of two parameters with a sample size of 10 28

Figure 3.2 Distributions of Control Sections and Section Subdivisions of a Fiber Element 29

Figure 3.3 Typical hysteretic stress-strain relations of the material models . 30

Figure 3.4 F2S2B Analytical Model 31

Figure 3.5 F5S4B Analytical Model 34

Figure 3.6 F5S4B Analytical Model 37

Figure 3.7 Rayleigh damping with 3% equivalent critical damping for reference structures 41

Figure 4.1 Capacity Curves and Inter-story Drift Ratios at Limit States . . . 45

Figure 4.2 Tornado Diagrams for F2S2B Building 48

Figure 4.3 Tornado Diagrams for F5S4B Building 49

Figure 4.4 Tornado Diagrams for F8S3B Building 50

Figure 4.5 Fragility curve calculation from MIDR results obtained from RTR scenario for NEHRP D site (a) F2S2B , (b) F5S4B (c) F8S3B . . 54

Figure 4.6 Fragility curves of F2S2B for IO, LS, and CP limit states for uncertainty scenarios for (a) NEHRP D, (b) NEHRP C, (c) generic rock, and (d) NEHRP B site conditions 55

Figure 4.7 Fragility curves of F5S4B for IO, LS, and CP limit states for uncertainty scenarios for (a) NEHRP D, (b) NEHRP C, (c) generic rock, and (d) NEHRP B site conditions 56

Figure 4.8 Fragility curves of F8S3B for IO, LS, and CP limit states for uncertainty scenarios for (a) NEHRP D, (b) NEHRP C, (c) generic rock, and (d) NEHRP B site conditions 57

Figure 4.9 Change in fragility function parameters (θ, β) for Immediate Occupancy limit state for uncertainty scenarios with respect to RTR scenario for (a) NEHRP D, (b) NEHRP C, (c) generic rock, and (d) NEHRP B site conditions 59

Figure 4.10 Change in fragility function parameters (θ, β) for Life Safety limit state for uncertainty scenarios with respect to RTR scenario for (a) NEHRP D, (b) NEHRP C, (c) generic rock, and (d) NEHRP B site conditions 60

Figure 4.11 Change in fragility function parameters (θ, β) for Collapse Prevention limit state for uncertainty scenarios with respect to RTR scenario for (a) NEHRP D, (b) NEHRP C, (c) generic rock, and (d) NEHRP B site conditions 61

Figure B.1 GM Suite Spectra for NEHRP Class D Site F2S2B Building . . . 156

Figure B.2 GM Suite Spectra for NEHRP Class D Site F5S4B Building . . . 157

Figure B.3 GM Suite Spectra for NEHRP Class D Site F8S3B Building . . . 158

Figure B.4 GM Suite Spectra for NEHRP Class C Site F2S2B Building . . . 159

Figure B.5 GM Suite Spectra for NEHRP Class C Site F5S4B Building . . . 160

Figure B.6 GM Suite Spectra for NEHRP Class C Site F8S3B Building . . . 161

Figure B.7 GM Suite Spectra for Generic Rock Site F2S2B Building 162

Figure B.8 GM Suite Spectra for Generic Rock Site F5S4B Building 163

Figure B.9 GM Suite Spectra for Generic Rock Site F8S3B Building 164

Figure B.10 GM Suite Spectra for NEHRP Class B Site F2S2B Building . . . 165

Figure B.11 GM Suite Spectra for NEHRP Class B Site F5S4B Building . . . 166

Figure B.12 GM Suite Spectra for NEHRP Class B Site F8S3B Building . . . 167

LIST OF ABBREVIATIONS

ALL	Uncertainty scenario where all parameters are considered as random variables
b	Width of column
β	Dispersion of the fragility curve
CMS	Conditional mean spectrum
$CONF$	Concrete confinement uncertainty scenario
CP	Collapse prevention limit state
$DAMP$	Structural damping uncertainty scenario
EDP	Engineering demand parameter
$f_c^{'}$	compressive strength of concrete
fy	Yield strength of steel
$GEOM$	Section geometry uncertainty scenario
GMM	Ground motion model
h	Depth of beam
IDA	Incremental dynamic analysis
IM	Intensity measure
IO	Immediate occupancy limit state
LHS	Latin hypercube sampling
LS	Life safety limit state
MAT	Material uncertainty scenario
MIDR	Maximum interstory drift ratio
$\text{MIDR}_{p_{avg}}$	Average maximum interstory drift ratio due to variation of a single parameter

$\text{MIDR}_{reference_{avg}}$	Average maximum interstory drift ratio of the reference structure
NAFZ	North Anatolian Fault Zone
NEHRP	National Earthquake Hazards Reduction Program
NLTHA	Non-linear time history analysis
PSHA	Probabilistic seismic hazard analysis
poe	Probability of exceedence
RC	Reinforced concrete
RP	Return period (years)
RTR	Record-to-record uncertainty scenario
s	Spacing of the transverse steel
Sa	Spectral acceleration (g)
SF	Scale factor
SIG	Significant parameters uncertainty scenario
t	Yhickness of concrete cover
θ	Median capacity of the fragility curve
UHS	Uniform hazard spectra
w	Weight density of concrete
ξ	Equivalent viscous damping

CHAPTER 1

INTRODUCTION

1.1 Motivation and Problem Definition

In structural engineering, the accurate assessment of structural fragility is a crucial aspect in ensuring the resilience of communities against potential seismic events. Numerous analytical approaches have been developed for generating fragility functions, which describe how susceptible structures are to earthquakes. Apart from the inherent uncertainty regarding the earthquake occurrences and ground motion levels, seismic loss assessment procedures also involve uncertainties concerning the fragility calculations. Uncertainty in the seismic inputs has been considered to be more dominant, yet the uncertainty regarding the structural fragilities cannot be dismissed. This statement has been recently verified during the 2023 Kahramanmaraş earthquakes. In this destructive earthquake sequence, similarly constructed buildings conceived different levels of damage under similar levels of seismic action and site conditions. There are many examples of such incidents in the affected 11 cities during the earthquakes. One typical example is from Adıyaman city where among 13 buildings with the same structural design and construction, one of them collapsed while the others experienced different damage levels from light to severe (Figure 1.1, adopted from [1]). These cases reveal that small variations in material or structural characteristics may cause abrupt changes in the seismic performance of similar constructions under similar site and seismic intensity conditions. More surprisingly, new constructions which were supposed to possess less variation compared to old constructions also experienced variable seismic performance during these events, which was hard to predict beforehand.

Figure 1.1: Block of similar RC constructions in Adıyaman after the 2023 earthquakes: one collapsed, the others experienced various degrees of damage

These uncertainties arise from diverse sources such as material properties, geometric complexities, and modeling assumptions as their propagation through fragility calculations can introduce considerable variability in predicted outcomes. Uncertainty quantification in fragility functions allows for the incorporation of uncertainties in model inputs and improves the accuracy of loss assessment analyses. Although the influence of modeling uncertainty on the seismic safety of the structures is recognized, uncertainty quantification and characterization are often simplified due to computational challenges. However, with advancements in computational resources and power, rigorous simulations for a wide range of random variables are viable.

In this thesis, fragility functions for reinforced concrete residential buildings are estimated considering various uncertainties in modeling parameters and the propagation of these uncertainties through fragility calculations is examined. By systematically analyzing the influence of modeling uncertainties on fragility predictions, this study aims to quantify the effects of different sources of uncertainty for well-constructed RC frame buildings by employing structural fragility as the analysis tool. In the long term, the outcomes of this study are expected to provide insights for enhancing the resilience of civil infrastructure.

1.2 Literature Review on Uncertainty Quantification in Fragility Analysis

The seismic risk assessment field in earthquake engineering has widely embraced the quantitative approach [[2]]. Early studies on the sensitivity of loss estimation to structural modeling parameters suggested that the seismic performance estimation is not significantly influenced by the uncertainty in the structural system [[3], [4]]. Bradley [5] later observed that when a broad range of ground motions is chosen without strict criteria, there is an overestimation of ground motion uncertainty, while the inclusion of only low-level uncertainties results in an underrepresentation of modeling uncertainties. This rationale could explain the findings of earlier studies, which primarily concentrated on measuring physical quantities and establishing correlations between measurable physical parameters and constitutive model parameters [[4], [6], [7]]. However, even with the consideration of high-level uncertainties, such as structural damping and alternative modeling techniques, Çelik and Ellingwood [8] concluded that the total uncertainty in the structural response of non-ductile reinforced concrete frames designed for gravity loads within low-to-moderate seismic areas is predominantly influenced by record-to-record variability.

Differing from previous claims, other researchers [[9], [10], [11]], while investigating uncertainties in fragility analysis, remarked that the variability in modeling must be considered. Likewise, many researchers working on portfolio risk assessment and addressing uncertainties, [[12], [13], [14], [15]], have come to the conclusion that not accounting for the variability in vulnerability functions can result in an underestimation of the variability in earthquake losses. In addition, Dolšek [7, 16], Liel [17] and Gökkaya [18] indicate that uncertainties associated with the modeling of the structural capacity have the potential to notably increase the logarithmic standard deviation of collapse fragility and slightly decrease its median. Recent studies propose that a substantial portion of the total dispersion in structural response arises from modeling uncertainties, especially when the structural behavior becomes highly nonlinear under intense ground shaking [[18], [19], [20]].

The Incremental Dynamic Analysis (IDA) method has been commonly used in most studies to analyze the collapse behavior of different kinds of structures [21, 22]. However, the robustness of the IDA procedure against scaling is questionable, as it does

not integrate information on the spectral shape of the seismic input.

Even though the sources of record-to-record uncertainties and modeling uncertainties are independent and uncorrelated, their contributions to the uncertainty in structural response will interact and interdependently influence each other, forming a coupled relationship [[23]]. A significant number of researchers have examined the impacts of parameters through tornado diagrams [[8], [24], [25]]. These diagrams are constructed by fixing all but a single parameter at their median value and evaluating the variance attributed to a single parameter, without taking into consideration this coupling.

While uncertainties on the collapse capacity of reinforced concrete frames designed for a high seismic region have been previously investigated [[18], [24]], the literature currently lacks a comprehensive exploration of uncertainty quantification in fragility calculations for ductile reinforced concrete frames exposed to intense ground shaking on various local soil conditions considering the coupling of parameters, the spectral shape of the seismic input, and study on a wide range of uncertainty scenarios.

1.3 Proposed Methodology

In this section, the methodology proposed in this thesis in order to quantify uncertainties in fragility function parameter estimation due to uncertainty in the model input parameters is presented (Figure 1.2).

This study examines three distinct well-designed and ductile RC frames without any structural irregularities. The modeling parameters such as material properties, geometric properties, damping, and the parameters related with the concrete confinement are selected as random variables. Probability distributions of these random variables are then defined based on previous research.

Engineering demand parameters used in fragility function estimations rely on hazard parameters derived from the probabilistic evaluation of seismic hazards. In this study, Düzce region, a densely populated and industrialized area prone to seismic events, is selected as the study area. Hazard calculations are performed at four arbitrary sites

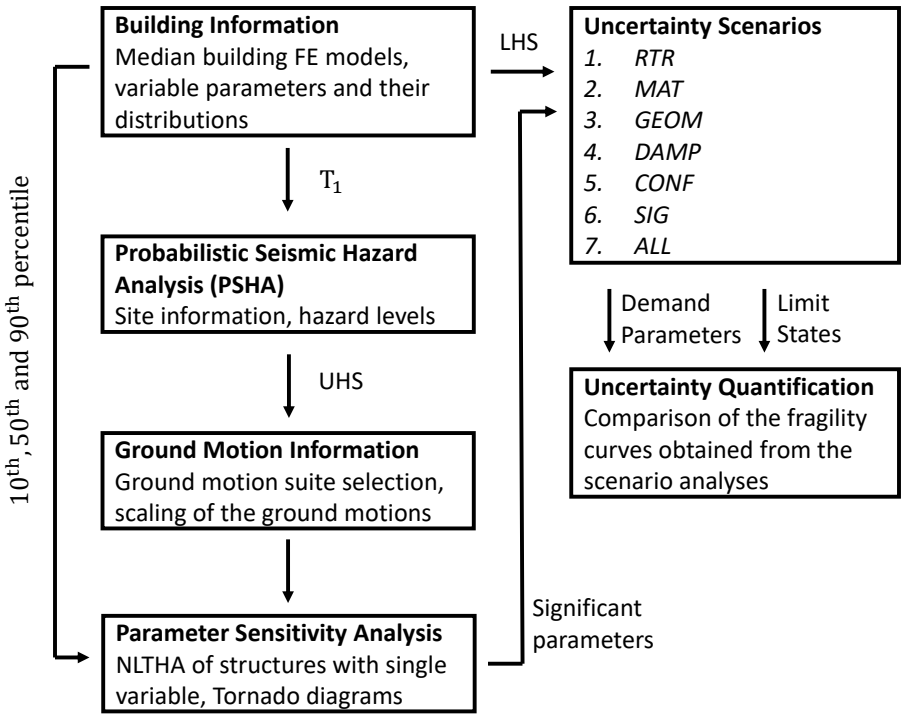

Figure 1.2: Quantification of Fragility Function Parameter Uncertainty Flowchart

with varying local soil conditions to account for the possible interaction of the prevalent periods of the soil and the structures. Moreover, six hazard levels are considered to represent engineering demand parameter and intensity measure relationships adequately.

Then, for each hazard level, local site conditions, and reference structure, distinct hazard consistent ground motion suites are selected. Ground motion records in the suites are selected based on their agreement with the target spectra within a specific period range. Selected ground motion records are scaled to represent the seismic input representing the site-specific hazard levels in the non-linear time history analyses of the selected structures.

Next, sensitivity of each parameter is investigated for its 10^{th}, 50^{th} (median), and 90^{th} percentile values. Based on the individual performance of each parameter, significant parameters are selected through tornado diagrams.

Uncertainty scenarios including different random variables based on input parameter groups are defined. Simulations with Latin hypercube sampling technique are employed to portray the probabilistic distribution of the random variables. The structured sampling approach of this method includes the entire input space in the calculations.

From the rigorous analyses of different structure realizations, engineering demand parameters are obtained for all uncertainty scenarios. Fragility function parameters are estimated with maximum likelihood method for the limit states defined herein. Finally, fragility function parameters of different uncertainty scenarios are compared with the parameters of the scenario where only the reference structures are analyzed.

In this thesis, fragility function parameters of ductile code compliant structure realizations without irregularities are estimated to quantify the impact of the uncertainty in the model input parameters. As stated before ,even small variations in construction or material seem to cause shifts in the damage states of two similar structures located on similar local site conditions with similar source-to-site distances, as observed during the recent earthquakes in Pazarcık (moment magnitude, Mw = 7.7) and Elbistan (Mw = 7.6) occurred on February 6, 2023, which resulted in numerous casualties and property losses. Therefore, it is crucial to incorporate all available information about structural variability in seismic designs to improve urban seismic resilience in seismically active regions. For this purpose, different from the majority of other research in the field, this study incorporates a broad range of structural input variables when calculating the fragility functions of three reinforced concrete buildings specifically designed to withstand high seismic loads. The reason for selecting well-designed RC frames in this study rather than deficient structures just like in most of the past studies is to investigate if the collapses of the new RC buildings after the 2023 Kahramanmaraş earthquake sequence may have been caused due to specific structural parameters considered in this study or due to some other factors. To account for uncertainties in the modeling parameters, a novel approach is used to quantify their impact through a series of uncertainty scenarios.

1.4 Objective and Scope

One of the primary objectives of this study is to gain insight into the impact of the uncertainty in the modeling inputs through rigorous analytical data processing and fragility function parameter estimations. Secondly, through uncertainty scenarios, another objective is to improve understanding of the significance of the variance of various input parameter groups.

Scope of this research contains fragility curve calculations of code compliant three reinforced concrete bare frame buildings which are designed for high seismic loads. Analyses are performed considering record-to-record variability as well as structural random variables of both high-level and low-level parameters herein. Finally, uncertainty quantification is performed for multiple scenarios to determine the most impactful parameter group.

- Chapter 2 presents the hazard calculations and the hazard compatible ground motion suites. In this chapter, seismotectonics of the selected study region is summarized. Next, seismic hazard analysis methodology and hazard levels considered in this study are described. Furthermore, seismic source models and ground motion models used in the hazard analysis are specified. The output of the hazard calculations are given in uniform hazard spectra format. Finally, methodologies used to obtain ground motion time histories compatible with the hazard calculations are explained in this chapter.

- Chapter 3 describes analytical structure models used in the study. The chapter begins with introducing reference model properties. Then, random variables in the structural model and their statistical properties are presented. Sampling methodology is next explained. Finally, analytical model assumptions and analysis parameters are summarized.

- In Chapter 4, analysis results are presented where the impact of random variables regarding the structural modeling on fragility function parameters are discussed. First, random variable sensitivity is investigated through single random variable analyses through which tornado diagram outputs are evaluated. Secondly, uncertainty scenarios are introduced. Then, the fragility function pa-

rameter estimation technique is described and the fragility curves are presented for the selected uncertainty scenarios. Finally, fragility function parameters are compared and impact of different uncertainty scenarios are discussed.

- In Chapter 5, the study is summarized and the main conclusions are presented. The chapter also contains a list of recommendations for future research.

The thesis also contains three appendices:

- In Appendix A, selected ground motion record properties are tabulated as the ground motion suite tables. In the tables, source, path, and site information about the selected ground motion records, the scale factor, and intensity measures of the scaled acceleration-time histories are presented.
- In Appendix B, figures depicting elastic acceleration response spectra with 5% damping of the selected and scaled ground motion record components, ground motion suite mean, and the target UHS are presented.
- In Appendix C, analysis input parameters for different structure realizations in the single random variable and multi random variable analyses are tabulated.

CHAPTER 2

SEISMIC HAZARD ANALYSIS AND GROUND MOTION SELECTION

2.1 Introduction

Seismic Hazard Analysis (SHA) is a crucial step for seismic loss estimation studies, providing information on the ground motion demand for structures to estimate losses over a specific period. The unpredictable nature of earthquakes makes it challenging to precisely assess their potential effects. However, within a probabilistic framework, SHA aims to predict these effects and describe them as ground motion intensity measures. Potential earthquake threat at a site is quantified through SHA, which is commonly approached through deterministic seismic hazard analysis (DSHA) or probabilistic seismic hazard analysis (PSHA). Deterministic seismic hazard analysis mostly deals with the most adverse earthquake scenario, while probabilistic seismic hazard analysis considers randomness in earthquake occurrences, integrates uncertainties through probability distributions, and provides ground motion parameters with associated probability distributions. In both type of analyses, to accurately incorporate intensity measures obtained from hazard calculations into structural response, ground motion selection and scaling is a crucial step in structural response history calculations.ion and scaling is crucial in structural response history calculations.

In this chapter, the principles and methodology of PSHA are introduced followed by the assumptions of PSHA performed in this study. Then, the methodology used to obtain scale factors and the ground motion suite selection process are explained.

2.1.1 Study Region and the Site of Interest

Türkiye is located at the junction of three major lithospheric plates, Eurasian, Arabian and African plates as shown in Figure 2.1, adopted from [26]. Therefore, formation of the Anatolian micro-plate in the neotectonic period are explained by the collision of the Eurasian and Arabian-African plates moving towards each other in a North-South direction [27]. Convergence of these three plates and the relative motion Arabian and African plates cause the Anatolian micro-plate to move west [28] and rotate counterclockwise [29]. Major portion of these plate movements are accommodated by North Anatolian Fault Zone's (NAFZ's) aprproximately 25mm/yr right-lateral motion [29]. NAFZ is located between the boundary of Eurasian and Anatolian plates and it is an approximately 1400 km long right-lateral strike slip transform fault system ranging from Karlıova triple junction to the north Aegean Sea. Along NAFZ, due to right-lateral strike-slip movements, several basins of different sizes (such as Erzincan, Bolu, Düzce and Adapazarı) are developed from the dilational bend and stepover geometry [30]. NAFZ is one of the major tectonic structures in the world, which experienced a major sequence of events in the last century: starting with the 27 December 1939 Erzincan earthquake (surface wave magnitude, Ms = 7.8 according to Barka [31]) in the easternmost section of the NAFZ to the west including the 17 August 1999 Kocaeli earthquake (moment magnitude, Mw = 7.6) and the 12 November 1999 Düzce earthquakes (Mw = 7.2).

In this study, seismic hazard calculations are performed in Düzce region. Düzce city is located in Northwestern Turkey and it is a highly populated and industrialized region. The region is located on an alluvial basin located within the proximity of the NAFZ. The seismicity of the region is well studied, active fault map of the region is presented in Figure 2.2, adopted from [32].

The selected site (40.9043 N, 31.1843 E) to be studied in this thesis is located 15 km away from the Düzce Fault, marked in Figure 2.2 with a star. While the spatial variability is not considered in this study, the site condition parameter is a fundamental variable in the loss assessment. Assuming four arbitrary site conditions with different Vs30, the time average seismic shear-wave velocity of the top 30 meters of the soil, the following different site conditions are considered in this study: NEHRP class

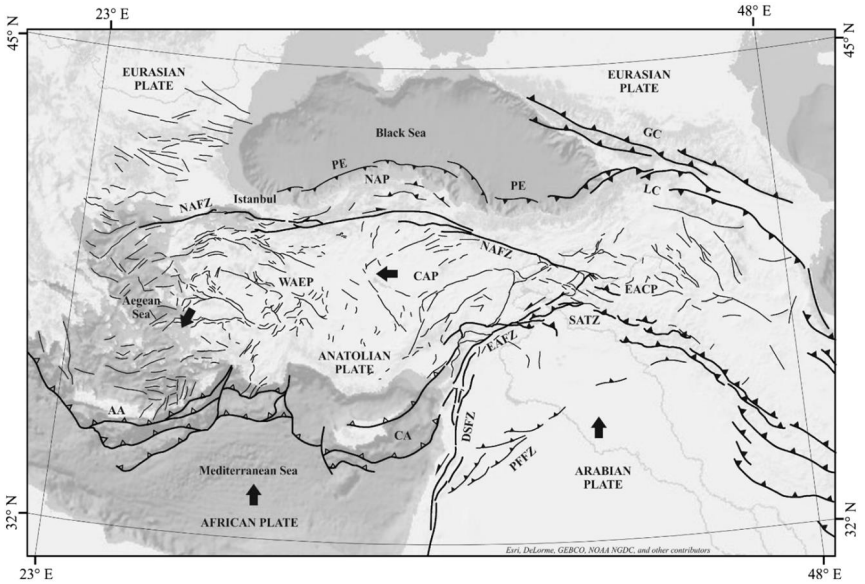

Figure 2.1: Tectonic map of Türkiye

B site (Vs30 = 1130 m/s), generic rock site (Vs30 = 760 m/s), NEHRP class C site (Vs30 = 560 m/s) and NEHRP class D site (Vs30 = 270 m/s).

2.2 Probabilistic Seismic Hazard Analysis

PSHA is a widely used methodology to estimate the probabilities of exceedance of selected ground motion intensity measures at any site of interest, within a certain time window by quantifying uncertainties related to earthquake recurrences, earthquake magnitudes and the resulting ground motions. In contrast to the deterministic seismic hazard assessment, where a single earthquake scenario is considered, probabilistic seismic hazard assessment takes into account various factors such as recurrence rates of the earthquakes, spatial variability in the source, and the variability of the log-normally distributed ground motion parameters.

The PSHA methodology is originally introduced by Cornell [2]. Computational requirements and the significance of this robust methodology have prompted the development of numerous software applications for conducting hazard calculations. The

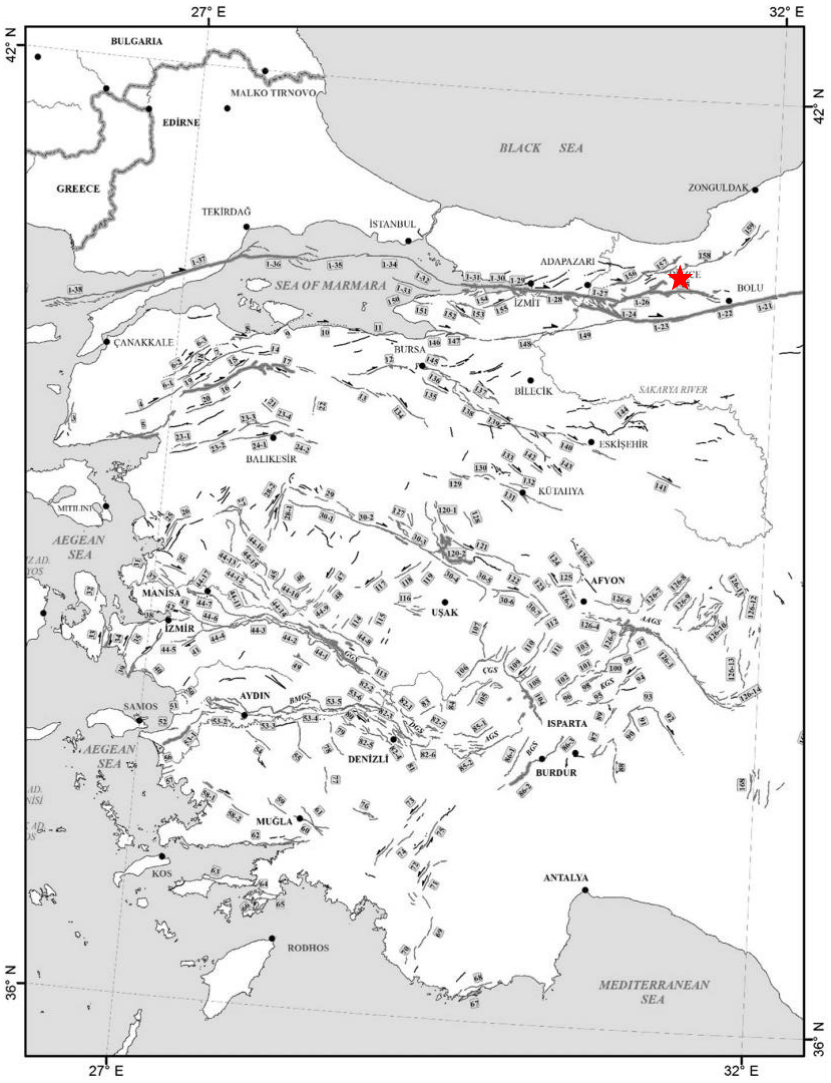

Figure 2.2: Active fault map of the Western Türkiye region

initial computer codes for PSHA were introduced in the 1970s with the launch of EQRISK [33] and FRISK [34]. Subsequent commonly utilized software includes SEISRISK II [35] and SEISRISK III [36], CRISIS [37], EQHAZ [38], EQRM [39], OpenSHA [40], and OpenQuake [41]. A very common and recent software, OpenQuake engine [41] is utilized in this study.

In this study, earthquakes are assumed to follow the homogeneous Poisson process (HPP). According to HPP, the number of events occurring in a period of time is independent of past occurrences, thus the probability of occurrence is proportional to the length of the time period and it is a memoryless process. Although earthquakes are

not memoryless physical events and this assumption is physically flawed, HPP provides accurate and practical results for the statistical modeling of earthquakes. The hazard levels considered in this thesis are selected to be 68%, 50%, 10%, 5%, 2% and 1% exceedance probability in 50 years (44, 72, 475, 975, 2475 and 4975-year return periods respectively). Therefore, both the elastic response and inelastic response of the structures could be captured in the fragility analyses.

The process of implementing PSHA involves several key steps, which include defining seismic sources with engineering importance within the range of site of interest, evaluating earthquake occurrence characteristics for each source, choosing the appropriate ground motion model, identifying site characteristics, and creating a computational algorithm that aggregates the effects from different sources, resulting in a probability distribution for the specified ground-motion parameter at the site of interest. Furthermore, in PSHA various sources of uncertainties, and their impacts on hazard results are addressed through logic tree or similar statistical approaches. Basic steps in PSHA are presented in Figure 2.3, adopted from [42].

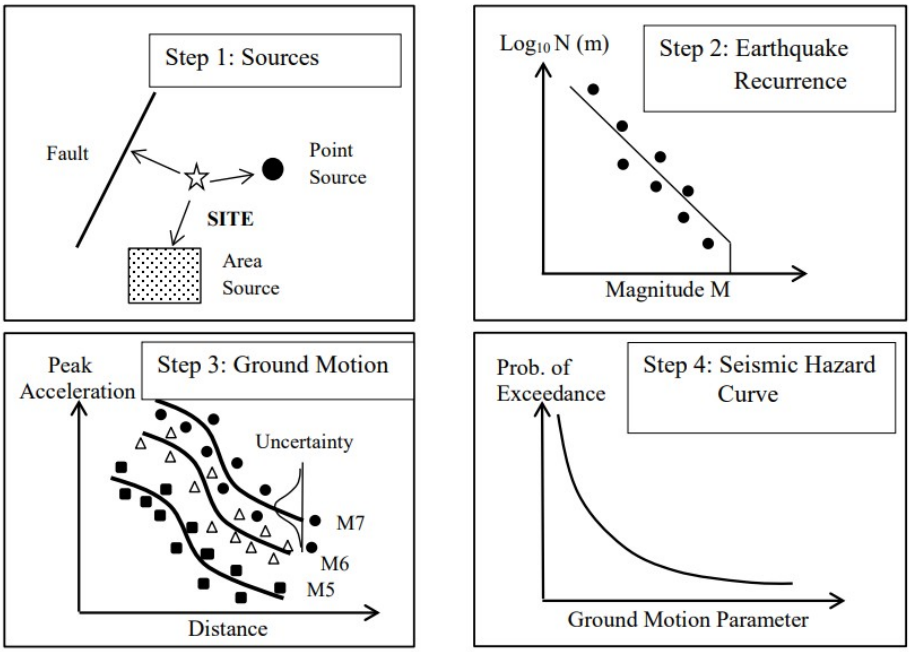

Figure 2.3: Basic 4 steps of PSHA: Source identification, source characterization, GMM selection, and computation of probability of exceedance of the ground motion parameter

Seismic source models that are used for the assessment of the recurrence rates of earthquakes are presented in the following subsection. The spatial variability of the source is assumed to be uniformly distributed. Finally, both regional and global ground motion models (GMMs) are utilized to address the variability of the ground motion parameters. GMMs used in this study and their logic tree weights are described in the subsection after the presentation of the source models.

2.2.1 Seismic Source Models

Seismic source models are used to describe the seismic activity of a region. These models may include maximum magnitude, depth, and distance parameters together with the earthquake recurrence rates. In this study, sources within 200 km of the site are considered with two different source models: an area source model [43] and a source model with both linear fault sources and smoothed seismicity sources [44]. These two models are combined with equal weights (50%) within the logic tree approach.

Maximum magnitudes of the area sources within the study area are estimated by considering the maximum probable magnitudes of the active faults that lie in the area source from the earthquake catalog. Focal depths are similarly estimated from the depth information of the active faults within the area source. The focal mechanisms of the area sources are estimated by combining normal, strike-slip, and reverse faulting with appropriate weights [43].

In the linear fault sources and smoothed seismicity sources model, events that occur within a 15 km buffer zone around a fault are assumed to have originated from that fault. Other events that are not within these buffer zones are incorporated into the source model as the smoothed seismicity sources [44]. Maximum moment, depth, and focal mechanisms of these smoothed seismicity sources are estimated similar to the calculations of area sources in [43].

2.2.2 Ground Motion Models

Ground motion models, formerly known as ground motion prediction equations and attenuation relationships, are mathematical models based on recorded ground motion databases that provide ground motion parameters for an earthquake with known source, path, and site parameters. These equations are mathematical formulations that fit parametric models to past ground motion data to predict future estimates. GMMs can be grouped into regional and global models.

In regional GMMs, the goal is to account for the unique effects of local seismic sources, propagation path, and site conditions on ground motion amplitudes, ensuring that data from other regions do not influence the indigenous dataset. However, regional GMMs may have relatively higher uncertainties because their databases inadequately represent large-magnitude earthquakes at close distances. On the other hand, global GMMs assumed that seismic data from countries sharing similar tectonic regimes are likely to demonstrate similar characteristics. This assumption results in more extensive ground-motion datasets, better distributed across magnitude and distance. Therefore, these models tend to have more stable parameters. Although, global GMMs rely on extensive databases, potentially lack accurate local representation, which can also introduce uncertainty and biased ground motion parameter estimations. While the aleatory uncertainty due to the nature of the earthquakes is already accommodated in the standard deviation of GMMs, the epistemic uncertainty due to mathematical model, methodology, or other differences between GMMs is considered in this study with a logic tree approach.

The GMMs used in this study are selected due to their ability to reflect regional tectonic behavior and the inclusion of the most recent earthquakes in their databases. Then, 5 GMMs are selected based on their ranking in [45] with a data driven GMM ranking tool, Euclidean Distance-Based Ranking (EDR) proposed by Kale and Akkar [46]. Selected GMMs and their logic tree weights are listed in Table 2.1.

Table 2.1: Ground Motion Models and Logic Tree Weights

GMM	Type	Applicable Range			Logic Tree Weight
		Magnitude (M_w)	Distance (km)	Period (s)	
ASK14 [47]	Global	3.0-8.5	$R_{RUP} \leq 300$	0-10	0.10
ASB14 [48]	Regional	4.0-8.0	$R_{JB} \leq 200$	0-4	0.25
BSSA14[49]	Global	3.0-8.5	$R_{JB} \leq 300$	0-10	0.20
CY14 [50]	Global	3.5-8.5	$R_{JB} \leq 300$	0-10	0.25
KAAH15 [51]	Regional	4.0-8.0	$R_{JB} \leq 200$	0-4	0.20

R_{RUP} is the minimum distance to the rapture plane and R_{JB}, Joyner-Boore distance, is the minimum distance to the surface projection of the rupture plane.

2.2.3 Target Spectra

The last step of PSHA is the calculation of ground motion parameters for a specified annual rate of exceedance. Assessment of the seismic performance of structural systems subjected to a set of ground-motion records that are scaled for a target response spectrum is the typical practice in earthquake engineering. The target spectrum is generally described as the uniform hazard spectra (UHS). In UHS, for each structural period, the probability of exceedance of the hazard is the same. Thus, each spectral acceleration (Sa), period (T) point represents the Sa value that the probability of exceedance 68%, 5%, 10%, 5%, 2%, and 1% in 50 years depending on the hazard level for this study. Another alternative representation of the PSHA results is the conditional mean spectrum (CMS) by Baker [52]. One of the main reasons that CMS was developed is to address the generally higher demands due to UHS enveloping the hazard contributions of multiple events with varying magnitude-distance for each period point where individual ground motion records may not be well represented. In CMS, the target mean response spectrum is defined, conditioned on the occurrence of a single spectral acceleration value at the selected period (T_1). This single conditional mean acceleration value is obtained through PSHA, then other periods (T_i) this conditional mean is multiplied with the correlation coefficients between (T_1) and (T_i), $\rho(T_i, T_1)$, that have been studied for global ground motion databases in [53, 54, 55]. However, as discussed in the previous subsection, empirical equations developed for regions with similar tectonic regimes may not represent local conditions accurately.

In this study, the hazard calculations are performed for 6 hazard levels and 4 site conditions and the resulting UHS are obtained for all cases. PSHA results are summarized in Figure 2.4. The limitations of UHS are addressed by selecting and scaling ground-motion records by considering the target mean to account for the variability in spectral ordinates.

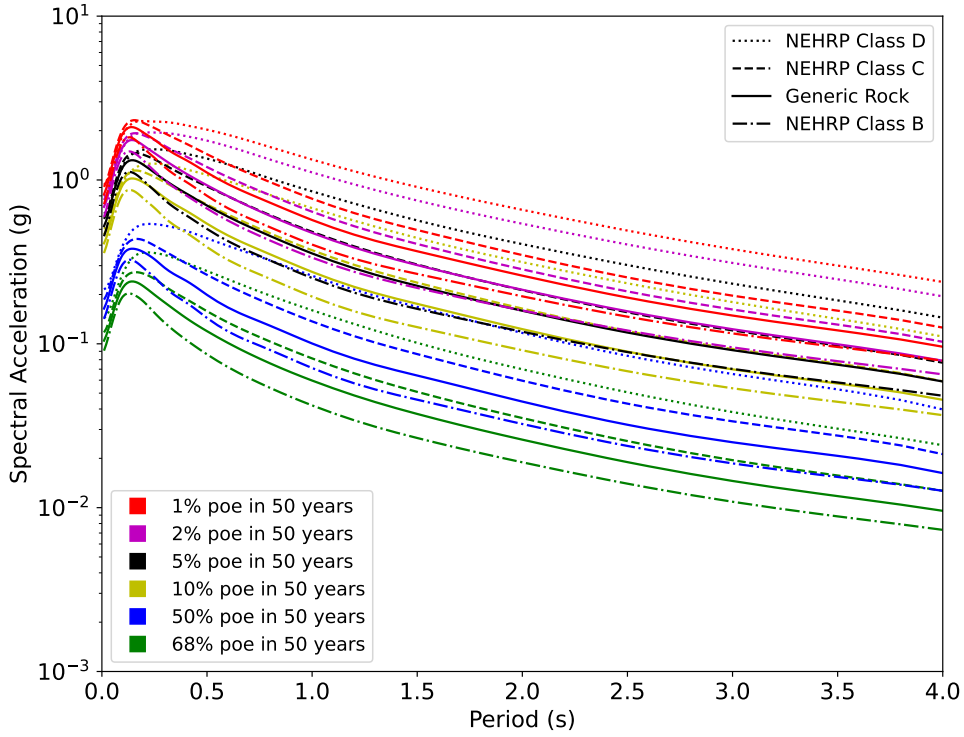

Figure 2.4: Target Uniform Hazard Spectra for Different Hazard Levels and for Different Site Conditions

2.3 Ground Motion Selection and Scaling

In the structural engineering practice, assessment of buildings with non-linear time history analyses (NLTHAs), requires a set of ground motion acceleration time histories, often referred to as the ground motion suite. Ground motion suites are constructed to represent the hazard conditions of interest at a certain location while incorporating uncertainty regarding ground motion variability. In this study, ground motion acceleration time histories which are compatible with the target hazard spectra presented in Figure 2.4 are obtained with basic scaling methodology.

2.3.1 Basic Scaling

Basic scaling methodology is fundamentally an error minimization procedure that is utilized to match the ground motion time histories to the target spectrum and rank the scaled ground motion time histories to determine ground motion suites. This approach, therefore, allows researchers to perform NLTHA with ground motion acceleration series that represent the target hazard spectra. The process of amplitude scaling involves adjusting the original ground-motion amplitudes linearly by multiplying the acceleration data with a scalar factor, known as the "scaling factor". Since outputs of basic scaling preserve their frequency content, this method is preferred for cases where record-to-record variation is investigated and spectral content of the records needs to be preserved. Alternatively, for cases where records closely matching with the target spectrum are needed, response spectrum matching techniques might be preferred. In spectral matching, spectral content of acceleration time histories is modified to match a target spectrum by the use of wavelets algorithm, initially proposed in [56], then improved in [57, 58].

The scaling methodology and, consequently, the calculation of scaling factors is influenced by whether a target spectral value at a single period or a spectrum defined for a period range is aimed. One of the early methodologies is to scale the ground motions based on a single period, generally the first fundamental period of the structure of interest. The method proposed by Shome et al. [59] advocates scaling each record in a bin to the target median spectral ordinate in order to mitigate dispersion in dynamic response. The scaling factor (SF) is calculated as follows:

$$SF_{record,i} = \frac{Sa_{(target)}(T = T_1)}{Sa_{(record,i)}(T = T_1)} \tag{2.1}$$

where, for each record i, $Sa_{(record,i)}(T = T_1)$ is the spectral acceleration of the record at the first fundamental period of the structure, T_1. Similarly, $Sa_{(target)}(T = T_1)$ is the target spectral acceleration at T_1. An alternative approach to amplitude scaling involves aligning only the mean spectral value of unscaled ground-motion records with the target spectral value at the first fundamental period of the structure. Instead of individually scaling each accelerogram in a ground motion bin to the target spec-

tral value, this method adjusts all records with the same scaling factor to align the mean spectral value of scaled accelerograms with the target spectral value [60]. The common scale factor for the ground motion suite is computed as follows:

$$SF_{suite} = \frac{Sa_{(target)}(T = T_1)}{Sa_{(\mu_{suite})}(T = T_1)} \tag{2.2}$$

where, $Sa_{(\mu_{suite})}(T = T_1)$ is the mean spectral acceleration of the ground motion suite at the first fundamental period of the structure, T_1, and $Sa_{(target)}(T = T_1)$ is the target spectral acceleration at T_1. Despite their effectiveness in producing a set of scaled records that have low variability in elastic spectral response parameters, these methods have limited use, especially for assessing the inelastic behavior of structures, where the uncertainty in structural response is highly susceptible to higher-mode effects.

As an another alternative, to account for higher mode effects and period shifts due to inelastic response, the scaling factor is computed while aiming for a match between the target spectral shape and the spectrum of each record within a predefined period interval, rather than scaling to the target spectral value just at the fundamental period. This scaling procedure, distributing equal weight to each intermediate period value, optimally matches the average spectral value for a certain period interval but does not guarantee a perfect match with the corresponding target at the fundamental period of the structure. In this study, selection and basic scaling of the ground motion suite is performed based on a specific period range. The main steps to obtain a hazard-compatible ground motion suite are explained in the following subsections.

2.3.1.1 Estimation of the Specific Period Range

The first step of the scaling procedure is to identify the period range of the error minimization to include periods that involve the potential structural response. This specific period range is defined to account for the shift in the fundamental period due to nonlinear behavior and contributions of the higher modes in the seismic response. In some of the current design codes (ASCE 7-16 [61] and Eurocode 8 [62]), this specific period range is bounded between $0.2T_1 - 2.0T_1$ with the constraint that max-

imum directional spectrum does not fall below 90% of the target spectrum in entire period range, where T_1 is the fundamental period of the structure. In this study, based on the most recent Turkish Earthquake Code (TEC) [63], the specific period range is defined to be $0.2T_1 - 1.5T_1$, where T_1 is the fundamental period of the structure. In this period range, the mean of the ground motion suite response spectra ($Sa_{(\mu_{suite})}$) is constrained to be always higher than the target response spectra.

2.3.1.2 Initial scale factor determination

It has been empirically verified in a previous study [64] that $Sa(T)$ is log-normally distributed. Thus, in recent ground-motion selection algorithms (e.g. [65, 66]), the sum of squared error function (SSE), shown as Equation 2.3 is used for representing the similarity between the target spectrum and the individual ground motion record of interest. In this study, the initial scale factors are obtained for each ground motion time history to rank the candidates for ground motion suites as follows:

$$SSE = \sum_{i=0.2T_1}^{1.5T_1} [\ln(Sa_{(target)}(T=i)) - \ln(Sa_{(scaled)}(T=i))]^2 \tag{2.3}$$

where, $\ln(Sa_{(scaled)}(T=i))$ is the logarithm of the spectral acceleration of the ground motion to be scaled at $T=i$, similarly $\ln(Sa_{(target)}(T=i))$ is the logarithm of the spectral acceleration value of the target spectrum at $T=i$. Period steps are selected in the SSE calculation consistent with the periods provided by the PEER NGA-West2 Database [66].

2.3.2 Ground motion suite selection

Recently, across the world, both the number and density of seismic monitoring stations as well as the number of recordings obtained from the current seismic sensors have shown an increasing trend. Thus, in parallel to the advances in the monitoring technologies and increasing density of the networks, the number of ground motion time history records has increased significantly. One of the main consequences of growing seismic monitoring networks is the trade-off between the ability to select

multiple suitable candidates for time history analyses and the resulting computational cost due to the increased number of ground motion time histories to be used in the analyses. In this study, 20 ground motion time histories per ground motion suite for each structure, each site condition, and each hazard level are selected. In the ground motion suite selection procedure, first, ground motion records are obtained from a ground motion database based on their properties, then the candidates are ranked based on their initial scale factors. For the ground motion suite selection, initially screening parameters based on the source, path, and site metadata of the records are applied to the PEER NGA-West2 database [[66], [67]]. The screening procedure is performed to eliminate record candidates that have incompatible source, path, and site parameters with the PSHA parameters. Ground motion records are selected from events that have strike-slip faulting and M_w greater than 5.5 consistent with the site of interest in this study. While the style of faulting does not directly impact the spectral shape of the ground motion significantly, since there remains a sufficient amount of ground motion record candidates consistent with the hazard calculations even after the inclusion of style of faulting screening parameters, source effects, especially for events at close distances, are selected consistent with the GMM parameters used in the PSHA. Ground motion records that are recorded more than 100 km away from the surface projection of the earthquake rupture plane are eliminated. Furthermore, Vs30 upper and lower bounds are selected between 0.5 and 1.5 times the reference Vs30 value as suggested in [68], not to disregard a disproportionate amount of ground motion records that could accurately match the target spectrum. Additionally, the lowest usable frequency is set to be 0.5 Hz and pulse-like records are screened out. In Table 2.2, screening parameters are presented for each site condition considered in this thesis.

Table 2.2: Screening Parameters for Ground Motion Suite Selection

Parameter	**Class B**	**Generic Rock**	**Class C**	**Class D**
$Vs30$ (m/s)	565-1695	380-1140	280-840	135-405
M_w	$\geq$5.5			
R_{jb} (km)	0-100			
Faulting	Strike Slip			

After screening procedure of the database is complete, ground motion suites are selected and scale factors are determined in four main steps:

- In the first step, for each record with 3-components, vertical acceleration-time records are discarded, and initial scale factors for both horizontal acceleration-time history components are calculated.
- Secondly, acceleration-time history components are ranked based on the absolute logarithms of the initial scale factors. Candidates that have the initial scale factors with values closer to 1 are ranked higher.
- Thirdly, the best performing, the highest ranking, 20 acceleration-time history components are selected for each ground motion suite.
- Finally, final scale factors of the acceleration-time histories are determined based on the criteria that the mean of the ground motion suite spectra is always above the target spectrum within the specific period range. In this step, scale factors are limited such that scaled acceleration time histories would be physically representative of the hazard estimation; especially since the significant duration of the acceleration time histories are not explicitly considered in the ground motion suite selection process. In recent research [[69], [70], [71]], it is shown that scale factors within the range of 0.2 to 5 do not bias the non-linear displacement results. Thus, these limits are incorporated into the ground motion selection and scaling process in this thesis.

In the ground motion record selection process, UHS is utilized to obtain hazard-consistent time histories with accurate spectral shapes by defining a period range to account for the shifts in the non-linearity in the dynamic behavior of the structures, selecting source, path, and site parameters consistent with those used in the seismic hazard analysis and limiting scale factors. Selected ground motion record components for the ground motion suites and their main intensity parameters as well as elastic acceleration response spectra with 5% damping are presented in Appendices A and B respectively. An example ground motion suite is presented in Table 2.3 and its spectra in Figure 2.5.

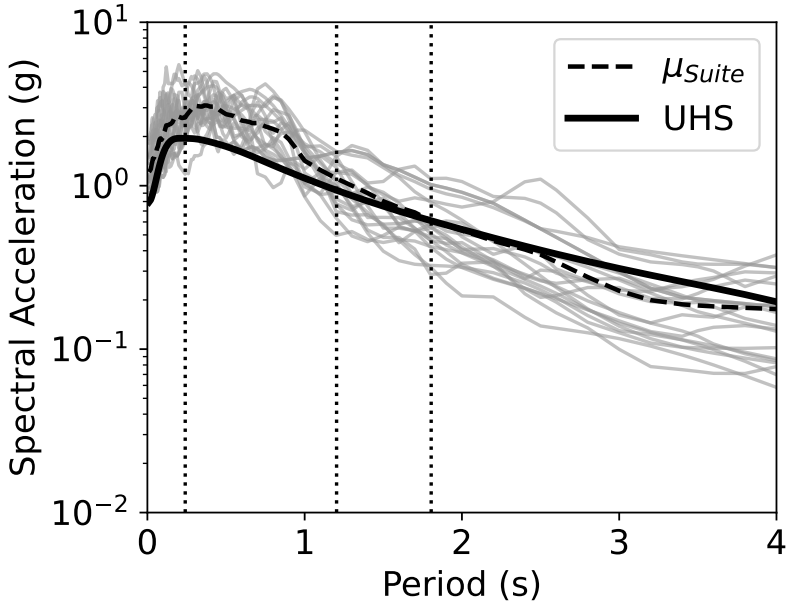

Figure 2.5: Ground Motion Suite Spectra for F8S3B Building with 2% Probability of Exceedence in 50 Years for NEHRP Class D Site

Table 2.3: Ground Motion Suite for F8S3B Building with 2% Probability of Exceedence in 50 Years for NEHRP Class D Site

Earthquake Name	Year	Station Name	Component	M_w	R_{jb} (km)	Vs30 (m/s)	Scale Factor	PGA (g)	PGV (cm/s)	Sa_{T1} (g)	Arias Intensity (cm/s)	Housner Intensity (cm)
Tottori Japan	2000	TTRH02	H-2	6.61	0.83	310	1.443	1.113	124.9	1.536	208.57	409.75
Parkfield-02 CA	2004	Parkfield - Fault Zone 14	H-1	6.0	8.45	246	1.464	1.917	122.0	2.470	167.57	367.61
Tottori Japan	2000	TTRH02	H-1	6.61	0.83	310	1.208	1.136	147.5	1.818	175.30	454.38
El Mayor-Cucapah Mexico	2010	El Centro Array 11	H-2	7.2	15.36	196	1.750	1.026	110.6	2.193	172.85	389.69
Imperial Valley-06	1979	Bonds Corner	H-2	6.53	0.44	223	1.928	1.498	86.6	3.420	229.56	361.84
El Mayor-Cucapah Mexico	2010	El Centro Array 11	H-1	7.2	15.36	196	2.222	0.982	128.3	1.978	248.41	361.70
Imperial Valley-06	1979	Bonds Corner	H-1	6.53	0.44	223	2.409	1.442	112.6	3.923	235.82	420.46
Kocaeli Turkey	1999	Duzce	H-2	7.51	13.6	282	2.481	0.903	138.0	1.530	83.66	562.63
Kocaeli Turkey	1999	Duzce	H-2	7.51	13.6	282	2.481	0.903	138.0	1.530	83.66	562.63
El Mayor-Cucapah Mexico	2010	El Centro Array 10	H-2	7.2	19.36	203	2.529	0.964	120.5	1.303	235.13	439.57
El Mayor-Cucapah Mexico	2010	MICHOACAN DE OCAMPO	H-1	7.2	13.21	242	2.553	1.372	157.1	2.490	404.77	555.98
Chalfant Valley-02	1986	Zack Brothers Ranch	H-1	6.19	6.44	316	2.591	1.159	95.3	2.423	132.65	389.98
Parkfield-02 CA	2004	Parkfield - Fault Zone 14	H-2	6.0	8.45	246	2.649	1.526	112.1	5.013	198.13	384.93
Landers	1992	Coolwater	H-2	7.28	19.74	353	2.685	1.120	116.6	1.313	160.33	386.36
El Mayor-Cucapah Mexico	2010	El Centro - Imperial & Ross	H-1	7.2	19.39	229	2.745	1.055	130.0	2.366	287.34	409.84
El Mayor-Cucapah Mexico	2010	RIITO	H-2	7.2	13.7	242	2.774	1.043	104.9	2.857	367.25	404.56
Kobe Japan	1995	Amagasaki	H-2	6.9	11.34	256	2.846	0.930	127.5	1.899	161.20	627.42
Westmorland	1981	Westmorland Fire Sta	H-1	5.9	6.18	194	2.919	1.101	128.8	2.258	152.69	523.64
Chalfant Valley-02	1986	Zack Brothers Ranch	H-2	6.19	6.44	316	2.923	1.171	130.7	1.873	173.81	444.32
Imperial Valley-06	1979	El Centro Array 8	H-1	6.53	3.86	206	2.981	1.819	162.4	2.785	148.14	547.85

CHAPTER 3

STRUCTURAL MODELING

3.1 Introduction

In this study, three reference structures are considered for the nonlinear time history analyses. The reference structures are reinforced concrete frame type structures that are designed before in another study [72]. All of the reference structures are code-compliant and they cover a wide fundamental period range (0.59 s to 1.20 s). Analytical models of the reference structures are developed using OpenSeesPy [73] a Python interpreter of the structural analysis platform OpenSees [74].

3.2 Reference Reinforced Concrete Frame Properties

Reference structures are intentionally selected to represent code-compliant residential reinforced concrete frame type structures, that are designed in California according to the Uniform Building Code-1982 [75]. Code-compliant buildings in Düzce and California have similar demand and capacity properties and RC frame structural systems are widely used in Düzce region. The abbreviation used to define the frames includes the number of stories and bays, i.e., F5S4B represents a structure with 5 stories and 4 bays. Hence in this study, the considered reference frames are labelled as F2S2B, F5S4B, and F8S3B. Basic dynamic parameters of the reference structures are given in Table 3.1. The median parameters of the reference structures are presented in Tables 3.3, 3.6, and 3.9. The section properties of the F2S2B reference structure are presented in Table 3.4 and Figure 3.4; the section properties of the F5S4B reference structure are presented in Table 3.7 and Figure 3.5 and the section properties of the

F8S3B reference structure are presented in Table 3.10 and Figure 3.6.

Table 3.1: Dynamic Parameters of the Reference Structures

Reference Structure	**Total Mass (t)**	**Total Height (m)**	T_1 **(s)**
F2S2B	275	7.9	0.592
F5S4B	1007	15.0	0.954
F8S3B	1816	31.7	1.203

3.3 Structural Parameters Used as Random Variables

While the improvements in manufacturing techniques and standardization have reduced the uncertainties of many construction materials; there are still uncertainties due to storage, transportation, and construction on site which could affect the the seismic performance of reinforced concrete structures. Moreover, uncertainties related to the modeling of the RC structures remain as a major source in fragility analyses. In this study, to account for this uncertainty, the following parameters have been selected as random variables during the dynamic analyses of structural models: the width of columns (b), the depth of beams (h), the compressive strength of concrete ($f_c^{'}$), yield strength of steel (f_y), the weight density of concrete (w), the equivalent viscous damping (ξ), the thickness of the concrete cover (t), and the spacing of the transverse steel (s). The probability distribution parameters of these random variables are listed in Table 3.2 by considering previous studies in the literature.

3.3.1 Sampling Methodology

Latin hypercube sampling (LHS) and Monte Carlo simulation are are two techniques that have been used in risk assessment and uncertainty analyses. LHS is a sampling technique that aims to evenly and systematically cover the entire input parameter space. The input parameter space is covered by dividing the space into equal intervals and it is ensured that each interval of each parameter is sampled exactly once while Monte Carlo simulation involves random sampling from the input parameter space without any specific structure or pattern. Random samples are generated according

Table 3.2: Statistical Parameters of the Selected Random Variables

Random Variable	**Distribution**	**Coefficient of Variation**	**Reference**
b	Normal	0.026	[76]
h	Normal	0.021	[76]
$f_c^{'}$	Normal	0.150	[77]
f_y	Lognormal	0.073	[78]
w	Normal	0.100	[76]
ξ	Lognormal	0.658	[18]
t	Normal	0.200	[79]
s	Normal	0.100	[79]

to the specified probability distributions for each parameter. Since Monte Carlo simulation relies on random sampling without enforcing a structured sampling strategy, it can cover the entire parameter space. However, it might require more samples to achieve similar coverage as LHS. Another benefit of LHS is that the number of random variables does not affect the computation time. Therefore, LHS is utilized in this study to evenly cover the input parameter space without increasing the computational effort.

An example application of LHS is depicted in Figure 3.1 for two parameters (p1, p2) for a sample size of 10. Here parameters p1 and p2 are assumed to have normal and log-normal distributions respectively.

LHS is a robust tool for uncertainty quantification that is not affected by the number of random variables in the study. However, the number of samples used for LHS is a crucial parameter for statistical reliability. Even though the LHS is a stratified sampling technique and covers the entire parameter space by the use of equal intervals, as the number of samples increases the coverage of the entire parameter space increases. This reduces the sampling error and allows for capturing distributions more accurately. On the other hand, there is a trade-off between the number of samples and the computational power requirements. The benefit of increasing the number of samples decays exponentially. For accurate results in RC frames, it is recommended to select the number of samples greater than twice the number of random variables

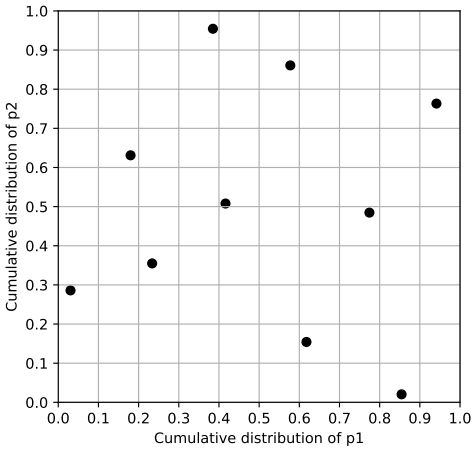

(a) Sampled cumulative distribution values in Unit Hypercube

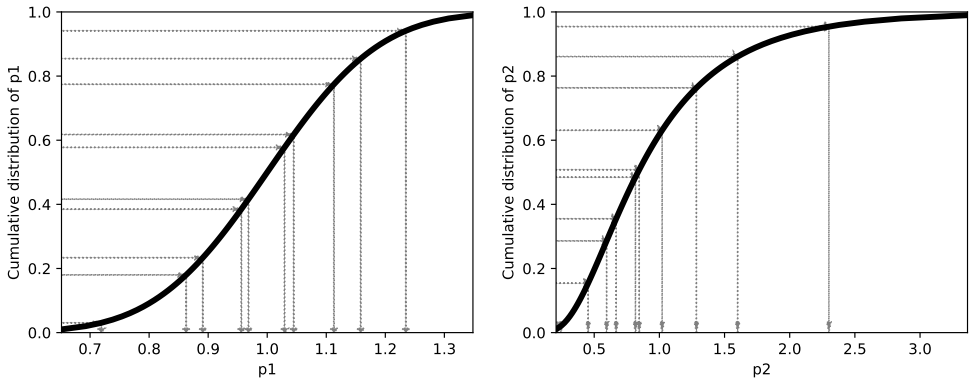

(b) Conversion of cumulative distribution values to parameters values

Figure 3.1: Example LHS of two parameters with a sample size of 10

[7]. In this study, 30 samples are used in the LHS procedure. Parameters used in the analyses are presented in Appendix C.

3.4 Analytical Models

OpenSees [74] is a general-purpose finite element analysis software used widely for earthquake engineering applications due to its modeling and non-linear time history analysis capabilities. One of the major advantages of using OpenSees is the ability to define structural elements at fiber level, thus allowing distributed plasticity to be modeled and analyzed. Fiber section [80] allows discretization of a section into longi-

tudinal steel and concrete (both confined and unconfined) fibers. Moreover, the nonlinear behavior of the element can be obtained from the stress-strain relations of the reinforcement and concrete fibers. Thus, force-deformation of the element does not need to be explicitly input and assumptions regarding the behavior of the structural system could be minimized. Figure 3.2, adopted from [80], represents the interaction of material constitutive models in the analytical fiber element model.

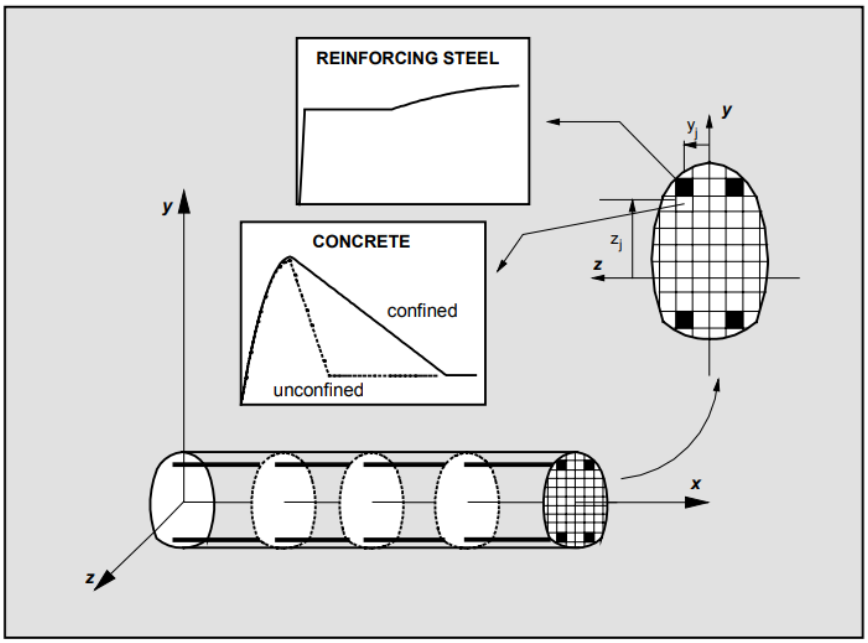

Figure 3.2: Distributions of Control Sections and Section Subdivisions of a Fiber Element

For the structural model, the force-based beam-column element is used for both beam and column elements. The plasticity of the beam elements is entirely modeled with fiber sections as distributed plasticity, while only the end sections of the column elements are modeled with fiber sections where the plasticity is known to be concentrated. The remaining mid-section of the column elements are modeled with elastic properties. The failure mechanism is assumed to be flexure for the well-designed structures and in the modeling, shear reinforcement details are not considered. There is a trade-off between modeling detail and the computational power requirements. For well-designed structures, modeling columns with lumped plasticity allows better utilization of the computational power in the analyses while impacting the behavior of the structural model minimally.

For the fiber sections, constitutive models for confined concrete, unconfined concrete, and steel reinforcements are defined separately. Concrete01 and Steel01 models are used for concrete and steel respectively. Typical hysteretic stress-strain relations of the material models are presented in Figure 3.3, adopted from [81]. Confined and unconfined concrete parameters are calculated by Modified Kent and Park [82] based on the reference model definitions of Kadaş [72]. Steel01 is a bi-linear model with strain hardening. In this study, the values of 200 GPa and 0.005 are used as the initial tangent of the model and the strain hardening ratio, respectively.

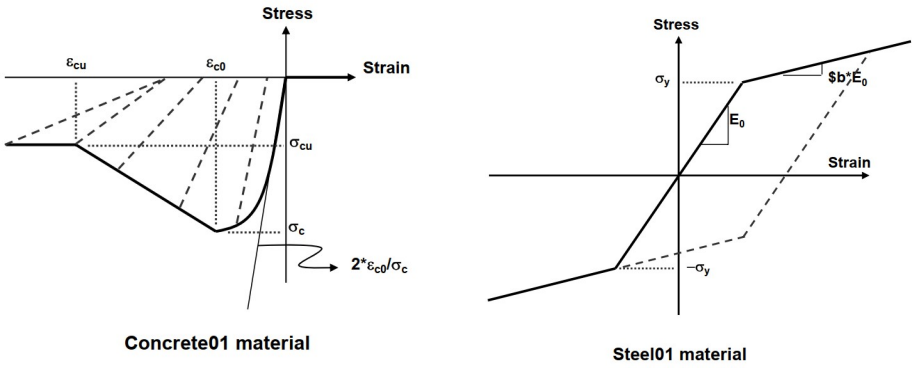

(a) Concrete01 (b) Steel01

Figure 3.3: Typical hysteretic stress-strain relations of the material models

The nonlinear behavior of the columns is modeled with the assumption that plasticity is concentrated at the column end zones, whose length is calculated based on plastic hinge length formulations of [83]. Cracked section properties, $E_{c_{cracked}} = 0.7E_c$, are used for the middle elastic section as in [63]. HingeMidpoint integration method is utilized for the columns whereas Gauss-Lobatto integration with 4 integration points is used for the beam elements. Integration point locations are presented in Figures 3.4, 3.5, and 3.6.

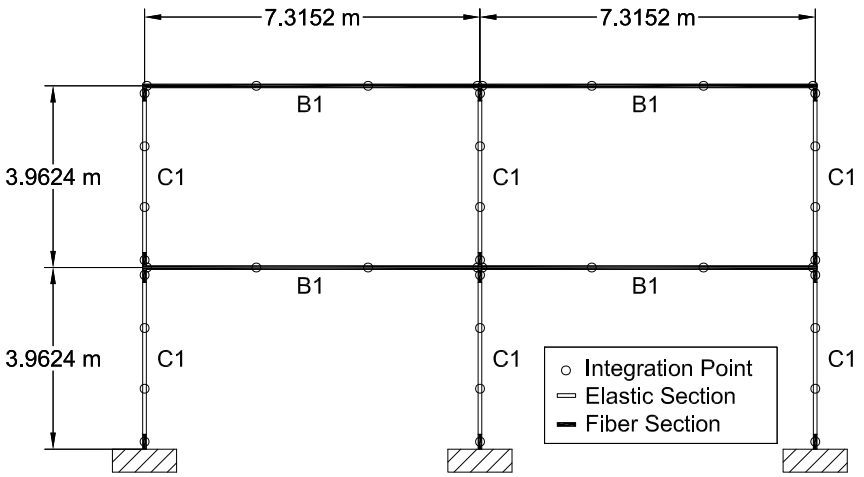

(a) Element Properties

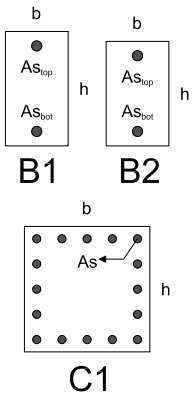

(b) Section Properties

Figure 3.4: F2S2B Analytical Model

Table 3.3: F2S2B Reference Model Material Properties

	Unconfined Concrete				Confined Concrete				Reinforcement	
Section	$f_c(MPa)$	ϵ_{c0}	$f_{cu}(MPa)$	ϵ_{cu}	$f_{cc}(MPa)$	ϵ_{c0c}	$f_{cuc}(MPa)$	ϵ_{cuc}	$f_y(MPa)$	$f_{yw}(MPa)$
C1	26.000	0.002	0.001	0.0057	34.153	0.0026	6.831	0.048	494.000	494.000
B1	26.000	0.002	0.001	0.0057	29.692	0.0023	5.938	0.017	494.000	494.000
B2	26.000	0.002	0.001	0.0057	29.670	0.0023	5.934	0.018	494.000	494.000

Table 3.4: F2S2B Reference Model Section Properties

Section	h (mm)	b (mm)	Cover (mm)	$As_{top}(mm^2)$	$As_{bot}(mm^2)$	Dead Load (kN/m)	Live Load (kN/m)
B1	556	305	56	1342	3148	24.71	1.95
B2	508	305	51	1342	2503	19.23	0.98
Section	h (mm)	b (mm)	Cover (mm)	$As(mm^2)$	Plastic hinge length (mm)		s (mm)
C1	609.6	609.6	61	645.2	325		100

Table 3.5: F2S2B Reference Model Story Masses

Story	Mass (ton)
1	177.7014
2	97.5535

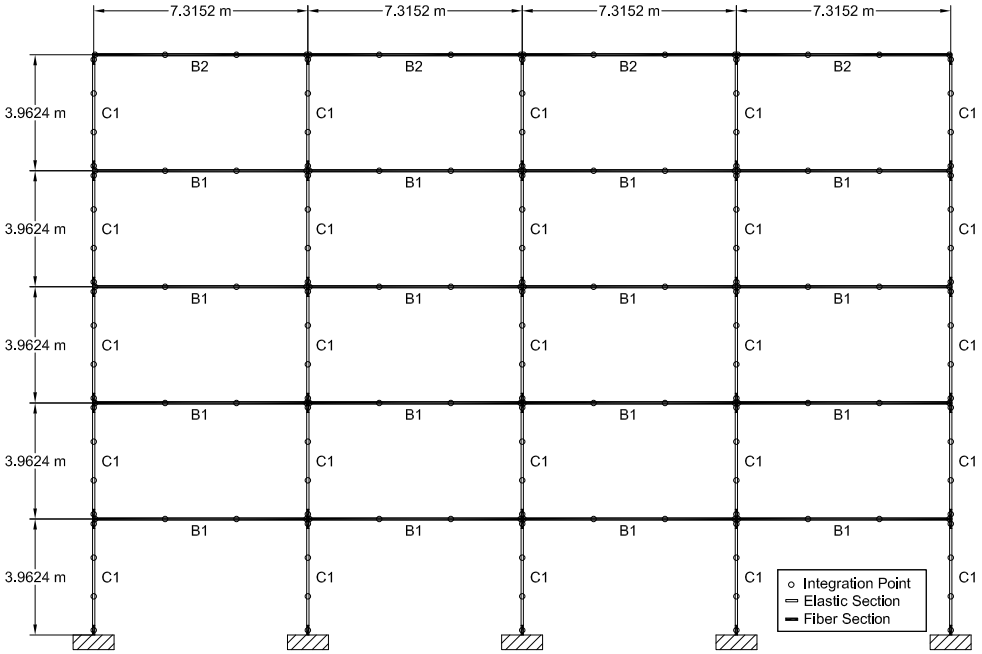

(a) Element Properties

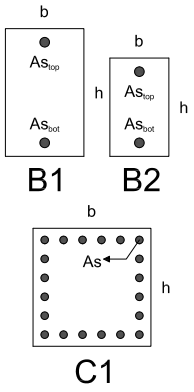

(b) Section Properties

Figure 3.5: F5S4B Analytical Model

Table 3.6: F5S4B Reference Model Material Properties

	Unconfined Concrete				Confined Concrete				Reinforcement	
Section	$f_c(MPa)$	ϵ_{c0}	$f_{cu}(MPa)$	ϵ_{cu}	$f_{cc}(MPa)$	ϵ_{c0c}	$f_{cuc}(MPa)$	ϵ_{cuc}	$f_y(MPa)$	$f_{yw}(MPa)$
C1	28.000	0.002	0.001	0.0054	36.173	0.0026	7.235	0.058	459.000	459.000
B1	28.000	0.002	0.001	0.0054	31.997	0.0023	6.399	0.022	459.000	459.000
B2	28.000	0.002	0.001	0.0054	33.328	0.0024	6.666	0.024	459.000	459.000

Table 3.7: F5S4B Reference Model Section Properties

Section	h (mm)	b (mm)	Cover (mm)	$As_{top}(mm^2)$	$As_{bot}(mm^2)$	Dead Load (kN/m)	Live Load (kN/m)
B1	660	406	66	5080	3150	20.49	1.31
B2	508	305	51	3790	2500	15.64	0.53
Section	h (mm)	b (mm)	Cover (mm)	$As(mm^2)$	Plastic hinge length (mm)		s (mm)
C1	711.0	711.0	46	885.8	339		100

Table 3.8: F5S4B Reference Model Story Masses

Story	Mass (ton)
1	212.430
2	212.430
3	212.430
4	212.430
5	157.400

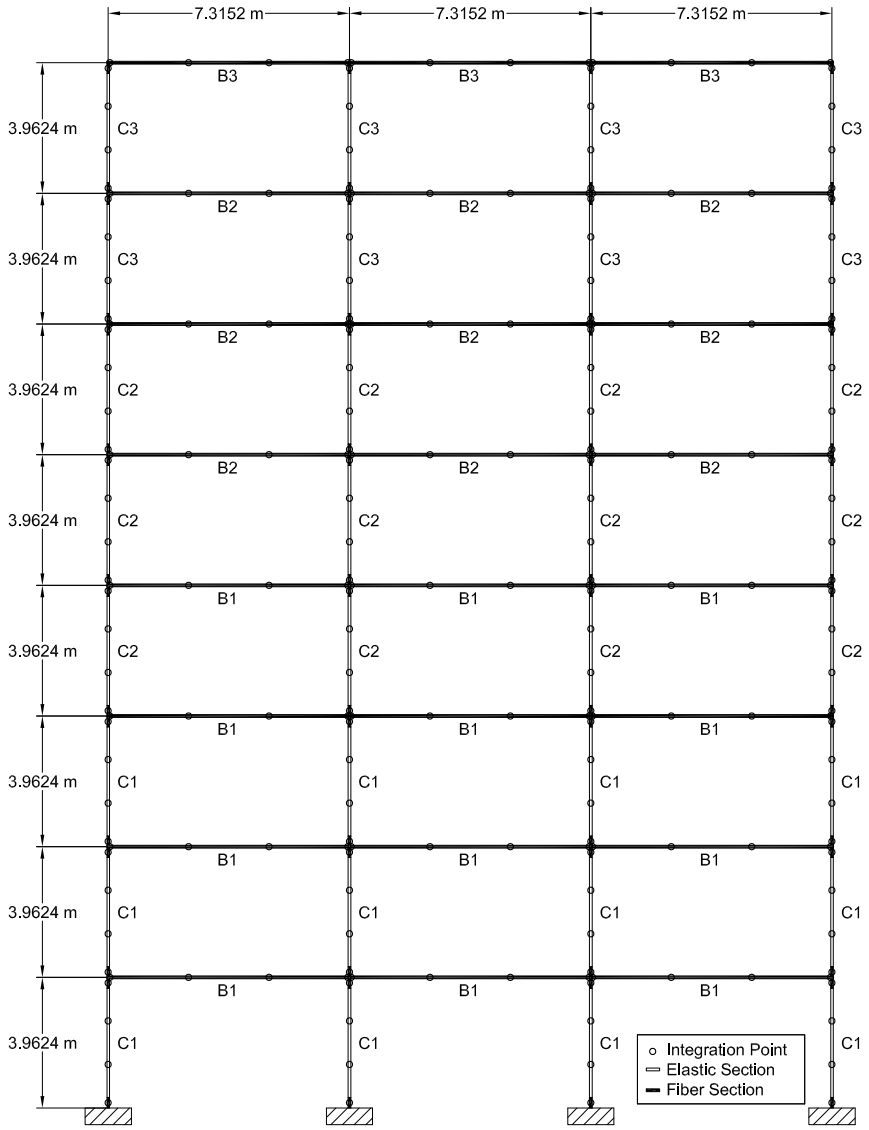

(a) Element Properties

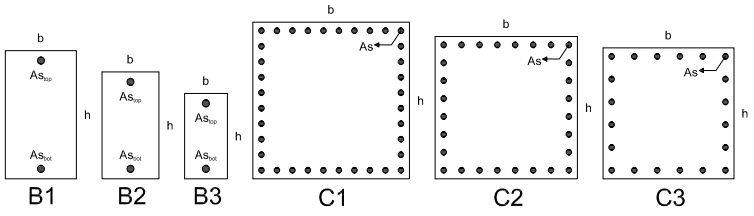

(b) Section Properties

Figure 3.6: F5S4B Analytical Model

Table 3.9: F8S3B Reference Model Material Properties

	Unconfined Concrete				Confined Concrete				Reinforcement	
Section	$f_c(MPa)$	ϵ_{c0}	$f_{cu}(MPa)$	ϵ_{cu}	$f_{cc}(MPa)$	ϵ_{c0c}	$f_{cuc}(MPa)$	ϵ_{cuc}	$f_y(MPa)$	$f_{yw}(MPa)$
C1	28.000	0.002	0.001	0.0054	33.880	0.0024	6.776	0.053	459.000	459.000
C2	28.000	0.002	0.001	0.0054	35.008	0.0025	7.002	0.059	459.000	459.000
C3	28.000	0.002	0.001	0.0054	38.367	0.0027	7.673	0.082	459.000	459.000
B1	28.000	0.002	0.001	0.0054	30.704	0.0022	6.141	0.019	459.000	459.000
B2	28.000	0.002	0.001	0.0054	31.513	0.0023	6.303	0.020	459.000	459.000
B3	28.000	0.002	0.001	0.0054	33.047	0.0024	6.609	0.023	459.000	459.000

Table 3.10: F8S3B Reference Model Section Properties

Section	h (mm)	b (mm)	Cover (mm)	$As_{top}(mm^2)$	$As_{bot}(mm^2)$	Dead Load (kN/m)	Live Load (kN/m)
B1	900	500	50	5400	4800	18.64	1.21
B2	750	400	50	4500	3600	18.64	1.21
B3	600	300	50	1800	1125	14.55	0.49
Section	h (mm)	b (mm)	Cover (mm)	$As(mm^2)$	Plastic hinge length (mm)		s (mm)
C1	1100.0	1100.0	50	510.0	363		100
C2	1000.0	1000.0	50	510.0	352		100
C3	920.0	920.0	50	510.0	349		100

Table 3.11: F8S3B Reference Model Story Masses

Story	Mass (ton)	Story	Mass (ton)
1	230.450	5	230.450
2	230.450	6	230.450
3	230.450	7	230.450
4	230.450	8	202.920

The mass contributions of the elements are calculated due to dead loads and 25% of the live loads and distributed to the nodes at each story with lumped masses. Story masses are tabulated in Tables 3.5, 3.8, and 3.11. In the analyses, P-Δ coordinate transformation is employed. This coordinate transformation is a linear transformation from the basic system to the global coordinate system that considers second-order P-Δ effects. For well designed ductile structures 3% equivalent critical damping is consistent with the previous studies [18]. Rayleigh damping is used with 3% equivalent critical damping in the first and second modes of the F2S2B and F5S4B structures, and the first and third modes of the F8S3B structure as presented in Figure 3.7. The corner frequencies for the Rayleigh damping are selected to include the modes until their cumulative mass contribution exceed 90%. Due to the Rayleigh damping formulation, the damping for the higher modes become very high and their contribution to the response becomes insignificant.

3.4.1 Analysis Parameters and Convergence Control

OpenSeesPy allows performing transient analysis with multiple solution algorithms and convergence tests in case a convergence could not be reached in the first iteration. In this study, the Newton-Raphson algorithm and Norm Displacement Increment Test are used as the solution algorithm and convergence test initially. The initial time step of the transient analyses is selected to be 0.005 s. Initially, fiber sections are subdivided into four and two sections in in-plane and out-of-plane directions respectively.

In case convergence could not be reached, combination of alternative solution algorithms (Krylov-Newton, secant Newton, modified Newton, Newton with Raphson

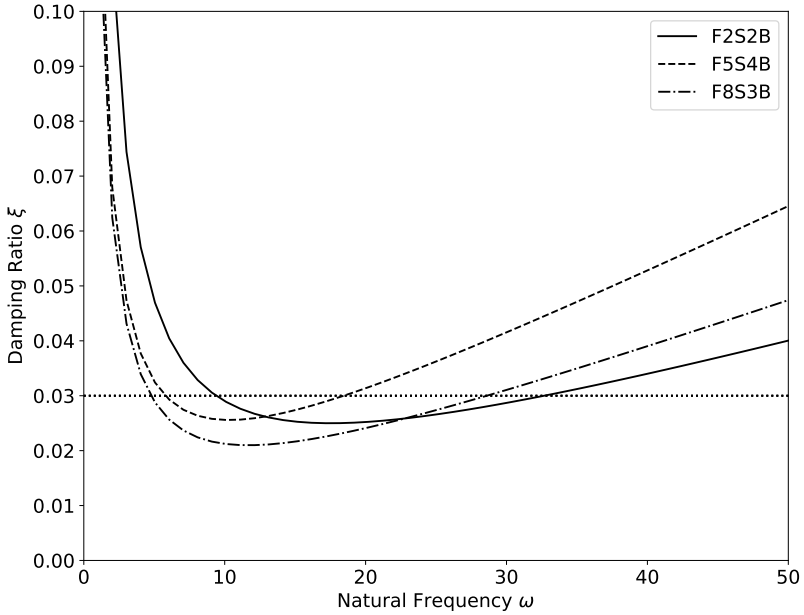

Figure 3.7: Rayleigh damping with 3% equivalent critical damping for reference structures

accelerator, Newton with periodic accelerator, Broyden–Fletcher–Goldfarb–Shanno (BFGS), Broyden, and Newton with line search) and convergence tests (Norm unbalance, relative norm unbalance, relative norm displacement increment, and relative energy increment) are employed while the time step is reduced to 0.0025 s. If the analysis still could not converge to a solution, in the rerun of the analysis the subdivisions of the fiber sections are doubled and the analysis is repeated until the number of subdivisions is 16 times the initial subdivisions. With these approaches, all analyses have converged to a solution in this study.

CHAPTER 4

ANALYSIS RESULTS AND UNCERTAINTY QUANTIFICATION

4.1 Introduction

In earthquake engineering, fragility functions are defined to represent the probability of the selected engineering demand parameter (EDP) exceeding a limit state for a given ground motion intensity measure (IM). EDPs, such as inter-story drift ratio and maximum top displacement, are estimated due to seismic excitations at a selected hazard level. As the hazard level increases, structures' seismic response becomes non-linear due to the inelastic deformations under forces that exceed the elastic limits of the system. Therefore, force-based calculations may fail to capture the post-elastic behavior and use of nonlinear displacement-based procedures may be required to capture the accurate behavior of the structures under seismic loads with higher intensity.

In this study, non-linear time history analyses are performed with structures with nonlinear analytical models consisting of nonlinear constitutive models with random variables. As the demand parameter maximum inter-story drift ratio is selected due to its correlation with the structural damage.

In the literature, the number of limit states used and their corresponding definitions are totally different. In this study, three limit states have been defined for the considered structural models. The first one, immediate occupancy (IO), indicates that there should be no or slight damage This limit state generally corresponds to the linear elastic behavior threshold of the structure. The second limit state, i.e. life safety (LS), can suggest significant damage, but there should still be enough protection against collapse. The third limit state, collapse prevention (CP), indicates that there is only a small margin against collapse. One approach for the attainment of limit states is

to carry out pushover analyses for the reference structures and monitor the progress of damage in the structural members. In this manner, IO limit state can be selected as the point where the sudden reduction in the slope of the capacity curve occurs as the overall stiffness of the structure is reduced due to the yielding within the structural members. CP limit state is adopted from the presented collapse mechanisms and the corresponding limit state values of the superior reinforced concrete structures in [84]. Finally, LS limit state is selected to be the arithmetic mean of IO and CP limit states in terms of the considered EDP. Maximum inter-story drift ratios (MIDR in %) associated with the defined limit states are tabulated in Table 4.1. Capacity curves and inter-story drift ratio distributions of the stories at limit states are presented in Figure 4.1 for all reference structures. In these figures, base shear coefficient is considered as the ratio of maximum base shear force to the total weight of the structure ($V_{base_{max}}/W_{total}$).

Table 4.1: MIDR values associated with the limit states

Structure	Maximum Inter-story Drift Ratio (%)		
	Immediate Occupancy	Life Safety	Collapse Prevention
F2S2B	1.5	2.7	3.9
F5S4B	0.9	2.2	3.5
F8S3B	0.6	1.6	2.7

Two types of analyses are performed to quantify the uncertainties in the fragility function calculation procedure. In the single random variable analyses, a single parameter is selected to be a random variable while the values of the other input parameters are fixed to the reference model parameters. While this method provides insight into the sensitivity of each parameter in the structural response variation, to represent variability caused by the entire input space, LHS technique is used in multi random variable analyses. LHS can be considered as a constrained Monte Carlo simulation technique, in which a smaller sample size can be sufficient by dividing the statistical distribution into intervals of equal probability. It is assumed that the results of the multi random variable analyses completely represent the engineering demand parameter space of the input parameters. The demand parameter space is then evaluated with respect to the reference model results. To estimate and compare the impact of model input un-

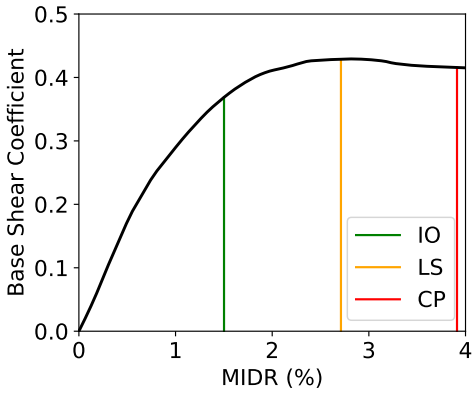

(a) F2S2B Capacity Curve

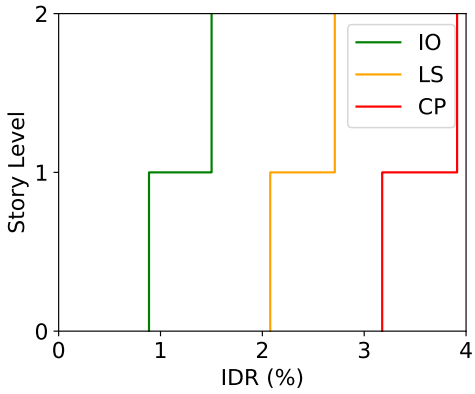

(b) F2S2B IDR with respect to height

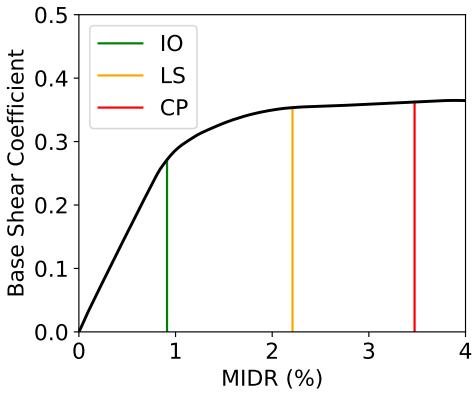

(c) F5S4B Capacity Curve

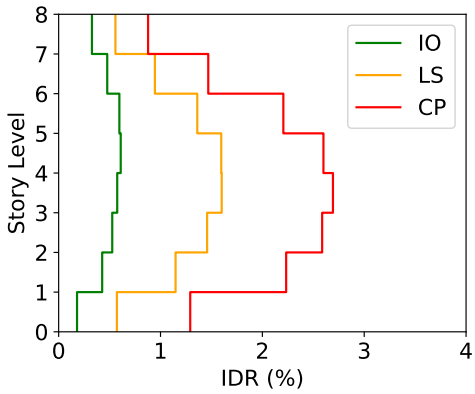

(d) F5S4B IDR with respect to height

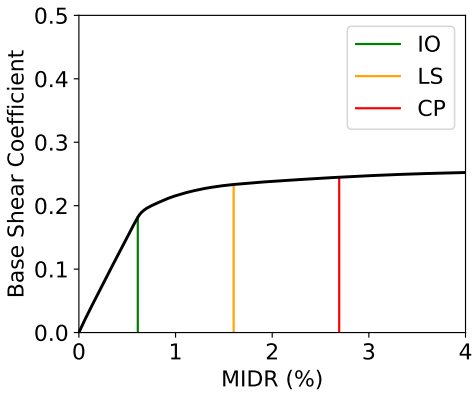

(e) F8S3B Capacity Curve

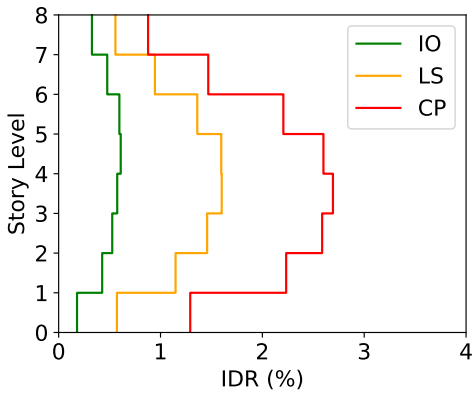

(f) F8S3B IDR with respect to height

Figure 4.1: Capacity Curves and Inter-story Drift Ratios at Limit States

certainties clearly, uncertainty scenarios are defined. The random variables listed in Table 3.2 are grouped into categories with respect to their type. In Table 4.2, different uncertainty scenarios are listed with the absence and presence of the considered random variables. For each scenario, an abbreviation has been used as shown in the first column of Table 4.2. Only the ground motion uncertainty is considered in the NLTHAs and consequently in the fragility parameter estimation in the first scenario, RTR. In MAT and $GEOM$ scenarios, uncertainties related with the material models ($f_c^{'}$,f_y, and w) and uncertainties related with the section geometries (b, h, and t) are considered respectively. Bradley [5] describes low-level modeling uncertainties as the constitutive model parameters and high-level uncertainties as uncertainties in the overall modeling methodology, such as the uncertainty in the constitutive model and structural damping. To investigate high-level modeling uncertainties as suggested by Bradley [5], equivalent viscous damping (ξ) is considered in a separate $DAMP$ scenario. Uncertainty in confinement effect is rarely included in the literature as a modeling uncertainty, thus in $CONF$ scenario, effect of the concrete cover thickness (t) and lateral reinforcement spacing (s) parameters are considered. SIG scenario includes input parameter uncertainties that are selected as the significant parameters from the single random variable analyses. Finally, all input parameters considered in this study are considered to be random variables in ALL scenario.

4.2 Single Random Variable Analyses

In single random variable analyses, first, each random variable except the investigated parameter is set to the median value (50^{th} percentile), and the response statistics is obtained accordingly. Then the investigated random variable is set to the extreme values (10^{th} percentile or 90^{th} percentile), and the structural response is calculated for each bound separately. Then, the variability in response statistics is illustrated by using tornado diagrams. In the tornado diagrams, maximum inter-story drift ratio is selected as the EDP. For each structure MIDR is calculated for 20 ground motion records, then the average of them is compared with the average MIDR obtained for the reference structures. Tornado diagrams of the single random variable analyses are presented in Figures 4.2, 4.3, and 4.4 for F2S2B, F5S4B, and F8S3B, respec-

tively. In these figures, different colors represent distinct site conditions. In tornado diagrams, swing term is the measure of the absolute difference between the extreme cases [3]. When ranking parameter sensitivities based on their impact on the structural response, higher swing values indicate more significance. Parameters with the largest swing values are included in the significant parameters scenario, SIG. Since sensitivity of the parameters are calculated with the consideration of the probability distributions listed in Table 3.2, although the parameters that are not included in the SIG scenario have considerable impact on the dynamic behavior of the structures, impact of their uncertainty on the structural response statistics is much lower compared to other parameters.

In Figures 4.2, 4.3, and 4.4, it is observed that damping has the largest variation of EDP across all hazard levels, site conditions and structure heights, which is consistent with the findings of Çelik and Elingwood [8]. On the other hand, variation in lateral reinforcement spacing and column width input parameters resulted in negligible variation in the EDP. In the case of steel yield strength, variation of the input parameter only starts to influence the variation of EDP at higher hazard levels due to increased nonlinear response of the structures. On the contrary, as the hazard level increases, impact of the variation in the concrete strength, concrete weight, beam depth and clear cover thickness in terms of EDP decreases or does not change at all. Finally, the effect of input parameter variation on the variation of EDP seems to be dependent on the site conditions. For instance, for F2S2B building where the hazard has the probability of exceedence of 50% in 50 years, variation of concrete weight resulted in only smaller MIDR with generic rock site and only higher MIDR with NEHRP class C site compared to the reference MIDR, in Figure 4.2. Moreover, in Figure 4.3 (f), swing due to yield strength of the steel is negligible for NEHRP class C site compared to other site conditions. Although impact of the different site conditions is not uniform, since these site conditions can have a significant impact on the variation of EDP, in fragility function parameter estimations, site effects should not be ignored.

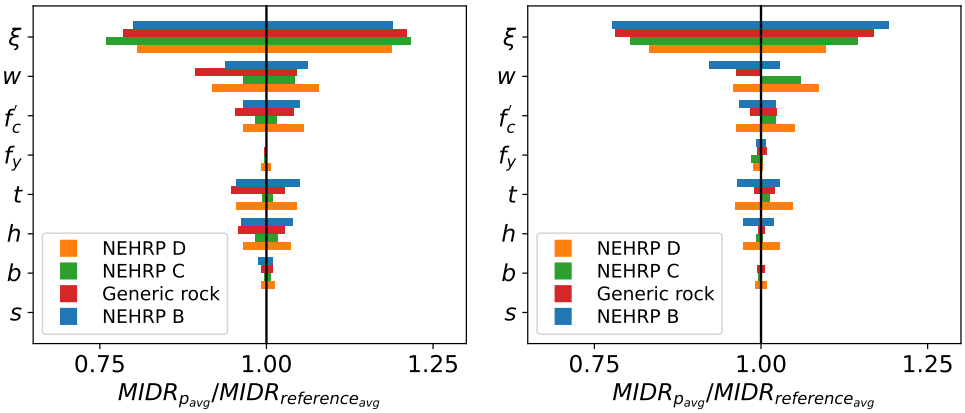

(a) 68% poe in 50 years

(b) 50% poe in 50 years

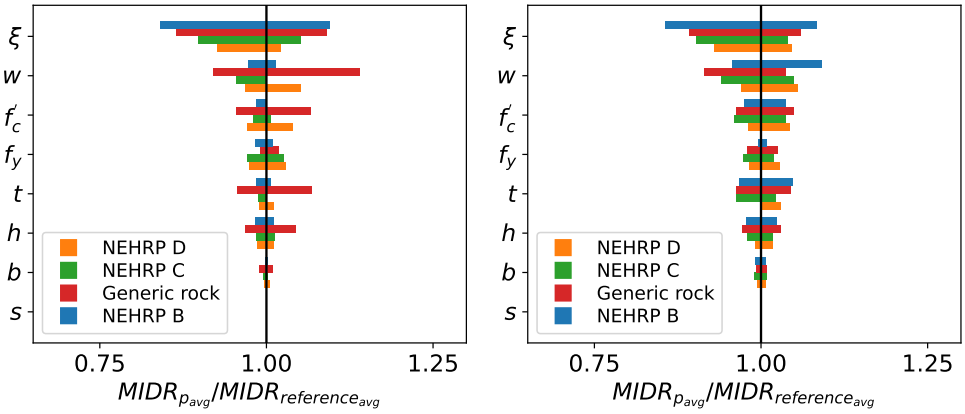

(c) 10% poe in 50 years

(d) 5% poe in 50 years

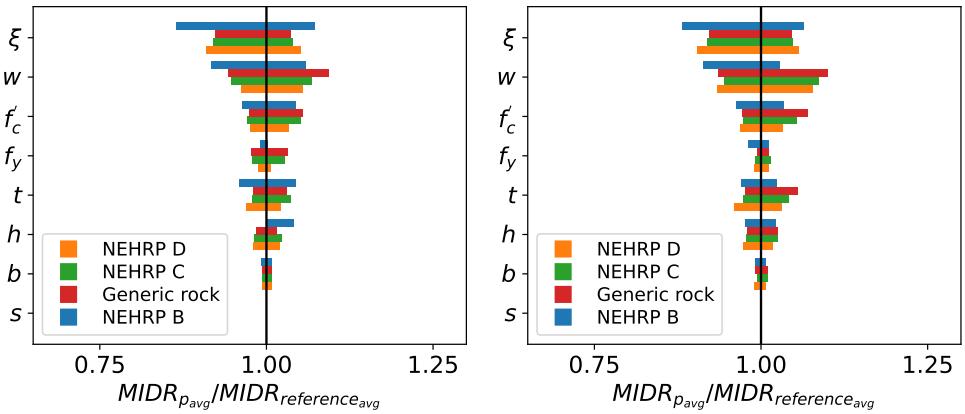

(e) 2% poe in 50 years

(f) 1% poe in 50 years

Figure 4.2: Tornado Diagrams for F2S2B Building

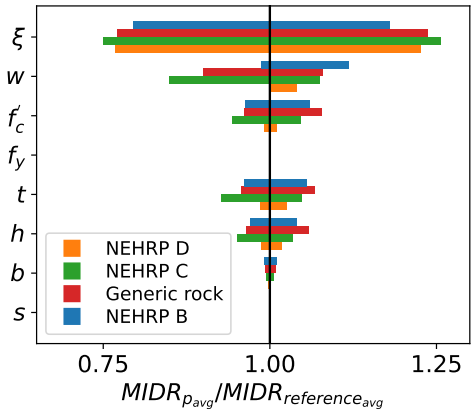

(a) 68% poe in 50 years

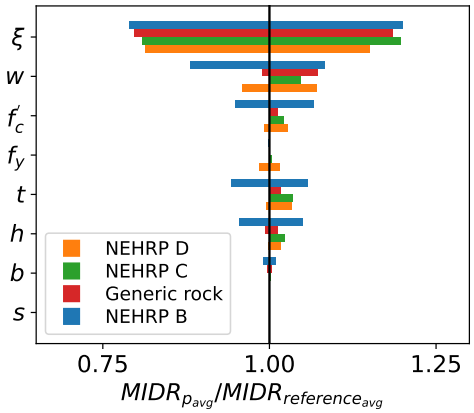

(b) 50% poe in 50 years

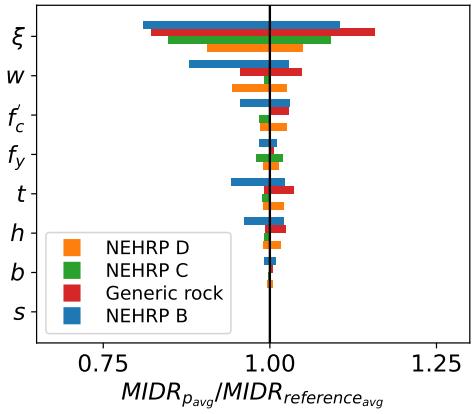

(c) 10% poe in 50 years

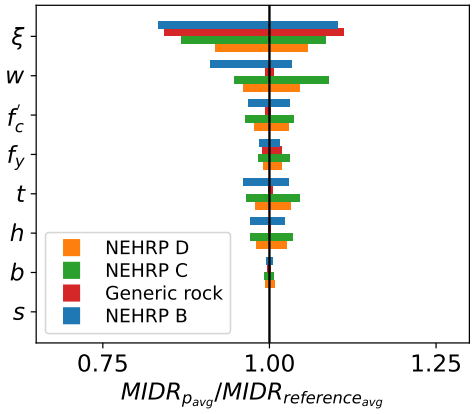

(d) 5% poe in 50 years

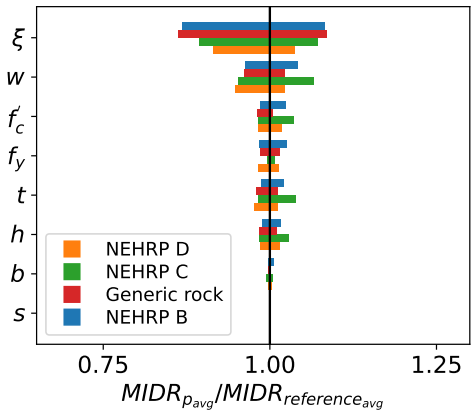

(e) 2% poe in 50 years

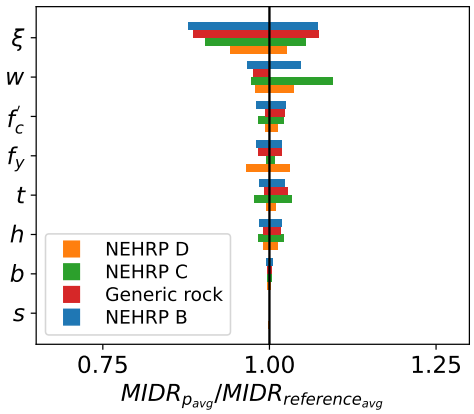

(f) 1% poe in 50 years

Figure 4.3: Tornado Diagrams for F5S4B Building

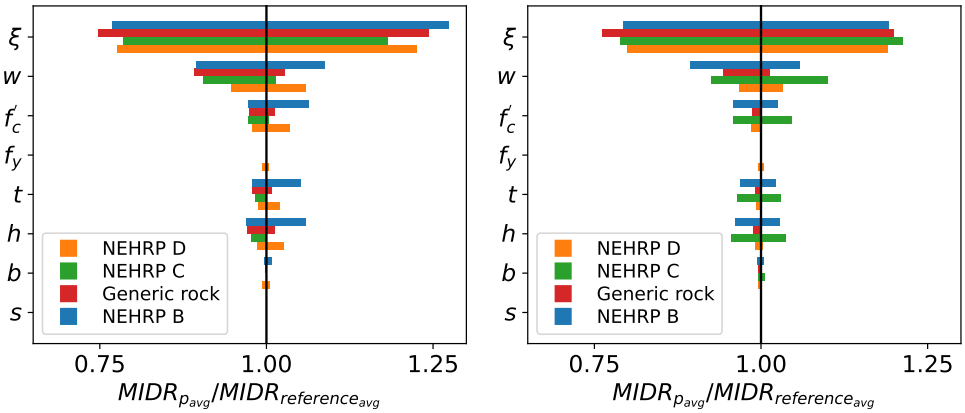

(a) 68% poe in 50 years

(b) 50% poe in 50 years

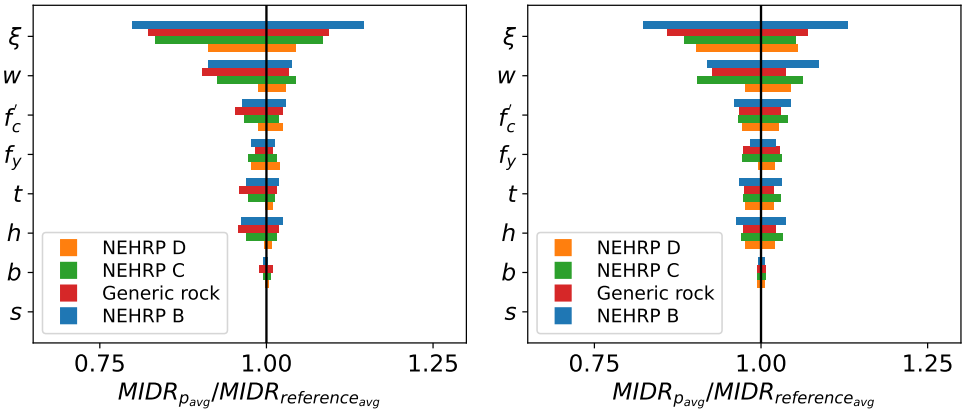

(c) 10% poe in 50 years

(d) 5% poe in 50 years

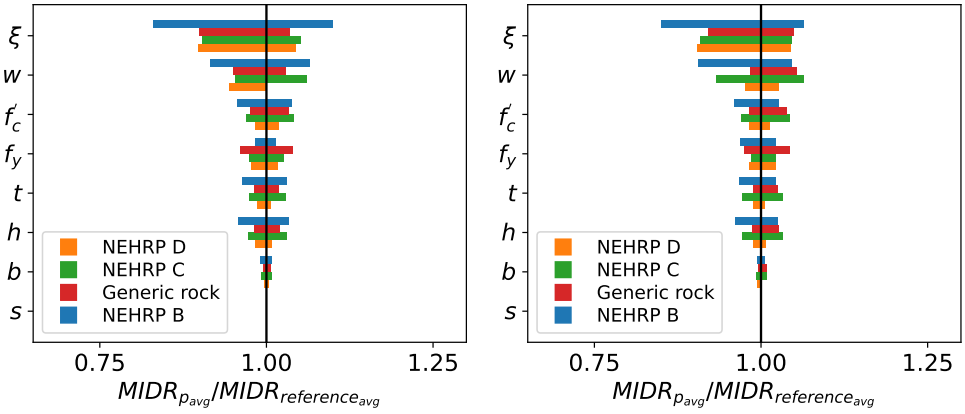

(e) 2% poe in 50 years

(f) 1% poe in 50 years

Figure 4.4: Tornado Diagrams for F8S3B Building

Table 4.2: Uncertainties Included in Uncertainty Scenarios

Scenario	Uncertainty Source								
	GM	b	h	$f_c^{'}$	f_y	w	ξ	t	s
RTR	•								
MAT	•			•	•	•			
$GEOM$	•	•	•					•	
$DAMP$	•						•		
$CONF$	•							•	•
SIG	•		•	•	•	•	•	•	
ALL	•	•	•	•	•	•	•	•	•

4.3 Multi Random Variable Analyses

In multi random variable analyses LHS technique is used to generate representative input parameters of the entire input space. Then, uncertainty quantification in fragility calculations is performed herein by comparing the fragility curves obtained. However, the influence of model input parameters is investigated through seven different uncertainty scenarios, where only the selected number of input parameters are considered as random variables.

In this section, analysis results are presented as fragility curves in Figures 4.6, 4.7, and 4.8 and the change in fragility function parameters are compared in Figures 4.9, 4.10, and 4.11.

4.3.1 Maximum likelihood method

In many studies (e.g. [85, 86]) the assumption that fragility functions are log-normally distributed has been confirmed. The log-normal cumulative distribution function that describes the fragility function is depicted in Equation 4.1.

$$P(Limitstate|IM = x) = \Phi\left(\frac{ln(x/\theta)}{\beta}\right) \tag{4.1}$$

In this equation, $P(Limitstate|IM = x)$ is the conditional probability of exceeding the limit state in terms of the engineering demand parameter due to a ground motion with intensity measure equal to x. $\Phi()$ is a standard normal cumulative distribution function (cdf). Parameter θ defines the median of the fragility function, where the probability of EDP exceeding limit state is 50%. Parameter β stands for the standard deviation of $ln(IM)$. Here, θ and β are also referred to as the fragility function parameters and their estimations are denoted as $\hat{\theta}$ and $\hat{\beta}$.

Error minimization techniques between observations and the fitted function are commonly used for fragility function parameter estimation. In the case of the sum of squared errors (SSE) minimization, errors between the observed fractions of limit state occurrences and probabilities of these occurrences predicted by the fragility function are used in the minimization equation, as given in Equation 4.2:

$$(\hat{\theta}, \hat{\beta}) = \min_{\theta,\beta} \sum_{j=1}^{m} \left[\frac{z_j}{n_j} - \Phi\left(\frac{ln(x_j/\theta)}{\beta} \right) \right]^2 \tag{4.2}$$

Maximum likelihood method (MLM) [86] is an alternative fragility function parameter estimation method based on binomial distribution. The binomial distribution is used to estimate the probability of z number of successes in n independent experiments. For the fragility parameter calculations, Baker [86], assumes that EDP observed from a ground motion record with $IM = x_j$ is independent from observations due to other ground motions with $IM = x_j$. Thus, the binomial distribution function of z_j out of n_j ground motions with $IM = x_j$ exceeding the limit state EDP is represented as in Equation 4.3. This assumption allows the method to be utilized even when there is only a single observation for an $IM = x_j$.

$$P(z_j \text{ in } n_j \text{ ground motions exceed the EDP}_{lim}) = \binom{n_j}{z_j} p_j^{z_j} (1 - p_j)^{n_j - z_j} \tag{4.3}$$

In Equation 4.3, $\binom{n_j}{z_j}$ is the binomial coefficient, p_j corresponds to the probability of a ground motion with $IM = x_j$ causing the limit state EDP (EDP$_{lim}$) to the structure, thus the EDP$_{lim}$ is exceeded z_j times with the probability of $p_j^{z_j}$, and the EDP$_{lim}$ is not exceeded $(n_j - z_j)$ times with the probability of $(1 - p_j)^{n_j - z_j}$.

In fragility function parameter estimations, commonly ground motions with multiple IM levels are considered. The likelihood function for m different IM levels is defined as the product of binomial distributions at each IM level as given in Equation 4.4:

$$\text{Likelihood} = \prod_{j=1}^{m} \binom{n_j}{z_j} p_j^{z_j} (1-p_j)^{n_j - z_j} \tag{4.4}$$

Moreover, p_j could be estimated with the fragility function parameters with the substitution of Equation 4.1 for p_j as presented in Equation 4.5:

$$\text{Likelihood} = \prod_{j=1}^{m} \binom{n_j}{z_j} \Phi\left(\frac{ln(x_j/\theta)}{\beta}\right)^{z_j} \left[1 - \Phi\left(\frac{ln(x_j/\theta)}{\beta}\right)\right]^{n_j - z_j} \tag{4.5}$$

Maximizing Equation 4.5 for known z_j and n_j with the estimates of fragility function parameters $(\hat{\theta}, \hat{\beta})$, results in the fragility function that has the best representation of the observed data. However, maximizing the logarithm of Equation 4.5 since in Equation 4.6 is preferred as it is both numerically simpler and equivalent in effectiveness [86]:

$$(\hat{\theta}, \hat{\beta}) = \max_{\theta,\beta} \sum_{j=1}^{m} ln\binom{n_j}{z_j} + z_j \Phi\left(\frac{ln(x_j/\theta)}{\beta}\right) + (n_j - z_j) ln\left[1 - \Phi\left(\frac{ln(x_j/\theta)}{\beta}\right)\right] \tag{4.6}$$

In this study, since the ground motions are scaled within a specific period range, each ground motion record used in the NLTHA have unique IMs. Consequently, each EDP observation has a unique IM parameter associated with it. Thus, in this study, fragility curve parameters are estimated with the maximum likelihood method. Illustration of the estimation of fragility functions from EDR calculated from RTR scenario is depicted in Figure 4.5.

Fragility functions for all scenarios and limit states are presented in Figures 4.6, 4.7, and 4.8 for structures F2S2B, F5S4B, and F8S3B respectively.

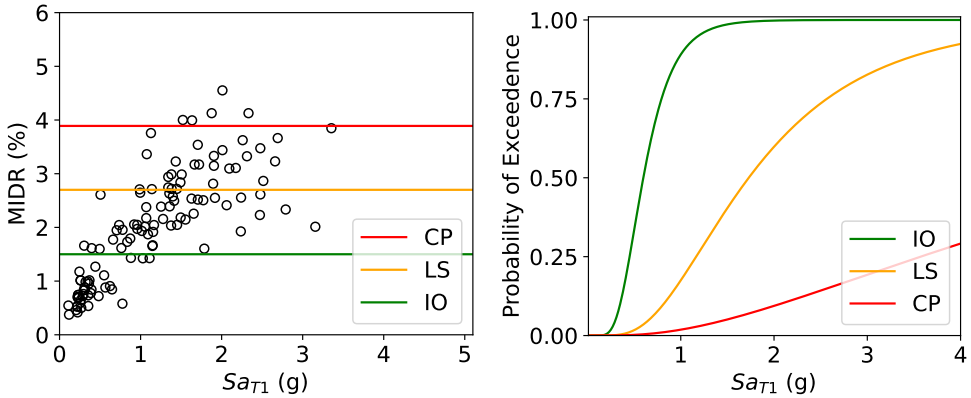

(a)

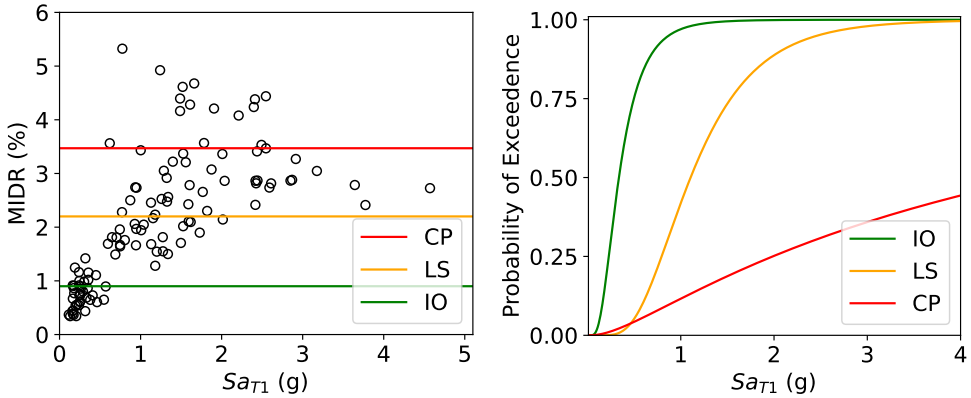

(b)

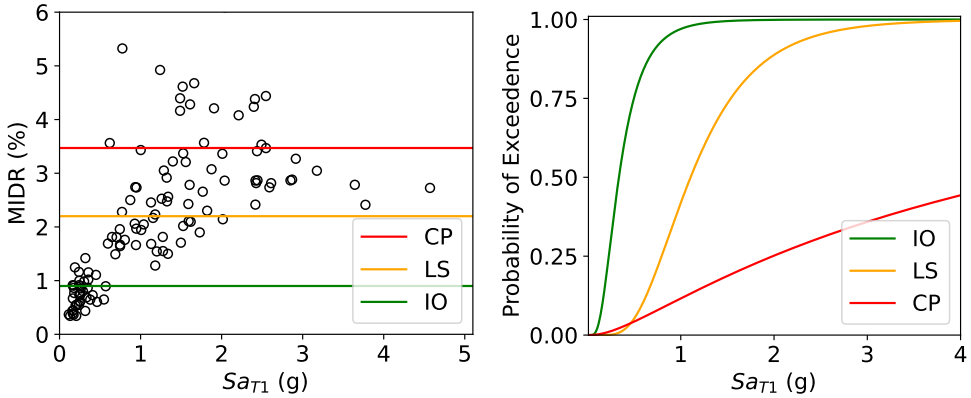

(c)

Figure 4.5: Fragility curve calculation from MIDR results obtained from RTR scenario for NEHRP D site (a) F2S2B , (b) F5S4B (c) F8S3B

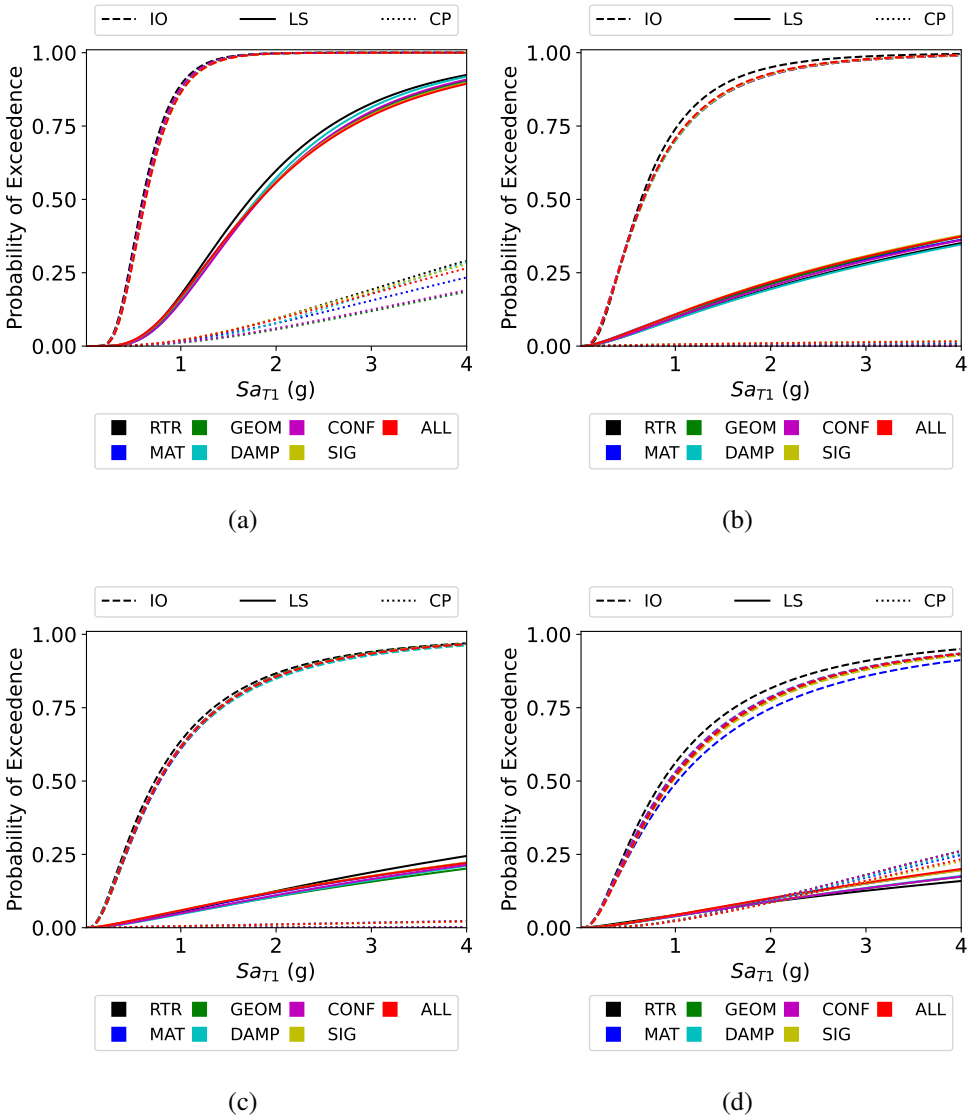

Figure 4.6: Fragility curves of F2S2B for IO, LS, and CP limit states for uncertainty scenarios for (a) NEHRP D, (b) NEHRP C, (c) generic rock, and (d) NEHRP B site conditions

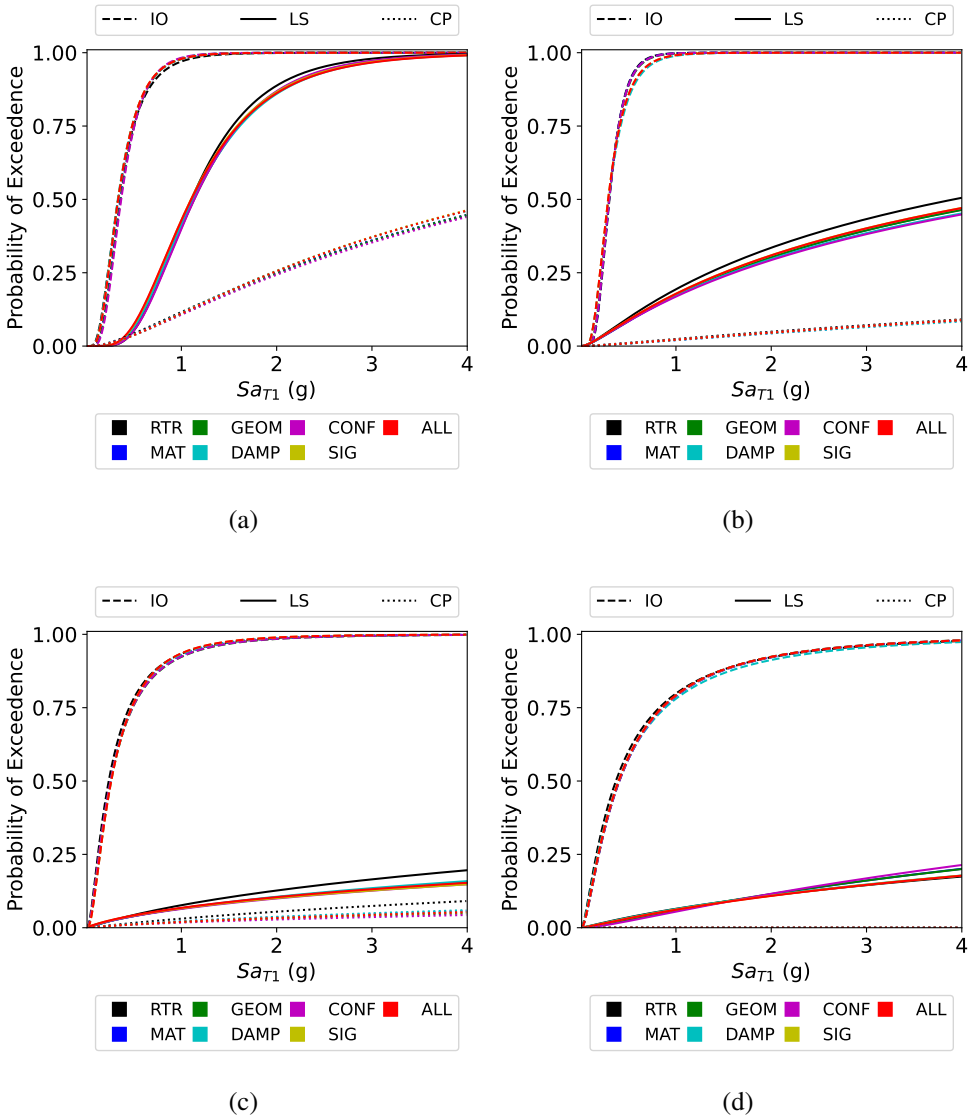

Figure 4.7: Fragility curves of F5S4B for IO, LS, and CP limit states for uncertainty scenarios for (a) NEHRP D, (b) NEHRP C, (c) generic rock, and (d) NEHRP B site conditions

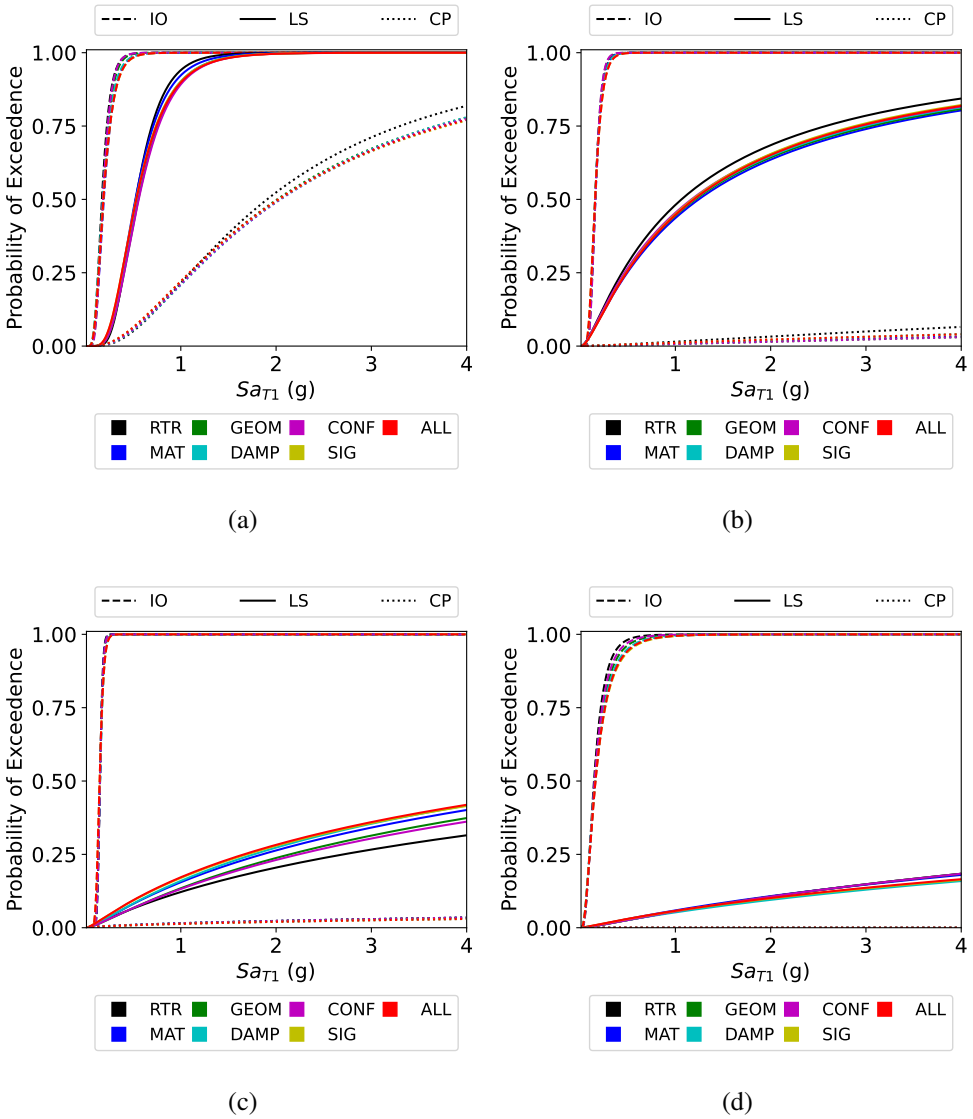

Figure 4.8: Fragility curves of F8S3B for IO, LS, and CP limit states for uncertainty scenarios for (a) NEHRP D, (b) NEHRP C, (c) generic rock, and (d) NEHRP B site conditions

From Figures 4.6, 4.7, and 4.8 it is first observed that the structural models are more vulnerable under softer soil conditions regardless of the number of stories as expected. There are abrupt changes especially in the LS and CP limit states. This reveals that even a high-code structure can exhibit different levels of damage if the soil conditions are not favorable. Second, the probability of exceeding the CP limit state seems to be low even for high hazard levels for all investigated structures and for all site conditions. This may be attributed to the fact that the reference structures are code compliant structures with both high ductility and strength. According to the conventional earthquake design philosophy, these structures are expected to sustain certain levels of damage, but they are not expected to collapse even under severe seismic action. Third, scenario based differences in fragility curves does not seem to be very significant. For IO limit state, a significant variation is not eventually expected since the structural responses at the onset of linear elastic behavior should not differ so much. There is only a significant difference for the 2-story building under hard soil conditions, which may be caused by the interaction of the short period of the structural model with the spectral shape of the ground motion records. For LS limit state, differences up to 10% can be observed in some cases. For CP limit state, the high variabilities observed for moderate and low code building models do not exist for the high-code building models in this study. For some cases, the probability of collapse is so low that it cannot be seen on the plot. Since the fragility function parameters estimated for continuous fragility curves, the fragility curves obtained for cases with very low probability of collapse numerically produced collapse prevention curves above life safety fragility curves as can be observed in Figure 4.6 for NEHRP class B site. For such cases collapse prevention fragility curve parameters are not included in the evaluations.

The impact of uncertainty scenarios is investigated by comparing fragility function parameters median capacity (θ_i) and dispersion (β_i) estimated for uncertainty scenario i with the fragility function parameters of the RTR scenario (θ_{RTR}, β_{RTR}), where only the ground motion uncertainty is considered. Comparisons are made for the ratios of these parameters, i.e. (θ_i/θ_{RTR} and β_i/β_{RTR}). While these comparisons allow evaluation of the impact of modeling uncertainty in fragility calculations, evaluation of each individual fragility curve is out of the scope of this study. Change in

the fragility function parameters with respect to each other are presented in Figures 4.9, 4.10, and 4.11 for limit states IO, LS, and CP respectively. In Figures 4.9, 4.10, and 4.11 different colors represent particular uncertainty scenarios, while different symbols are used to represent distinct structures.

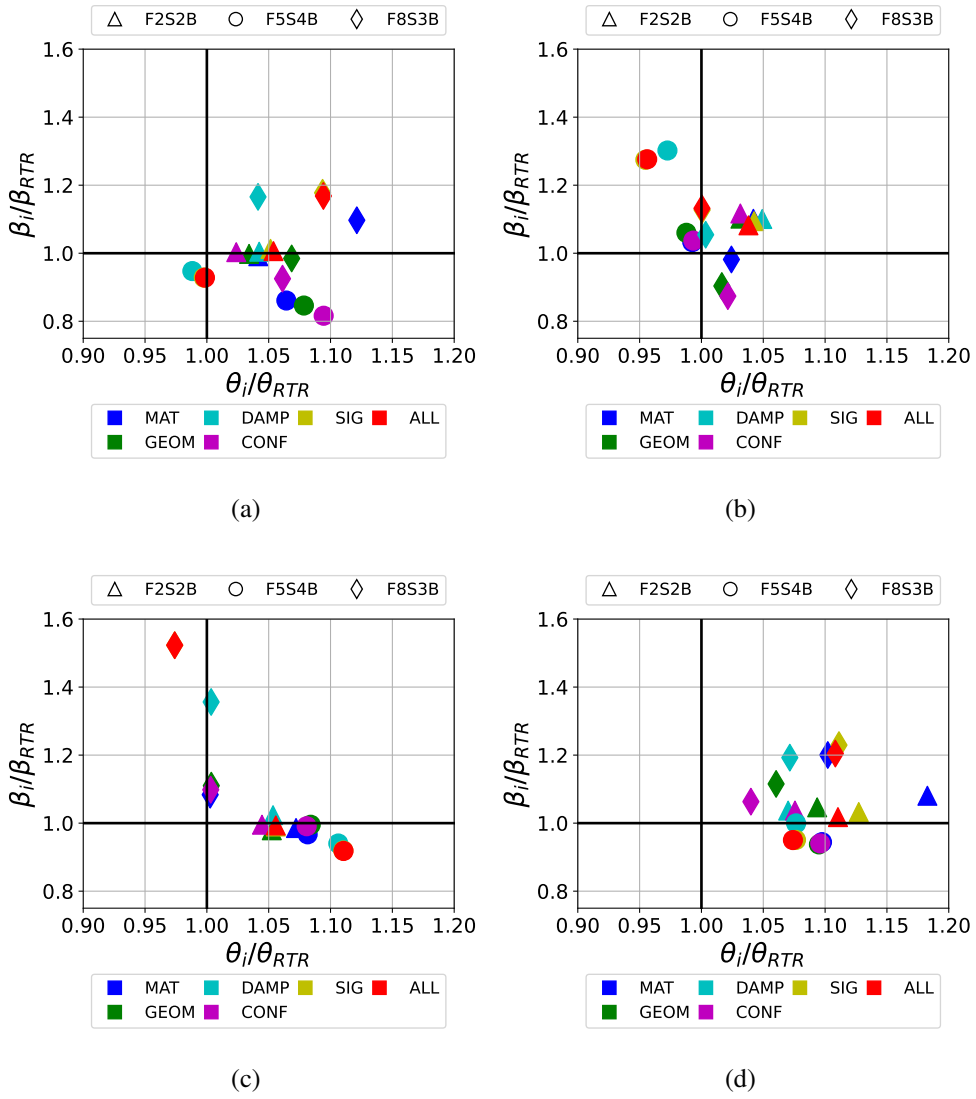

Figure 4.9: Change in fragility function parameters (θ, β) for Immediate Occupancy limit state for uncertainty scenarios with respect to RTR scenario for (a) NEHRP D, (b) NEHRP C, (c) generic rock, and (d) NEHRP B site conditions

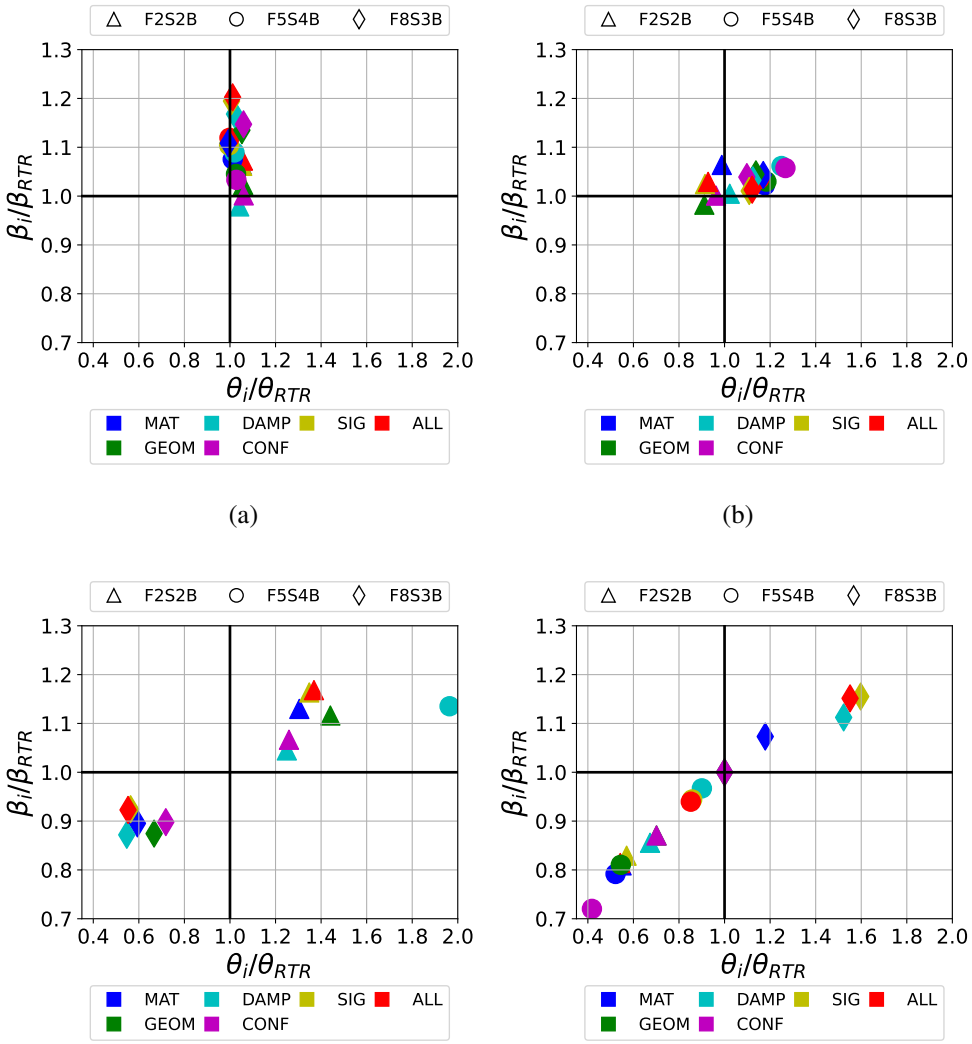

Figure 4.10: Change in fragility function parameters (θ, β) for Life Safety limit state for uncertainty scenarios with respect to RTR scenario for (a) NEHRP D, (b) NEHRP C, (c) generic rock, and (d) NEHRP B site conditions

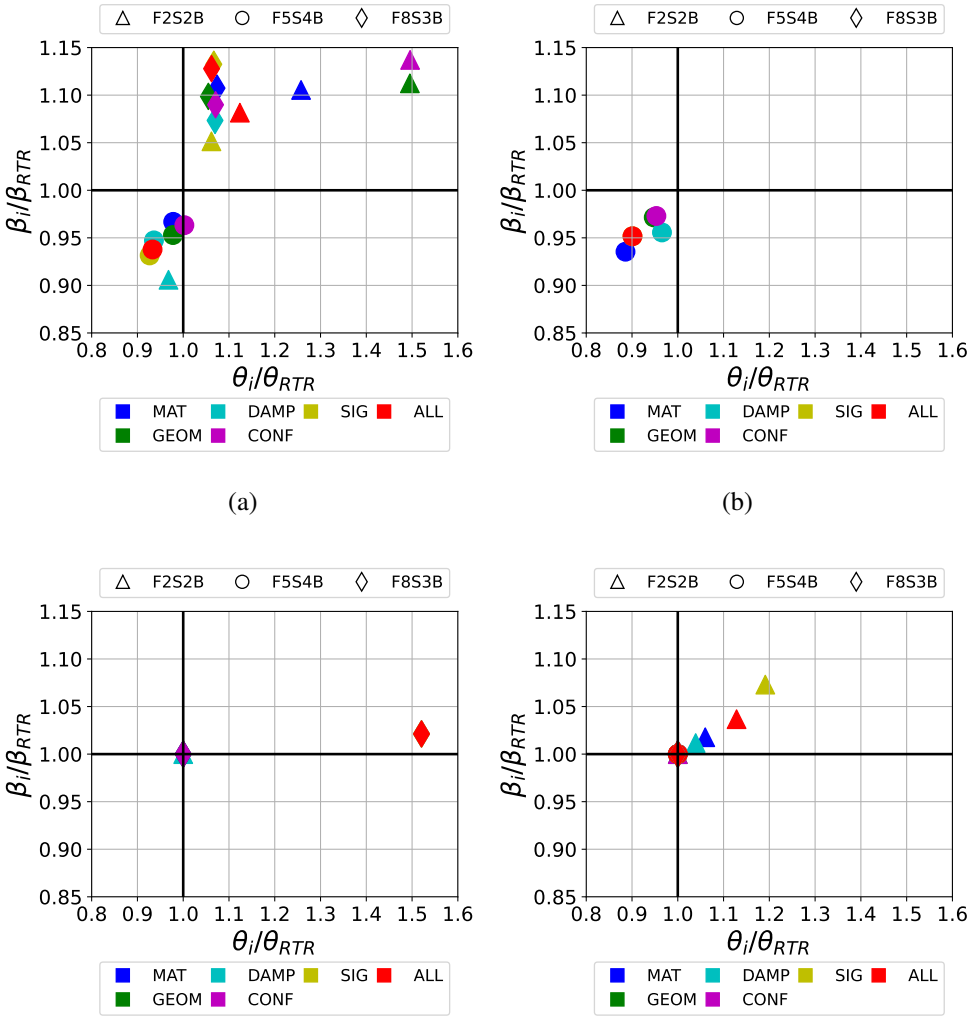

Figure 4.11: Change in fragility function parameters (θ, β) for Collapse Prevention limit state for uncertainty scenarios with respect to RTR scenario for (a) NEHRP D, (b) NEHRP C, (c) generic rock, and (d) NEHRP B site conditions

In Figures 4.9, 4.10, and 4.11, $\theta_i/\theta_{RTR} = 1$ and $\beta_i/\beta_{RTR} = 1$ lines represent the thresholds for reduction of median capacity and increased dispersion respectively. Median capacity reductions are observed for all limit states, especially, the uncertainty scenarios that include material and damping uncertainties are observed to influence the fragility function parameters the most. The change in the fragility function parameter θ shifts the fragility curve and the parameter β controls the shape of the fragility curve, larger β values flattens the fragility curve whereas $\beta = 0$ indicates a vertical line. Therefore, by comparing only a single fragility curve parameter impact of the uncertainty in the modeling parameters may not be evaluated accurately. However, the combination of low θ_i/θ_{RTR} and high β_i/β_{RTR} may result in unconservative shifts in the damage states and may be important for the decision making for loss calculations.

For CP limit state, only NEHRP class D site is considered, as the median collapse capacity is very high for all other site conditions. In the case of CP limit state at NEHRP class D site, up to 8% median capacity reductions and a reduction of the dispersion parameter by 10% is observed for the cases where capacity reductions are observed. These values are lower compared to the maximum median collapse capacity reduction of 20% and the maximum increase of the dispersion parameter for collapse limit state of 70% reported in [18]. However, these findings are consistent with the findings of Kwon and Elnashai [4] and Gökkaya et al. [18] that irregularities of the buildings may result in a cliff edge effect where variation of the model parameters change the failure mechanism. For the case of code-compliant ductile buildings without irregularities, the impact of the variation of the model parameters to the fragility function parameter variation is not affected by the variation of the failure mode. On the other hand, for the case of non-ductile buildings or ductile buildings with irregularities, failure mode with the lowest capacity is observed based on the input parameter variation. These abrupt shifts in the failure modes could increase the model input parameters' impact on the fragility function parameters. Therefore, in this study input parameter variance effects on the fragility parameters are investigated through code-compliant buildings with a single governing failure mode. Moreover, the reduction of the capacity and the increase of the dispersion effects of variation of the input parameters are not negligible even for code-compliant buildings.

For the IO and LS limit states, up to 5% and 60% capacity reductions are observed respectively. For the cases where capacity reductions are observed, increases in the dispersion are observed up to 55% and 12% for IO and LS limit states respectively. Lower median capacity reductions are observed for F2S2B structures except for the stiff soil conditions at LS limit state. Furthermore, for all uncertainty scenarios, F8S3B median capacity is less than θ_{RTR} for LS limit state and generic rock site conditions. Median capacity reductions at lower limit states underline the significance of incorporation of model input parameter uncertainties into fragility function calculations. Damage states related with these limit states have immense social and economic consequences in the case of a catastrophic event as in the cases of the February 6, 2023 earthquakes in Pazarcık (Mw = 7.7) and Elbistan (Mw = 7.6).

CHAPTER 5

CONCLUSIONS

5.1 Summary

In this study, the fragility function parameters of three code-compliant ductile reinforced concrete frames are investigated for the propagation of the modeling uncertainties. Various modeling parameters are used as random variables and their impact on structural capacity uncertainties is examined. Hazard assessments are conducted at four arbitrary sites with high seismicity, considering different soil conditions and hazard levels. Ground motion records are selected and scaled for nonlinear time history analyses. Sensitivities of individual random variables are evaluated followed by identification of the significant ones using tornado diagrams. The Latin hypercube sampling technique is used to represent the probabilistic distribution of the random variables in the nonlinear dynamic structural analyses. Fragility function parameters, median capacity and dispersion, are estimated for different uncertainty scenarios and compared with the scenario in which modeling uncertainties are not considered. The importance of accounting for structural variability in fragility calculations is emphasized and expressed quantitatively.

Hazard calculations in this thesis are performed with site-specific probabilistic seismic hazard analysis. Düzce region, an alluvial basin located within the proximity of the North Anatolian Fault Zone, is selected as the study region. Four arbitrary soil conditions are considered in the PSHA with the Vs30 values 270 m/s, 560 m/s, 760 m/s, and 1130 m/s. Ground motion intensity parameters are estimated for six hazard levels (68%, 50%, 10%, 5%, 2%, and 1% exceedance probability in 50 years). As a result of the PSHA, uniform hazard spectra for all site conditions and hazard levels

are produced. Ground motion records consistent with the seismotectonic conditions, source-to-site distances, and Vs30 values, are selected based on their similarity with the UHS within a specific period range. Selected ground motion records are then scaled to provide hazard-compatible time histories for nonlinear time history analysis of the structures.

Buildings analyzed in this study are deliberately chosen as code-compliant ductile reinforced concrete frames. Analytical modeling of the structures is performed on OpenSees as 2D bare frame structures. The beams are modeled with distributed plasticity and the columns are modeled with plastic hinges and elastic mid-sections. Plastic regions are defined with fiber sections, where distinct modeling of confined concrete, concrete cover and reinforcing steel is incorporated. Concrete material properties are defined with zero-tensile strength by using Concrete01, whereas the bi-linear Steel01 is used as the constitutive model for reinforcing steel in OpenSees. Eight modeling input parameters regarding material properties, section geometry, damping, and confinement of concrete are selected as random variables with probability distributions obtained from previous studies. Their variability is projected onto structure realizations with Latin hypercube sampling.

In this thesis, first, the sensitivity of each random variable is investigated through tornado diagrams. Then, through the uncertainty scenarios, the effects of the entire input space on the fragility calculations are examined. Fragility function parameters are calculated for these scenarios. Finally, median capacity and dispersion estimated for scenarios including modeling uncertainties are compared with the fragility curve parameters of the scenario containing only the ground motion record-to-record uncertainty.

This study contributes to the field of probabilistic structure response assessment by considering a wide range of structural input variables and employing a novel approach to quantify their impact on fragility with the use of uncertainty scenarios. Recognizing the impacts of the uncertainties in modeling parameters and integrating them into seismic performance assessment of structures, especially in light of recent earthquakes causing significant damage and casualties, will result in safer and more resilient environments.

5.2 Conclusions

Based on the selected sites, building models, structural parameters, and uncertainty quantification analyses performed herein, the following main conclusions could be drawn:

- Performance of the structures, even when they are designed according to seismic codes, regardless of the story height, is influenced significantly by the different soil conditions. For instance, for life safety limit state with NEHRP class D site, no median capacity reduction is observed, yet up to 10%, 50%, and 60% median capacity reductions are found in NEHRP class C, generic rock, and NEHRP class B site conditions respectively. Similarly, for life safety limit state, up to 12% and 6% increase in dispersion is observed for NEHRP class D site and NEHRP class C site respectively, yet for generic rock, and NEHRP class B site dispersion increase is not observed. Therefore, accurate representation of the local site parameters in the hazard analyses is crucial.

- Among different uncertainty scenarios, the ones that include constitutive model parameters and damping uncertainties are observed to influence the fragility function parameters the most. While the uncertainty of material properties is addressed to a degree in the current design codes, uncertainty due to damping is often overlooked. In the probabilistic seismic performance assessment procedures, damping should be incorporated for accurate estimation of the engineering demand parameters.

- Regarding the immediate occupancy limit state, a significant variation is not observed except for the 2-story building under stiff soil conditions, where an interaction of the short period of the structural model with the spectral shape of the ground motion records is expected. In this limit state, a maximum median capacity reduction of 5% and a maximum 55% increase in dispersion are observed.

- For the life safety limit state, the impact of variability in the model parameters to the fragility curve parameters is found to be more significant than other limit states. This may be a more critical issue knowing that life safety limit state

is more difficult to define physically when compared to other limit states. As high as 60% reduction of the median capacity is observed compared to the case including only the ground motion record-to-record uncertainty. Furthermore, with the consideration of the uncertainties in modeling input parameters, the dispersion of the fragility curve is increased up to 12%. Shifts of such amplitudes highlight the significance of the variability of modeling parameters in fragility calculations.

- In the collapse prevention limit state, fragility curves are flat in some cases due to the probability of collapse being very low. However, for NEHRP class D site conditions, -8% shift in the median collapse capacity is observed without any increase in the dispersion. Higher variabilities can be expected for non-ductile or irregular buildings that could switch the failure mode suddenly based on the minimum capacity of the different failure mechanisms.

- For well-designed RC frames, the combined effect of reduction in the median capacity and dispersion increase due to uncertainty in the modeling parameters may ultimately result in an unconservative shift of the damage states in the loss calculations. Even slight shifts in the damage states could cause immense social and economic consequences for the local communities as in the case of the 2023 Kahramanmaraş earthquake sequence. This is especially valid for the life safety limit state. In other words, variations in structural parameters have a considerable probability of causing shifts from moderate to severe damage. On the other hand, based on the analyses of the considered building models, since the probability of collapse is low for well-designed buildings, the corresponding variability is also low. This result indicates that the collapse of new buildings during the 2023 earthquakes may not have originated from small variations in material or structural parameters that have been used during the design but due to some major deficiencies during the construction and service-life of the building.

5.3 Recommendations for Future Work

This work has some inherent limitations due to its scope and assumptions in its methodology. Following points can be investigated further in future works:

- One limitation of basic scaling is that the significant duration of an earthquake may not be represented accurately. Thus in future work, physics-based broadband ground motion simulations can be utilized for analyzing the seismic hazard and obtaining ground motion time histories.
- Through physics based ground motion simulations it is possible to model complex fault raptures such as multi-segment fault raptures and large magnitude earthquake sequences. In the future studies to investigate the impact of the modeling uncertianties for the collapse fragilities, incorporating these rare events in the hazard calculations might lead to more accurate estimates.
- In this study, the local site conditions are employed in terms of Vs30 value in the GMMs within the hazard analyses. Effects of nonlinear soil conditions on fragility functions could be explored with more rigorous modeling of the soil layers in future studies.
- Similar to structural damping, uncertainty in the soil damping could also be a significant parameter to be considered in the future studies. Moreover, the energy dissipation due to soil material damping and the dissipation due to soil radiation damping could be investigated and compared.
- In this study, the spatial variation of the hazard is not considered. However, investigating the variation in the distance parameter combined with the variation in the soil conditions in the future studies may provide insight into the abrupt structural behavior differences between similarly designed structures.
- In this study, 2D frame models are utilized to idealize the reference structures. In future work structural idealization can be considered as an uncertainty source by using 3D models or different idealization techniques, thus the impact of structural idealization can be expanded upon. This modeling approach can also provide a chance to discuss the effect of plan irregularity on seismic fragility.

- This study deals with well-designed RC frame structures for novelty since there are many past studies on the seismic risk assessment of deficient RC structures. Yet, such structures can also be considered as a continuation of this study to compare the propagation of uncertainty and its effects on structural fragility with the outcomes of this study.

- Investigation of the impact of modeling uncertainties on the fragility curves for various structural system types, including RC frames with shear walls, base isolation, flat slab systems and structures made from other construction materials such as masonry, wood, and steel is suggested for future studies.

- One of the limitations of this study is considering deterministic limit states. In the future studies, uncertainty in the limit state or limit state estimation methodology could be considered together with the propagation of the modeling uncertainties in the fragility calculations.

- Exploring the uncertainty propagation of modeling input parameters in direct seismic loss calculations is the ultimate goal. To achieve this task, a larger domain of structural model parameters should be considered in order to cover all building typologies that exist in the current building stock.

REFERENCES

[1] Ensonhaber, "13 bloklu sitede yıkılan tek binanın kolonlarının kesildiği öne sürüldü." `https://www.ensonhaber.com/`, 2023. Accessed on 2024-02-27.

[2] C. A. Cornell, "Engineering seismic risk analysis," *Bulletin of the Seismological Society of America*, vol. 58, no. 5, pp. 1583–1606, 1968.

[3] K. A. Porter, J. L. Beck, and R. V. Shaikhutdinov, "Sensitivity of building loss estimates to major uncertain variables," *Earthquake Spectra*, vol. 18, no. 4, pp. 719–743, 2002.

[4] O. S. Kwon and A. Elnashai, "The effect of material and ground motion uncertainty on the seismic vulnerability curves of rc structure," *Engineering Structures*, vol. 28, no. 2, pp. 289–303, 2006.

[5] B. A. Bradley, "A critical examination of seismic response uncertainty analysis in earthquake engineering," *Earthquake Engineering & Structural Dynamics*, vol. 42, no. 11, pp. 1717–1729, 2013.

[6] A. J. Kappos, M. K. Chryssanthopoulos, and C. Dymiotis, "Uncertainty analysis of strength and ductility of confined reinforced concrete members," *Engineering Structures*, vol. 21, no. 3, pp. 195–208, 1999.

[7] M. Dolšek, "Incremental dynamic analysis with consideration of modeling uncertainties," *Earthquake Engineering & Structural Dynamics*, vol. 38, no. 6, pp. 805–825, 2009.

[8] O. C. Çelik and B. R. Ellingwood, "Seismic fragilities for non-ductile reinforced concrete frames–role of aleatoric and epistemic uncertainties," *Structural Safety*, vol. 32, no. 1, pp. 1–12, 2010.

[9] T. Choudhury and H. B. Kaushik, "Treatment of uncertainties in seismic

fragility assessment of rc frames with masonry infill walls," *Soil Dynamics and Earthquake Engineering*, vol. 126, p. 105771, 2019.

[10] L. Jiang, Z. Hong, and Y. Hu, "Effects of various uncertainties on seismic risk of steel frame equipped with steel panel wall," *Bulletin of Earthquake Engineering*, vol. 16, pp. 5995–6012, 2018.

[11] G. J. O'Reilly and T. J. Sullivan, "Quantification of modelling uncertainty in existing italian rc frames," *Earthquake Engineering & Structural Dynamics*, vol. 47, no. 4, pp. 1054–1074, 2018.

[12] H. Crowley, J. J. Bommer, R. Pinho, and J. Bird, "The impact of epistemic uncertainty on an earthquake loss model," *Earthquake engineering & structural dynamics*, vol. 34, no. 14, pp. 1653–1685, 2005.

[13] H. Aslani, C. Cabrera, and M. Rahnama, "Analysis of the sources of uncertainty for portfolio-level earthquake loss estimation," *Earthquake engineering & structural dynamics*, vol. 41, no. 11, pp. 1549–1568, 2012.

[14] M. Rota, A. Penna, and G. Magenes, "A framework for the seismic assessment of existing masonry buildings accounting for different sources of uncertainty," *Earthquake engineering & structural dynamics*, vol. 43, no. 7, pp. 1045–1066, 2014.

[15] L. Sousa, V. Silva, M. Marques, and H. Crowley, "On the treatment of uncertainty in seismic vulnerability and portfolio risk assessment," *Earthquake Engineering & Structural Dynamics*, vol. 47, no. 1, pp. 87–104, 2018.

[16] M. Dolšek, "Simplified method for seismic risk assessment of buildings with consideration of aleatory and epistemic uncertainty," *Structure and Infrastructure Engineering*, vol. 8, no. 10, pp. 939–953, 2012.

[17] A. B. Liel, C. B. Haselton, G. G. Deierlein, and J. W. Baker, "Incorporating modeling uncertainties in the assessment of seismic collapse risk of buildings," *Structural safety*, vol. 31, no. 2, pp. 197–211, 2009.

[18] B. U. Gökkaya, J. W. Baker, and G. G. Deierlein, "Quantifying the impacts of modeling uncertainties on the seismic drift demands and collapse risk of build-

ings with implications on seismic design checks," *Earthquake Engineering & Structural Dynamics*, vol. 45, no. 10, pp. 1661–1683, 2016.

[19] E. Tubaldi, M. Barbato, and A. Dall'Asta, "Influence of model parameter uncertainty on seismic transverse response and vulnerability of steel–concrete composite bridges with dual load path," *Journal of Structural Engineering*, vol. 138, no. 3, pp. 363–374, 2012.

[20] M. Bovo and N. Buratti, "Evaluation of the variability contribution due to epistemic uncertainty on constitutive models in the definition of fragility curves of rc frames," *Engineering Structures*, vol. 188, pp. 700–716, 2019.

[21] F. Zareian and H. Krawinkler, "Assessment of probability of collapse and design for collapse safety," *Earthquake Engineering & Structural Dynamics*, vol. 36, no. 13, pp. 1901–1914, 2007.

[22] Y. J. Yin and Y. Li, "Seismic collapse risk of light-frame wood construction considering aleatoric and epistemic uncertainties," *Structural Safety*, vol. 32, no. 4, pp. 250–261, 2010.

[23] P. Deng, S. Pei, J. W. van de Lindt, and C. Zhang, "Uncertainty quantification for seismic responses of bilinear sdof systems: A semi-closed-form estimation," *Soil Dynamics and Earthquake Engineering*, vol. 93, pp. 18–28, 2017.

[24] C. B. Haselton, *Assessing seismic collapse safety of modern reinforced concrete moment frame buildings*. PhD thesis, Stanford University, 2006.

[25] M. A. Hariri-Ardebili and S. Sattar, "Sensitivity Analysis of Reinforced Concrete Structures: A Review," Technical Note NIST TN 2254, National Institute of Standards and Technology, Gaithersburg, MD, 2023.

[26] T. Y. Duman, T. Çan, Ö. Emre, F. T. Kadirioğlu, N. Başarır Baştürk, T. Kılıç, S. Arslan, S. Özalp, R. F. Kartal, and D. Kalafat, "Seismotectonic database of turkey," *Bulletin of Earthquake Engineering*, vol. 16, pp. 3277–3316, 2018.

[27] A. M. C. Şengör and Y. Yılmaz, "Tethyan evolution of turkey: a plate tectonic approach," *Tectonophysics*, vol. 75, no. 3-4, pp. 181–241, 1981.

[28] A. M. C. Şengör, N. Görür, and F. Şaroğlu, "Strike-slip faulting and related basin formation in zones of tectonic escape: Turkey as a case study," in *Strike-Slip Deformation, Basin Formation, and Sedimentation*, SEPM Society for Sedimentary Geology, 01 1985.

[29] R. Reilinger, S. McClusky, P. Vernant, S. Lawrence, S. Ergintav, R. Cakmak, H. Ozener, F. Kadirov, I. Guliev, and R. Stepanyan, "Gps constraints on continental deformation in the africa-arabia-eurasia continental collision zone and implications for the dynamics of plate interactions," *Journal of Geophysical Research: Solid Earth*, vol. 111, no. B5, pp. 1–12, 2006.

[30] A. M. C. Şengör, O. Tüysüz, C. Imren, M. Sakınç, H. Eyidoğan, N. Görür, X. Le Pichon, and C. Rangin, "The north anatolian fault: A new look," *Annu. Rev. Earth Planet. Sci.*, vol. 33, pp. 37–112, 2005.

[31] A. Barka, "Slip distribution along the north anatolian fault associated with the large earthquakes of the period 1939 to 1967," *Bulletin of the Seismological Society of America*, vol. 86, no. 5, pp. 1238–1254, 1996.

[32] Ö. Emre, T. Y. Duman, S. Özalp, F. Şaroğlu, Ş. Olgun, H. Elmacı, and T. Çan, "Active fault database of turkey," *Bulletin of Earthquake Engineering*, vol. 16, no. 8, pp. 3229–3275, 2018.

[33] R. K. McGuire, *FORTRAN computer program for seismic risk analysis*, 1976.

[34] R. K. McGuire, *FRISK: computer program for seismic risk analysis using faults as earthquake sources*, 1978.

[35] B. Bender and D. M. Perkins, "SEISRISK II; a computer program for seismic hazard estimation," Report 82-293, U.S. Geological Survey, 1982.

[36] B. Bender and D. M. Perkins, *SEISRISK III: a computer program for seismic hazard estimation*. No. 1772 in Bulletin (US Geological Survey), US Government Printing Office, 1987.

[37] M. Ordaz, F. Martinelli, V. D'Amico, and C. Meletti, "Crisis2008: A flexible tool to perform probabilistic seismic hazard assessment," *Seismological Research Letters*, vol. 84, no. 3, pp. 495–504, 2013.

[38] K. Assatourians and G. M. Atkinson, "Eqhaz: An open-source probabilistic seismic-hazard code based on the monte carlo simulation approach," *Seismological Research Letters*, vol. 84, no. 3, pp. 516–524, 2013.

[39] D. Robinson, T. Dhu, and J. Schneider, "Practical probabilistic seismic risk analysis: A demonstration of capability," *Seismological Research Letters*, vol. 77, no. 4, pp. 453–459, 2006.

[40] E. H. Field, T. H. Jordan, and C. A. Cornell, "Opensha: A developing community-modeling environment for seismic hazard analysis," *Seismological Research Letters*, vol. 74, no. 4, pp. 406–419, 2003.

[41] M. Pagani, D. Monelli, G. Weatherill, L. Danciu, H. Crowley, V. Silva, P. Henshaw, L. Butler, M. Nastasi, and L. Panzeri, "Openquake engine: An open hazard (and risk) software for the global earthquake model," *Seismological Research Letters*, vol. 85, no. 3, pp. 692–702, 2014.

[42] Federal Energy Regulatory Commission, *FERC Engineering Guidelines, Risk-Informed Decision Making Chapter R20: Probabilistic Seismic Hazard Analysis - Draft*. Federal Energy Regulatory Commission, 2014.

[43] K. Sesetyan, M. B. Demircioğlu, T. Y. Duman, T. Çan, S. Tekin, T. E. Azak, and Ö. Z. Fercan, "A probabilistic seismic hazard assessment for the turkish territory—part i: the area source model," *Bulletin of Earthquake Engineering*, vol. 16, pp. 3367–3397, 2018.

[44] M. B. Demircioğlu, K. Şeşetyan, T. Y. Duman, T. Çan, S. Tekin, and S. Ergintav, "A probabilistic seismic hazard assessment for the turkish territory: part ii—fault source and background seismicity model," *Bulletin of Earthquake Engineering*, vol. 16, pp. 3399–3438, 2018.

[45] Ö. Kale, "Some discussions on data-driven testing of ground-motion prediction equations under the turkish ground-motion database," *Journal of Earthquake Engineering*, vol. 23, no. 1, pp. 160–181, 2019.

[46] Ö. Kale and S. Akkar, "A new procedure for selecting and ranking ground-motion prediction equations (gmpes): The euclidean distance-based ranking

(edr) method," *Bulletin of the Seismological Society of America*, vol. 103, no. 2A, pp. 1069–1084, 2013.

[47] N. A. Abrahamson, W. J. Silva, and R. Kamai, "Summary of the ask14 ground motion relation for active crustal regions," *Earthquake Spectra*, vol. 30, no. 3, pp. 1025–1055, 2014.

[48] S. Akkar, M. A. Sandıkkaya, and J. J. Bommer, "Empirical ground-motion models for point-and extended-source crustal earthquake scenarios in europe and the middle east," *Bulletin of earthquake engineering*, vol. 12, pp. 359–387, 2014.

[49] D. M. Boore, J. P. Stewart, E. Seyhan, and G. M. Atkinson, "Nga-west2 equations for predicting pga, pgv, and 5% damped psa for shallow crustal earthquakes," *Earthquake Spectra*, vol. 30, no. 3, pp. 1057–1085, 2014.

[50] B. S. J. Chiou and R. R. Youngs, "Update of the chiou and youngs nga model for the average horizontal component of peak ground motion and response spectra," *Earthquake Spectra*, vol. 30, no. 3, pp. 1117–1153, 2014.

[51] Ö. Kale, S. Akkar, A. Ansari, and H. Hamzehloo, "A ground-motion predictive model for iran and turkey for horizontal pga, pgv, and 5% damped response spectrum: Investigation of possible regional effects," *Bulletin of the Seismological Society of America*, vol. 105, no. 2A, pp. 963–980, 2015.

[52] J. W. Baker, "Conditional mean spectrum: Tool for ground-motion selection," *Journal of Structural Engineering*, vol. 137, no. 3, pp. 322–331, 2011.

[53] J. W. Baker and C. A. Cornell, "Correlation of response spectral values for multicomponent ground motions," *Bulletin of the Seismological Society of America*, vol. 96, no. 1, pp. 215–227, 2006.

[54] J. W. Baker and N. Jayaram, "Correlation of spectral acceleration values from nga ground motion models," *Earthquake Spectra*, vol. 24, no. 1, pp. 299–317, 2008.

[55] N. Jayaram and J. W. Baker, "Correlation model for spatially distributed ground-motion intensities," *Earthquake Engineering & Structural Dynamics*, vol. 38, no. 15, pp. 1687–1708, 2009.

[56] N. Abrahamson, "Non-stationary spectral matching," *Seismological research letters*, vol. 63, no. 1, p. 30, 1992.

[57] J. Hancock, J. Watson-Lamprey, N. A. Abrahamson, J. J. Bommer, A. Markatis, E. McCoy, and R. Mendis, "An improved method of matching response spectra of recorded earthquake ground motion using wavelets," *Journal of earthquake engineering*, vol. 10, no. spec01, pp. 67–89, 2006.

[58] L. Al Atik and N. Abrahamson, "An improved method for nonstationary spectral matching," *Earthquake spectra*, vol. 26, no. 3, pp. 601–617, 2010.

[59] N. Shome, C. A. Cornell, P. Bazzurro, and J. E. Carballo, "Earthquakes, records, and nonlinear responses," *Earthquake spectra*, vol. 14, no. 3, pp. 469–500, 1998.

[60] P. Giovenale, C. A. Cornell, and L. Esteva, "Comparing the adequacy of alternative ground motion intensity measures for the estimation of structural responses," *Earthquake engineering & structural dynamics*, vol. 33, no. 8, pp. 951–979, 2004.

[61] American Society of Civil Engineers, "Minimum design loads for buildings and other structures," ASCE 7-16, American Society of Civil Engineers, 2016.

[62] European Committee for Standardization (CEN), "Eurocode 8: Design Provisions for Earthquake Resistance of Structures, Part 1.1: General Rules, Seismic Actions and Rules for Buildings," 2004. EN 1998-1.

[63] Turkish Building Earthquake Code (TEC), 2019.

[64] N. Jayaram and J. W. Baker, "Statistical tests of the joint distribution of spectral acceleration values," *Bulletin of the Seismological Society of America*, vol. 98, no. 5, pp. 2231–2243, 2008.

[65] N. Jayaram, T. Lin, and J. W. Baker, "A computationally efficient ground-motion selection algorithm for matching a target response spectrum mean and variance," *Earthquake spectra*, vol. 27, no. 3, pp. 797–815, 2011.

[66] Pacific Earthquake Engineering Research (PEER) Center, "Technical report for the peer ground motion database web application," 2010.

[67] Y. Bozorgnia, N. A. Abrahamson, L. Al Atik, T. D. Ancheta, G. M. Atkinson, J. W. Baker, A. Baltay, D. M. Boore, K. W. Campbell, and B. S.-J. Chiou, "Nga-west2 research project," *Earthquake Spectra*, vol. 30, no. 3, pp. 973–987, 2014.

[68] K. Tarbali and B. A. Bradley, "The effect of causal parameter bounds in psha-based ground motion selection," *Earthquake Engineering & Structural Dynamics*, vol. 45, no. 9, pp. 1515–1535, 2016.

[69] W. Du, C. Ning, and G. Wang, "The effect of amplitude scaling limits on conditional spectrum-based ground motion selection," *Earthquake Engineering & Structural Dynamics*, vol. 48, no. 9, pp. 1030–1044, 2019.

[70] I. Iervolino and C. A. Cornell, "Record selection for nonlinear seismic analysis of structures," *Earthquake Spectra*, vol. 21, no. 3, pp. 685–713, 2005.

[71] A. Kottke and E. M. Rathje, "A semi-automated procedure for selecting and scaling recorded earthquake motions for dynamic analysis," *Earthquake Spectra*, vol. 24, no. 4, pp. 911–932, 2008.

[72] K. Kadaş, "Influence of idealized pushover curves on seismic response," Master's thesis, Middle East Technical University, 2006.

[73] M. Zhu, F. McKenna, and M. H. Scott, "Openseespy: Python library for the opensees finite element framework," *SoftwareX*, vol. 7, pp. 6–11, 2018.

[74] F. McKenna, M. H. Scott, and G. L. Fenves, "Nonlinear finite-element analysis software architecture using object composition," *Journal of Computing in Civil Engineering*, vol. 24, no. 1, pp. 95–107, 2010.

[75] International Conference of Building Officials (ICBO), "Uniform Building Code," Whittier, CA, 1982.

[76] R. Ranganathan, *Structural reliability analysis and design*. Jaico publishing house, 1999.

[77] S. A. Mirza, J. G. MacGregor, and M. Hatzinikolas, "Statistical descriptions of strength of concrete," *Journal of the Structural Division*, vol. 105, no. 6, pp. 1021–1037, 1979.

[78] S. A. Mirza and J. G. MacGregor, "Variability of mechanical properties of reinforcing bars," *Journal of the Structural Division*, vol. 105, no. 5, pp. 921–937, 1979.

[79] B. Binici and K. M. Mosalam, "Analysis of reinforced concrete columns retrofitted with fiber reinforced polymer lamina," *Composites Part B: Engineering*, vol. 38, no. 2, pp. 265–276, 2007.

[80] F. Taucer, E. Spacone, and F. C. Filippou, *A fiber beam-column element for seismic response analysis of reinforced concrete structures*, vol. 91. Earthquake Engineering Research Center, College of Engineering, University, 1991.

[81] S. Mazzoni, F. McKenna, M. H. Scott, and G. L. Fenves, "Opensees command language manual," *Pacific earthquake engineering research (PEER) center*, vol. 264, no. 1, pp. 137–158, 2006.

[82] D. C. Kent and R. Park, "Flexural members with confined concrete," *Journal of the structural division*, vol. 97, no. 7, pp. 1969–1990, 1971.

[83] British Standard, "Eurocode 8: Design of Structures for Earthquake Resistance," *BS EN 1998-3*, 2005.

[84] B. Özer AY and M. A. Erberik, "Vulnerability of turkish low-rise and mid-rise reinforced concrete frame structures," *Journal of Earthquake Engineering*, vol. 12, no. S2, pp. 2–11, 2008.

[85] K. Porter, R. Kennedy, and R. Bachman, "Creating fragility functions for performance-based earthquake engineering," *Earthquake spectra*, vol. 23, no. 2, pp. 471–489, 2007.

[86] J. W. Baker, "Efficient analytical fragility function fitting using dynamic structural analysis," *Earthquake Spectra*, vol. 31, no. 1, pp. 579–599, 2015.

Appendix A

GROUND MOTION SUITE TABLES

Table A.1: Ground Motion Suite for F2S2B Building with 68% Probability of Exceedence in 50 Years for NEHRP Class D Site

Earthquake Name	Year	Station Name	Component	M_w	R_{jb} (km)	Vs30 (m/s)	Scale Factor	PGA (g)	PGV (cm/s)	Sa_{T1} (g)	Arias Intensity (cm/s)	Housner Intensity (cm)
Landers	1992	Desert Hot Springs	H-2	7.28	21.78	359	1.248	0.192	26.1	0.265	10.74	102.91
Parkfield-02 CA	2004	Parkfield - Gold Hill 2W	H-1	6.0	2.13	290	1.246	0.205	18.6	0.522	3.79	41.08
Kocaeli Turkey	1999	Atakoy	H-2	7.51	56.49	310	1.246	0.209	22.2	0.418	4.45	60.20
Parkfield-02 CA	2004	Parkfield - Vineyard Cany 5W	H-1	6.0	9.2	320	1.246	0.211	13.5	0.449	4.49	47.80
Trinidad	1980	Rio Dell Overpass W Ground	H-1	7.2	76.06	312	1.246	0.188	11.0	0.353	6.14	36.89
Parkfield-02 CA	2004	Parkfield - Vineyard Cany 5W	H-2	6.0	9.2	320	1.241	0.245	13.4	1.085	4.14	56.65
Parkfield-02 CA	2004	Parkfield - Vineyard Cany 1W	H-1	6.0	1.0	284	1.256	0.210	22.9	0.485	4.20	81.01
Darfield New Zealand	2010	RKAC	H-2	7.0	13.37	296	1.238	0.237	22.1	0.545	7.93	64.81
Darfield New Zealand	2010	RKAC	H-1	7.0	13.37	296	1.231	0.205	13.0	0.423	6.74	54.28
Superstition Hills-02	1987	Salton Sea Wildlife Refuge	H-2	6.54	25.88	191	1.268	0.177	23.0	0.287	5.86	88.26
Parkfield-02 CA	2004	Parkfield - Vineyard Cany 1W	H-2	6.0	1.0	284	1.271	0.172	14.9	0.497	3.89	59.26
Tottori Japan	2000	SMN003	H-1	6.61	25.52	344	1.273	0.644	24.6	2.185	33.80	33.12
Big Bear-01	1992	North Palm Springs Fire Sta 36	H-2	6.46	40.87	368	1.273	0.165	14.9	0.344	6.44	61.27
El Mayor-Cucapah Mexico	2010	Salton City	H-1	7.2	72.44	324	1.221	0.239	11.1	0.575	5.48	45.16
El Mayor-Cucapah Mexico	2010	Brawley Airport	H-1	7.2	41.15	209	1.276	0.170	14.5	0.614	9.48	52.10
Landers	1992	North Palm Springs	H-1	7.28	26.84	345	1.286	0.175	14.3	0.397	10.82	78.99
Kobe Japan	1995	Abeno	H-2	6.9	24.85	256	1.208	0.279	29.9	0.679	8.66	87.27
Morgan Hill	1984	Gilroy Array 3	H-1	6.19	13.01	350	1.208	0.235	13.3	0.605	5.04	58.70
Tottori Japan	2000	TTR005	H-1	6.61	45.98	169	1.288	0.248	13.8	0.504	6.16	31.13
Imperial Valley-06	1979	El Centro Array 12	H-1	6.53	17.94	197	1.291	0.187	27.7	0.382	6.77	94.30

Table A.2: Ground Motion Suite for F5S4B Building with 68% Probability of Exceedence in 50 Years for NEHRP Class D Site

Earthquake Name	Year	Station Name	Component	M_w	R_{jb} (km)	Vs30 (m/s)	Scale Factor	PGA (g)	PGV (cm/s)	Sa_{T1} (g)	Arias Intensity (cm/s)	Housner Intensity (cm)
Tottori Japan	2000	TTRH04	H-1	6.61	32.75	254	1.079	0.202	18.2	0.905	6.16	49.25
Parkfield-02 CA	2004	Parkfield - Vineyard Cany 1W	H-1	6.0	1.0	284	1.075	0.180	19.6	0.415	3.08	69.35
Chi-Chi Taiwan-04	1999	CHY047	H-2	6.2	38.59	170	1.075	0.141	12.0	0.265	2.62	48.29
Kocaeli Turkey	1999	Bursa Tofas	H-2	7.51	60.43	290	1.068	0.107	19.5	0.144	5.72	87.17
Darfield New Zealand	2010	SBRC	H-1	7.0	21.31	263	1.064	0.158	21.6	0.289	7.06	46.82
Imperial Valley-06	1979	El Centro Array 12	H-1	6.53	17.94	197	1.062	0.154	22.8	0.314	4.59	77.60
Landers	1992	North Palm Springs	H-2	7.28	26.84	345	1.060	0.142	15.4	0.276	7.99	84.05
Darfield New Zealand	2010	SBRC	H-2	7.0	21.31	263	1.060	0.162	29.1	0.325	7.51	56.27
Chalfant Valley-02	1986	Benton	H-1	6.19	21.55	371	1.056	0.221	14.4	0.686	4.13	70.63
Big Bear-01	1992	North Palm Springs Fire Sta 36	H-2	6.46	40.87	368	1.110	0.143	13.0	0.300	4.89	53.40
Darfield New Zealand	2010	FDCS	H-1	7.0	90.17	390	1.112	0.114	14.8	0.182	3.70	70.80
Mammoth Lakes-06	1980	Convict Creek	H-2	5.94	6.44	382	1.049	0.330	17.1	1.142	5.72	48.02
Livermore-01	1980	San Ramon - Eastman Kodak	H-1	5.8	15.19	378	1.114	0.167	23.1	0.201	2.67	90.07
Landers	1992	North Palm Springs	H-1	7.28	26.84	345	1.114	0.152	12.4	0.344	8.12	68.44
Kocaeli Turkey	1999	Atakoy	H-2	7.51	56.49	310	1.047	0.176	18.6	0.351	3.14	50.59
Chi-Chi Taiwan-04	1999	CHY101	H-1	6.2	21.62	259	1.047	0.160	19.7	0.360	3.63	62.76
Kobe Japan	1995	Abeno	H-2	6.9	24.85	256	1.047	0.242	25.9	0.588	6.50	75.62
Chi-Chi Taiwan-04	1999	CHY034	H-2	6.2	28.45	379	1.116	0.115	10.5	0.177	2.70	54.50
Trinidad	1980	Rio Dell Overpass E Ground	H-2	7.2	76.06	312	1.116	0.150	10.8	0.328	4.88	43.35
Parkfield-02 CA	2004	Parkfield - Fault Zone 6	H-1	6.0	0.87	267	1.043	0.186	25.2	0.662	3.50	65.45

Table A.3: Ground Motion Suite for F8S3B Building with 68% Probability of Exceedence in 50 Years for NEHRP Class D Site

Earthquake Name	Year	Station Name	Component	M_w	R_{jb} (km)	Vs30 (m/s)	Scale Factor	PGA (g)	PGV (cm/s)	Sa_{T1} (g)	Arias Intensity (cm/s)	Housner Intensity (cm)
Parkfield-02 CA	2004	Parkfield - Vineyard Cany 1W	H-1	6.0	1.0	284	1.103	0.185	20.2	0.426	3.24	71.15
Parkfield	1966	Cholame - Shandon Array 8	H-2	6.19	12.9	257	1.103	0.300	12.5	0.544	4.76	49.81
Landers	1992	North Palm Springs	H-1	7.28	26.84	345	1.096	0.149	12.2	0.339	7.87	67.35
Kocaeli Turkey	1999	Atakoy	H-2	7.51	56.49	310	1.105	0.185	19.7	0.371	3.50	53.40
Mammoth Lakes-02	1980	Mammoth Lakes H. S.	H-1	5.69	1.45	347	1.094	0.425	26.4	1.211	7.73	46.72
Parkfield-02 CA	2004	Parkfield - Cholame 6W	H-1	6.0	8.16	252	1.106	0.258	13.3	0.506	4.76	41.12
Tottori Japan	2000	TTRH04	H-1	6.61	32.75	254	1.109	0.208	18.7	0.930	6.51	50.63
Darfield New Zealand	2010	FDCS	H-1	7.0	90.17	390	1.085	0.112	14.4	0.178	3.53	69.10
Parkfield-02 CA	2004	Parkfield - Fault Zone 4	H-1	6.0	0.73	221	1.116	0.147	18.6	0.256	3.19	60.25
Chi-Chi Taiwan-04	1999	CHY015	H-1	6.2	50.02	229	1.116	0.114	16.6	0.184	2.88	72.27
Darfield New Zealand	2010	SBRC	H-2	7.0	21.31	263	1.116	0.171	30.6	0.342	8.33	59.25
Joshua Tree CA	1992	Thousand Palms Post Office	H-2	6.1	17.15	334	1.118	0.219	13.9	0.664	6.83	49.60
Landers	1992	Amboy	H-1	7.28	69.21	383	1.120	0.129	20.4	0.300	7.19	71.29
Kobe Japan	1995	Tadoka	H-2	6.9	31.69	312	1.120	0.218	16.5	0.374	8.61	55.56
Landers	1992	Thousand Palms Post Office	H-2	7.28	36.93	334	1.076	0.125	14.9	0.253	5.64	67.14
Joshua Tree CA	1992	North Palm Springs Fire Sta 36	H-1	6.1	21.4	368	1.126	0.182	9.7	0.424	4.29	42.96
Chi-Chi Taiwan-04	1999	CHY034	H-2	6.2	28.45	379	1.127	0.116	10.6	0.178	2.75	55.03
Superstition Hills-02	1987	Plaster City	H-1	6.54	22.25	317	1.127	0.154	11.1	0.343	3.87	55.25
Landers	1992	Indio - Coachella Canal	H-2	7.28	54.25	339	1.129	0.124	17.1	0.175	4.28	74.75
Mammoth Lakes-06	1980	Convict Creek	H-2	5.94	6.44	382	1.134	0.357	18.5	1.234	6.68	51.88

Table A.4: Ground Motion Suite for F2S2B Building with 68% Probability of Exceedence in 50 Years for NEHRP Class C Site

Earthquake Name	Year	Station Name	Component	M_w	R_{jb} (km)	Vs30 (m/s)	Scale Factor	PGA (g)	PGV (cm/s)	Sa_{T1} (g)	Arias Intensity (cm/s)	Housner Intensity (cm)
Tottori Japan	2000	HRSH03	H-2	6.61	73.91	487	1.067	0.372	9.8	1.195	33.97	14.56
Manjil Iran	1990	Tonekabun	H-1	7.37	93.3	290	1.069	0.095	9.5	0.119	2.81	52.87
Parkfield-02 CA	2004	Parkfield - Vineyard Cany 4W	H-1	6.0	6.74	386	1.062	0.108	7.5	0.392	1.14	25.10
Tottori Japan	2000	SMN003	H-2	6.61	25.52	344	1.061	0.335	8.8	1.259	16.59	16.51
Hector Mine	1999	Fort Irwin	H-1	7.13	65.04	367	1.071	0.114	7.0	0.265	2.04	21.33
Mammoth Lakes-04	1980	Long Valley Dam (L Abut)	H-1	5.7	12.75	537	1.060	0.104	8.5	0.207	0.67	23.90
Big Bear-01	1992	Fun Valley	H-1	6.46	49.35	389	1.073	0.110	6.0	0.358	1.79	24.83
Parkfield-02 CA	2004	Parkfield - Gold Hill 3E	H-2	6.0	5.79	451	1.075	0.119	7.4	0.290	1.55	21.38
Darfield New Zealand	2010	LSRC	H-2	7.0	79.53	561	1.056	0.104	13.8	0.129	1.80	46.99
Hector Mine	1999	Morongo Valley Fire Station	H-2	7.13	53.21	396	1.082	0.093	12.6	0.144	2.33	68.22
Landers	1992	San Bernardino - E & Hospitality	H-1	7.28	79.76	297	1.050	0.082	20.8	0.135	4.39	92.66
Tottori Japan	2000	HRS003	H-1	6.61	65.8	336	1.050	0.117	9.6	0.337	1.99	17.93
Morgan Hill	1984	Corralitos	H-1	6.19	23.23	462	1.084	0.088	7.2	0.164	0.78	28.67
El Mayor-Cucapah Mexico	2010	Ocotillo Wells - Veh. Rec. Area	H-1	7.2	67.71	361	1.084	0.102	13.9	0.186	1.54	31.99
Westmorland	1981	Superstition Mtn Camera	H-2	5.9	19.26	362	1.084	0.113	8.6	0.345	0.97	23.71
Landers	1992	Forest Falls Post Office	H-2	7.28	45.34	436	1.047	0.091	9.6	0.232	3.09	34.64
Chi-Chi Taiwan-04	1999	CHY046	H-2	6.2	38.11	442	1.047	0.126	9.4	0.243	1.20	35.52
Darfield New Zealand	2010	PEEC	H-2	7.0	52.13	551	1.047	0.122	4.8	0.281	2.59	25.33
Coyote Lake	1979	San Juan Bautista - Hwy 101/156 Overpass	H-2	5.74	20.44	363	1.043	0.125	8.7	0.155	1.01	23.70
Parkfield-02 CA	2004	Parkfield - Vineyard Cany 6W	H-2	6.0	13.33	392	1.041	0.109	8.2	0.308	1.65	30.14

Table A.5: Ground Motion Suite for F5S4B Building with 68% Probability of Exceedence in 50 Years for NEHRP Class C Site

Earthquake Name	Year	Station Name	Component	M_w	R_{jb} (km)	Vs30 (m/s)	Scale Factor	PGA (g)	PGV (cm/s)	Sa_{T1} (g)	Arias Intensity (cm/s)	Housner Intensity (cm)
Big Bear-01	1992	Fun Valley	H-2	6.46	49.35	389	1.050	0.120	5.8	0.302	2.02	21.06
Hector Mine	1999	Fun Valley	H-2	7.13	54.68	389	1.051	0.092	6.9	0.198	2.14	26.40
El Mayor-Cucapah Mexico	2010	Ocotillo Wells - Veh. Rec. Area	H-2	7.2	67.71	361	1.051	0.074	10.6	0.096	1.29	36.96
Big Bear-01	1992	Fun Valley	H-1	6.46	49.35	389	1.051	0.107	5.9	0.350	1.72	24.33
Trinidad offshore	1983	Rio Dell Overpass E Ground	H-2	5.7	68.02	312	1.053	0.148	6.4	0.375	1.85	19.63
Duzce Turkey	1999	Lamont 1058	H-2	7.14	0.21	529	1.047	0.112	16.6	0.276	1.28	49.47
Darfield New Zealand	2010	WSFC	H-1	7.0	24.36	344	1.060	0.071	9.1	0.138	1.69	37.00
Darfield New Zealand	2010	DORC	H-2	7.0	29.96	280	1.060	0.092	12.6	0.261	2.30	40.28
Tottori Japan	2000	KGW001	H-2	6.61	99.39	325	1.038	0.119	5.5	0.265	1.66	17.48
Tottori Japan	2000	HRSH06	H-2	6.61	54.62	281	1.064	0.261	11.5	0.470	6.41	20.41
Double Springs	1994	Woodfords	H-1	5.9	12.48	393	1.037	0.063	6.6	0.185	0.88	26.95
Landers	1992	Baker Fire Station	H-1	7.28	87.94	325	1.035	0.111	9.6	0.245	2.61	37.99
Mammoth Lakes-03	1980	Long Valley Dam (L Abut)	H-1	5.91	10.31	537	1.032	0.089	7.0	0.166	0.78	25.38
Parkfield-02 CA	2004	Parkfield - Stone Corral 3E	H-1	6.0	7.68	565	1.072	0.211	9.4	0.785	2.84	35.55
Mammoth Lakes-04	1980	Long Valley Dam (L Abut)	H-1	5.7	12.75	537	1.024	0.100	8.2	0.200	0.63	23.09
Hector Mine	1999	Beaumont - 6th & Maple	H-2	7.13	89.67	315	1.022	0.065	14.7	0.125	1.52	44.36
Darfield New Zealand	2010	DORC	H-1	7.0	29.96	280	1.081	0.089	11.3	0.294	2.23	36.23
Darfield New Zealand	2010	PEEC	H-2	7.0	52.13	551	1.081	0.126	5.0	0.290	2.76	26.14
Parkfield-02 CA	2004	Parkfield - Vineyard Cany 4W	H-2	6.0	6.74	386	1.020	0.094	7.8	0.261	0.98	29.48
Landers	1992	Palm Springs Airport	H-1	7.28	36.15	312	1.018	0.077	11.0	0.223	3.55	51.46

Table A.6: Ground Motion Suite for F8S3B Building with 68% Probability of Exceedence in 50 Years for NEHRP Class C Site

Earthquake Name	Year	Station Name	Component	M_w	R_{jb} (km)	Vs30 (m/s)	Scale Factor	PGA (g)	PGV (cm/s)	Sa_{T1} (g)	Arias Intensity (cm/s)	Housner Intensity (cm)
Morgan Hill	1984	Gilroy Array 7	H-1	6.19	12.06	334	1.067	0.203	7.8	0.405	3.30	21.37
Tottori Japan	2000	SMN004	H-1	6.61	34.64	281	1.067	0.151	9.2	0.429	4.19	24.30
Tottori Japan	2000	SMNH03	H-1	6.61	52.3	440	1.070	0.169	10.2	0.260	4.67	23.58
Hector Mine	1999	Forest Falls Post Office	H-2	7.13	74.92	436	1.070	0.065	11.5	0.199	1.00	28.87
Livermore-01	1980	San Ramon - Eastman Kodak	H-2	5.8	15.19	378	1.072	0.068	8.9	0.124	0.96	31.94
Mammoth Lakes-03	1980	Long Valley Dam (L Abut)	H-1	5.91	10.31	537	1.072	0.093	7.3	0.173	0.84	26.36
Hector Mine	1999	Fun Valley	H-2	7.13	54.68	389	1.072	0.094	7.0	0.202	2.22	26.93
Coyote Lake	1979	San Juan Bautista 24 Polk St	H-1	5.74	19.46	336	1.061	0.119	7.5	0.194	1.32	26.38
Chi-Chi Taiwan-04	1999	CHY042	H-1	6.2	34.1	665	1.075	0.089	7.5	0.145	1.05	33.00
Chi-Chi Taiwan-04	1999	CHY024	H-2	6.2	19.67	428	1.077	0.079	14.0	0.140	1.02	47.51
Chi-Chi Taiwan-04	1999	CHY024	H-1	6.2	19.67	428	1.057	0.073	15.0	0.145	1.00	37.38
Mammoth Lakes-04	1980	Long Valley Dam (L Abut)	H-1	5.7	12.75	537	1.079	0.105	8.6	0.210	0.70	24.32
Chalfant Valley-02	1986	Long Valley Dam (L Abut)	H-2	6.19	18.3	537	1.055	0.079	8.4	0.177	0.78	40.44
Darfield New Zealand	2010	WSFC	H-2	7.0	24.36	344	1.055	0.073	9.0	0.144	1.38	37.64
Darfield New Zealand	2010	TRCS	H-2	7.0	93.7	425	1.055	0.080	8.5	0.331	2.47	47.22
Parkfield-02 CA	2004	Parkfield - Gold Hill 4W	H-1	6.0	7.74	421	1.080	0.443	12.8	1.597	10.86	27.86
El Mayor-Cucapah Mexico	2010	Bombay Beach	H-2	7.2	77.72	349	1.086	0.066	9.6	0.090	1.45	37.95
El Mayor-Cucapah Mexico	2010	North Shore - Durmid	H-2	7.2	84.54	382	1.087	0.069	9.7	0.135	1.24	40.47
Big Bear-01	1992	Hesperia - 4th & Palm	H-2	6.46	44.48	358	1.090	0.098	10.8	0.173	1.24	33.09
Hector Mine	1999	Desert Hot Springs	H-1	7.13	56.4	359	1.045	0.070	7.8	0.131	1.24	32.13

Table A.7: Ground Motion Suite for F2S2B Building with 68% Probability of Exceedence in 50 Years for Generic Rock Site

Earthquake Name	Year	Station Name	Component	M_w	R_{jb} (km)	Vs30 (m/s)	Scale Factor	PGA (g)	PGV (cm/s)	Sa_{T1} (g)	Arias Intensity (cm/s)	Housner Intensity (cm)
Tottori Japan	2000	OKY008	H-1	6.61	50.35	451	1.036	0.169	8.4	0.505	3.31	17.64
Mammoth Lakes-05	1980	Long Valley Dam (Upr L Abut)	H-2	5.7	14.91	537	1.034	0.075	6.7	0.117	0.61	17.75
Caldiran Turkey	1976	Maku	H-2	7.21	50.78	433	1.043	0.102	7.1	0.237	1.00	16.39
Tottori Japan	2000	SMN008	H-1	6.61	88.13	405	1.028	0.184	5.8	0.496	2.47	11.44
Denali Alaska	2002	Carlo (temp)	H-1	7.9	49.94	399	1.028	0.098	7.1	0.242	1.64	21.11
Potenza Italy	1990	Brienza	H-1	5.8	25.89	561	1.048	0.103	4.0	0.179	0.54	14.31
Chalfant Valley-02	1986	Long Valley Dam (L Abut)	H-1	6.19	18.3	537	1.048	0.086	7.4	0.192	0.78	26.82
Mammoth Lakes-02	1980	Long Valley Dam (Upr L Abut)	H-2	5.69	14.28	537	1.025	0.068	4.5	0.119	0.58	16.03
Darfield New Zealand	2010	LSRC	H-1	7.0	79.53	561	1.025	0.078	10.1	0.101	1.45	47.71
Chi-Chi Taiwan-04	1999	CHY024	H-1	6.2	19.67	428	1.051	0.072	15.0	0.144	0.99	37.14
Chi-Chi Taiwan-04	1999	CHY010	H-2	6.2	31.6	539	1.053	0.103	6.6	0.187	1.06	24.50
Morgan Hill	1984	San Justo Dam (L Abut)	H-2	6.19	31.88	544	1.053	0.074	5.5	0.110	1.14	25.39
Tottori Japan	2000	OKY013	H-2	6.61	69.28	472	1.059	0.110	8.2	0.386	2.46	25.16
Potenza Italy	1990	Rionero In Vulture	H-2	5.8	34.5	575	1.013	0.088	5.4	0.332	0.90	19.47
Sitka Alaska	1972	Sitka Observatory	H-2	7.68	34.61	650	1.013	0.087	14.3	0.351	1.66	18.15
Morgan Hill	1984	UCSC Lick Observatory	H-2	6.19	45.47	714	1.062	0.081	4.2	0.142	0.95	17.42
Chi-Chi Taiwan-04	1999	TCU116	H-2	6.2	28.72	493	1.062	0.093	11.2	0.109	0.87	40.05
Big Bear-01	1992	Snow Creek	H-1	6.46	37.04	524	1.011	0.166	4.8	0.374	3.00	17.17
Kobe Japan	1995	Chihaya	H-1	6.9	49.91	609	1.065	0.098	5.7	0.199	1.37	17.45
Tottori Japan	2000	HRS021	H-1	6.61	36.32	409	1.065	0.271	6.8	0.551	13.89	12.27

Table A.8: Ground Motion Suite for F5S4B Building with 68% Probability of Exceedence in 50 Years for Generic Rock Site

Earthquake Name	Year	Station Name	Component	M_w	R_{jb} (km)	Vs30 (m/s)	Scale Factor	PGA (g)	PGV (cm/s)	Sa_{T1} (g)	Arias Intensity (cm/s)	Housner Intensity (cm)
El Mayor-Cucapah Mexico	2010	Bombay Beach - Bertram	H-1	7.2	81.42	491	1.091	0.054	8.0	0.076	0.84	27.98
Morgan Hill	1984	UCSC Lick Observatory	H-2	6.19	45.47	714	1.091	0.083	4.3	0.146	1.00	17.90
Big Bear-01	1992	Temecula - 6th & Mercedes	H-2	6.46	76.13	416	1.091	0.052	5.1	0.080	0.81	25.09
Denali Alaska	2002	Carlo (temp)	H-1	7.9	49.94	399	1.084	0.103	7.5	0.256	1.82	22.27
Mammoth Lakes-02	1980	Long Valley Dam (Upr L Abut)	H-2	5.69	14.28	537	1.094	0.072	4.8	0.127	0.66	17.11
Hector Mine	1999	San Jacinto - Soboba	H-2	7.13	92.71	447	1.078	0.060	7.7	0.105	0.64	26.27
Potenza Italy	1990	Rionero In Vulture	H-2	5.8	34.5	575	1.078	0.094	5.8	0.354	1.02	20.71
Tottori Japan	2000	OKY013	H-2	6.61	69.28	472	1.099	0.115	8.5	0.400	2.65	26.12
Parkfield-02 CA	2004	PARKFIELD - STOCKDALE MTN	H-2	6.0	4.0	394	1.104	0.390	8.9	1.211	2.85	23.86
Tottori Japan	2000	SMN006	H-1	6.61	72.4	627	1.104	0.088	7.8	0.148	1.20	19.48
Kobe Japan	1995	Chihaya	H-1	6.9	49.91	609	1.106	0.102	5.9	0.207	1.48	18.12
Darfield New Zealand	2010	KOKS	H-2	7.0	95.18	511	1.107	0.060	7.4	0.066	0.94	45.16
Chalfant Valley-02	1986	Long Valley Dam (Downst)	H-1	6.19	18.3	537	1.110	0.107	5.4	0.132	0.74	23.05
Duzce Turkey	1999	Lamont 1058	H-1	7.14	0.21	529	1.060	0.082	15.1	0.120	0.76	45.23
Big Bear-01	1992	Wrightwood - Swarthout	H-1	6.46	70.83	477	1.117	0.080	4.9	0.167	1.26	17.80
Kobe Japan	1995	OKA	H-1	6.9	86.93	609	1.117	0.088	5.8	0.130	1.18	15.48
Duzce Turkey	1999	Mudurnu	H-2	7.14	34.3	535	1.054	0.062	18.4	0.096	1.02	26.62
Hector Mine	1999	Heart Bar State Park	H-2	7.13	61.21	625	1.123	0.092	11.6	0.265	1.82	19.94
Chi-Chi Taiwan-04	1999	CHY029	H-2	6.2	25.75	545	1.127	0.069	13.1	0.102	0.73	43.31
Tottori Japan	2000	OKYH14	H-1	6.61	26.51	710	1.128	0.302	12.7	1.617	7.78	24.41

Table A.9: Ground Motion Suite for F8S3B Building with 68% Probability of Exceedence in 50 Years for Generic Rock Site

Earthquake Name	Year	Station Name	Component	M_w	R_{jb} (km)	Vs30 (m/s)	Scale Factor	PGA (g)	PGV (cm/s)	Sa_{T1} (g)	Arias Intensity (cm/s)	Housner Intensity (cm)
Hector Mine	1999	Whitewater Trout Farm	H-2	7.13	62.91	425	1.081	0.061	10.7	0.133	0.88	23.01
Chi-Chi Taiwan-04	1999	TCU084	H-2	6.2	26.83	665	1.076	0.046	6.4	0.052	0.50	31.16
Tottori Japan	2000	OKY013	H-2	6.61	69.28	472	1.074	0.112	8.3	0.391	2.53	25.53
Tottori Japan	2000	OKYH08	H-2	6.61	24.84	694	1.074	0.259	12.8	1.026	6.78	26.85
El Mayor-Cucapah Mexico	2010	North Shore - Hwy 111	H-1	7.2	95.72	388	1.072	0.050	13.7	0.089	1.22	37.52
Hector Mine	1999	Joshua Tree N.M. - Keys View	H-2	7.13	50.42	686	1.098	0.096	7.1	0.205	1.28	17.36
Chalfant Valley-02	1986	Convict Creek	H-2	6.19	29.35	382	1.066	0.076	3.9	0.173	0.60	23.08
Potenza Italy	1990	Rionero In Vulture	H-2	5.8	34.5	575	1.103	0.096	5.9	0.362	1.06	21.19
Livermore-01	1980	San Ramon Fire Station	H-2	5.8	15.84	384	1.105	0.040	4.9	0.068	0.63	26.21
Chalfant Valley-02	1986	Long Valley Dam (Downst)	H-1	6.19	18.3	537	1.105	0.106	5.4	0.132	0.73	22.94
Chi-Chi Taiwan-04	1999	TCU084	H-1	6.2	26.83	665	1.059	0.060	7.1	0.074	0.62	32.49
Denali Alaska	2002	Carlo (temp)	H-1	7.9	49.94	399	1.059	0.101	7.4	0.250	1.74	21.76
Hector Mine	1999	San Jacinto - Soboba	H-2	7.13	92.71	447	1.051	0.059	7.6	0.102	0.61	25.62
Chalfant Valley-02	1986	Lake Crowley - Shehorn Res.	H-2	6.19	22.08	457	1.050	0.096	5.9	0.198	1.06	18.20
Chi-Chi Taiwan-04	1999	TTN041	H-2	6.2	47.59	418	1.121	0.105	6.0	0.259	1.29	15.68
Darfield New Zealand	2010	KOKS	H-1	7.0	95.18	511	1.044	0.046	7.6	0.064	0.75	31.53
Darfield New Zealand	2010	TRCS	H-1	7.0	93.7	425	1.042	0.072	8.6	0.262	1.95	32.62
Hector Mine	1999	San Jacinto - Soboba	H-1	7.13	92.71	447	1.131	0.068	8.8	0.088	0.65	24.89
Mammoth Lakes-02	1980	Long Valley Dam (Upr L Abut)	H-2	5.69	14.28	537	1.137	0.075	5.0	0.132	0.71	17.79
Mammoth Lakes-05	1980	Long Valley Dam (Upr L Abut)	H-2	5.7	14.91	537	1.027	0.074	6.6	0.116	0.60	17.62

Table A.10: Ground Motion Suite for F2S2B Building with 68% Probability of Exceedence in 50 Years for NEHRP Class B Site

Earthquake Name	Year	Station Name	Component	M_w	R_{jb} (km)	Vs30 (m/s)	Scale Factor	PGA (g)	PGV (cm/s)	Sa_{T1} (g)	Arias Intensity (cm/s)	Housner Intensity (cm)
Kobe Japan	1995	OKA	H-2	6.9	86.93	609	1.010	0.061	3.7	0.120	0.62	10.04
Tottori Japan	2000	SMN006	H-2	6.61	72.4	627	1.010	0.070	3.2	0.162	0.82	10.16
Kobe Japan	1995	MZH	H-2	6.9	69.04	609	1.046	0.056	5.0	0.078	0.71	19.91
Darfield New Zealand	2010	RPZ	H-2	7.0	57.37	638	1.061	0.052	5.9	0.116	0.58	20.55
Tottori Japan	2000	OKY002	H-1	6.61	54.7	592	1.092	0.119	3.8	0.196	1.41	11.15
Tottori Japan	2000	OKY002	H-2	6.61	54.7	592	0.939	0.175	4.1	0.344	1.84	9.55
Kocaeli Turkey	1999	Bursa Sivil	H-1	7.51	65.53	613	1.106	0.050	9.0	0.072	0.88	42.29
Chi-Chi Taiwan-04	1999	CHY052	H-2	6.2	45.33	573	1.110	0.051	4.2	0.109	0.45	17.18
Hector Mine	1999	Twentynine Palms	H-1	7.13	42.06	635	0.925	0.061	6.5	0.147	0.61	18.53
Tottori Japan	2000	SMNH12	H-2	6.61	45.07	590	0.923	0.241	5.7	1.241	9.04	8.42
Kocaeli Turkey	1999	Bursa Sivil	H-2	7.51	65.53	613	1.126	0.061	10.2	0.073	0.98	43.54
Chi-Chi Taiwan-04	1999	CHY052	H-1	6.2	45.33	573	0.915	0.054	4.8	0.090	0.40	15.04
Morgan Hill	1984	Gilroy Array 1	H-2	6.19	14.9	1428	1.131	0.112	3.3	0.236	0.78	12.31
Livermore-01	1980	Tracy - Sewage Treatm Plant	H-1	5.8	53.35	650	1.138	0.055	7.6	0.062	0.78	39.37
Duzce Turkey	1999	Lamont 1060	H-2	7.14	25.78	782	1.140	0.061	6.6	0.140	0.57	18.57
Chi-Chi Taiwan-04	1999	TTN051	H-2	6.2	37.54	665	1.140	0.076	7.4	0.240	0.48	18.22
Chi-Chi Taiwan-04	1999	TTN051	H-1	6.2	37.54	665	0.888	0.067	4.2	0.150	0.57	13.04
Coyote Lake	1979	Gilroy Array 1	H-1	5.74	10.21	1428	1.162	0.109	4.9	0.293	0.87	13.13
Chalfant Valley-01	1986	Bishop - Paradise Lodge	H-2	5.77	14.99	585	0.876	0.077	7.9	0.281	0.33	17.27
Potenza Italy	1990	Rionero In Vulture	H-1	5.8	34.5	575	0.866	0.078	4.8	0.230	0.73	15.52

Table A.11: Ground Motion Suite for F5S4B Building with 68% Probability of Exceedence in 50 Years for NEHRP Class B Site

Earthquake Name	Year	Station Name	Component	M_w	R_{jb} (km)	Vs30 (m/s)	Scale Factor	PGA (g)	PGV (cm/s)	Sa_{T1} (g)	Arias Intensity (cm/s)	Housner Intensity (cm)
Chi-Chi Taiwan-04	1999	TTN051	H-2	6.2	37.54	665	1.017	0.068	6.6	0.214	0.39	16.25
Tottori Japan	2000	OKYH08	H-1	6.61	24.84	694	1.001	0.228	6.6	1.111	5.90	20.05
Tottori Japan	2000	SMNH12	H-1	6.61	45.07	590	0.999	0.232	9.9	1.271	8.85	15.58
Chi-Chi Taiwan-04	1999	CHY052	H-2	6.2	45.33	573	0.978	0.045	3.7	0.096	0.35	15.14
Kobe Japan	1995	Chihaya	H-2	6.9	49.91	609	0.976	0.107	4.0	0.340	1.48	12.24
Darfield New Zealand	2010	RPZ	H-1	7.0	57.37	638	1.098	0.052	3.7	0.108	0.37	16.09
Tottori Japan	2000	OKYH07	H-2	6.61	15.23	940	1.106	0.141	14.0	0.281	3.63	31.74
Duzce Turkey	1999	Lamont 1060	H-2	7.14	25.78	782	1.129	0.060	6.5	0.138	0.56	18.38
El Mayor-Cucapah Mexico	2010	Anza Borrego S.P. - Tierra Blan	H-1	7.2	57.94	585	0.948	0.038	11.8	0.073	0.51	20.40
Kocaeli Turkey	1999	Istanbul	H-1	7.51	49.66	595	1.133	0.048	8.7	0.104	0.61	20.06
Kobe Japan	1995	OKA	H-2	6.9	86.93	609	1.135	0.068	4.1	0.134	0.79	11.28
Chi-Chi Taiwan-04	1999	TCU138	H-2	6.2	33.53	653	1.168	0.056	10.3	0.113	0.55	33.92
Tottori Japan	2000	SMN006	H-2	6.61	72.4	627	1.175	0.082	3.7	0.188	1.11	11.81
Tottori Japan	2000	OKYH05	H-1	6.61	46.75	610	1.175	0.128	8.9	0.444	2.00	20.59
Kocaeli Turkey	1999	Istanbul	H-2	7.51	49.66	595	1.195	0.072	10.3	0.109	0.57	20.57
Chi-Chi Taiwan-04	1999	TTN051	H-1	6.2	37.54	665	0.893	0.068	4.2	0.150	0.58	13.10
Darfield New Zealand	2010	RPZ	H-2	7.0	57.37	638	0.883	0.043	4.9	0.096	0.40	17.09
Sitka Alaska	1972	Sitka Observatory	H-1	7.68	34.61	650	0.878	0.085	8.0	0.220	0.99	16.09
Bam Iran	2003	Mohammad Abad-e-Madkoon	H-2	6.6	46.2	575	1.231	0.088	5.1	0.283	0.96	19.54
Chalfant Valley-01	1986	Bishop - Paradise Lodge	H-2	5.77	14.99	585	0.868	0.076	7.9	0.279	0.32	17.11

Table A.12: Ground Motion Suite for F8S3B Building with 68% Probability of Exceedence in 50 Years for NEHRP Class B Site

Earthquake Name	Year	Station Name	Component	M_w	R_{jb} (km)	Vs30 (m/s)	Scale Factor	PGA (g)	PGV (cm/s)	Sa_{T1} (g)	Arias Intensity (cm/s)	Housner Intensity (cm)
El Mayor-Cucapah Mexico	2010	Anza Borrego S.P. - Tierra Blan	H-2	7.2	57.94	585	1.125	0.041	8.8	0.075	0.55	25.14
Chi-Chi Taiwan-04	1999	TCU138	H-2	6.2	33.53	653	1.108	0.053	9.8	0.107	0.49	32.17
Tottori Japan	2000	OKYH08	H-1	6.61	24.84	694	1.108	0.253	7.3	1.230	7.23	22.20
Darfield New Zealand	2010	RPZ	H-1	7.0	57.37	638	1.138	0.054	3.8	0.112	0.40	16.68
Chi-Chi Taiwan-04	1999	TTN051	H-2	6.2	37.54	665	1.100	0.073	7.2	0.232	0.45	17.57
Duzce Turkey	1999	Lamont 1060	H-2	7.14	25.78	782	1.167	0.062	6.7	0.143	0.59	19.01
Kocaeli Turkey	1999	Istanbul	H-1	7.51	49.66	595	1.170	0.050	8.9	0.107	0.65	20.71
Kobe Japan	1995	Chihaya	H-2	6.9	49.91	609	1.189	0.131	4.9	0.414	2.20	14.91
Tottori Japan	2000	OKYH07	H-2	6.61	15.23	940	1.044	0.133	13.2	0.265	3.23	29.95
Kocaeli Turkey	1999	Istanbul	H-2	7.51	49.66	595	1.210	0.073	10.4	0.111	0.58	20.82
Tottori Japan	2000	OKYH05	H-1	6.61	46.75	610	1.216	0.133	9.2	0.460	2.15	21.31
Tottori Japan	2000	SMNH12	H-1	6.61	45.07	590	1.221	0.283	12.2	1.555	13.24	19.06
Chi-Chi Taiwan-04	1999	CHY052	H-2	6.2	45.33	573	1.026	0.047	3.9	0.101	0.38	15.88
Hector Mine	1999	San Bernardino - Del Rosa Wk Sta	H-2	7.13	96.91	643	1.276	0.032	10.2	0.068	0.38	30.21
Chi-Chi Taiwan-04	1999	TTN051	H-1	6.2	37.54	665	0.983	0.074	4.6	0.166	0.70	14.43
Kobe Japan	1995	MZH	H-1	6.9	69.04	609	0.983	0.067	4.9	0.097	0.68	14.93
Bam Iran	2003	Mohammad Abad-e-Madkoon	H-2	6.6	46.2	575	1.282	0.092	5.3	0.295	1.04	20.35
El Mayor-Cucapah Mexico	2010	Glamis Black Mountain Rd	H-2	7.2	89.69	743	1.282	0.047	4.9	0.096	0.68	18.22
Sitka Alaska	1972	Sitka Observatory	H-1	7.68	34.61	650	0.974	0.094	8.9	0.244	1.22	17.85
Hector Mine	1999	San Bernardino - Del Rosa Wk Sta	H-1	7.13	96.91	643	1.320	0.042	9.3	0.087	0.37	20.67

Table A.13: Ground Motion Suite for F2S2B Building with 50% Probability of Exceedence in 50 Years for NEHRP Class D Site

Earthquake Name	Year	Station Name	Component	M_w	R_{jb} (km)	Vs30 (m/s)	Scale Factor	PGA (g)	PGV (cm/s)	Sa_{T1} (g)	Arias Intensity (cm/s)	Housner Intensity (cm)
Parkfield-02 CA	2004	PARKFIELD - 1-STORY SCHOOL BLDG	H-2	6.0	0.95	270	1.085	0.314	51.4	0.381	11.69	169.87
Tottori Japan	2000	SMN001	H-2	6.61	14.42	331	1.078	0.271	20.6	0.621	6.84	69.19
El Mayor-Cucapah Mexico	2010	El Centro - Meadows Union School	H-1	7.2	27.81	276	1.091	0.203	26.0	0.550	14.50	77.63
Tottori Japan	2000	OKY005	H-1	6.61	28.81	293	1.074	0.310	13.3	0.655	9.92	49.42
Mammoth Lakes-04	1980	Convict Creek	H-1	5.7	1.37	382	1.098	0.408	14.5	1.171	7.94	39.97
Mammoth Lakes-06	1980	Convict Creek	H-1	5.94	6.44	382	1.069	0.284	20.4	0.798	4.58	45.33
Morgan Hill	1984	Gilroy Array 4	H-1	6.19	11.53	222	1.065	0.239	20.3	0.447	8.28	77.51
Darfield New Zealand	2010	Papanui High School	H-1	7.0	18.73	263	1.063	0.224	54.5	0.332	14.58	172.13
Parkfield-02 CA	2004	PARKFIELD - UPSAR 01	H-1	6.0	9.63	358	1.106	0.203	16.7	0.453	6.84	51.71
Tottori Japan	2000	SMN001	H-1	6.61	14.42	331	1.106	0.261	14.1	0.764	7.21	47.64
Imperial Valley-02	1940	El Centro Array 9	H-2	6.95	6.09	213	1.111	0.234	34.8	0.366	14.69	127.27
El Mayor-Cucapah Mexico	2010	El Centro Array 4	H-1	7.2	35.08	209	1.111	0.273	29.2	0.485	16.38	80.14
Darfield New Zealand	2010	Papanui High School	H-2	7.0	18.73	263	1.117	0.204	87.2	0.294	16.48	198.66
Mammoth Lakes-03	1980	Convict Creek	H-1	5.91	2.67	382	1.119	0.261	22.2	0.587	5.70	78.50
Kobe Japan	1995	Shin-Osaka	H-2	6.9	19.14	256	1.043	0.243	22.8	0.451	7.09	113.18
Big Bear-01	1992	Desert Hot Springs	H-1	6.46	39.52	359	1.126	0.254	21.4	0.429	7.97	81.79
Tottori Japan	2000	OKY005	H-2	6.61	28.81	293	1.126	0.380	22.3	0.767	9.74	55.52
Parkfield-02 CA	2004	PARKFIELD - HOG CANYON	H-2	6.0	0.73	364	1.041	0.265	20.5	0.605	6.57	67.01
El Mayor-Cucapah Mexico	2010	TAMAULIPAS	H-2	7.2	25.32	242	1.041	0.236	55.0	0.787	20.44	119.38
Darfield New Zealand	2010	Pages Road Pumping Station	H-1	7.0	24.55	206	1.132	0.224	33.3	0.520	13.50	103.11

Table A.14: Ground Motion Suite for F5S4B Building with 50% Probability of Exceedence in 50 Years for NEHRP Class D Site

Earthquake Name	Year	Station Name	Component	M_w	R_{jb} (km)	Vs30 (m/s)	Scale Factor	PGA (g)	PGV (cm/s)	Sa_{T1} (g)	Arias Intensity (cm/s)	Housner Intensity (cm)
Big Bear-01	1992	Desert Hot Springs	H-2	6.46	39.52	359	1.250	0.225	20.7	0.519	9.70	86.80
Parkfield-02 CA	2004	Parkfield - Vineyard Cany 3W	H-1	6.0	4.43	309	1.250	0.353	23.9	1.011	14.00	91.14
Imperial Valley-06	1979	Aeropuerto Mexicali	H-2	6.53	0.0	260	1.248	0.338	30.2	1.105	13.94	87.11
Parkfield-02 CA	2004	Parkfield - Fault Zone 8	H-1	6.0	3.05	309	1.245	0.715	27.4	1.576	24.10	57.12
Parkfield-02 CA	2004	Parkfield - Vineyard Cany 3W	H-2	6.0	4.43	309	1.258	0.390	25.6	1.111	15.30	79.17
Kobe Japan	1995	Yae	H-1	6.9	27.77	256	1.260	0.199	26.7	0.212	17.30	151.37
Chalfant Valley-02	1986	Bishop - LADWP South St	H-1	6.19	14.38	303	1.260	0.313	24.7	0.578	8.15	92.71
Mammoth Lakes-02	1980	Mammoth Lakes H. S.	H-2	5.69	1.45	347	1.238	0.547	29.7	1.640	19.75	61.77
Big Bear-01	1992	Desert Hot Springs	H-1	6.46	39.52	359	1.235	0.278	23.5	0.471	9.59	89.76
Northwest China-01	1997	Jiashi	H-2	5.9	12.62	240	1.265	0.296	20.6	0.647	9.97	58.92
El Mayor-Cucapah Mexico	2010	El Centro Array 7	H-1	7.2	27.42	211	1.225	0.312	26.4	0.767	24.54	83.50
Darfield New Zealand	2010	Christchurch Hospital	H-1	7.0	18.4	194	1.275	0.267	85.7	0.320	20.55	219.08
Darfield New Zealand	2010	Christchurch Hospital	H-2	7.0	18.4	194	1.278	0.195	27.6	0.255	11.39	115.52
Landers	1992	Morongo Valley Hall (GEOS 58)	H-1	7.28	40.67	368	1.278	0.240	21.3	0.332	16.03	102.79
Parkfield-02 CA	2004	Parkfield - Cholame 6W	H-2	6.0	8.16	252	1.280	0.484	22.1	0.848	13.89	56.33
Darfield New Zealand	2010	SPFS	H-1	7.0	29.86	390	1.218	0.195	24.9	0.342	15.24	111.14
Landers	1992	Fun Valley	H-2	7.28	25.02	389	1.218	0.251	21.2	0.382	18.43	77.09
El Mayor-Cucapah Mexico	2010	Meloland E Holton Rd.	H-1	7.2	30.18	196	1.215	0.240	36.4	0.582	27.81	110.67
Darfield New Zealand	2010	SPFS	H-2	7.0	29.86	390	1.285	0.206	27.7	0.368	15.71	105.52
Parkfield-02 CA	2004	Hog Canyon	H-1	6.0	4.51	376	1.288	0.333	25.8	0.758	10.33	84.02

Table A.15: Ground Motion Suite for F8S3B Building with 50% Probability of Exceedence in 50 Years for NEHRP Class D Site

Earthquake Name	Year	Station Name	Component	M_w	R_{jb} (km)	Vs30 (m/s)	Scale Factor	PGA (g)	PGV (cm/s)	Sa_{T1} (g)	Arias Intensity (cm/s)	Housner Intensity (cm)
Parkfield-02 CA	2004	PARKFIELD - JOAQUIN CANYON	H-1	6.0	3.83	379	1.328	0.824	33.7	2.009	32.69	90.42
Big Bear-01	1992	Desert Hot Springs	H-1	6.46	39.52	359	1.330	0.300	25.3	0.507	11.12	96.61
Parkfield-02 CA	2004	Parkfield - Cholame 4AW	H-1	6.0	4.81	283	1.330	0.402	35.7	1.053	9.13	93.07
El Mayor-Cucapah Mexico	2010	El Centro - Meadows Union School	H-2	7.2	27.81	276	1.332	0.264	39.6	0.387	16.22	139.96
Landers	1992	Fun Valley	H-1	7.28	25.02	389	1.320	0.285	31.9	0.432	21.56	88.58
El Mayor-Cucapah Mexico	2010	TAMAULIPAS	H-2	7.2	25.32	242	1.338	0.303	70.6	1.012	33.75	153.39
Landers	1992	Morongo Valley Hall (GEOS 58)	H-1	7.28	40.67	368	1.319	0.248	22.0	0.343	17.08	106.09
Kobe Japan	1995	Kakogawa	H-1	6.9	22.5	312	1.314	0.316	27.3	0.936	18.13	128.65
El Mayor-Cucapah Mexico	2010	Meloland E Holton Rd.	H-1	7.2	30.18	196	1.314	0.259	39.3	0.629	32.49	119.63
Darfield New Zealand	2010	Christchurch Hospital	H-2	7.0	18.4	194	1.346	0.205	29.1	0.269	12.63	121.64
Morgan Hill	1984	Gilroy Array 4	H-2	6.19	11.53	222	1.348	0.470	23.3	0.713	14.32	85.55
Darfield New Zealand	2010	SPFS	H-2	7.0	29.86	390	1.348	0.216	29.1	0.386	17.28	110.68
Imperial Valley-06	1979	Calexico Fire Station	H-1	6.53	10.45	231	1.308	0.362	29.4	0.783	15.00	85.30
Morgan Hill	1984	Gilroy Array 4	H-1	6.19	11.53	222	1.351	0.303	25.8	0.567	13.32	98.33
El Mayor-Cucapah Mexico	2010	El Centro Array 7	H-2	7.2	27.42	211	1.306	0.313	30.9	0.823	23.96	111.02
Hector Mine	1999	Joshua Tree	H-2	7.13	31.06	379	1.295	0.247	32.0	0.264	10.74	94.55
Parkfield-02 CA	2004	PARKFIELD - UPSAR 10	H-1	6.0	8.65	342	1.364	0.420	32.4	0.538	16.41	82.72
Parkfield	1966	Cholame - Shandon Array 5	H-2	6.19	9.58	290	1.367	0.503	30.8	0.653	11.97	76.58
Landers	1992	Fun Valley	H-2	7.28	25.02	389	1.367	0.282	23.8	0.429	23.22	86.53
El Mayor-Cucapah Mexico	2010	Bonds Corner	H-2	7.2	30.75	223	1.272	0.350	24.9	1.051	30.49	104.32

Table A.16: Ground Motion Suite for F2S2B Building with 50% Probability of Exceedence in 50 Years for NEHRP Class C Site

Earthquake Name	Year	Station Name	Component	M_w	R_{jb} (km)	Vs30 (m/s)	Scale Factor	PGA (g)	PGV (cm/s)	Sa_{T1} (g)	Arias Intensity (cm/s)	Housner Intensity (cm)
Parkfield-02 CA	2004	Parkfield - Fault Zone 15	H-1	6.0	0.8	308	1.105	0.160	25.2	0.440	4.05	83.10
Duzce Turkey	1999	Lamont 531	H-1	7.14	8.03	638	1.100	0.176	12.0	0.262	5.51	32.23
Landers	1992	Indio - Jackson Road	H-2	7.28	48.84	292	1.116	0.141	15.6	0.272	9.35	85.21
Trinidad	1980	Rio Dell Overpass E Ground	H-2	7.2	76.06	312	1.116	0.150	10.8	0.328	4.87	43.33
Mammoth Lakes-03	1980	Long Valley Dam (Upr L Abut)	H-2	5.91	10.31	537	1.096	0.213	14.5	0.425	4.35	33.49
Parkfield-02 CA	2004	Parkfield - Gold Hill 5W	H-1	6.0	11.11	441	1.122	0.277	9.1	0.458	4.48	30.12
Kocaeli Turkey	1999	Cekmece	H-1	7.51	64.95	346	1.089	0.193	18.4	0.402	5.79	38.93
Duzce Turkey	1999	Lamont 531	H-2	7.14	8.03	638	1.087	0.134	14.6	0.254	4.97	47.20
Morgan Hill	1984	Gilroy Array 3	H-1	6.19	13.01	350	1.127	0.219	12.4	0.564	4.38	54.74
Trinidad	1980	Rio Dell Overpass W Ground	H-2	7.2	76.06	312	1.082	0.170	11.9	0.419	5.34	40.93
Coyote Lake	1979	Coyote Lake Dam - Southwest Abutment	H-1	5.74	5.3	561	1.131	0.159	13.3	0.368	2.47	35.89
El Mayor-Cucapah Mexico	2010	Salton City	H-1	7.2	72.44	324	1.138	0.222	10.3	0.535	4.76	42.09
Livermore-01	1980	Del Valle Dam (Toe)	H-2	5.8	23.92	403	1.071	0.274	16.5	0.356	2.51	63.08
Chi-Chi Taiwan-04	1999	CHY035	H-2	6.2	25.01	573	1.142	0.153	17.0	0.221	3.84	67.60
Landers	1992	Amboy	H-2	7.28	69.21	383	1.069	0.156	21.2	0.424	8.78	88.50
Darfield New Zealand	2010	RKAC	H-1	7.0	13.37	296	1.147	0.191	12.1	0.394	5.85	50.57
Darfield New Zealand	2010	RKAC	H-2	7.0	13.37	296	1.153	0.221	20.6	0.507	6.88	60.36
Parkfield-02 CA	2004	Parkfield - Vineyard Cany 5W	H-2	6.0	9.2	320	1.155	0.228	12.4	1.011	3.59	52.75
Chi-Chi Taiwan-04	1999	CHY028	H-2	6.2	17.63	543	1.054	0.216	14.8	0.462	3.70	36.54
Parkfield-02 CA	2004	Parkfield - Gold Hill 2W	H-1	6.0	2.13	290	1.162	0.191	17.3	0.487	3.30	38.32

Table A.17: Ground Motion Suite for F5S4B Building with 50% Probability of Exceedence in 50 Years for NEHRP Class C Site

Earthquake Name	Year	Station Name	Component	M_w	R_{jb} (km)	Vs30 (m/s)	Scale Factor	PGA (g)	PGV (cm/s)	Sa_{T1} (g)	Arias Intensity (cm/s)	Housner Intensity (cm)
Kocaeli Turkey	1999	Zeytinburnu	H-2	7.51	51.98	342	1.278	0.140	20.2	0.225	5.63	58.86
Landers	1992	North Palm Springs Fire Sta 36	H-1	7.28	26.95	368	1.283	0.178	18.7	0.330	11.66	106.19
Mammoth Lakes-03	1980	Convict Creek	H-2	5.91	2.67	382	1.283	0.238	20.8	0.655	5.79	50.79
Superstition Hills-02	1987	Plaster City	H-1	6.54	22.25	317	1.271	0.173	12.5	0.386	4.92	62.29
Landers	1992	Amboy	H-1	7.28	69.21	383	1.286	0.148	23.4	0.345	9.47	81.82
Landers	1992	Thousand Palms Post Office	H-2	7.28	36.93	334	1.289	0.150	17.8	0.303	8.09	80.37
Livermore-01	1980	San Ramon - Eastman Kodak	H-1	5.8	15.19	378	1.266	0.189	26.3	0.228	3.44	102.32
Trinidad	1980	Rio Dell Overpass E Ground	H-2	7.2	76.06	312	1.266	0.170	12.3	0.372	6.27	49.15
Chi-Chi Taiwan-04	1999	CHY034	H-2	6.2	28.45	379	1.266	0.130	11.9	0.200	3.47	61.79
Landers	1992	North Palm Springs	H-1	7.28	26.84	345	1.266	0.172	14.1	0.391	10.48	77.75
Darfield New Zealand	2010	FDCS	H-1	7.0	90.17	390	1.263	0.130	16.8	0.207	4.77	80.42
Trinidad	1980	Rio Dell Overpass W Ground	H-2	7.2	76.06	312	1.292	0.203	14.2	0.501	7.62	48.86
Big Bear-01	1992	North Palm Springs Fire Sta 36	H-2	6.46	40.87	368	1.260	0.163	14.7	0.340	6.31	60.65
Hector Mine	1999	Mecca - CVWD Yard	H-1	7.13	91.96	318	1.296	0.131	32.0	0.154	4.51	98.16
Parkfield-02 CA	2004	PARKFIELD - DONNA LEE	H-1	6.0	4.25	657	1.258	0.370	19.1	0.724	5.77	48.31
Darfield New Zealand	2010	CSHS	H-2	7.0	43.6	638	1.308	0.151	15.6	0.225	6.70	77.30
Mammoth Lakes-02	1980	Convict Creek	H-2	5.69	2.91	382	1.309	0.239	17.3	0.438	3.53	59.51
Chi-Chi Taiwan-04	1999	CHY035	H-1	6.2	25.01	573	1.240	0.145	21.2	0.246	3.10	64.80
Chi-Chi Taiwan-04	1999	CHY080	H-2	6.2	12.44	496	1.319	0.177	21.6	0.361	5.18	62.70
Landers	1992	North Palm Springs Fire Sta 36	H-2	7.28	26.95	368	1.322	0.183	15.2	0.349	10.29	71.56

Table A.18: Ground Motion Suite for F8S3B Building with 50% Probability of Exceedence in 50 Years for NEHRP Class C Site

Earthquake Name	Year	Station Name	Component	M_w	R_{jb} (km)	Vs30 (m/s)	Scale Factor	PGA (g)	PGV (cm/s)	Sa_{T1} (g)	Arias Intensity (cm/s)	Housner Intensity (cm)
Landers	1992	Thousand Palms Post Office	H-1	7.28	36.93	334	1.079	0.108	21.8	0.315	5.60	79.33
Landers	1992	San Bernardino - E & Hospitality	H-1	7.28	79.76	297	1.063	0.083	21.1	0.136	4.50	93.81
Big Bear-01	1992	San Bernardino - E & Hospitality	H-2	6.46	34.98	297	1.084	0.109	12.8	0.180	3.50	69.19
Big Bear-01	1992	San Bernardino - E & Hospitality	H-1	6.46	34.98	297	1.060	0.098	14.6	0.157	3.12	65.19
Big Bear-01	1992	North Palm Springs Fire Sta 36	H-2	6.46	40.87	368	1.060	0.137	12.4	0.286	4.46	51.02
Upland	1990	Pomona - 4th & Locust FF	H-1	5.63	7.17	384	1.060	0.197	11.2	0.387	3.30	36.84
Joshua Tree CA	1992	Whitewater Trout Farm	H-1	6.1	28.97	425	1.086	0.233	12.7	0.430	4.06	36.69
Darfield New Zealand	2010	RKAC	H-2	7.0	13.37	296	1.058	0.202	18.9	0.465	5.79	55.39
Mammoth Lakes-04	1980	Convict Creek	H-1	5.7	1.37	382	1.088	0.404	14.4	1.161	7.81	39.63
Trinidad	1980	Rio Dell Overpass E Ground	H-2	7.2	76.06	312	1.088	0.147	10.6	0.320	4.64	42.27
Landers	1992	North Palm Springs Fire Sta 36	H-2	7.28	26.95	368	1.054	0.146	12.2	0.279	6.54	57.06
Chi-Chi Taiwan-04	1999	CHY086	H-2	6.2	33.63	665	1.093	0.120	12.1	0.160	2.18	46.61
Mammoth Lakes-02	1980	Convict Creek	H-2	5.69	2.91	382	1.093	0.199	14.4	0.366	2.46	49.67
Kocaeli Turkey	1999	Fatih	H-2	7.51	53.34	387	1.095	0.177	16.8	0.415	8.26	37.12
Imperial Valley-06	1979	Coachella Canal 4	H-2	6.53	49.1	336	1.050	0.134	16.8	0.146	2.27	46.77
Parkfield-02 CA	2004	PARKFIELD - DONNA LEE	H-2	6.0	4.25	657	1.047	0.390	14.7	1.799	7.99	41.53
Chi-Chi Taiwan-04	1999	CHY080	H-1	6.2	12.44	496	1.103	0.133	19.5	0.240	2.74	57.81
Kocaeli Turkey	1999	Zeytinburnu	H-2	7.51	51.98	342	1.037	0.113	16.4	0.182	3.71	47.73
Hector Mine	1999	Fort Irwin	H-2	7.13	65.04	367	1.111	0.140	15.8	0.230	3.15	54.71
Mammoth Lakes-06	1980	Convict Creek	H-2	5.94	6.44	382	1.032	0.325	16.8	1.124	5.54	47.25

Table A.19: Ground Motion Suite for F2S2B Building with 50% Probability of Exceedence in 50 Years for Generic Rock Site

Earthquake Name	Year	Station Name	Component	M_w	R_{jb} (km)	Vs30 (m/s)	Scale Factor	PGA (g)	PGV (cm/s)	Sa_{T1} (g)	Arias Intensity (cm/s)	Housner Intensity (cm)
Chi-Chi Taiwan-04	1999	CHY035	H-1	6.2	25.01	573	1.029	0.120	17.6	0.204	2.13	53.79
Tottori Japan	2000	OKYH10	H-1	6.61	46.36	554	1.033	0.296	9.4	0.626	11.31	20.44
Bam Iran	2003	Mohammad Abad-e-Madkoon	H-1	6.6	46.2	575	1.022	0.126	13.0	0.282	1.74	44.31
Darfield New Zealand	2010	CSHS	H-2	7.0	43.6	638	1.039	0.120	12.4	0.178	4.23	61.40
Darfield New Zealand	2010	PEEC	H-1	7.0	52.13	551	1.018	0.124	11.3	0.267	3.03	35.72
Helena Montana-01	1935	Carroll College	H-2	6.0	2.07	593	1.014	0.158	14.0	0.399	1.04	39.18
Parkfield-02 CA	2004	Parkfield - Stone Corral 2E	H-2	6.0	5.23	566	1.014	0.190	9.6	0.424	2.09	28.22
Darfield New Zealand	2010	OXZ	H-1	7.0	30.63	482	1.012	0.127	11.8	0.300	5.12	47.45
Tottori Japan	2000	SMNH03	H-1	6.61	52.3	440	1.051	0.166	10.0	0.255	4.50	23.16
Duzce Turkey	1999	Lamont 1061	H-2	7.14	11.46	481	1.008	0.132	12.2	0.202	2.54	35.26
Chi-Chi Taiwan-04	1999	CHY086	H-2	6.2	33.63	665	1.005	0.110	11.1	0.147	1.85	42.86
Parkfield-02 CA	2004	Bear Valley Ranch Parkfield CA USA	H-2	6.0	3.38	528	1.002	0.161	9.2	0.370	1.67	38.07
Duzce Turkey	1999	Lamont 1059	H-1	7.14	4.17	551	1.002	0.153	12.9	0.414	3.90	25.95
Parkfield-02 CA	2004	Bear Valley Ranch Parkfield CA USA	H-1	6.0	3.38	528	0.995	0.162	8.6	0.399	2.10	27.07
Darfield New Zealand	2010	OXZ	H-2	7.0	30.63	482	0.995	0.145	11.4	0.269	4.13	46.82
Tottori Japan	2000	SMNH10	H-1	6.61	15.58	967	0.986	0.156	8.5	0.420	1.99	31.32
Tottori Japan	2000	OKYH09	H-1	6.61	21.22	519	0.983	0.182	7.5	1.019	10.64	27.38
Parkfield-02 CA	2004	PARKFIELD - JACK CANYON	H-2	6.0	9.12	576	0.983	0.167	10.5	0.533	1.70	24.81
Tottori Japan	2000	OKYH09	H-2	6.61	21.22	519	1.079	0.313	9.1	1.778	15.75	28.82
Parkfield-02 CA	2004	Parkfield - Stone Corral 2E	H-1	6.0	5.23	566	1.088	0.197	14.0	0.656	2.55	41.43

Table A.20: Ground Motion Suite for F5S4B Building with 50% Probability of Exceedence in 50 Years for Generic Rock Site

Earthquake Name	Year	Station Name	Component	M_w	R_{jb} (km)	Vs30 (m/s)	Scale Factor	PGA (g)	PGV (cm/s)	Sa_{T1} (g)	Arias Intensity (cm/s)	Housner Intensity (cm)
Parkfield-02 CA	2004	Bear Valley Ranch Parkfield CA USA	H-2	6.0	3.38	528	1.072	0.172	9.9	0.396	1.92	40.76
Duzce Turkey	1999	Lamont 1059	H-1	7.14	4.17	551	1.083	0.165	13.9	0.448	4.56	28.06
Chi-Chi Taiwan-04	1999	CHY006	H-2	6.2	24.58	438	1.094	0.119	10.6	0.231	2.05	36.48
Upland	1990	Pomona - 4th & Locust FF	H-2	5.63	7.17	384	1.049	0.217	8.2	0.639	2.59	34.45
Duzce Turkey	1999	Lamont 1061	H-1	7.14	11.46	481	1.044	0.106	11.7	0.235	2.53	35.56
Chi-Chi Taiwan-04	1999	TCU116	H-1	6.2	28.72	493	1.100	0.121	21.0	0.140	1.42	62.76
Basso Tirreno Italy	1978	Naso	H-1	6.0	17.15	621	1.040	0.156	8.5	0.262	2.89	24.46
Darfield New Zealand	2010	FDCS	H-2	7.0	90.17	390	1.036	0.129	9.8	0.237	2.87	42.11
Landers	1992	Big Bear Lake - Civic Center	H-2	7.28	45.48	430	1.110	0.183	8.4	0.512	7.03	33.12
Bam Iran	2003	Mohammad Abad-e-Madkoon	H-1	6.6	46.2	575	1.032	0.127	13.1	0.284	1.77	44.72
Parkfield-02 CA	2004	Parkfield - Gold Hill 3W	H-2	6.0	4.66	511	1.032	0.447	16.2	1.085	4.78	34.81
Morgan Hill	1984	San Justo Dam (L Abut)	H-1	6.19	31.88	544	1.113	0.090	8.1	0.131	2.33	31.38
Landers	1992	Forest Falls Post Office	H-1	7.28	45.34	436	1.027	0.118	10.8	0.293	3.48	45.22
Chi-Chi Taiwan-04	1999	TCU122	H-1	6.2	23.14	475	1.027	0.121	14.9	0.159	1.24	49.22
Darfield New Zealand	2010	LSRC	H-2	7.0	79.53	561	1.026	0.101	13.5	0.125	1.70	45.66
Tottori Japan	2000	SMNH10	H-1	6.61	15.58	967	1.119	0.178	9.7	0.477	2.57	35.55
Parkfield-02 CA	2004	Parkfield - Gold Hill 3E	H-1	6.0	5.79	451	1.123	0.235	14.1	0.493	3.10	27.00
Parkfield-02 CA	2004	PARKFIELD - JACK CANYON	H-2	6.0	9.12	576	1.130	0.192	12.0	0.613	2.25	28.52
Hector Mine	1999	Morongo Valley Fire Station	H-2	7.13	53.21	396	1.008	0.087	11.7	0.135	2.03	63.58
Parkfield-02 CA	2004	PARKFIELD - TEMBLOR	H-1	6.0	12.29	525	1.139	0.118	7.2	0.271	1.90	29.45

Table A.21: Ground Motion Suite for F8S3B Building with 50% Probability of Exceedence in 50 Years for Generic Rock Site

Earthquake Name	Year	Station Name	Component	M_w	R_{jb} (km)	Vs30 (m/s)	Scale Factor	PGA (g)	PGV (cm/s)	Sa_{T1} (g)	Arias Intensity (cm/s)	Housner Intensity (cm)
Double Springs	1994	Woodfords	H-2	5.9	12.48	393	1.135	0.099	8.9	0.175	1.46	39.83
Parkfield-02 CA	2004	Parkfield - Gold Hill 5W	H-1	6.0	11.11	441	1.135	0.281	9.2	0.463	4.58	30.46
Parkfield-02 CA	2004	Bear Valley Ranch Parkfield CA USA	H-2	6.0	3.38	528	1.115	0.179	10.3	0.412	2.07	42.38
Duzce Turkey	1999	Lamont 1061	H-1	7.14	11.46	481	1.115	0.113	12.5	0.250	2.88	37.96
Parkfield-02 CA	2004	Parkfield - Gold Hill 3W	H-2	6.0	4.66	511	1.140	0.494	17.9	1.199	5.83	38.45
Chi-Chi Taiwan-04	1999	CHY006	H-2	6.2	24.58	438	1.142	0.124	11.1	0.241	2.24	38.08
Upland	1990	Pomona - 4th & Locust FF	H-2	5.63	7.17	384	1.106	0.229	8.7	0.673	2.88	36.32
Chi-Chi Taiwan-04	1999	CHY042	H-2	6.2	34.1	665	1.169	0.111	10.6	0.161	1.72	41.67
Parkfield-02 CA	2004	Parkfield - Stone Corral 2E	H-1	6.0	5.23	566	1.182	0.214	15.2	0.713	3.01	45.02
Darfield New Zealand	2010	LSRC	H-1	7.0	79.53	561	1.070	0.082	10.5	0.106	1.58	49.81
Darfield New Zealand	2010	FDCS	H-2	7.0	90.17	390	1.070	0.133	10.1	0.245	3.06	43.49
Landers	1992	Big Bear Lake - Civic Center	H-2	7.28	45.48	430	1.193	0.197	9.1	0.550	8.11	35.59
Darfield New Zealand	2010	PEEC	H-1	7.0	52.13	551	1.052	0.128	11.7	0.275	3.24	36.90
Mammoth Lakes-03	1980	Long Valley Dam (Upr L Abut)	H-2	5.91	10.31	537	1.051	0.204	13.9	0.408	4.00	32.12
Chi-Chi Taiwan-04	1999	CHY046	H-2	6.2	38.11	442	1.205	0.145	10.8	0.280	1.59	40.86
Chi-Chi Taiwan-04	1999	CHY028	H-2	6.2	17.63	543	1.047	0.215	14.8	0.459	3.65	36.32
Tottori Japan	2000	SMNH02	H-2	6.61	23.64	503	1.209	0.386	12.6	1.373	16.34	30.53
Tottori Japan	2000	SMNH10	H-1	6.61	15.58	967	1.209	0.192	10.5	0.515	2.99	38.41
Morgan Hill	1984	San Justo Dam (L Abut)	H-1	6.19	31.88	544	1.214	0.098	8.9	0.143	2.77	34.23
Tottori Japan	2000	OKYH14	H-2	6.61	26.51	710	1.038	0.470	24.1	2.536	13.54	45.54

Table A.22: Ground Motion Suite for F2S2B Building with 50% Probability of Exceedence in 50 Years for NEHRP Class B Site

Earthquake Name	Year	Station Name	Component	M_w	R_{jb} (km)	Vs30 (m/s)	Scale Factor	PGA (g)	PGV (cm/s)	Sa_{T1} (g)	Arias Intensity (cm/s)	Housner Intensity (cm)
Tottori Japan	2000	OKYH07	H-1	6.61	15.23	940	1.032	0.191	8.8	0.317	2.84	25.37
Tottori Japan	2000	OKYH14	H-1	6.61	26.51	710	1.055	0.282	11.9	1.513	6.81	22.84
Chalfant Valley-02	1986	Bishop - Paradise Lodge	H-2	6.19	14.97	585	1.069	0.172	13.6	0.541	2.30	39.96
Chi-Chi Taiwan-04	1999	CHY042	H-2	6.2	34.1	665	0.994	0.095	9.0	0.137	1.24	35.44
Parkfield-02 CA	2004	PARKFIELD - JACK CANYON	H-1	6.0	9.12	576	0.993	0.145	6.1	0.313	1.57	19.68
Tottori Japan	2000	SMNH12	H-1	6.61	45.07	590	1.075	0.249	10.7	1.368	10.25	16.77
Tottori Japan	2000	OKYH08	H-2	6.61	24.84	694	0.972	0.234	11.5	0.928	5.55	24.30
Darfield New Zealand	2010	CSHS	H-1	7.0	43.6	638	0.945	0.084	7.7	0.178	2.88	41.61
Parkfield-02 CA	2004	Parkfield - Stone Corral 3E	H-1	6.0	7.68	565	0.944	0.185	8.3	0.691	2.20	31.28
Basso Tirreno Italy	1978	Naso	H-2	6.0	17.15	621	0.939	0.122	6.3	0.239	1.73	17.12
Coyote Lake	1979	Gilroy Array 1	H-2	5.74	10.21	1428	1.162	0.136	12.6	0.409	1.09	28.95
Livermore-01	1980	Tracy - Sewage Treatm Plant	H-2	5.8	53.35	650	1.174	0.093	7.9	0.137	1.12	38.71
Hector Mine	1999	Joshua Tree N.M. - Keys View	H-2	7.13	50.42	686	1.180	0.103	7.6	0.220	1.48	18.65
Helena Montana-01	1935	Carroll College	H-1	6.0	2.07	593	1.183	0.190	6.9	0.454	0.99	17.59
Chi-Chi Taiwan-04	1999	CHY042	H-1	6.2	34.1	665	1.183	0.098	8.3	0.159	1.27	36.33
Hector Mine	1999	Heart Bar State Park	H-1	7.13	61.21	625	1.195	0.090	15.5	0.204	1.97	31.11
Tottori Japan	2000	OKYH08	H-1	6.61	24.84	694	1.226	0.280	8.1	1.362	8.86	24.58
Hector Mine	1999	Heart Bar State Park	H-2	7.13	61.21	625	1.239	0.102	12.8	0.292	2.22	21.99
Chi-Chi Taiwan-04	1999	CHY086	H-1	6.2	33.63	665	0.855	0.098	11.4	0.107	2.03	39.79
Parkfield-02 CA	2004	Parkfield - Stone Corral 3E	H-2	6.0	7.68	565	0.846	0.183	8.4	0.437	1.61	28.70

Table A.23: Ground Motion Suite for F5S4B Building with 50% Probability of Exceedence in 50 Years for NEHRP Class B Site

Earthquake Name	Year	Station Name	Component	M_w	R_{jb} (km)	Vs30 (m/s)	Scale Factor	PGA (g)	PGV (cm/s)	Sa_{T1} (g)	Arias Intensity (cm/s)	Housner Intensity (cm)
Basso Tirreno Italy	1978	Naso	H-2	6.0	17.15	621	1.042	0.135	6.9	0.265	2.12	18.99
Chi-Chi Taiwan-04	1999	CHY042	H-1	6.2	34.1	665	1.029	0.085	7.2	0.138	0.96	31.61
Hector Mine	1999	Heart Bar State Park	H-1	7.13	61.21	625	1.054	0.080	13.7	0.180	1.54	27.44
Tottori Japan	2000	OKYH07	H-1	6.61	15.23	940	1.092	0.202	9.3	0.335	3.18	26.83
Parkfield-02 CA	2004	Parkfield - Stone Corral 3E	H-1	6.0	7.68	565	0.990	0.194	8.7	0.725	2.42	32.81
Parkfield-02 CA	2004	PARKFIELD - JACK CANYON	H-1	6.0	9.12	576	1.104	0.162	6.7	0.348	1.95	21.88
Chalfant Valley-02	1986	Bishop - Paradise Lodge	H-2	6.19	14.97	585	1.113	0.179	14.2	0.563	2.49	41.58
Coyote Lake	1979	Gilroy Array 1	H-2	5.74	10.21	1428	1.117	0.130	12.1	0.393	1.00	27.81
Kocaeli Turkey	1999	Bursa Sivil	H-2	7.51	65.53	613	1.184	0.064	10.7	0.077	1.09	45.76
Livermore-01	1980	Tracy - Sewage Treatm Plant	H-1	5.8	53.35	650	1.194	0.058	7.9	0.065	0.86	41.29
Livermore-01	1980	Tracy - Sewage Treatm Plant	H-2	5.8	53.35	650	0.902	0.071	6.1	0.105	0.66	29.76
Tottori Japan	2000	OKYH08	H-2	6.61	24.84	694	1.213	0.292	14.4	1.158	8.64	30.30
Hector Mine	1999	Joshua Tree N.M. - Keys View	H-2	7.13	50.42	686	1.213	0.106	7.8	0.226	1.56	19.17
Kocaeli Turkey	1999	Bursa Sivil	H-1	7.51	65.53	613	1.219	0.055	9.9	0.080	1.06	46.61
Hector Mine	1999	Joshua Tree N.M. - Keys View	H-1	7.13	50.42	686	1.221	0.094	10.6	0.185	1.29	28.01
Parkfield-02 CA	2004	Parkfield - Stone Corral 3E	H-2	6.0	7.68	565	0.865	0.187	8.6	0.447	1.68	29.32
Potenza Italy	1990	Rionero In Vulture	H-2	5.8	34.5	575	1.261	0.110	6.8	0.414	1.39	24.23
Morgan Hill	1984	UCSC Lick Observatory	H-2	6.19	45.47	714	1.275	0.097	5.0	0.170	1.37	20.92
Parkfield-02 CA	2004	Parkfield - Stone Corral 2E	H-2	6.0	5.23	566	0.840	0.157	8.0	0.351	1.43	23.37
Tottori Japan	2000	SMN006	H-1	6.61	72.4	627	1.292	0.102	9.1	0.173	1.64	22.81

Table A.24: Ground Motion Suite for F8S3B Building with 50% Probability of Exceedence in 50 Years for NEHRP Class B Site

Earthquake Name	Year	Station Name	Component	M_w	R_{jb} (km)	Vs30 (m/s)	Scale Factor	PGA (g)	PGV (cm/s)	Sa_{T1} (g)	Arias Intensity (cm/s)	Housner Intensity (cm)
Livermore-01	1980	Tracy - Sewage Treatm Plant	H-1	5.8	53.35	650	1.122	0.055	7.5	0.061	0.76	38.80
Hector Mine	1999	Heart Bar State Park	H-1	7.13	61.21	625	1.130	0.085	14.7	0.193	1.76	29.41
Kocaeli Turkey	1999	Bursa Sivil	H-1	7.51	65.53	613	1.099	0.049	8.9	0.072	0.86	42.02
Chalfant Valley-02	1986	Bishop - Paradise Lodge	H-2	6.19	14.97	585	1.094	0.176	13.9	0.554	2.41	40.89
Tottori Japan	2000	OKYH07	H-1	6.61	15.23	940	1.139	0.210	9.7	0.350	3.46	27.99
Kocaeli Turkey	1999	Bursa Sivil	H-2	7.51	65.53	613	1.065	0.058	9.6	0.069	0.88	41.19
Parkfield-02 CA	2004	Parkfield - Stone Corral 3E	H-1	6.0	7.68	565	1.052	0.207	9.3	0.770	2.74	34.87
Chi-Chi Taiwan-04	1999	CHY042	H-1	6.2	34.1	665	1.034	0.085	7.2	0.139	0.97	31.75
Coyote Lake	1979	Gilroy Array 1	H-2	5.74	10.21	1428	1.206	0.141	13.0	0.424	1.17	30.03
Parkfield-02 CA	2004	PARKFIELD - JACK CANYON	H-1	6.0	9.12	576	1.268	0.186	7.7	0.400	2.57	25.13
Basso Tirreno Italy	1978	Naso	H-2	6.0	17.15	621	1.273	0.165	8.5	0.324	3.17	23.20
Hector Mine	1999	Joshua Tree N.M. - Keys View	H-1	7.13	50.42	686	1.284	0.099	11.1	0.194	1.43	29.46
Chi-Chi Taiwan-04	1999	TCU084	H-1	6.2	26.83	665	1.333	0.075	9.0	0.094	0.98	40.89
Tottori Japan	2000	OKYH08	H-2	6.61	24.84	694	1.349	0.325	16.0	1.287	10.69	33.70
Parkfield-02 CA	2004	Parkfield - Stone Corral 3E	H-2	6.0	7.68	565	0.922	0.199	9.2	0.477	1.91	31.27
Chi-Chi Taiwan-04	1999	TCU084	H-2	6.2	26.83	665	1.350	0.057	8.0	0.066	0.79	39.11
Parkfield-02 CA	2004	PARKFIELD - JACK CANYON	H-2	6.0	9.12	576	0.904	0.154	9.6	0.490	1.44	22.83
Hector Mine	1999	Joshua Tree N.M. - Keys View	H-2	7.13	50.42	686	1.380	0.121	8.9	0.257	2.02	21.82
Basso Tirreno Italy	1978	Naso	H-1	6.0	17.15	621	0.901	0.135	7.4	0.227	2.17	21.19
Potenza Italy	1990	Rionero In Vulture	H-2	5.8	34.5	575	1.383	0.121	7.4	0.454	1.67	26.59

Table A.25: Ground Motion Suite for F2S2B Building with 10% Probability of Exceedence in 50 Years for NEHRP Class D Site

Earthquake Name	Year	Station Name	Component	M_w	R_{jb} (km)	Vs30 (m/s)	Scale Factor	PGA (g)	PGV (cm/s)	Sa_{T1} (g)	Arias Intensity (cm/s)	Housner Intensity (cm)
El Mayor-Cucapah Mexico	2010	El Centro Differential Array	H-1	7.2	22.83	202	1.064	0.590	31.2	1.625	50.16	116.79
Chalfant Valley-02	1986	Zack Brothers Ranch	H-1	6.19	6.44	316	1.077	0.481	39.6	1.006	22.89	162.01
El Mayor-Cucapah Mexico	2010	El Centro Array 11	H-1	7.2	15.36	196	0.958	0.423	55.3	0.852	46.12	155.86
El Mayor-Cucapah Mexico	2010	RIITO	H-2	7.2	13.7	242	1.109	0.417	42.0	1.143	58.74	161.80
Imperial Valley-06	1979	Bonds Corner	H-1	6.53	0.44	223	0.919	0.550	42.9	1.496	34.30	160.34
Parkfield-02 CA	2004	Parkfield - Fault Zone 14	H-2	6.0	8.45	246	0.890	0.513	37.7	1.684	22.36	129.30
Parkfield-02 CA	2004	Parkfield - Fault Zone 14	H-2	6.0	8.45	246	0.890	0.513	37.7	1.684	22.36	129.30
El Mayor-Cucapah Mexico	2010	MICHOACAN DE OCAMPO	H-1	7.2	13.21	242	1.179	0.634	72.5	1.150	86.36	256.81
El Mayor-Cucapah Mexico	2010	El Centro Differential Array	H-2	7.2	22.83	202	1.181	0.598	45.9	1.904	57.78	177.53
El Mayor-Cucapah Mexico	2010	El Centro - Imperial & Ross	H-1	7.2	19.39	229	1.195	0.460	56.6	1.030	54.51	178.50
El Mayor-Cucapah Mexico	2010	RIITO	H-1	7.2	13.7	242	1.198	0.475	62.7	1.490	58.32	175.00
Managua Nicaragua-01	1972	Managua ESSO	H-2	6.24	3.51	289	1.240	0.408	38.1	0.865	31.46	137.32
Darfield New Zealand	2010	DFHS	H-2	7.0	11.86	344	1.255	0.643	37.3	1.397	45.27	129.02
El Mayor-Cucapah Mexico	2010	El Centro Array 10	H-2	7.2	19.36	203	1.261	0.481	60.1	0.649	58.46	219.18
Chalfant Valley-02	1986	Zack Brothers Ranch	H-2	6.19	6.44	316	1.278	0.512	57.1	0.818	33.20	194.19
Parkfield-02 CA	2004	PARKFIELD - JOAQUIN CANYON	H-2	6.0	3.83	379	1.283	0.632	39.1	1.962	40.63	94.59
Landers	1992	Coolwater	H-2	7.28	19.74	353	1.310	0.547	56.9	0.641	38.17	188.53
El Mayor-Cucapah Mexico	2010	MICHOACAN DE OCAMPO	H-2	7.2	13.21	242	1.316	0.537	57.3	0.992	85.24	219.74
Westmorland	1981	Westmorland Fire Sta	H-2	5.9	6.18	194	1.335	0.665	47.8	1.351	34.54	195.84
El Mayor-Cucapah Mexico	2010	El Centro Array 11	H-2	7.2	15.36	196	0.783	0.459	49.5	0.982	34.64	174.46

Table A.26: Ground Motion Suite for F5S4B Building with 10% Probability of Exceedence in 50 Years for NEHRP Class D Site

Earthquake Name	Year	Station Name	Component	M_w	R_{jb} (km)	Vs30 (m/s)	Scale Factor	PGA (g)	PGV (cm/s)	Sa_{T1} (g)	Arias Intensity (cm/s)	Housner Intensity (cm)
Parkfield-02 CA	2004	Parkfield - Fault Zone 14	H-2	6.0	8.45	246	1.356	0.781	57.4	2.566	51.92	197.06
Imperial Valley-06	1979	Bonds Corner	H-1	6.53	0.44	223	1.372	0.822	64.1	2.235	76.52	239.51
El Mayor-Cucapah Mexico	2010	El Centro Array 11	H-1	7.2	15.36	196	1.265	0.559	73.0	1.126	80.47	205.86
Chalfant Valley-02	1986	Zack Brothers Ranch	H-1	6.19	6.44	316	1.445	0.646	53.2	1.351	41.25	217.49
El Mayor-Cucapah Mexico	2010	El Centro Array 10	H-2	7.2	19.36	203	1.460	0.556	69.6	0.752	78.33	253.70
El Mayor-Cucapah Mexico	2010	MICHOACAN DE OCAMPO	H-1	7.2	13.21	242	1.498	0.805	92.2	1.462	139.43	326.31
Landers	1992	Coolwater	H-2	7.28	19.74	353	1.519	0.634	66.0	0.743	51.33	218.61
El Mayor-Cucapah Mexico	2010	RIITO	H-2	7.2	13.7	242	1.559	0.586	59.0	1.606	116.04	227.41
El Mayor-Cucapah Mexico	2010	El Centro - Imperial & Ross	H-1	7.2	19.39	229	1.570	0.603	74.3	1.353	93.99	234.39
Kocaeli Turkey	1999	Duzce	H-2	7.51	13.6	282	1.572	0.573	87.5	0.970	33.61	356.62
Chalfant Valley-02	1986	Zack Brothers Ranch	H-2	6.19	6.44	316	1.639	0.656	73.3	1.050	54.63	249.10
El Mayor-Cucapah Mexico	2010	RIITO	H-1	7.2	13.7	242	1.700	0.674	89.1	2.115	117.49	248.39
El Mayor-Cucapah Mexico	2010	El Centro Array 10	H-1	7.2	19.36	203	1.726	0.629	78.7	0.990	91.70	235.73
El Mayor-Cucapah Mexico	2010	El Centro - Imperial & Ross	H-2	7.2	19.39	229	1.737	0.643	82.7	2.042	100.86	290.77
Imperial Valley-06	1979	Bonds Corner	H-2	6.53	0.44	223	1.002	0.779	45.0	1.778	62.05	188.12
Westmorland	1981	Westmorland Fire Sta	H-1	5.9	6.18	194	1.754	0.661	77.4	1.357	55.14	314.67
El Mayor-Cucapah Mexico	2010	El Centro Array 11	H-2	7.2	15.36	196	0.989	0.580	62.5	1.240	55.23	220.28
El Mayor-Cucapah Mexico	2010	El Centro Differential Array	H-2	7.2	22.83	202	1.778	0.901	69.0	2.866	130.93	267.23
El Mayor-Cucapah Mexico	2010	El Centro Differential Array	H-1	7.2	22.83	202	1.782	0.988	52.2	2.722	140.63	195.55
Managua Nicaragua-01	1972	Managua ESSO	H-2	6.24	3.51	289	1.787	0.589	54.9	1.247	65.40	197.99

Table A.27: Ground Motion Suite for F8S3B Building with 10% Probability of Exceedence in 50 Years for NEHRP Class D Site

Earthquake Name	Year	Station Name	Component	M_w	R_{jb} (km)	Vs30 (m/s)	Scale Factor	PGA (g)	PGV (cm/s)	Sa_{T1} (g)	Arias Intensity (cm/s)	Housner Intensity (cm)
El Mayor-Cucapah Mexico	2010	El Centro Array 11	H-1	7.2	15.36	196	1.262	0.558	72.9	1.123	80.10	205.39
Imperial Valley-06	1979	Bonds Corner	H-1	6.53	0.44	223	1.369	0.820	64.0	2.230	76.16	238.95
Kocaeli Turkey	1999	Duzce	H-2	7.51	13.6	282	1.410	0.513	78.4	0.870	27.02	319.74
Kocaeli Turkey	1999	Duzce	H-2	7.51	13.6	282	1.410	0.513	78.4	0.870	27.02	319.74
El Mayor-Cucapah Mexico	2010	El Centro Array 10	H-2	7.2	19.36	203	1.434	0.547	68.3	0.739	75.59	249.23
El Mayor-Cucapah Mexico	2010	MICHOACAN DE OCAMPO	H-1	7.2	13.21	242	1.448	0.779	89.1	1.413	130.25	315.39
Chalfant Valley-02	1986	Zack Brothers Ranch	H-1	6.19	6.44	316	1.472	0.658	54.2	1.376	42.82	221.57
Imperial Valley-06	1979	Bonds Corner	H-2	6.53	0.44	223	1.098	0.853	49.3	1.947	74.39	205.98
Parkfield-02 CA	2004	Parkfield - Fault Zone 14	H-2	6.0	8.45	246	1.499	0.863	63.4	2.836	63.43	217.79
Landers	1992	Coolwater	H-2	7.28	19.74	353	1.522	0.635	66.1	0.744	51.50	218.98
El Mayor-Cucapah Mexico	2010	El Centro - Imperial & Ross	H-1	7.2	19.39	229	1.558	0.599	73.8	1.342	92.54	232.59
El Mayor-Cucapah Mexico	2010	RIITO	H-2	7.2	13.7	242	1.572	0.591	59.4	1.619	117.91	229.23
Kobe Japan	1995	Amagasaki	H-2	6.9	11.34	256	1.616	0.528	72.4	1.079	52.00	356.37
El Mayor-Cucapah Mexico	2010	El Centro Array 11	H-2	7.2	15.36	196	0.992	0.581	62.7	1.243	55.53	220.87
Westmorland	1981	Westmorland Fire Sta	H-1	5.9	6.18	194	1.656	0.624	73.1	1.281	49.14	297.05
Chalfant Valley-02	1986	Zack Brothers Ranch	H-2	6.19	6.44	316	1.656	0.663	74.0	1.061	55.77	251.70
Imperial Valley-06	1979	El Centro Array 8	H-1	6.53	3.86	206	1.690	1.031	92.1	1.579	47.62	310.62
Joshua Tree CA	1992	Indio - Jackson Road	H-2	6.1	25.04	292	1.706	0.694	90.5	0.851	37.94	276.69
El Mayor-Cucapah Mexico	2010	El Centro - Imperial & Ross	H-2	7.2	19.39	229	1.709	0.632	81.4	2.009	97.69	286.17
El Mayor-Cucapah Mexico	2010	El Centro Array 10	H-1	7.2	19.36	203	1.717	0.626	78.3	0.985	90.72	234.47

Table A.28: Ground Motion Suite for F2S2B Building with 10% Probability of Exceedence in 50 Years for NEHRP Class C Site

Earthquake Name	Year	Station Name	Component	M_w	R_{jb} (km)	Vs30 (m/s)	Scale Factor	PGA (g)	PGV (cm/s)	Sa_{T1} (g)	Arias Intensity (cm/s)	Housner Intensity (cm)
Darfield New Zealand	2010	Heathcote Valley Primary School	H-2	7.0	24.36	422	1.235	0.780	28.0	1.658	64.05	68.33
Tottori Japan	2000	TTR009	H-1	6.61	8.82	420	1.209	0.762	48.1	2.578	36.40	107.59
Landers	1992	Coolwater	H-2	7.28	19.74	353	1.184	0.494	51.4	0.579	31.15	170.30
Victoria Mexico	1980	Cerro Prieto	H-1	6.33	13.8	472	1.171	0.756	39.3	1.232	27.76	165.88
Kocaeli Turkey	1999	Duzce	H-2	7.51	13.6	282	1.282	0.467	71.3	0.791	22.33	290.67
Parkfield-02 CA	2004	PARKFIELD - JOAQUIN CANYON	H-2	6.0	3.83	379	1.159	0.571	35.4	1.773	33.18	85.49
Chalfant Valley-02	1986	Zack Brothers Ranch	H-2	6.19	6.44	316	1.157	0.463	51.7	0.741	27.22	175.82
Big Bear-01	1992	Big Bear Lake - Civic Center	H-2	6.46	7.31	430	1.298	0.625	36.5	1.472	57.03	81.85
Tottori Japan	2000	SMNH01	H-2	6.61	5.83	446	1.143	0.705	40.5	2.082	63.01	110.50
Darfield New Zealand	2010	DFHS	H-2	7.0	11.86	344	1.135	0.582	33.8	1.263	37.01	116.65
Tottori Japan	2000	TTR007	H-2	6.61	11.28	470	1.323	0.741	34.3	2.217	61.87	77.04
Mammoth Lakes-06	1980	Long Valley Dam (Upr L Abut)	H-2	5.94	9.65	537	1.328	0.550	45.3	0.958	22.32	168.30
Tottori Japan	2000	OKY004	H-2	6.61	19.72	476	1.127	0.930	26.6	1.637	93.15	83.46
Mammoth Lakes-06	1980	Long Valley Dam (Upr L Abut)	H-1	5.94	9.65	537	1.125	1.063	34.1	1.083	19.77	92.59
Managua Nicaragua-01	1972	Managua ESSO	H-2	6.24	3.51	289	1.122	0.370	34.5	0.783	25.79	124.34
Parkfield-02 CA	2004	Parkfield - Fault Zone 11	H-2	6.0	3.12	542	1.342	1.517	37.0	4.421	56.97	66.24
Big Bear-01	1992	Big Bear Lake - Civic Center	H-1	6.46	7.31	430	1.093	0.595	37.7	1.233	34.77	79.18
Parkfield-02 CA	2004	PARKFIELD - JOAQUIN CANYON	H-1	6.0	3.83	379	1.371	0.850	34.8	2.074	34.83	93.33
Parkfield-02 CA	2004	Parkfield - Vineyard Cany 1E	H-2	6.0	1.59	381	1.392	0.403	35.6	0.972	20.12	113.54
Kobe Japan	1995	Nishi-Akashi	H-2	6.9	7.08	609	1.076	0.500	41.2	0.830	26.76	148.23

Table A.29: Ground Motion Suite for F5S4B Building with 10% Probability of Exceedence in 50 Years for NEHRP Class C Site

Earthquake Name	Year	Station Name	Component	M_w	R_{jb} (km)	Vs30 (m/s)	Scale Factor	PGA (g)	PGV (cm/s)	Sa_{T1} (g)	Arias Intensity (cm/s)	Housner Intensity (cm)
Darfield New Zealand	2010	DFHS	H-2	7.0	11.86	344	1.252	0.642	37.3	1.394	45.06	128.71
Mammoth Lakes-06	1980	Long Valley Dam (Upr L Abut)	H-1	5.94	9.65	537	1.233	1.166	37.4	1.187	23.76	101.52
Hector Mine	1999	Hector	H-2	7.13	10.35	726	1.211	0.397	54.2	0.668	27.87	196.89
Mammoth Lakes-06	1980	Long Valley Dam (Upr L Abut)	H-2	5.94	9.65	537	1.206	0.499	41.1	0.870	18.40	152.79
Superstition Hills-02	1987	Poe Road (temp)	H-1	6.54	11.16	317	1.308	0.621	53.8	0.783	36.99	160.13
Big Bear-01	1992	Big Bear Lake - Civic Center	H-1	6.46	7.31	430	1.319	0.719	45.5	1.488	50.65	95.57
Duzce Turkey	1999	IRIGM 496	H-1	7.14	4.21	760	1.323	1.363	53.2	2.162	238.40	129.39
Morgan Hill	1984	Anderson Dam (Downstream)	H-2	6.19	3.22	489	1.338	0.387	37.2	0.667	15.47	140.91
Kocaeli Turkey	1999	Duzce	H-1	7.51	13.6	282	1.349	0.421	79.4	0.601	20.13	210.30
Tottori Japan	2000	TTR009	H-2	6.61	8.82	420	1.365	0.822	35.5	2.269	55.00	101.80
Manjil Iran	1990	Abbar	H-1	7.37	12.55	724	1.134	0.583	48.1	1.675	60.81	153.14
Landers	1992	Joshua Tree	H-2	7.28	11.03	379	1.368	0.388	58.2	0.461	44.73	224.24
Joshua Tree CA	1992	Indio - Jackson Road	H-2	6.1	25.04	292	1.126	0.458	59.7	0.562	16.54	182.69
Managua Nicaragua-01	1972	Managua ESSO	H-2	6.24	3.51	289	1.117	0.368	34.3	0.780	25.56	123.78
Darfield New Zealand	2010	Heathcote Valley Primary School	H-1	7.0	24.36	422	1.400	0.807	59.2	2.236	76.56	122.99
Duzce Turkey	1999	Lamont 375	H-1	7.14	3.93	454	1.102	0.981	41.0	2.061	123.44	86.19
Landers	1992	Joshua Tree	H-1	7.28	11.03	379	1.409	0.385	38.1	0.383	33.24	179.23
Managua Nicaragua-01	1972	Managua ESSO	H-1	6.24	3.51	289	1.423	0.529	41.3	0.990	32.40	163.20
Kobe Japan	1995	Nishi-Akashi	H-2	6.9	7.08	609	1.081	0.502	41.4	0.834	27.03	148.98
Tottori Japan	2000	SMNH01	H-1	6.61	5.83	446	1.080	0.792	38.5	1.383	63.93	104.36

Table A.30: Ground Motion Suite for F8S3B Building with 10% Probability of Exceedence in 50 Years for NEHRP Class C Site

Earthquake Name	Year	Station Name	Component	M_w	R_{jb} (km)	Vs30 (m/s)	Scale Factor	PGA (g)	PGV (cm/s)	Sa_{T1} (g)	Arias Intensity (cm/s)	Housner Intensity (cm)
Landers	1992	Joshua Tree	H-2	7.28	11.03	379	1.138	0.323	48.5	0.383	30.96	186.55
Kocaeli Turkey	1999	Duzce	H-1	7.51	13.6	282	1.138	0.355	67.0	0.507	14.32	177.38
Tottori Japan	2000	SMNH01	H-1	6.61	5.83	446	1.128	0.827	40.2	1.444	69.69	108.97
Superstition Hills-02	1987	Poe Road (temp)	H-1	6.54	11.16	317	1.170	0.556	48.1	0.700	29.58	143.20
Mammoth Lakes-06	1980	Long Valley Dam (Upr L Abut)	H-2	5.94	9.65	537	1.092	0.452	37.3	0.788	15.10	138.43
Manjil Iran	1990	Abbar	H-1	7.37	12.55	724	1.079	0.555	45.8	1.594	55.08	145.75
Landers	1992	Joshua Tree	H-1	7.28	11.03	379	1.203	0.329	32.5	0.327	24.22	152.99
Darfield New Zealand	2010	DFHS	H-2	7.0	11.86	344	1.206	0.618	35.9	1.343	41.82	124.00
Duzce Turkey	1999	IRIGM 496	H-2	7.14	4.21	760	1.063	0.798	42.1	1.787	75.08	103.29
Morgan Hill	1984	Anderson Dam (Downstream)	H-2	6.19	3.22	489	1.226	0.355	34.1	0.611	13.00	129.17
Duzce Turkey	1999	Lamont 375	H-1	7.14	3.93	454	1.226	1.092	45.6	2.293	152.79	95.88
Kobe Japan	1995	Kakogawa	H-2	6.9	22.5	312	1.247	0.404	33.5	0.921	26.74	174.74
Managua Nicaragua-01	1972	Managua ESSO	H-2	6.24	3.51	289	1.029	0.339	31.6	0.718	21.67	113.98
Hector Mine	1999	Hector	H-2	7.13	10.35	726	1.027	0.337	46.0	0.566	20.04	166.94
Managua Nicaragua-01	1972	Managua ESSO	H-1	6.24	3.51	289	1.292	0.481	37.5	0.899	26.74	148.26
Landers	1992	Indio - Jackson Road	H-1	7.28	48.84	292	1.295	0.397	46.2	0.397	25.78	166.45
Mammoth Lakes-06	1980	Long Valley Dam (Upr L Abut)	H-1	5.94	9.65	537	1.295	1.224	39.2	1.246	26.19	106.57
Darfield New Zealand	2010	DFHS	H-1	7.0	11.86	344	1.301	0.614	52.0	1.027	43.36	156.58
Duzce Turkey	1999	IRIGM 496	H-1	7.14	4.21	760	1.305	1.345	52.5	2.133	231.93	127.62
Morgan Hill	1984	Halls Valley	H-2	6.19	3.45	282	1.306	0.408	51.4	0.737	15.15	142.58

Table A.31: Ground Motion Suite for F2S2B Building with 10% Probability of Exceedence in 50 Years for Generic Rock Site

Earthquake Name	Year	Station Name	Component	M_w	R_{jb} (km)	Vs30 (m/s)	Scale Factor	PGA (g)	PGV (cm/s)	Sa_{T1} (g)	Arias Intensity (cm/s)	Housner Intensity (cm)
Hector Mine	1999	Hector	H-2	7.13	10.35	726	1.239	0.407	55.5	0.683	29.18	201.44
Parkfield-02 CA	2004	PARKFIELD - UPSAR 05	H-1	6.0	9.14	441	1.260	0.463	28.6	0.970	21.38	83.66
Morgan Hill	1984	Anderson Dam (Downstream)	H-2	6.19	3.22	489	1.265	0.366	35.2	0.630	13.83	133.22
Parkfield-02 CA	2004	Parkfield - Gold Hill 3W	H-1	6.0	4.66	511	1.283	1.008	29.8	2.005	19.38	57.54
Tottori Japan	2000	SMNH02	H-1	6.61	23.64	503	1.291	0.743	27.3	2.556	45.00	61.95
Duzce Turkey	1999	IRIGM 498	H-2	7.14	3.58	425	1.186	0.419	29.9	0.880	16.90	74.76
Parkfield-02 CA	2004	Parkfield - Cholame 2E	H-2	6.0	3.22	523	1.295	0.655	29.8	1.695	24.89	55.79
Parkfield-02 CA	2004	PARKFIELD - UPSAR 07	H-2	6.0	9.14	441	1.297	0.487	21.8	1.121	24.80	76.22
Parkfield-02 CA	2004	Parkfield - Vineyard Cany 2W	H-1	6.0	2.33	439	1.300	0.699	36.9	1.056	25.17	65.35
Morgan Hill	1984	Anderson Dam (Downstream)	H-1	6.19	3.22	489	1.307	0.553	33.2	0.775	11.91	83.70
Parkfield-02 CA	2004	PARKFIELD - UPSAR 11	H-1	6.0	8.93	466	1.173	0.546	31.7	0.703	20.73	82.28
Parkfield-02 CA	2004	PARKFIELD - MIDDLE MOUNTAIN	H-2	6.0	0.61	398	1.324	0.543	38.7	0.784	10.77	92.10
Parkfield-02 CA	2004	PARKFIELD - UPSAR 11	H-2	6.0	8.93	466	1.336	0.476	26.8	0.680	20.84	85.46
Parkfield-02 CA	2004	Parkfield - Vineyard Cany 1E	H-2	6.0	1.59	381	1.138	0.330	29.1	0.795	13.46	92.86
Duzce Turkey	1999	Lamont 375	H-2	7.14	3.93	454	1.369	0.703	28.0	1.072	38.85	73.99
Parkfield-02 CA	2004	PARKFIELD - UPSAR 07	H-1	6.0	9.14	441	1.369	0.446	25.4	1.126	22.17	82.00
Parkfield-02 CA	2004	Parkfield - Fault Zone 11	H-2	6.0	3.12	542	1.101	1.245	30.4	3.628	38.38	54.36
Parkfield-02 CA	2004	Parkfield - Cholame 2E	H-1	6.0	3.22	523	1.394	0.664	32.1	1.738	17.77	82.10
Mammoth Lakes-06	1980	Long Valley Dam (Upr L Abut)	H-2	5.94	9.65	537	1.086	0.449	37.1	0.784	14.93	137.64
Tottori Japan	2000	TTR007	H-2	6.61	11.28	470	1.083	0.606	28.1	1.814	41.41	63.02

Table A.32: Ground Motion Suite for F5S4B Building with 10% Probability of Exceedence in 50 Years for Generic Rock Site

Earthquake Name	Year	Station Name	Component	M_w	R_{jb} (km)	Vs30 (m/s)	Scale Factor	PGA (g)	PGV (cm/s)	Sa_{T1} (g)	Arias Intensity (cm/s)	Housner Intensity (cm)
Duzce Turkey	1999	IRIGM 498	H-2	7.14	3.58	425	1.517	0.536	38.3	1.125	27.67	95.64
Parkfield-02 CA	2004	PARKFIELD - UPSAR 11	H-2	6.0	8.93	466	1.521	0.543	30.5	0.774	27.04	97.34
Parkfield-02 CA	2004	PARKFIELD - UPSAR 05	H-1	6.0	9.14	441	1.526	0.560	34.7	1.174	31.36	101.31
Tottori Japan	2000	TTR009	H-1	6.61	8.82	420	1.463	0.921	58.1	3.117	53.23	130.12
Parkfield-02 CA	2004	PARKFIELD - UPSAR 09	H-1	6.0	8.86	466	1.548	0.434	34.3	0.530	25.15	111.94
Tottori Japan	2000	OKY004	H-2	6.61	19.72	476	1.454	1.199	34.3	2.111	154.87	107.61
Landers	1992	Morongo Valley Fire Station	H-1	7.28	17.36	396	1.566	0.349	46.9	0.507	30.09	186.31
Parkfield-02 CA	2004	PARKFIELD - UPSAR 11	H-1	6.0	8.93	466	1.438	0.670	38.9	0.862	31.17	100.90
Darfield New Zealand	2010	Heathcote Valley Primary School	H-2	7.0	24.36	422	1.577	0.996	35.8	2.117	104.42	87.24
Kobe Japan	1995	Kobe University	H-2	6.9	0.9	1043	1.431	0.446	44.2	1.045	17.09	186.22
Parkfield-02 CA	2004	PARKFIELD - MIDDLE MOUNTAIN	H-2	6.0	0.61	398	1.586	0.650	46.3	0.938	15.45	110.29
Big Bear-01	1992	Big Bear Lake - Civic Center	H-2	6.46	7.31	430	1.612	0.776	45.4	1.828	87.96	101.65
Parkfield-02 CA	2004	Parkfield - Vineyard Cany 1E	H-1	6.0	1.59	381	1.625	0.436	47.7	1.028	19.27	156.34
Parkfield-02 CA	2004	Parkfield - Vineyard Cany 1E	H-2	6.0	1.59	381	1.375	0.398	35.1	0.961	19.64	112.18
Tottori Japan	2000	TTR007	H-2	6.61	11.28	470	1.661	0.930	43.1	2.783	97.49	96.70
Tottori Japan	2000	SMNH01	H-2	6.61	5.83	446	1.354	0.836	48.0	2.466	88.42	130.89
Parkfield-02 CA	2004	PARKFIELD - UPSAR 07	H-2	6.0	9.14	441	1.684	0.632	28.3	1.455	41.78	98.94
Parkfield-02 CA	2004	PARKFIELD - UPSAR 07	H-1	6.0	9.14	441	1.697	0.553	31.5	1.396	34.07	101.66
Morgan Hill	1984	Anderson Dam (Downstream)	H-1	6.19	3.22	489	1.702	0.720	43.2	1.009	20.18	108.98
Landers	1992	Fun Valley	H-1	7.28	25.02	389	1.706	0.368	41.2	0.558	36.01	114.48

Table A.33: Ground Motion Suite for F8S3B Building with 10% Probability of Exceedence in 50 Years for Generic Rock Site

Earthquake Name	Year	Station Name	Component	M_w	R_{jb} (km)	Vs30 (m/s)	Scale Factor	PGA (g)	PGV (cm/s)	Sa_{T1} (g)	Arias Intensity (cm/s)	Housner Intensity (cm)
Parkfield-02 CA	2004	PARKFIELD - UPSAR 11	H-1	6.0	8.93	466	1.458	0.679	39.4	0.874	32.00	102.23
Tottori Japan	2000	SMNH01	H-2	6.61	5.83	446	1.375	0.848	48.8	2.504	91.16	132.90
Darfield New Zealand	2010	Heathcote Valley Primary School	H-1	7.0	24.36	422	1.375	0.793	58.2	2.196	73.84	120.78
Parkfield-02 CA	2004	Parkfield - Vineyard Cany 1E	H-2	6.0	1.59	381	1.372	0.398	35.1	0.958	19.55	111.93
Tottori Japan	2000	TTR009	H-2	6.61	8.82	420	1.371	0.826	35.7	2.278	55.45	102.21
Parkfield-02 CA	2004	Parkfield - Vineyard Cany 1E	H-1	6.0	1.59	381	1.483	0.398	43.6	0.939	16.05	142.69
Tottori Japan	2000	TTR009	H-1	6.61	8.82	420	1.486	0.936	59.1	3.167	54.95	132.21
Duzce Turkey	1999	IRIGM 498	H-2	7.14	3.58	425	1.512	0.534	38.1	1.122	27.48	95.32
Parkfield-02 CA	2004	PARKFIELD - UPSAR 11	H-2	6.0	8.93	466	1.532	0.546	30.8	0.779	27.41	98.00
Parkfield-02 CA	2004	PARKFIELD - UPSAR 09	H-1	6.0	8.86	466	1.533	0.429	33.9	0.525	24.66	110.84
Landers	1992	Morongo Valley Fire Station	H-1	7.28	17.36	396	1.315	0.293	39.4	0.426	21.21	156.44
Big Bear-01	1992	Big Bear Lake - Civic Center	H-1	6.46	7.31	430	1.307	0.712	45.1	1.474	49.69	94.66
Parkfield-02 CA	2004	PARKFIELD - UPSAR 05	H-1	6.0	9.14	441	1.576	0.579	35.8	1.213	33.44	104.63
Parkfield-02 CA	2004	PARKFIELD - MIDDLE MOUNTAIN	H-2	6.0	0.61	398	1.583	0.648	46.2	0.936	15.39	110.07
Tottori Japan	2000	OKY004	H-2	6.61	19.72	476	1.606	1.324	37.8	2.332	188.98	118.87
Duzce Turkey	1999	IRIGM 496	H-1	7.14	4.21	760	1.253	1.291	50.4	2.047	213.73	122.51
Darfield New Zealand	2010	SPFS	H-1	7.0	29.86	390	1.627	0.261	33.3	0.456	27.20	148.47
Mammoth Lakes-06	1980	Long Valley Dam (Upr L Abut)	H-1	5.94	9.65	537	1.243	1.175	37.7	1.196	24.13	102.29
Victoria Mexico	1980	Cerro Prieto	H-2	6.33	13.8	472	1.631	1.032	28.7	1.214	27.27	118.96
Kobe Japan	1995	Kobe University	H-2	6.9	0.9	1043	1.233	0.384	38.1	0.901	12.68	160.42

Table A.34: Ground Motion Suite for F2S2B Building with 10% Probability of Exceedence in 50 Years for NEHRP Class B Site

Earthquake Name	Year	Station Name	Component	M_w	R_{jb} (km)	Vs30 (m/s)	Scale Factor	PGA (g)	PGV (cm/s)	Sa_{T1} (g)	Arias Intensity (cm/s)	Housner Intensity (cm)
Kobe Japan	1995	Kobe University	H-1	6.9	0.9	1043	1.132	0.312	62.6	0.797	15.96	241.72
Tottori Japan	2000	SMNH10	H-2	6.61	15.58	967	1.237	0.285	26.5	0.737	7.56	86.25
Kobe Japan	1995	Kobe University	H-2	6.9	0.9	1043	1.072	0.334	33.1	0.783	9.58	139.47
Parkfield-02 CA	2004	PARKFIELD - DONNA LEE	H-2	6.0	4.25	657	1.304	0.486	18.3	2.240	12.39	51.72
Hector Mine	1999	Hector	H-1	7.13	10.35	726	1.311	0.348	34.1	0.576	14.55	134.06
Hector Mine	1999	Hector	H-2	7.13	10.35	726	0.891	0.292	39.9	0.491	15.08	144.84
Tottori Japan	2000	SMN015	H-2	6.61	9.1	617	1.562	0.427	23.9	0.565	9.45	72.01
Tottori Japan	2000	OKYH14	H-2	6.61	26.51	710	1.650	0.747	38.3	4.029	34.18	72.37
Parkfield-02 CA	2004	PARKFIELD - DONNA LEE	H-1	6.0	4.25	657	1.665	0.490	25.3	0.959	10.12	63.96
Tottori Japan	2000	SMN015	H-1	6.61	9.1	617	1.667	0.253	32.0	0.640	9.89	119.08
Parkfield-02 CA	2004	PARKFIELD - TURKEY FLAT 1 (0M)	H-1	6.0	4.66	907	1.834	0.450	26.8	0.672	5.87	52.58
Duzce Turkey	1999	Lamont 531	H-2	7.14	8.03	638	1.885	0.233	25.3	0.441	14.95	81.87
Parkfield-02 CA	2004	PARKFIELD - TURKEY FLAT 1 (0M)	H-2	6.0	4.66	907	1.893	0.371	22.3	0.566	6.89	61.49
Duzce Turkey	1999	Lamont 531	H-1	7.14	8.03	638	1.904	0.305	20.7	0.453	16.51	55.78
Chi-Chi Taiwan-04	1999	CHY035	H-2	6.2	25.01	573	1.980	0.264	29.4	0.382	11.54	117.20
Kobe Japan	1995	Nishi-Akashi	H-2	6.9	7.08	609	0.632	0.294	24.2	0.487	9.24	87.11
Basso Tirreno Italy	1978	Naso	H-1	6.0	17.15	621	2.186	0.327	17.9	0.551	12.76	51.41
Duzce Turkey	1999	IRIGM 496	H-1	7.14	4.21	760	0.630	0.649	25.3	1.029	54.04	61.60
Parkfield-02 CA	2004	PARKFIELD - JACK CANYON	H-2	6.0	9.12	576	2.293	0.389	24.4	1.243	9.27	57.86
Tottori Japan	2000	SMNH10	H-1	6.61	15.58	967	2.296	0.364	19.9	0.978	10.80	72.92

Table A.35: Ground Motion Suite for F5S4B Building with 10% Probability of Exceedence in 50 Years for NEHRP Class B Site

Earthquake Name	Year	Station Name	Component	M_w	R_{jb} (km)	Vs30 (m/s)	Scale Factor	PGA (g)	PGV (cm/s)	Sa_{T1} (g)	Arias Intensity (cm/s)	Housner Intensity (cm)
Tottori Japan	2000	SMNH10	H-2	6.61	15.58	967	1.237	0.285	26.5	0.736	7.55	86.20
Hector Mine	1999	Hector	H-1	7.13	10.35	726	1.031	0.274	26.8	0.453	8.99	105.35
Tottori Japan	2000	SMN015	H-1	6.61	9.1	617	1.342	0.204	25.7	0.515	6.41	95.84
Chi-Chi Taiwan-04	1999	CHY035	H-2	6.2	25.01	573	1.430	0.191	21.2	0.276	6.02	84.63
Tottori Japan	2000	SMN015	H-2	6.61	9.1	617	1.497	0.409	22.9	0.541	8.68	69.01
Duzce Turkey	1999	Lamont 531	H-2	7.14	8.03	638	1.525	0.188	20.4	0.356	9.79	66.22
Parkfield-02 CA	2004	PARKFIELD - DONNA LEE	H-2	6.0	4.25	657	1.584	0.591	22.3	2.721	18.28	62.82
Kobe Japan	1995	Kobe University	H-2	6.9	0.9	1043	0.813	0.253	25.1	0.594	5.51	105.76
Chi-Chi Taiwan-04	1999	CHY035	H-1	6.2	25.01	573	1.725	0.201	29.5	0.342	5.99	90.14
Parkfield-02 CA	2004	PARKFIELD - DONNA LEE	H-1	6.0	4.25	657	1.748	0.515	26.6	1.007	11.15	67.15
Darfield New Zealand	2010	CSHS	H-2	7.0	43.6	638	1.813	0.210	21.7	0.311	12.88	107.16
Parkfield-02 CA	2004	PARKFIELD - TURKEY FLAT 1 (0M)	H-2	6.0	4.66	907	1.836	0.360	21.7	0.549	6.48	59.64
Chi-Chi Taiwan-04	1999	CHY086	H-2	6.2	33.63	665	1.844	0.202	20.3	0.270	6.22	78.68
Kobe Japan	1995	Kobe University	H-1	6.9	0.9	1043	0.735	0.203	40.7	0.518	6.74	157.09
Duzce Turkey	1999	Lamont 531	H-1	7.14	8.03	638	1.862	0.299	20.2	0.443	15.79	54.56
Parkfield-02 CA	2004	PARKFIELD - TURKEY FLAT 1 (0M)	H-1	6.0	4.66	907	1.932	0.474	28.2	0.708	6.51	55.39
Duzce Turkey	1999	IRIGM 496	H-1	7.14	4.21	760	0.705	0.727	28.3	1.152	67.70	68.95
Chi-Chi Taiwan-04	1999	CHY086	H-1	6.2	33.63	665	2.008	0.229	26.8	0.252	11.23	93.48
Darfield New Zealand	2010	CSHS	H-1	7.0	43.6	638	2.070	0.185	16.9	0.391	13.84	91.21
Tottori Japan	2000	OKYH14	H-2	6.61	26.51	710	2.102	0.952	48.8	5.134	55.48	92.20

Table A.36: Ground Motion Suite for F8S3B Building with 10% Probability of Exceedence in 50 Years for NEHRP Class B Site

Earthquake Name	Year	Station Name	Component	M_w	R_{jb} (km)	Vs30 (m/s)	Scale Factor	PGA (g)	PGV (cm/s)	Sa_{T1} (g)	Arias Intensity (cm/s)	Housner Intensity (cm)
Tottori Japan	2000	SMNH10	H-2	6.61	15.58	967	1.212	0.280	26.0	0.722	7.26	84.50
Tottori Japan	2000	SMN015	H-1	6.61	9.1	617	1.282	0.195	24.6	0.492	5.85	91.57
Chi-Chi Taiwan-04	1999	CHY035	H-2	6.2	25.01	573	1.380	0.184	20.5	0.267	5.61	81.71
Hector Mine	1999	Hector	H-1	7.13	10.35	726	0.986	0.262	25.6	0.433	8.22	100.77
Duzce Turkey	1999	Lamont 531	H-2	7.14	8.03	638	1.545	0.191	20.7	0.361	10.05	67.11
Tottori Japan	2000	SMN015	H-2	6.61	9.1	617	1.567	0.429	23.9	0.567	9.52	72.27
Darfield New Zealand	2010	CSHS	H-2	7.0	43.6	638	1.587	0.184	19.0	0.273	9.87	93.82
Chi-Chi Taiwan-04	1999	CHY035	H-1	6.2	25.01	573	1.668	0.195	28.5	0.331	5.60	87.15
Parkfield-02 CA	2004	PARKFIELD - DONNA LEE	H-2	6.0	4.25	657	1.706	0.636	24.0	2.930	21.20	67.65
Chi-Chi Taiwan-04	1999	CHY086	H-2	6.2	33.63	665	1.780	0.195	19.6	0.260	5.79	75.93
Duzce Turkey	1999	IRIGM 496	H-1	7.14	4.21	760	0.747	0.770	30.1	1.222	76.10	73.10
Kobe Japan	1995	Kobe University	H-2	6.9	0.9	1043	0.736	0.229	22.7	0.538	4.52	95.75
Parkfield-02 CA	2004	PARKFIELD - DONNA LEE	H-1	6.0	4.25	657	1.865	0.549	28.3	1.074	12.69	71.64
Chi-Chi Taiwan-04	1999	CHY086	H-1	6.2	33.63	665	1.892	0.216	25.2	0.237	9.96	88.06
Parkfield-02 CA	2004	PARKFIELD - TURKEY FLAT 1 (0M)	H-2	6.0	4.66	907	1.920	0.376	22.6	0.574	7.08	62.36
Duzce Turkey	1999	Lamont 531	H-1	7.14	8.03	638	2.038	0.327	22.2	0.485	18.92	59.71
Bam Iran	2003	Mohammad Abad-e-Madkoon	H-1	6.6	46.2	575	2.064	0.255	26.2	0.569	7.10	89.46
Darfield New Zealand	2010	CSHS	H-1	7.0	43.6	638	2.074	0.185	17.0	0.392	13.90	91.38
Helena Montana-01	1935	Carroll College	H-2	6.0	2.07	593	2.074	0.324	28.5	0.817	4.34	80.15
Parkfield-02 CA	2004	PARKFIELD - TURKEY FLAT 1 (0M)	H-1	6.0	4.66	907	2.099	0.515	30.7	0.769	7.68	60.16

Table A.37: Ground Motion Suite for F2S2B Building with 5% Probability of Exceedence in 50 Years for NEHRP Class D Site

Earthquake Name	Year	Station Name	Component	M_w	R_{jb} (km)	Vs30 (m/s)	Scale Factor	PGA (g)	PGV (cm/s)	Sa_{T1} (g)	Arias Intensity (cm/s)	Housner Intensity (cm)
El Mayor-Cucapah Mexico	2010	El Centro Array 11	H-2	7.2	15.36	196	1.023	0.600	64.7	1.282	59.11	227.89
Parkfield-02 CA	2004	Parkfield - Fault Zone 14	H-2	6.0	8.45	246	1.163	0.670	49.2	2.200	38.17	168.96
Imperial Valley-06	1979	Bonds Corner	H-1	6.53	0.44	223	1.199	0.718	56.1	1.953	58.47	209.36
El Mayor-Cucapah Mexico	2010	El Centro Array 11	H-1	7.2	15.36	196	1.251	0.553	72.2	1.114	78.72	203.62
Imperial Valley-06	1979	Bonds Corner	H-2	6.53	0.44	223	0.851	0.661	38.2	1.510	44.75	159.76
Tottori Japan	2000	TTRH02	H-2	6.61	0.83	310	0.836	0.645	72.4	0.890	70.05	237.46
El Mayor-Cucapah Mexico	2010	El Centro Differential Array	H-1	7.2	22.83	202	1.389	0.770	40.7	2.121	85.40	152.40
Chalfant Valley-02	1986	Zack Brothers Ranch	H-1	6.19	6.44	316	1.405	0.628	51.7	1.313	38.98	211.41
El Mayor-Cucapah Mexico	2010	RIITO	H-2	7.2	13.7	242	1.449	0.545	54.8	1.492	100.20	211.32
El Mayor-Cucapah Mexico	2010	MICHOACAN DE OCAMPO	H-1	7.2	13.21	242	1.539	0.827	94.7	1.501	147.15	335.22
El Mayor-Cucapah Mexico	2010	MICHOACAN DE OCAMPO	H-1	7.2	13.21	242	1.539	0.827	94.7	1.501	147.15	335.22
El Mayor-Cucapah Mexico	2010	El Centro Differential Array	H-2	7.2	22.83	202	1.543	0.782	59.9	2.488	98.67	231.98
El Mayor-Cucapah Mexico	2010	El Centro - Imperial & Ross	H-1	7.2	19.39	229	1.561	0.600	73.9	1.345	92.89	233.03
El Mayor-Cucapah Mexico	2010	RIITO	H-1	7.2	13.7	242	1.564	0.621	81.9	1.946	99.46	228.53
Tottori Japan	2000	TTRH02	H-1	6.61	0.83	310	0.724	0.681	88.5	1.090	63.05	272.50
Managua Nicaragua-01	1972	Managua ESSO	H-2	6.24	3.51	289	1.619	0.533	49.7	1.130	53.64	179.31
Darfield New Zealand	2010	DFHS	H-2	7.0	11.86	344	1.638	0.840	48.7	1.824	77.13	168.41
El Mayor-Cucapah Mexico	2010	El Centro Array 10	H-2	7.2	19.36	203	1.648	0.628	78.5	0.849	99.79	286.36
Chalfant Valley-02	1986	Zack Brothers Ranch	H-2	6.19	6.44	316	1.667	0.668	74.5	1.068	56.53	253.40
Parkfield-02 CA	2004	PARKFIELD - JOAQUIN CANYON	H-2	6.0	3.83	379	1.672	0.823	51.0	2.558	69.07	123.34

Table A.38: Ground Motion Suite for F5S4B Building with 5% Probability of Exceedence in 50 Years for NEHRP Class D Site

Earthquake Name	Year	Station Name	Component	M_w	R_{jb} (km)	Vs30 (m/s)	Scale Factor	PGA (g)	PGV (cm/s)	Sa_{T1} (g)	Arias Intensity (cm/s)	Housner Intensity (cm)
Imperial Valley-06	1979	Bonds Corner	H-2	6.53	0.44	223	1.352	1.051	60.8	2.399	112.92	253.78
El Mayor-Cucapah Mexico	2010	El Centro Array 11	H-2	7.2	15.36	196	1.334	0.782	84.3	1.671	100.42	297.02
El Mayor-Cucapah Mexico	2010	El Centro Array 11	H-1	7.2	15.36	196	1.704	0.753	98.4	1.517	146.08	277.36
Parkfield-02 CA	2004	Parkfield - Fault Zone 14	H-2	6.0	8.45	246	1.829	1.053	77.4	3.460	94.39	265.69
Imperial Valley-06	1979	Bonds Corner	H-1	6.53	0.44	223	1.849	1.107	86.4	3.011	138.89	322.68
Parkfield-02 CA	2004	Parkfield - Fault Zone 14	H-1	6.0	8.45	246	1.086	1.422	90.6	1.833	92.27	272.78
Tottori Japan	2000	TTRH02	H-2	6.61	0.83	310	1.056	0.815	91.4	1.124	111.72	299.88
Chalfant Valley-02	1986	Zack Brothers Ranch	H-1	6.19	6.44	316	1.947	0.871	71.7	1.821	74.92	293.08
El Mayor-Cucapah Mexico	2010	El Centro Array 10	H-2	7.2	19.36	203	1.966	0.749	93.7	1.013	142.08	341.70
El Mayor-Cucapah Mexico	2010	MICHOACAN DE OCAMPO	H-1	7.2	13.21	242	2.023	1.088	124.5	1.974	254.29	440.68
Landers	1992	Coolwater	H-2	7.28	19.74	353	2.052	0.856	89.1	1.004	93.61	295.23
El Mayor-Cucapah Mexico	2010	RIITO	H-2	7.2	13.7	242	2.108	0.793	79.7	2.171	212.05	307.41
El Mayor-Cucapah Mexico	2010	El Centro - Imperial & Ross	H-1	7.2	19.39	229	2.121	0.815	100.4	1.828	171.51	316.64
Kocaeli Turkey	1999	Duzce	H-2	7.51	13.6	282	2.121	0.772	118.0	1.308	61.13	480.94
Tottori Japan	2000	TTRH02	H-1	6.61	0.83	310	0.959	0.901	117.1	1.443	110.42	360.63
Chalfant Valley-02	1986	Zack Brothers Ranch	H-2	6.19	6.44	316	2.211	0.886	98.9	1.416	99.42	336.05
El Mayor-Cucapah Mexico	2010	RIITO	H-1	7.2	13.7	242	2.294	0.910	120.2	2.854	213.97	335.20
El Mayor-Cucapah Mexico	2010	El Centro Array 10	H-1	7.2	19.36	203	2.331	0.849	106.3	1.337	167.19	318.31
El Mayor-Cucapah Mexico	2010	El Centro - Imperial & Ross	H-2	7.2	19.39	229	2.342	0.867	111.5	2.754	183.45	392.15
Westmorland	1981	Westmorland Fire Sta	H-1	5.9	6.18	194	2.365	0.892	104.4	1.829	100.26	424.32

Table A.39: Ground Motion Suite for F8S3B Building with 5% Probability of Exceedence in 50 Years for NEHRP Class D Site

Earthquake Name	Year	Station Name	Component	M_w	R_{jb} (km)	Vs30 (m/s)	Scale Factor	PGA (g)	PGV (cm/s)	Sa_{T1} (g)	Arias Intensity (cm/s)	Housner Intensity (cm)
El Mayor-Cucapah Mexico	2010	El Centro Array 11	H-2	7.2	15.36	196	1.314	0.770	83.0	1.647	97.48	292.65
Imperial Valley-06	1979	Bonds Corner	H-2	6.53	0.44	223	1.451	1.127	65.2	2.574	130.03	272.33
Parkfield-02 CA	2004	Parkfield - Fault Zone 14	H-1	6.0	8.45	246	1.100	1.441	91.8	1.857	94.71	276.37
Tottori Japan	2000	TTRH02	H-2	6.61	0.83	310	1.084	0.837	93.8	1.154	117.77	307.90
El Mayor-Cucapah Mexico	2010	El Centro Array 11	H-1	7.2	15.36	196	1.669	0.737	96.3	1.485	140.05	271.58
Imperial Valley-06	1979	Bonds Corner	H-1	6.53	0.44	223	1.811	1.084	84.6	2.949	133.29	316.11
Kocaeli Turkey	1999	Duzce	H-2	7.51	13.6	282	1.865	0.679	103.8	1.150	47.27	422.93
Kocaeli Turkey	1999	Duzce	H-2	7.51	13.6	282	1.865	0.679	103.8	1.150	47.27	422.93
El Mayor-Cucapah Mexico	2010	El Centro Array 10	H-2	7.2	19.36	203	1.898	0.724	90.5	0.978	132.48	329.94
El Mayor-Cucapah Mexico	2010	MICHOACAN DE OCAMPO	H-1	7.2	13.21	242	1.919	1.031	118.1	1.872	228.65	417.87
Chalfant Valley-02	1986	Zack Brothers Ranch	H-1	6.19	6.44	316	1.947	0.871	71.6	1.820	74.86	292.98
Tottori Japan	2000	TTRH02	H-1	6.61	0.83	310	0.908	0.854	110.9	1.367	99.10	341.64
Parkfield-02 CA	2004	Parkfield - Fault Zone 14	H-2	6.0	8.45	246	1.988	1.145	84.1	3.762	111.60	288.90
Landers	1992	Coolwater	H-2	7.28	19.74	353	2.015	0.841	87.5	0.986	90.30	289.96
El Mayor-Cucapah Mexico	2010	El Centro - Imperial & Ross	H-1	7.2	19.39	229	2.064	0.793	97.7	1.779	162.43	308.14
El Mayor-Cucapah Mexico	2010	RIITO	H-2	7.2	13.7	242	2.085	0.784	78.9	2.147	207.53	304.12
Kobe Japan	1995	Amagasaki	H-2	6.9	11.34	256	2.139	0.699	95.9	1.427	91.07	471.59
Chalfant Valley-02	1986	Zack Brothers Ranch	H-2	6.19	6.44	316	2.193	0.878	98.1	1.405	97.80	333.30
Westmorland	1981	Westmorland Fire Sta	H-1	5.9	6.18	194	2.194	0.827	96.8	1.697	86.27	393.59
Imperial Valley-06	1979	El Centro Array 8	H-1	6.53	3.86	206	2.240	1.367	122.0	2.093	83.62	411.59

Table A.40: Ground Motion Suite for F2S2B Building with 5% Probability of Exceedence in 50 Years for NEHRP Class C Site

Earthquake Name	Year	Station Name	Component	M_w	R_{jb} (km)	Vs30 (m/s)	Scale Factor	PGA (g)	PGV (cm/s)	Sa_{T1} (g)	Arias Intensity (cm/s)	Housner Intensity (cm)
Manjil Iran	1990	Abbar	H-1	7.37	12.55	724	1.335	0.687	56.7	1.973	84.36	180.36
Chalfant Valley-02	1986	Zack Brothers Ranch	H-1	6.19	6.44	316	1.348	0.603	49.6	1.261	35.91	202.92
Kobe Japan	1995	Nishi-Akashi	H-1	6.9	7.08	609	1.279	0.618	59.9	0.935	55.92	188.96
Manjil Iran	1990	Abbar	H-2	7.37	12.55	724	1.380	0.686	69.8	2.637	145.84	304.14
Baja California	1987	Cerro Prieto	H-1	5.5	3.43	472	1.240	1.587	57.5	3.631	56.00	206.25
Darfield New Zealand	2010	Heathcote Valley Primary School	H-1	7.0	24.36	422	1.462	0.843	61.9	2.335	83.51	128.44
Tottori Japan	2000	TTR009	H-2	6.61	8.82	420	1.476	0.889	38.4	2.452	64.24	110.02
Duzce Turkey	1999	IRIGM 496	H-1	7.14	4.21	760	1.482	1.527	59.6	2.422	299.23	144.96
Kobe Japan	1995	Nishi-Akashi	H-2	6.9	7.08	609	1.489	0.691	56.9	1.148	51.25	205.13
Big Bear-01	1992	Big Bear Lake - Civic Center	H-1	6.46	7.31	430	1.514	0.825	52.2	1.707	66.70	109.67
Managua Nicaragua-01	1972	Managua ESSO	H-2	6.24	3.51	289	1.554	0.512	47.7	1.084	49.42	172.11
Duzce Turkey	1999	Lamont 375	H-1	7.14	3.93	454	1.123	1.000	41.8	2.099	128.13	87.81
Mammoth Lakes-06	1980	Long Valley Dam (Upr L Abut)	H-1	5.94	9.65	537	1.560	1.475	47.3	1.502	38.04	128.44
Tottori Japan	2000	SMNH01	H-1	6.61	5.83	446	1.121	0.821	39.9	1.435	68.81	108.28
Tottori Japan	2000	OKY004	H-2	6.61	19.72	476	1.563	1.289	36.8	2.270	179.06	115.71
Darfield New Zealand	2010	DFHS	H-2	7.0	11.86	344	1.574	0.807	46.8	1.752	71.18	161.78
Tottori Japan	2000	SMNH01	H-2	6.61	5.83	446	1.584	0.977	56.2	2.885	120.99	153.11
Chalfant Valley-02	1986	Zack Brothers Ranch	H-2	6.19	6.44	316	1.601	0.641	71.6	1.026	52.16	243.41
Parkfield-02 CA	2004	PARKFIELD - JOAQUIN CANYON	H-2	6.0	3.83	379	1.609	0.792	49.1	2.462	63.95	118.68
Victoria Mexico	1980	Cerro Prieto	H-1	6.33	13.8	472	1.621	1.046	54.4	1.705	53.17	229.57

Table A.41: Ground Motion Suite for F5S4B Building with 5% Probability of Exceedence in 50 Years for NEHRP Class C Site

Earthquake Name	Year	Station Name	Component	M_w	R_{jb} (km)	Vs30 (m/s)	Scale Factor	PGA (g)	PGV (cm/s)	Sa_{T1} (g)	Arias Intensity (cm/s)	Housner Intensity (cm)
Kocaeli Turkey	1999	Duzce	H-2	7.51	13.6	282	1.161	0.423	64.6	0.716	18.31	263.23
Landers	1992	Coolwater	H-2	7.28	19.74	353	1.126	0.470	48.9	0.551	28.21	162.05
Tottori Japan	2000	TTR007	H-1	6.61	11.28	470	1.123	0.824	48.0	3.007	66.55	133.85
Duzce Turkey	1999	IRIGM 496	H-2	7.14	4.21	760	1.177	0.883	46.6	1.978	92.00	114.34
Baja California	1987	Cerro Prieto	H-1	5.5	3.43	472	1.190	1.524	55.2	3.486	51.63	198.04
Manjil Iran	1990	Abbar	H-2	7.37	12.55	724	1.206	0.599	61.0	2.306	111.45	265.87
Chalfant Valley-02	1986	Zack Brothers Ranch	H-2	6.19	6.44	316	1.213	0.486	54.3	0.777	29.95	184.43
Chalfant Valley-02	1986	Zack Brothers Ranch	H-1	6.19	6.44	316	1.069	0.478	39.3	0.999	22.58	160.89
Chalfant Valley-02	1986	Zack Brothers Ranch	H-1	6.19	6.44	316	1.069	0.478	39.3	0.999	22.58	160.89
Victoria Mexico	1980	Cerro Prieto	H-1	6.33	13.8	472	1.245	0.804	41.8	1.310	31.38	176.35
Kobe Japan	1995	Nishi-Akashi	H-1	6.9	7.08	609	1.037	0.501	48.5	0.758	36.74	153.15
Kobe Japan	1995	Nishi-Akashi	H-2	6.9	7.08	609	1.275	0.592	48.8	0.983	37.60	175.69
Tottori Japan	2000	SMNH01	H-1	6.61	5.83	446	1.277	0.936	45.5	1.636	89.43	123.44
Duzce Turkey	1999	Lamont 375	H-1	7.14	3.93	454	1.305	1.162	48.5	2.439	172.94	102.01
Managua Nicaragua-01	1972	Managua ESSO	H-2	6.24	3.51	289	1.319	0.435	40.5	0.920	35.60	146.07
Joshua Tree CA	1992	Indio - Jackson Road	H-2	6.1	25.04	292	1.329	0.541	70.5	0.663	23.04	215.59
Manjil Iran	1990	Abbar	H-1	7.37	12.55	724	1.339	0.689	56.8	1.979	84.88	180.92
Mammoth Lakes-06	1980	Long Valley Dam (Upr L Abut)	H-2	5.94	9.65	537	1.425	0.590	48.6	1.028	25.69	180.57
Hector Mine	1999	Hector	H-2	7.13	10.35	726	1.432	0.470	64.1	0.790	38.98	232.84
Mammoth Lakes-06	1980	Long Valley Dam (Upr L Abut)	H-1	5.94	9.65	537	1.456	1.376	44.1	1.402	33.12	119.85

Table A.42: Ground Motion Suite for F8S3B Building with 5% Probability of Exceedence in 50 Years for NEHRP Class C Site

Earthquake Name	Year	Station Name	Component	M_w	R_{jb} (km)	Vs30 (m/s)	Scale Factor	PGA (g)	PGV (cm/s)	Sa_{T1} (g)	Arias Intensity (cm/s)	Housner Intensity (cm)
Manjil Iran	1990	Abbar	H-2	7.37	12.55	724	1.070	0.532	54.1	2.045	87.67	235.81
Landers	1992	Coolwater	H-2	7.28	19.74	353	1.068	0.446	46.4	0.522	25.35	153.65
Kobe Japan	1995	Nishi-Akashi	H-1	6.9	7.08	609	1.057	0.511	49.5	0.772	38.16	156.10
Baja California	1987	Cerro Prieto	H-1	5.5	3.43	472	1.133	1.451	52.6	3.319	46.80	188.55
Chalfant Valley-02	1986	Zack Brothers Ranch	H-1	6.19	6.44	316	1.031	0.461	37.9	0.964	20.99	155.12
Chalfant Valley-02	1986	Zack Brothers Ranch	H-2	6.19	6.44	316	1.162	0.465	52.0	0.744	27.46	176.60
Tottori Japan	2000	TTR007	H-1	6.61	11.28	470	1.183	0.867	50.6	3.167	73.81	140.96
Joshua Tree CA	1992	Indio - Jackson Road	H-2	6.1	25.04	292	1.196	0.487	63.4	0.596	18.65	193.97
Kobe Japan	1995	Nishi-Akashi	H-2	6.9	7.08	609	1.203	0.559	46.0	0.928	33.48	165.79
Kocaeli Turkey	1999	Duzce	H-2	7.51	13.6	282	0.987	0.359	54.9	0.609	13.24	223.86
Victoria Mexico	1980	Cerro Prieto	H-1	6.33	13.8	472	1.214	0.784	40.8	1.277	29.82	171.94
Managua Nicaragua-01	1972	Managua ESSO	H-2	6.24	3.51	289	1.271	0.419	39.1	0.887	33.07	140.80
Hector Mine	1999	Hector	H-2	7.13	10.35	726	1.271	0.417	56.9	0.701	30.71	206.67
Duzce Turkey	1999	IRIGM 496	H-2	7.14	4.21	760	1.315	0.987	52.1	2.210	114.84	127.75
Manjil Iran	1990	Abbar	H-1	7.37	12.55	724	1.333	0.686	56.6	1.970	84.12	180.11
Mammoth Lakes-06	1980	Long Valley Dam (Upr L Abut)	H-2	5.94	9.65	537	1.350	0.558	46.0	0.974	23.04	171.00
Tottori Japan	2000	SMNH01	H-1	6.61	5.83	446	1.393	1.021	49.6	1.784	106.39	134.64
Landers	1992	Joshua Tree	H-2	7.28	11.03	379	1.409	0.400	60.0	0.475	47.43	230.92
Kocaeli Turkey	1999	Duzce	H-1	7.51	13.6	282	1.409	0.439	82.9	0.627	21.94	219.57
Superstition Hills-02	1987	Poe Road (temp)	H-1	6.54	11.16	317	1.448	0.688	59.6	0.866	45.32	177.25

Table A.43: Ground Motion Suite for F2S2B Building with 5% Probability of Exceedence in 50 Years for Generic Rock Site

Earthquake Name	Year	Station Name	Component	M_w	R_{jb} (km)	Vs30 (m/s)	Scale Factor	PGA (g)	PGV (cm/s)	Sa_{T1} (g)	Arias Intensity (cm/s)	Housner Intensity (cm)
Victoria Mexico	1980	Cerro Prieto	H-1	6.33	13.8	472	1.355	0.875	45.5	1.425	37.15	191.90
Tottori Japan	2000	TTR009	H-1	6.61	8.82	420	1.399	0.881	55.6	2.981	48.69	124.44
Tottori Japan	2000	SMNH01	H-2	6.61	5.83	446	1.321	0.815	46.8	2.406	84.14	127.69
Tottori Japan	2000	OKY004	H-2	6.61	19.72	476	1.309	1.079	30.8	1.901	125.56	96.90
Mammoth Lakes-06	1980	Long Valley Dam (Upr L Abut)	H-1	5.94	9.65	537	1.303	1.232	39.5	1.255	26.54	107.29
Darfield New Zealand	2010	Heathcote Valley Primary School	H-2	7.0	24.36	422	1.429	0.902	32.4	1.918	85.71	79.05
Big Bear-01	1992	Big Bear Lake - Civic Center	H-1	6.46	7.31	430	1.265	0.689	43.6	1.427	46.58	91.65
Kobe Japan	1995	Nishi-Akashi	H-2	6.9	7.08	609	1.243	0.577	47.6	0.959	35.75	171.31
Duzce Turkey	1999	IRIGM 496	H-1	7.14	4.21	760	1.239	1.277	49.8	2.025	209.20	121.21
Big Bear-01	1992	Big Bear Lake - Civic Center	H-2	6.46	7.31	430	1.501	0.723	42.3	1.703	76.30	94.68
Tottori Japan	2000	TTR009	H-2	6.61	8.82	420	1.232	0.742	32.1	2.048	44.82	91.89
Darfield New Zealand	2010	Heathcote Valley Primary School	H-1	7.0	24.36	422	1.219	0.703	51.6	1.947	58.01	107.06
Tottori Japan	2000	TTR007	H-2	6.61	11.28	470	1.534	0.859	39.8	2.570	83.11	89.28
Mammoth Lakes-06	1980	Long Valley Dam (Upr L Abut)	H-2	5.94	9.65	537	1.538	0.636	52.5	1.109	29.92	194.85
Parkfield-02 CA	2004	Parkfield - Fault Zone 11	H-2	6.0	3.12	542	1.554	1.757	42.9	5.121	76.45	76.72
Parkfield-02 CA	2004	Parkfield - Vineyard Cany 1E	H-2	6.0	1.59	381	1.611	0.467	41.2	1.126	26.97	131.44
Manjil Iran	1990	Abbar	H-2	7.37	12.55	724	1.151	0.572	58.2	2.199	101.37	253.57
Parkfield-02 CA	2004	PARKFIELD - UPSAR 11	H-1	6.0	8.93	466	1.661	0.773	44.9	0.995	41.54	116.47
Manjil Iran	1990	Abbar	H-1	7.37	12.55	724	1.115	0.574	47.3	1.648	58.86	150.65
Duzce Turkey	1999	IRIGM 498	H-2	7.14	3.58	425	1.677	0.593	42.3	1.244	33.82	105.74

Table A.44: Ground Motion Suite for F5S4B Building with 5% Probability of Exceedence in 50 Years for Generic Rock Site

Earthquake Name	Year	Station Name	Component	M_w	R_{jb} (km)	Vs30 (m/s)	Scale Factor	PGA (g)	PGV (cm/s)	Sa_{T1} (g)	Arias Intensity (cm/s)	Housner Intensity (cm)
Mammoth Lakes-06	1980	Long Valley Dam (Upr L Abut)	H-1	5.94	9.65	537	1.056	0.998	32.0	1.017	17.42	86.91
Hector Mine	1999	Hector	H-2	7.13	10.35	726	1.038	0.341	46.4	0.572	20.47	168.73
Mammoth Lakes-06	1980	Long Valley Dam (Upr L Abut)	H-2	5.94	9.65	537	1.031	0.427	35.2	0.744	13.45	130.67
Big Bear-01	1992	Big Bear Lake - Civic Center	H-1	6.46	7.31	430	1.130	0.615	39.0	1.274	37.14	81.84
Duzce Turkey	1999	IRIGM 496	H-1	7.14	4.21	760	1.133	1.168	45.6	1.852	174.82	110.80
Morgan Hill	1984	Anderson Dam (Downstream)	H-2	6.19	3.22	489	1.146	0.332	31.8	0.571	11.34	120.67
Tottori Japan	2000	TTR009	H-2	6.61	8.82	420	1.171	0.706	30.5	1.947	40.49	87.34
Manjil Iran	1990	Abbar	H-1	7.37	12.55	724	0.969	0.499	41.1	1.432	44.45	130.93
Kobe Japan	1995	Kobe University	H-1	6.9	0.9	1043	1.185	0.327	65.5	0.834	17.51	253.19
Darfield New Zealand	2010	Heathcote Valley Primary School	H-1	7.0	24.36	422	1.198	0.691	50.7	1.914	56.06	105.24
Duzce Turkey	1999	Lamont 375	H-1	7.14	3.93	454	0.946	0.842	35.2	1.768	90.83	73.93
Tottori Japan	2000	SMNH01	H-1	6.61	5.83	446	0.927	0.680	33.0	1.188	47.14	89.62
Kobe Japan	1995	Nishi-Akashi	H-2	6.9	7.08	609	0.924	0.429	35.4	0.713	19.75	127.35
Tottori Japan	2000	SMNH01	H-2	6.61	5.83	446	1.239	0.764	43.9	2.256	73.99	119.74
Parkfield-02 CA	2004	Parkfield - Vineyard Cany 1E	H-2	6.0	1.59	381	1.258	0.364	32.1	0.879	16.44	102.62
Victoria Mexico	1980	Cerro Prieto	H-1	6.33	13.8	472	0.903	0.583	30.3	0.950	16.49	127.85
Manjil Iran	1990	Abbar	H-2	7.37	12.55	724	0.875	0.435	44.3	1.672	58.63	192.84
Kobe Japan	1995	Kobe University	H-2	6.9	0.9	1043	1.309	0.408	40.4	0.957	14.31	170.40
Parkfield-02 CA	2004	PARKFIELD - UPSAR 11	H-1	6.0	8.93	466	1.314	0.612	35.5	0.788	26.00	92.14
Baja California	1987	Cerro Prieto	H-1	5.5	3.43	472	0.864	1.107	40.1	2.531	27.22	143.80

Table A.45: Ground Motion Suite for F8S3B Building with 5% Probability of Exceedence in 50 Years for Generic Rock Site

Earthquake Name	Year	Station Name	Component	M_w	R_{jb} (km)	Vs30 (m/s)	Scale Factor	PGA (g)	PGV (cm/s)	Sa_{T1} (g)	Arias Intensity (cm/s)	Housner Intensity (cm)
Tottori Japan	2000	SMNH01	H-1	6.61	5.83	446	1.293	0.948	46.0	1.655	91.59	124.92
Kobe Japan	1995	Kobe University	H-1	6.9	0.9	1043	1.285	0.354	71.0	0.905	20.57	274.45
Mammoth Lakes-06	1980	Long Valley Dam (Upr L Abut)	H-2	5.94	9.65	537	1.253	0.518	42.8	0.904	19.87	158.78
Duzce Turkey	1999	Lamont 375	H-1	7.14	3.93	454	1.408	1.253	52.3	2.631	201.28	110.05
Morgan Hill	1984	Anderson Dam (Downstream)	H-2	6.19	3.22	489	1.408	0.407	39.1	0.701	17.13	148.26
Manjil Iran	1990	Abbar	H-1	7.37	12.55	724	1.237	0.637	52.5	1.828	72.44	167.14
Duzce Turkey	1999	IRIGM 496	H-2	7.14	4.21	760	1.221	0.917	48.4	2.053	99.12	118.69
Kobe Japan	1995	Kobe University	H-2	6.9	0.9	1043	1.475	0.460	45.6	1.078	18.16	191.97
Hector Mine	1999	Hector	H-2	7.13	10.35	726	1.179	0.387	52.8	0.650	26.43	191.72
Mammoth Lakes-06	1980	Long Valley Dam (Upr L Abut)	H-1	5.94	9.65	537	1.486	1.404	45.0	1.430	34.49	122.30
Duzce Turkey	1999	IRIGM 496	H-1	7.14	4.21	760	1.499	1.545	60.3	2.450	306.06	146.61
Victoria Mexico	1980	Cerro Prieto	H-1	6.33	13.8	472	1.126	0.727	37.8	1.184	25.66	159.48
Kobe Japan	1995	Nishi-Akashi	H-2	6.9	7.08	609	1.116	0.518	42.7	0.860	28.78	153.72
Big Bear-01	1992	Big Bear Lake - Civic Center	H-1	6.46	7.31	430	1.566	0.853	54.0	1.767	71.40	113.47
Landers	1992	Morongo Valley Fire Station	H-1	7.28	17.36	396	1.570	0.350	47.0	0.508	30.24	186.78
Tottori Japan	2000	TTR007	H-1	6.61	11.28	470	1.098	0.806	47.0	2.942	63.69	130.93
Tottori Japan	2000	TTR009	H-2	6.61	8.82	420	1.639	0.987	42.7	2.724	79.28	122.21
Parkfield-02 CA	2004	Parkfield - Vineyard Cany 1E	H-2	6.0	1.59	381	1.642	0.476	42.0	1.147	27.99	133.91
Darfield New Zealand	2010	Heathcote Valley Primary School	H-1	7.0	24.36	422	1.644	0.948	69.6	2.626	105.60	144.44
Tottori Japan	2000	SMNH01	H-2	6.61	5.83	446	1.646	1.015	58.3	2.997	130.58	159.06

Table A.46: Ground Motion Suite for F2S2B Building with 5% Probability of Exceedence in 50 Years for NEHRP Class B Site

Earthquake Name	Year	Station Name	Component	M_w	R_{jb} (km)	Vs30 (m/s)	Scale Factor	PGA (g)	PGV (cm/s)	Sa_{T1} (g)	Arias Intensity (cm/s)	Housner Intensity (cm)
Hector Mine	1999	Hector	H-2	7.13	10.35	726	1.126	0.370	50.4	0.621	24.11	183.12
Kobe Japan	1995	Kobe University	H-2	6.9	0.9	1043	1.355	0.422	41.8	0.990	15.32	176.32
Kobe Japan	1995	Kobe University	H-1	6.9	0.9	1043	1.431	0.395	79.1	1.008	25.52	305.70
Tottori Japan	2000	SMNH10	H-2	6.61	15.58	967	1.566	0.361	33.6	0.932	12.11	109.18
Parkfield-02 CA	2004	PARKFIELD - DONNA LEE	H-2	6.0	4.25	657	1.649	0.615	23.2	2.833	19.81	65.40
Hector Mine	1999	Hector	H-1	7.13	10.35	726	1.660	0.441	43.2	0.730	23.32	169.68
Kobe Japan	1995	Nishi-Akashi	H-2	6.9	7.08	609	0.799	0.371	30.6	0.616	14.77	110.13
Duzce Turkey	1999	IRIGM 496	H-1	7.14	4.21	760	0.797	0.821	32.1	1.303	86.52	77.95
Manjil Iran	1990	Abbar	H-2	7.37	12.55	724	0.740	0.368	37.4	1.415	41.97	163.16
Manjil Iran	1990	Abbar	H-1	7.37	12.55	724	0.716	0.368	30.4	1.058	24.27	96.74
Kobe Japan	1995	Nishi-Akashi	H-1	6.9	7.08	609	0.686	0.332	32.1	0.501	16.08	101.33
Tottori Japan	2000	SMN015	H-2	6.61	9.1	617	1.977	0.541	30.2	0.715	15.15	91.19
Tottori Japan	2000	OKYH14	H-2	6.61	26.51	710	2.088	0.945	48.5	5.100	54.76	91.60
Parkfield-02 CA	2004	PARKFIELD - DONNA LEE	H-1	6.0	4.25	657	2.106	0.620	32.0	1.213	16.18	80.88
Tottori Japan	2000	SMN015	H-1	6.61	9.1	617	2.107	0.320	40.4	0.809	15.79	150.45
Parkfield-02 CA	2004	PARKFIELD - TURKEY FLAT 1 (0M)	H-1	6.0	4.66	907	2.318	0.569	33.9	0.850	9.37	66.45
Duzce Turkey	1999	Lamont 531	H-2	7.14	8.03	638	2.383	0.294	31.9	0.557	23.90	103.50
Parkfield-02 CA	2004	PARKFIELD - TURKEY FLAT 1 (0M)	H-2	6.0	4.66	907	2.394	0.470	28.2	0.716	11.02	77.78
Duzce Turkey	1999	Lamont 531	H-1	7.14	8.03	638	2.406	0.386	26.2	0.572	26.37	70.50
Duzce Turkey	1999	IRIGM 496	H-2	7.14	4.21	760	0.541	0.406	21.4	0.909	19.42	52.53

Table A.47: Ground Motion Suite for F5S4B Building with 5% Probability of Exceedence in 50 Years for NEHRP Class B Site

Earthquake Name	Year	Station Name	Component	M_w	R_{jb} (km)	Vs30 (m/s)	Scale Factor	PGA (g)	PGV (cm/s)	Sa_{T1} (g)	Arias Intensity (cm/s)	Housner Intensity (cm)
Kobe Japan	1995	Kobe University	H-2	6.9	0.9	1043	0.977	0.305	30.2	0.714	7.97	127.17
Hector Mine	1999	Hector	H-1	7.13	10.35	726	1.240	0.329	32.2	0.545	13.00	126.72
Kobe Japan	1995	Kobe University	H-1	6.9	0.9	1043	0.885	0.244	48.9	0.623	9.77	189.12
Duzce Turkey	1999	IRIGM 496	H-1	7.14	4.21	760	0.848	0.874	34.1	1.386	98.01	82.96
Tottori Japan	2000	SMNH10	H-2	6.61	15.58	967	1.485	0.343	31.9	0.884	10.90	103.55
Hector Mine	1999	Hector	H-2	7.13	10.35	726	0.776	0.255	34.7	0.428	11.45	126.20
Tottori Japan	2000	SMN015	H-1	6.61	9.1	617	1.613	0.245	30.9	0.619	9.26	115.22
Manjil Iran	1990	Abbar	H-1	7.37	12.55	724	0.726	0.373	30.8	1.072	24.93	98.05
Chi-Chi Taiwan-04	1999	CHY035	H-2	6.2	25.01	573	1.723	0.230	25.6	0.333	8.73	101.96
Kobe Japan	1995	Nishi-Akashi	H-2	6.9	7.08	609	0.691	0.321	26.4	0.533	11.03	95.18
Tottori Japan	2000	SMN015	H-2	6.61	9.1	617	1.800	0.492	27.5	0.651	12.55	83.01
Manjil Iran	1990	Abbar	H-2	7.37	12.55	724	0.654	0.325	33.1	1.249	32.71	144.05
Duzce Turkey	1999	Lamont 531	H-2	7.14	8.03	638	1.833	0.226	24.6	0.429	14.14	79.62
Duzce Turkey	1999	IRIGM 496	H-2	7.14	4.21	760	0.638	0.479	25.3	1.073	27.08	62.03
Parkfield-02 CA	2004	PARKFIELD - DONNA LEE	H-2	6.0	4.25	657	1.905	0.710	26.8	3.272	26.43	75.54
Chi-Chi Taiwan-04	1999	CHY035	H-1	6.2	25.01	573	2.072	0.242	35.5	0.411	8.65	108.30
Parkfield-02 CA	2004	PARKFIELD - DONNA LEE	H-1	6.0	4.25	657	2.102	0.619	31.9	1.210	16.12	80.74
Kobe Japan	1995	Nishi-Akashi	H-1	6.9	7.08	609	0.562	0.271	26.3	0.411	10.78	82.97
Darfield New Zealand	2010	CSHS	H-2	7.0	43.6	638	2.180	0.252	26.1	0.374	18.62	128.84
Parkfield-02 CA	2004	PARKFIELD - TURKEY FLAT 1 (0M)	H-2	6.0	4.66	907	2.211	0.434	26.1	0.661	9.40	71.83

Table A.48: Ground Motion Suite for F8S3B Building with 5% Probability of Exceedence in 50 Years for NEHRP Class B Site

Earthquake Name	Year	Station Name	Component	M_w	R_{jb} (km)	Vs30 (m/s)	Scale Factor	PGA (g)	PGV (cm/s)	Sa_{T1} (g)	Arias Intensity (cm/s)	Housner Intensity (cm)
Hector Mine	1999	Hector	H-1	7.13	10.35	726	1.135	0.301	29.5	0.499	10.91	116.08
Duzce Turkey	1999	IRIGM 496	H-1	7.14	4.21	760	0.862	0.888	34.7	1.409	101.22	84.31
Kobe Japan	1995	Kobe University	H-2	6.9	0.9	1043	0.847	0.264	26.2	0.619	5.99	110.28
Tottori Japan	2000	SMNH10	H-2	6.61	15.58	967	1.399	0.323	30.0	0.833	9.67	97.55
Kobe Japan	1995	Kobe University	H-1	6.9	0.9	1043	0.739	0.204	40.8	0.520	6.80	157.83
Tottori Japan	2000	SMN015	H-1	6.61	9.1	617	1.478	0.224	28.3	0.567	7.77	105.53
Manjil Iran	1990	Abbar	H-1	7.37	12.55	724	0.712	0.366	30.2	1.052	23.97	96.15
Duzce Turkey	1999	IRIGM 496	H-2	7.14	4.21	760	0.701	0.526	27.8	1.179	32.68	68.15
Chi-Chi Taiwan-04	1999	CHY035	H-2	6.2	25.01	573	1.590	0.212	23.6	0.307	7.44	94.14
Hector Mine	1999	Hector	H-2	7.13	10.35	726	0.676	0.222	30.3	0.373	8.69	109.96
Kobe Japan	1995	Nishi-Akashi	H-2	6.9	7.08	609	0.641	0.298	24.5	0.494	9.49	88.29
Duzce Turkey	1999	Lamont 531	H-2	7.14	8.03	638	1.778	0.220	23.8	0.416	13.31	77.24
Tottori Japan	2000	SMN015	H-2	6.61	9.1	617	1.806	0.494	27.6	0.653	12.64	83.30
Darfield New Zealand	2010	CSHS	H-2	7.0	43.6	638	1.828	0.212	21.9	0.314	13.10	108.09
Manjil Iran	1990	Abbar	H-2	7.37	12.55	724	0.571	0.284	28.9	1.091	24.95	125.80
Chi-Chi Taiwan-04	1999	CHY035	H-1	6.2	25.01	573	1.920	0.224	32.9	0.381	7.43	100.34
Kobe Japan	1995	Nishi-Akashi	H-1	6.9	7.08	609	0.564	0.272	26.4	0.412	10.85	83.23
Parkfield-02 CA	2004	PARKFIELD - DONNA LEE	H-2	6.0	4.25	657	1.966	0.733	27.6	3.376	28.14	77.96
Chi-Chi Taiwan-04	1999	CHY086	H-2	6.2	33.63	665	2.050	0.225	22.6	0.300	7.68	87.44
Parkfield-02 CA	2004	PARKFIELD - DONNA LEE	H-1	6.0	4.25	657	2.148	0.632	32.6	1.237	16.83	82.50

Table A.49: Ground Motion Suite for F2S2B Building with 2% Probability of Exceedence in 50 Years for NEHRP Class D Site

Earthquake Name	Year	Station Name	Component	M_w	R_{jb} (km)	Vs30 (m/s)	Scale Factor	PGA (g)	PGV (cm/s)	Sa_{T1} (g)	Arias Intensity (cm/s)	Housner Intensity (cm)
Tottori Japan	2000	TTRH02	H-2	6.61	0.83	310	1.060	0.818	91.7	1.128	112.48	300.90
Imperial Valley-06	1979	Bonds Corner	H-2	6.53	0.44	223	1.081	0.840	48.6	1.917	72.14	202.85
Tottori Japan	2000	TTRH02	H-1	6.61	0.83	310	0.919	0.864	112.3	1.383	101.56	345.86
El Mayor-Cucapah Mexico	2010	El Centro Array 11	H-2	7.2	15.36	196	1.300	0.762	82.1	1.629	95.35	289.43
Parkfield-02 CA	2004	Parkfield - Fault Zone 14	H-1	6.0	8.45	246	0.858	1.123	71.5	1.448	57.57	215.47
Parkfield-02 CA	2004	Parkfield - Fault Zone 14	H-2	6.0	8.45	246	1.475	0.849	62.4	2.790	61.39	214.26
Imperial Valley-06	1979	Bonds Corner	H-1	6.53	0.44	223	1.521	0.911	71.1	2.478	94.07	265.55
El Mayor-Cucapah Mexico	2010	El Centro Array 11	H-1	7.2	15.36	196	1.588	0.702	91.7	1.414	126.89	258.51
El Mayor-Cucapah Mexico	2010	El Centro Differential Array	H-1	7.2	22.83	202	1.762	0.977	51.6	2.692	137.57	193.42
Chalfant Valley-02	1986	Zack Brothers Ranch	H-1	6.19	6.44	316	1.783	0.797	65.6	1.666	62.77	268.27
El Mayor-Cucapah Mexico	2010	RIITO	H-2	7.2	13.7	242	1.840	0.692	69.6	1.895	161.59	268.36
El Mayor-Cucapah Mexico	2010	MICHOACAN DE OCAMPO	H-1	7.2	13.21	242	1.953	1.050	120.1	1.905	236.81	425.26
El Mayor-Cucapah Mexico	2010	MICHOACAN DE OCAMPO	H-1	7.2	13.21	242	1.953	1.050	120.1	1.905	236.81	425.26
El Mayor-Cucapah Mexico	2010	El Centro Differential Array	H-2	7.2	22.83	202	1.958	0.992	76.0	3.156	158.76	294.26
El Mayor-Cucapah Mexico	2010	El Centro - Imperial & Ross	H-1	7.2	19.39	229	1.980	0.761	93.8	1.707	149.54	295.66
El Mayor-Cucapah Mexico	2010	RIITO	H-1	7.2	13.7	242	1.986	0.788	104.1	2.472	160.48	290.29
Managua Nicaragua-01	1972	Managua ESSO	H-2	6.24	3.51	289	2.054	0.677	63.1	1.434	86.41	227.59
Darfield New Zealand	2010	DFHS	H-2	7.0	11.86	344	2.077	1.065	61.8	2.312	123.98	213.51
El Mayor-Cucapah Mexico	2010	El Centro Array 10	H-2	7.2	19.36	203	2.089	0.797	99.6	1.076	160.48	363.14
Chalfant Valley-02	1986	Zack Brothers Ranch	H-2	6.19	6.44	316	2.115	0.847	94.6	1.355	90.99	321.48

Table A.50: Ground Motion Suite for F5S4B Building with 2% Probability of Exceedence in 50 Years for NEHRP Class D Site

Earthquake Name	Year	Station Name	Component	M_w	R_{jb} (km)	Vs30 (m/s)	Scale Factor	PGA (g)	PGV (cm/s)	Sa_{T1} (g)	Arias Intensity (cm/s)	Housner Intensity (cm)
Parkfield-02 CA	2004	Parkfield - Fault Zone 14	H-1	6.0	8.45	246	1.437	1.882	119.8	2.425	161.56	360.97
Tottori Japan	2000	TTRH02	H-2	6.61	0.83	310	1.397	1.078	120.9	1.487	195.66	396.86
Tottori Japan	2000	TTRH02	H-1	6.61	0.83	310	1.267	1.191	154.7	1.906	192.77	476.49
El Mayor-Cucapah Mexico	2010	El Centro Array 11	H-2	7.2	15.36	196	1.763	1.034	111.4	2.210	175.57	392.74
Imperial Valley-06	1979	Bonds Corner	H-2	6.53	0.44	223	1.790	1.391	80.4	3.175	197.84	335.92
El Mayor-Cucapah Mexico	2010	El Centro Array 11	H-1	7.2	15.36	196	2.257	0.997	130.3	2.009	256.25	367.36
Parkfield-02 CA	2004	Parkfield - Fault Zone 14	H-2	6.0	8.45	246	2.416	1.391	102.2	4.571	164.73	351.00
Imperial Valley-06	1979	Bonds Corner	H-1	6.53	0.44	223	2.450	1.467	114.5	3.989	243.86	427.56
Chalfant Valley-02	1986	Zack Brothers Ranch	H-1	6.19	6.44	316	2.579	1.153	94.9	2.411	131.38	388.11
El Mayor-Cucapah Mexico	2010	El Centro Array 10	H-2	7.2	19.36	203	2.601	0.992	124.0	1.340	248.68	452.05
El Mayor-Cucapah Mexico	2010	MICHOACAN DE OCAMPO	H-1	7.2	13.21	242	2.676	1.439	164.7	2.610	444.81	582.82
Landers	1992	Coolwater	H-2	7.28	19.74	353	2.711	1.131	117.7	1.326	163.43	390.08
El Mayor-Cucapah Mexico	2010	RIITO	H-2	7.2	13.7	242	2.786	1.048	105.4	2.869	370.52	406.36
El Mayor-Cucapah Mexico	2010	El Centro - Imperial & Ross	H-1	7.2	19.39	229	2.804	1.078	132.8	2.416	299.82	418.65
Kocaeli Turkey	1999	Duzce	H-2	7.51	13.6	282	2.804	1.021	156.0	1.730	106.86	635.88
Chalfant Valley-02	1986	Zack Brothers Ranch	H-2	6.19	6.44	316	2.927	1.173	130.9	1.875	174.30	444.95
El Mayor-Cucapah Mexico	2010	RIITO	H-1	7.2	13.7	242	3.033	1.203	158.9	3.774	374.12	443.23
El Mayor-Cucapah Mexico	2010	El Centro Array 10	H-1	7.2	19.36	203	3.082	1.123	140.5	1.767	292.20	420.81
El Mayor-Cucapah Mexico	2010	El Centro - Imperial & Ross	H-2	7.2	19.39	229	3.099	1.147	147.5	3.643	321.13	518.84
Westmorland	1981	Westmorland Fire Sta	H-1	5.9	6.18	194	3.126	1.179	137.9	2.418	175.08	560.72

Table A.51: Ground Motion Suite for F8S3B Building with 2% Probability of Exceedence in 50 Years for NEHRP Class D Site

Earthquake Name	Year	Station Name	Component	M_w	R_{jb} (km)	Vs30 (m/s)	Scale Factor	PGA (g)	PGV (cm/s)	Sa_{T1} (g)	Arias Intensity (cm/s)	Housner Intensity (cm)
Tottori Japan	2000	TTRH02	H-2	6.61	0.83	310	1.443	1.113	124.9	1.536	208.57	409.75
Parkfield-02 CA	2004	Parkfield - Fault Zone 14	H-1	6.0	8.45	246	1.464	1.917	122.0	2.470	167.57	367.61
Tottori Japan	2000	TTRH02	H-1	6.61	0.83	310	1.208	1.136	147.5	1.818	175.30	454.38
El Mayor-Cucapah Mexico	2010	El Centro Array 11	H-2	7.2	15.36	196	1.750	1.026	110.6	2.193	172.85	389.69
Imperial Valley-06	1979	Bonds Corner	H-2	6.53	0.44	223	1.928	1.498	86.6	3.420	229.56	361.84
El Mayor-Cucapah Mexico	2010	El Centro Array 11	H-1	7.2	15.36	196	2.222	0.982	128.3	1.978	248.41	361.70
Imperial Valley-06	1979	Bonds Corner	H-1	6.53	0.44	223	2.409	1.442	112.6	3.923	235.82	420.46
Kocaeli Turkey	1999	Duzce	H-2	7.51	13.6	282	2.481	0.903	138.0	1.530	83.66	562.63
Kocaeli Turkey	1999	Duzce	H-2	7.51	13.6	282	2.481	0.903	138.0	1.530	83.66	562.63
El Mayor-Cucapah Mexico	2010	El Centro Array 10	H-2	7.2	19.36	203	2.529	0.964	120.5	1.303	235.13	439.57
El Mayor-Cucapah Mexico	2010	MICHOACAN DE OCAMPO	H-1	7.2	13.21	242	2.553	1.372	157.1	2.490	404.77	555.98
Chalfant Valley-02	1986	Zack Brothers Ranch	H-1	6.19	6.44	316	2.591	1.159	95.3	2.423	132.65	389.98
Parkfield-02 CA	2004	Parkfield - Fault Zone 14	H-2	6.0	8.45	246	2.649	1.526	112.1	5.013	198.13	384.93
Landers	1992	Coolwater	H-2	7.28	19.74	353	2.685	1.120	116.6	1.313	160.33	386.36
El Mayor-Cucapah Mexico	2010	El Centro - Imperial & Ross	H-1	7.2	19.39	229	2.745	1.055	130.0	2.366	287.34	409.84
El Mayor-Cucapah Mexico	2010	RIITO	H-2	7.2	13.7	242	2.774	1.043	104.9	2.857	367.25	404.56
Kobe Japan	1995	Amagasaki	H-2	6.9	11.34	256	2.846	0.930	127.5	1.899	161.20	627.42
Westmorland	1981	Westmorland Fire Sta	H-1	5.9	6.18	194	2.919	1.101	128.8	2.258	152.69	523.64
Chalfant Valley-02	1986	Zack Brothers Ranch	H-2	6.19	6.44	316	2.923	1.171	130.7	1.873	173.81	444.32
Imperial Valley-06	1979	El Centro Array 8	H-1	6.53	3.86	206	2.981	1.819	162.4	2.785	148.14	547.85

Table A.52: Ground Motion Suite for F2S2B Building with 2% Probability of Exceedence in 50 Years for NEHRP Class C Site

Earthquake Name	Year	Station Name	Component	M_w	R_{jb} (km)	Vs30 (m/s)	Scale Factor	PGA (g)	PGV (cm/s)	Sa_{T1} (g)	Arias Intensity (cm/s)	Housner Intensity (cm)
Duzce Turkey	1999	IRIGM 496	H-2	7.14	4.21	760	1.279	0.960	50.7	2.150	108.75	124.32
Tottori Japan	2000	TTR007	H-1	6.61	11.28	470	1.297	0.952	55.5	3.474	88.83	154.63
Baja California	1987	Cerro Prieto	H-2	5.5	3.43	472	1.313	1.187	72.4	2.717	56.74	251.43
Tottori Japan	2000	SMNH01	H-1	6.61	5.83	446	1.428	1.046	50.8	1.828	111.71	137.96
Duzce Turkey	1999	Lamont 375	H-1	7.14	3.93	454	1.433	1.276	53.3	2.678	208.52	112.02
Baja California	1987	Cerro Prieto	H-1	5.5	3.43	472	1.577	2.019	73.2	4.620	90.66	262.42
Tottori Japan	2000	TTRH02	H-2	6.61	0.83	310	1.021	0.788	88.4	1.087	104.42	289.91
Kobe Japan	1995	Nishi-Akashi	H-1	6.9	7.08	609	1.623	0.785	76.0	1.186	90.03	239.76
Manjil Iran	1990	Abbar	H-1	7.37	12.55	724	1.696	0.873	72.0	2.507	136.19	229.17
Chalfant Valley-02	1986	Zack Brothers Ranch	H-1	6.19	6.44	316	1.716	0.767	63.1	1.604	58.14	258.18
Manjil Iran	1990	Abbar	H-2	7.37	12.55	724	1.754	0.871	88.7	3.352	235.55	386.52
Tottori Japan	2000	TTRH02	H-1	6.61	0.83	310	0.885	0.832	108.1	1.332	94.16	333.02
Darfield New Zealand	2010	Heathcote Valley Primary School	H-1	7.0	24.36	422	1.858	1.071	78.6	2.967	134.76	163.17
Tottori Japan	2000	TTR009	H-2	6.61	8.82	420	1.877	1.131	48.9	3.119	103.94	139.94
Duzce Turkey	1999	IRIGM 496	H-1	7.14	4.21	760	1.888	1.946	75.9	3.086	485.70	184.69
Kobe Japan	1995	Nishi-Akashi	H-2	6.9	7.08	609	1.892	0.879	72.4	1.459	82.78	260.71
Big Bear-01	1992	Big Bear Lake - Civic Center	H-1	6.46	7.31	430	1.924	1.048	66.4	2.170	107.74	139.39
Managua Nicaragua-01	1972	Managua ESSO	H-2	6.24	3.51	289	1.975	0.651	60.7	1.378	79.88	218.82
Mammoth Lakes-06	1980	Long Valley Dam (Upr L Abut)	H-1	5.94	9.65	537	1.984	1.876	60.1	1.910	61.51	163.34
Tottori Japan	2000	OKY004	H-2	6.61	19.72	476	1.988	1.639	46.9	2.888	289.73	147.19

Table A.53: Ground Motion Suite for F5S4B Building with 2% Probability of Exceedence in 50 Years for NEHRP Class C Site

Earthquake Name	Year	Station Name	Component	M_w	R_{jb} (km)	Vs30 (m/s)	Scale Factor	PGA (g)	PGV (cm/s)	Sa_{T1} (g)	Arias Intensity (cm/s)	Housner Intensity (cm)
Baja California	1987	Cerro Prieto	H-2	5.5	3.43	472	1.183	1.070	65.2	2.448	46.06	226.54
Kobe Japan	1995	Nishi-Akashi	H-1	6.9	7.08	609	1.438	0.695	67.3	1.051	70.63	212.36
Chalfant Valley-02	1986	Zack Brothers Ranch	H-1	6.19	6.44	316	1.481	0.662	54.5	1.385	43.34	222.92
Tottori Japan	2000	TTR007	H-1	6.61	11.28	470	1.556	1.141	66.6	4.167	127.79	185.47
Tottori Japan	2000	TTR007	H-1	6.61	11.28	470	1.556	1.141	66.6	4.167	127.79	185.47
Landers	1992	Coolwater	H-2	7.28	19.74	353	1.561	0.651	67.7	0.763	54.16	224.56
Kocaeli Turkey	1999	Duzce	H-2	7.51	13.6	282	1.611	0.587	89.7	0.994	35.29	365.45
Duzce Turkey	1999	IRIGM 496	H-2	7.14	4.21	760	1.632	1.225	64.7	2.743	176.94	158.57
Baja California	1987	Cerro Prieto	H-1	5.5	3.43	472	1.651	2.114	76.6	4.836	99.33	274.68
Manjil Iran	1990	Abbar	H-2	7.37	12.55	724	1.673	0.831	84.6	3.197	214.25	368.64
Chalfant Valley-02	1986	Zack Brothers Ranch	H-2	6.19	6.44	316	1.684	0.674	75.3	1.079	57.66	255.92
Victoria Mexico	1980	Cerro Prieto	H-1	6.33	13.8	472	1.727	1.115	58.0	1.816	60.34	244.55
Tottori Japan	2000	SMNH01	H-1	6.61	5.83	446	1.770	1.298	63.0	2.267	171.76	171.07
Kobe Japan	1995	Nishi-Akashi	H-2	6.9	7.08	609	1.770	0.822	67.7	1.365	72.47	243.93
Tottori Japan	2000	TTRH02	H-2	6.61	0.83	310	0.802	0.619	69.4	0.854	64.45	227.77
Duzce Turkey	1999	Lamont 375	H-1	7.14	3.93	454	1.811	1.612	67.3	3.386	333.21	141.60
Managua Nicaragua-01	1972	Managua ESSO	H-2	6.24	3.51	289	1.831	0.603	56.2	1.277	68.61	202.79
Joshua Tree CA	1992	Indio - Jackson Road	H-2	6.1	25.04	292	1.840	0.749	97.6	0.918	44.17	298.54
Manjil Iran	1990	Abbar	H-1	7.37	12.55	724	1.853	0.954	78.7	2.739	162.57	250.38
Mammoth Lakes-06	1980	Long Valley Dam (Upr L Abut)	H-2	5.94	9.65	537	1.974	0.817	67.4	1.424	49.29	250.10

Table A.54: Ground Motion Suite for F8S3B Building with 2% Probability of Exceedence in 50 Years for NEHRP Class C Site

Earthquake Name	Year	Station Name	Component	M_w	R_{jb} (km)	Vs30 (m/s)	Scale Factor	PGA (g)	PGV (cm/s)	Sa_{T1} (g)	Arias Intensity (cm/s)	Housner Intensity (cm)
Baja California	1987	Cerro Prieto	H-2	5.5	3.43	472	1.155	1.045	63.7	2.391	43.93	221.23
Kocaeli Turkey	1999	Duzce	H-2	7.51	13.6	282	1.404	0.511	78.1	0.866	26.81	318.48
Kocaeli Turkey	1999	Duzce	H-2	7.51	13.6	282	1.404	0.511	78.1	0.866	26.81	318.48
Chalfant Valley-02	1986	Zack Brothers Ranch	H-1	6.19	6.44	316	1.468	0.656	54.0	1.372	42.56	220.89
Kobe Japan	1995	Nishi-Akashi	H-1	6.9	7.08	609	1.503	0.726	70.4	1.098	77.17	221.98
Landers	1992	Coolwater	H-2	7.28	19.74	353	1.521	0.634	66.0	0.744	51.42	218.80
Manjil Iran	1990	Abbar	H-2	7.37	12.55	724	1.521	0.756	76.9	2.906	177.07	335.12
Baja California	1987	Cerro Prieto	H-1	5.5	3.43	472	1.612	2.064	74.8	4.722	94.73	268.25
Chalfant Valley-02	1986	Zack Brothers Ranch	H-2	6.19	6.44	316	1.655	0.663	74.0	1.060	55.70	251.54
Tottori Japan	2000	TTR007	H-1	6.61	11.28	470	1.684	1.235	72.1	4.511	149.72	200.75
Tottori Japan	2000	TTRH02	H-2	6.61	0.83	310	0.816	0.630	70.6	0.869	66.74	231.79
Joshua Tree CA	1992	Indio - Jackson Road	H-2	6.1	25.04	292	1.701	0.692	90.2	0.848	37.73	275.90
Kobe Japan	1995	Nishi-Akashi	H-2	6.9	7.08	609	1.711	0.795	65.5	1.320	67.71	235.78
Victoria Mexico	1980	Cerro Prieto	H-1	6.33	13.8	472	1.725	1.114	57.9	1.815	60.22	244.32
Hector Mine	1999	Hector	H-2	7.13	10.35	726	1.807	0.593	80.9	0.997	62.04	293.75
Managua Nicaragua-01	1972	Managua ESSO	H-2	6.24	3.51	289	1.807	0.595	55.5	1.261	66.81	200.12
Duzce Turkey	1999	IRIGM 496	H-2	7.14	4.21	760	1.870	1.404	74.1	3.143	232.35	181.72
Manjil Iran	1990	Abbar	H-1	7.37	12.55	724	1.898	0.977	80.6	2.805	170.53	256.44
Mammoth Lakes-06	1980	Long Valley Dam (Upr L Abut)	H-2	5.94	9.65	537	1.921	0.795	65.5	1.386	46.66	243.35
Tottori Japan	2000	SMNH01	H-1	6.61	5.83	446	1.982	1.453	70.6	2.538	215.23	191.50

Table A.55: Ground Motion Suite for F2S2B Building with 2% Probability of Exceedence in 50 Years for Generic Rock Site

Earthquake Name	Year	Station Name	Component	M_w	R_{jb} (km)	Vs30 (m/s)	Scale Factor	PGA (g)	PGV (cm/s)	Sa_{T1} (g)	Arias Intensity (cm/s)	Housner Intensity (cm)
Baja California	1987	Cerro Prieto	H-1	5.5	3.43	472	1.484	1.901	68.9	4.348	80.29	246.96
Kobe Japan	1995	Nishi-Akashi	H-1	6.9	7.08	609	1.532	0.740	71.7	1.119	80.14	226.20
Manjil Iran	1990	Abbar	H-1	7.37	12.55	724	1.597	0.822	67.8	2.359	120.64	215.69
Duzce Turkey	1999	Lamont 375	H-1	7.14	3.93	454	1.346	1.198	50.0	2.515	183.94	105.21
Tottori Japan	2000	SMNH01	H-1	6.61	5.83	446	1.341	0.983	47.8	1.718	98.60	129.62
Manjil Iran	1990	Abbar	H-2	7.37	12.55	724	1.650	0.820	83.4	3.153	208.39	363.56
Darfield New Zealand	2010	Heathcote Valley Primary School	H-1	7.0	24.36	422	1.749	1.008	74.0	2.793	119.41	153.59
Baja California	1987	Cerro Prieto	H-2	5.5	3.43	472	1.234	1.116	68.0	2.554	50.12	236.31
Tottori Japan	2000	TTR009	H-2	6.61	8.82	420	1.768	1.065	46.0	2.938	92.22	131.81
Duzce Turkey	1999	IRIGM 496	H-1	7.14	4.21	760	1.775	1.829	71.4	2.901	429.25	173.62
Tottori Japan	2000	TTR007	H-1	6.61	11.28	470	1.219	0.894	52.2	3.264	78.42	145.29
Kobe Japan	1995	Nishi-Akashi	H-2	6.9	7.08	609	1.784	0.828	68.2	1.376	73.59	245.81
Duzce Turkey	1999	IRIGM 496	H-2	7.14	4.21	760	1.204	0.904	47.7	2.024	96.34	117.01
Big Bear-01	1992	Big Bear Lake - Civic Center	H-1	6.46	7.31	430	1.815	0.989	62.6	2.047	95.87	131.49
Mammoth Lakes-06	1980	Long Valley Dam (Upr L Abut)	H-1	5.94	9.65	537	1.868	1.766	56.6	1.799	54.53	153.78
Tottori Japan	2000	OKY004	H-2	6.61	19.72	476	1.874	1.545	44.2	2.722	257.44	138.75
Tottori Japan	2000	SMNH01	H-2	6.61	5.83	446	1.895	1.169	67.2	3.451	173.08	183.13
Victoria Mexico	1980	Cerro Prieto	H-1	6.33	13.8	472	1.943	1.254	65.3	2.044	76.40	275.20
Tottori Japan	2000	TTR009	H-1	6.61	8.82	420	2.005	1.263	79.7	4.274	100.07	178.41
Darfield New Zealand	2010	Heathcote Valley Primary School	H-2	7.0	24.36	422	2.044	1.291	46.4	2.743	175.38	113.07

Table A.56: Ground Motion Suite for F5S4B Building with 2% Probability of Exceedence in 50 Years for Generic Rock Site

Earthquake Name	Year	Station Name	Component	M_w	R_{jb} (km)	Vs30 (m/s)	Scale Factor	PGA (g)	PGV (cm/s)	Sa_{T1} (g)	Arias Intensity (cm/s)	Housner Intensity (cm)
Tottori Japan	2000	TTR007	H-1	6.61	11.28	470	1.157	0.849	49.5	3.099	70.66	137.91
Duzce Turkey	1999	IRIGM 496	H-2	7.14	4.21	760	1.212	0.910	48.0	2.037	97.62	117.78
Baja California	1987	Cerro Prieto	H-1	5.5	3.43	472	1.228	1.572	57.0	3.597	54.96	204.32
Kobe Japan	1995	Nishi-Akashi	H-1	6.9	7.08	609	1.070	0.517	50.1	0.782	39.09	157.98
Manjil Iran	1990	Abbar	H-2	7.37	12.55	724	1.244	0.618	62.9	2.378	118.53	274.19
Victoria Mexico	1980	Cerro Prieto	H-1	6.33	13.8	472	1.284	0.829	43.1	1.351	33.37	181.88
Kobe Japan	1995	Nishi-Akashi	H-2	6.9	7.08	609	1.315	0.611	50.3	1.014	40.01	181.24
Tottori Japan	2000	SMNH01	H-1	6.61	5.83	446	1.318	0.966	46.9	1.687	95.15	127.33
Duzce Turkey	1999	Lamont 375	H-1	7.14	3.93	454	1.350	1.202	50.2	2.523	185.06	105.53
Manjil Iran	1990	Abbar	H-1	7.37	12.55	724	1.381	0.711	58.6	2.040	90.23	186.54
Mammoth Lakes-06	1980	Long Valley Dam (Upr L Abut)	H-2	5.94	9.65	537	1.470	0.608	50.2	1.061	27.35	186.30
Hector Mine	1999	Hector	H-2	7.13	10.35	726	1.477	0.485	66.1	0.815	41.49	240.21
Baja California	1987	Cerro Prieto	H-2	5.5	3.43	472	0.879	0.795	48.5	1.820	25.46	168.42
Mammoth Lakes-06	1980	Long Valley Dam (Upr L Abut)	H-1	5.94	9.65	537	1.501	1.419	45.5	1.446	35.22	123.58
Big Bear-01	1992	Big Bear Lake - Civic Center	H-1	6.46	7.31	430	1.605	0.874	55.4	1.810	74.93	116.24
Duzce Turkey	1999	IRIGM 496	H-1	7.14	4.21	760	1.612	1.661	64.8	2.634	353.76	157.62
Morgan Hill	1984	Anderson Dam (Downstream)	H-2	6.19	3.22	489	1.630	0.472	45.3	0.812	22.96	171.66
Tottori Japan	2000	TTR009	H-2	6.61	8.82	420	1.667	1.004	43.4	2.770	81.96	124.27
Kobe Japan	1995	Kobe University	H-1	6.9	0.9	1043	1.687	0.465	93.3	1.188	35.47	360.41
Darfield New Zealand	2010	Heathcote Valley Primary School	H-1	7.0	24.36	422	1.704	0.983	72.1	2.722	113.46	149.72

Table A.57: Ground Motion Suite for F8S3B Building with 2% Probability of Exceedence in 50 Years for Generic Rock Site

Earthquake Name	Year	Station Name	Component	M_w	R_{jb} (km)	Vs30 (m/s)	Scale Factor	PGA (g)	PGV (cm/s)	Sa_{T1} (g)	Arias Intensity (cm/s)	Housner Intensity (cm)
Manjil Iran	1990	Abbar	H-2	7.37	12.55	724	1.202	0.597	60.8	2.297	110.65	264.92
Kobe Japan	1995	Nishi-Akashi	H-1	6.9	7.08	609	1.188	0.574	55.6	0.868	48.19	175.40
Baja California	1987	Cerro Prieto	H-1	5.5	3.43	472	1.274	1.632	59.1	3.732	59.18	212.02
Tottori Japan	2000	TTR007	H-1	6.61	11.28	470	1.330	0.976	56.9	3.562	93.35	158.52
Kobe Japan	1995	Nishi-Akashi	H-2	6.9	7.08	609	1.352	0.628	51.7	1.042	42.24	186.22
Victoria Mexico	1980	Cerro Prieto	H-1	6.33	13.8	472	1.366	0.882	45.9	1.437	37.75	193.43
Hector Mine	1999	Hector	H-2	7.13	10.35	726	1.427	0.468	63.9	0.788	38.74	232.11
Duzce Turkey	1999	IRIGM 496	H-2	7.14	4.21	760	1.479	1.110	58.6	2.486	145.38	143.74
Manjil Iran	1990	Abbar	H-1	7.37	12.55	724	1.500	0.772	63.7	2.216	106.44	202.59
Mammoth Lakes-06	1980	Long Valley Dam (Upr L Abut)	H-2	5.94	9.65	537	1.518	0.628	51.8	1.095	29.14	192.31
Kobe Japan	1995	Kobe University	H-1	6.9	0.9	1043	1.556	0.429	86.0	1.096	30.18	332.44
Tottori Japan	2000	SMNH01	H-1	6.61	5.83	446	1.566	1.148	55.8	2.005	134.39	151.32
Baja California	1987	Cerro Prieto	H-2	5.5	3.43	472	0.913	0.826	50.3	1.890	27.46	174.90
Duzce Turkey	1999	Lamont 375	H-1	7.14	3.93	454	1.703	1.516	63.3	3.184	294.65	133.16
Morgan Hill	1984	Anderson Dam (Downstream)	H-2	6.19	3.22	489	1.706	0.494	47.4	0.850	25.14	179.64
Kobe Japan	1995	Kobe University	H-2	6.9	0.9	1043	1.783	0.556	55.0	1.302	26.52	232.00
Mammoth Lakes-06	1980	Long Valley Dam (Upr L Abut)	H-1	5.94	9.65	537	1.801	1.702	54.6	1.734	50.67	148.24
Duzce Turkey	1999	IRIGM 496	H-1	7.14	4.21	760	1.814	1.870	73.0	2.965	448.28	177.43
Big Bear-01	1992	Big Bear Lake - Civic Center	H-1	6.46	7.31	430	1.894	1.032	65.3	2.136	104.35	137.18
Landers	1992	Morongo Valley Fire Station	H-1	7.28	17.36	396	1.903	0.425	57.0	0.616	44.42	226.38

Table A.58: Ground Motion Suite for F2S2B Building with 2% Probability of Exceedence in 50 Years for NEHRP Class B Site

Earthquake Name	Year	Station Name	Component	M_w	R_{jb} (km)	Vs30 (m/s)	Scale Factor	PGA (g)	PGV (cm/s)	Sa_{T1} (g)	Arias Intensity (cm/s)	Housner Intensity (cm)
Kobe Japan	1995	Nishi-Akashi	H-2	6.9	7.08	609	1.066	0.495	40.8	0.822	26.30	146.94
Duzce Turkey	1999	IRIGM 496	H-1	7.14	4.21	760	1.064	1.097	42.8	1.739	154.24	104.08
Manjil Iran	1990	Abbar	H-2	7.37	12.55	724	0.987	0.491	49.9	1.887	74.65	217.60
Manjil Iran	1990	Abbar	H-1	7.37	12.55	724	0.955	0.491	40.5	1.411	43.15	129.00
Kobe Japan	1995	Nishi-Akashi	H-1	6.9	7.08	609	0.917	0.443	42.9	0.670	28.70	135.36
Hector Mine	1999	Hector	H-2	7.13	10.35	726	1.501	0.493	67.2	0.828	42.83	244.05
Kobe Japan	1995	Kobe University	H-2	6.9	0.9	1043	1.808	0.564	55.8	1.321	27.26	235.23
Duzce Turkey	1999	IRIGM 496	H-2	7.14	4.21	760	0.720	0.541	28.5	1.211	34.47	69.99
Kobe Japan	1995	Kobe University	H-1	6.9	0.9	1043	1.910	0.527	105.6	1.345	45.45	407.95
Tottori Japan	2000	SMNH10	H-2	6.61	15.58	967	2.091	0.482	44.9	1.245	21.59	145.76
Parkfield-02 CA	2004	PARKFIELD - DONNA LEE	H-2	6.0	4.25	657	2.203	0.821	31.0	3.782	35.32	87.33
Hector Mine	1999	Hector	H-1	7.13	10.35	726	2.213	0.587	57.6	0.973	41.45	226.23
Tottori Japan	2000	SMN015	H-2	6.61	9.1	617	2.638	0.722	40.3	0.954	26.96	121.65
Tottori Japan	2000	OKYH14	H-2	6.61	26.51	710	2.788	1.262	64.7	6.809	97.60	122.29
Parkfield-02 CA	2004	PARKFIELD - DONNA LEE	H-1	6.0	4.25	657	2.809	0.827	42.7	1.618	28.79	107.89
Tottori Japan	2000	SMN015	H-1	6.61	9.1	617	2.810	0.426	53.9	1.079	28.10	200.68
Parkfield-02 CA	2004	PARKFIELD - TURKEY FLAT 1 (0M)	H-1	6.0	4.66	907	3.094	0.759	45.2	1.134	16.69	88.68
Duzce Turkey	1999	Lamont 531	H-2	7.14	8.03	638	3.175	0.392	42.6	0.742	42.43	137.90
Parkfield-02 CA	2004	PARKFIELD - TURKEY FLAT 1 (0M)	H-2	6.0	4.66	907	3.193	0.626	37.7	0.955	19.60	103.73
Duzce Turkey	1999	Lamont 531	H-1	7.14	8.03	638	3.210	0.515	34.9	0.764	46.93	94.05

Table A.59: Ground Motion Suite for F5S4B Building with 2% Probability of Exceedence in 50 Years for NEHRP Class B Site

Earthquake Name	Year	Station Name	Component	M_w	R_{jb} (km)	Vs30 (m/s)	Scale Factor	PGA (g)	PGV (cm/s)	Sa_{T1} (g)	Arias Intensity (cm/s)	Housner Intensity (cm)
Duzce Turkey	1999	IRIGM 496	H-1	7.14	4.21	760	1.124	1.159	45.2	1.837	172.17	109.96
Hector Mine	1999	Hector	H-2	7.13	10.35	726	1.028	0.337	46.0	0.567	20.10	167.19
Kobe Japan	1995	Kobe University	H-1	6.9	0.9	1043	1.174	0.324	64.9	0.827	17.19	250.87
Manjil Iran	1990	Abbar	H-1	7.37	12.55	724	0.963	0.495	40.9	1.423	43.86	130.05
Kobe Japan	1995	Kobe University	H-2	6.9	0.9	1043	1.297	0.404	40.0	0.947	14.03	168.75
Kobe Japan	1995	Nishi-Akashi	H-2	6.9	7.08	609	0.917	0.426	35.1	0.707	19.44	126.33
Manjil Iran	1990	Abbar	H-2	7.37	12.55	724	0.867	0.431	43.8	1.656	57.51	190.99
Duzce Turkey	1999	IRIGM 496	H-2	7.14	4.21	760	0.845	0.634	33.5	1.420	47.42	82.10
Kobe Japan	1995	Nishi-Akashi	H-1	6.9	7.08	609	0.744	0.360	34.8	0.544	18.93	109.94
Hector Mine	1999	Hector	H-1	7.13	10.35	726	1.644	0.436	42.8	0.723	22.87	168.05
Tottori Japan	2000	SMNH10	H-2	6.61	15.58	967	1.968	0.454	42.2	1.172	19.12	137.18
Tottori Japan	2000	SMN015	H-1	6.61	9.1	617	2.142	0.325	41.0	0.822	16.32	152.93
Chi-Chi Taiwan-04	1999	CHY035	H-2	6.2	25.01	573	2.282	0.305	33.9	0.441	15.33	135.09
Tottori Japan	2000	SMN015	H-2	6.61	9.1	617	2.384	0.652	36.4	0.862	22.01	109.92
Duzce Turkey	1999	Lamont 531	H-2	7.14	8.03	638	2.430	0.300	32.6	0.568	24.85	105.53
Parkfield-02 CA	2004	PARKFIELD - DONNA LEE	H-2	6.0	4.25	657	2.527	0.942	35.5	4.339	46.48	100.18
Chi-Chi Taiwan-04	1999	CHY035	H-1	6.2	25.01	573	2.750	0.321	47.1	0.546	15.23	143.68
Parkfield-02 CA	2004	PARKFIELD - DONNA LEE	H-1	6.0	4.25	657	2.787	0.820	42.3	1.605	28.34	107.03
Darfield New Zealand	2010	CSHS	H-2	7.0	43.6	638	2.891	0.335	34.6	0.497	32.77	170.92
Parkfield-02 CA	2004	PARKFIELD - TURKEY FLAT 1 (0M)	H-2	6.0	4.66	907	2.930	0.574	34.5	0.876	16.50	95.16

Table A.60: Ground Motion Suite for F8S3B Building with 2% Probability of Exceedence in 50 Years for NEHRP Class B Site

Earthquake Name	Year	Station Name	Component	M_w	R_{jb} (km)	Vs30 (m/s)	Scale Factor	PGA (g)	PGV (cm/s)	Sa_{T1} (g)	Arias Intensity (cm/s)	Housner Intensity (cm)
Kobe Japan	1995	Kobe University	H-1	6.9	0.9	1043	0.995	0.274	55.0	0.700	12.34	212.53
Kobe Japan	1995	Kobe University	H-2	6.9	0.9	1043	1.141	0.356	35.2	0.833	10.86	148.45
Duzce Turkey	1999	IRIGM 496	H-1	7.14	4.21	760	1.160	1.195	46.6	1.895	183.22	113.43
Manjil Iran	1990	Abbar	H-1	7.37	12.55	724	0.957	0.492	40.6	1.414	43.34	129.28
Duzce Turkey	1999	IRIGM 496	H-2	7.14	4.21	760	0.944	0.709	37.4	1.587	59.25	91.76
Hector Mine	1999	Hector	H-2	7.13	10.35	726	0.910	0.299	40.8	0.502	15.76	148.05
Kobe Japan	1995	Nishi-Akashi	H-2	6.9	7.08	609	0.864	0.401	33.0	0.666	17.26	119.05
Manjil Iran	1990	Abbar	H-2	7.37	12.55	724	0.769	0.382	38.9	1.469	45.27	169.45
Kobe Japan	1995	Nishi-Akashi	H-1	6.9	7.08	609	0.758	0.366	35.5	0.554	19.65	112.00
Hector Mine	1999	Hector	H-1	7.13	10.35	726	1.527	0.405	39.7	0.671	19.74	156.14
Tottori Japan	2000	SMNH10	H-2	6.61	15.58	967	1.882	0.434	40.4	1.121	17.49	131.20
Tottori Japan	2000	SMN015	H-1	6.61	9.1	617	1.987	0.301	38.1	0.763	14.04	141.88
Chi-Chi Taiwan-04	1999	CHY035	H-2	6.2	25.01	573	2.141	0.286	31.8	0.413	13.49	126.72
Duzce Turkey	1999	Lamont 531	H-2	7.14	8.03	638	2.395	0.296	32.1	0.560	24.14	104.00
Tottori Japan	2000	SMN015	H-2	6.61	9.1	617	2.430	0.665	37.1	0.879	22.88	112.07
Darfield New Zealand	2010	CSHS	H-2	7.0	43.6	638	2.462	0.285	29.4	0.423	23.76	145.54
Chi-Chi Taiwan-04	1999	CHY035	H-1	6.2	25.01	573	2.586	0.302	44.3	0.513	13.47	135.12
Parkfield-02 CA	2004	PARKFIELD - DONNA LEE	H-2	6.0	4.25	657	2.648	0.987	37.2	4.547	51.05	104.99
Chi-Chi Taiwan-04	1999	CHY086	H-2	6.2	33.63	665	2.758	0.302	30.4	0.403	13.91	117.65
Parkfield-02 CA	2004	PARKFIELD - DONNA LEE	H-1	6.0	4.25	657	2.893	0.852	44.0	1.666	30.54	111.12

Table A.61: Ground Motion Suite for F2S2B Building with 1% Probability of Exceedence in 50 Years for NEHRP Class D Site

Earthquake Name	Year	Station Name	Component	M_w	R_{jb} (km)	Vs30 (m/s)	Scale Factor	PGA (g)	PGV (cm/s)	Sa_{T1} (g)	Arias Intensity (cm/s)	Housner Intensity (cm)
Tottori Japan	2000	TTRH02	H-1	6.61	0.83	310	1.086	1.021	132.6	1.635	141.77	408.63
Parkfield-02 CA	2004	Parkfield - Fault Zone 14	H-1	6.0	8.45	246	1.014	1.328	84.5	1.711	80.39	254.62
Tottori Japan	2000	TTRH02	H-2	6.61	0.83	310	1.252	0.966	108.3	1.332	156.97	355.46
Imperial Valley-06	1979	Bonds Corner	H-2	6.53	0.44	223	1.277	0.992	57.4	2.266	100.76	239.73
El Mayor-Cucapah Mexico	2010	El Centro Array 11	H-2	7.2	15.36	196	1.533	0.899	96.9	1.922	132.76	341.52
Parkfield-02 CA	2004	Parkfield - Fault Zone 14	H-2	6.0	8.45	246	1.743	1.004	73.7	3.297	85.71	253.18
Imperial Valley-06	1979	Bonds Corner	H-1	6.53	0.44	223	1.798	1.077	84.0	2.928	131.38	313.84
El Mayor-Cucapah Mexico	2010	El Centro Array 11	H-1	7.2	15.36	196	1.876	0.829	108.3	1.670	177.01	305.32
El Mayor-Cucapah Mexico	2010	El Centro Differential Array	H-1	7.2	22.83	202	2.081	1.154	61.0	3.178	191.77	228.36
Chalfant Valley-02	1986	Zack Brothers Ranch	H-1	6.19	6.44	316	2.105	0.942	77.5	1.968	87.56	316.85
El Mayor-Cucapah Mexico	2010	RIITO	H-2	7.2	13.7	242	2.172	0.817	82.1	2.236	225.08	316.72
El Mayor-Cucapah Mexico	2010	MICHOACAN DE OCAMPO	H-1	7.2	13.21	242	2.306	1.240	141.9	2.250	330.32	502.25
El Mayor-Cucapah Mexico	2010	MICHOACAN DE OCAMPO	H-1	7.2	13.21	242	2.306	1.240	141.9	2.250	330.32	502.25
El Mayor-Cucapah Mexico	2010	El Centro Differential Array	H-2	7.2	22.83	202	2.308	1.169	89.6	3.721	220.66	346.92
El Mayor-Cucapah Mexico	2010	El Centro - Imperial & Ross	H-1	7.2	19.39	229	2.340	0.900	110.8	2.017	208.86	349.42
El Mayor-Cucapah Mexico	2010	RIITO	H-1	7.2	13.7	242	2.343	0.930	122.8	2.916	223.32	342.45
Managua Nicaragua-01	1972	Managua ESSO	H-2	6.24	3.51	289	2.423	0.799	74.5	1.691	120.24	268.46
Darfield New Zealand	2010	DFHS	H-2	7.0	11.86	344	2.453	1.258	73.0	2.732	173.02	252.22
El Mayor-Cucapah Mexico	2010	El Centro Array 10	H-2	7.2	19.36	203	2.468	0.941	117.6	1.271	223.93	428.97
Chalfant Valley-02	1986	Zack Brothers Ranch	H-2	6.19	6.44	316	2.500	1.001	111.8	1.602	127.16	380.05

Table A.62: Ground Motion Suite for F5S4B Building with 1% Probability of Exceedence in 50 Years for NEHRP Class D Site

Earthquake Name	Year	Station Name	Component	M_w	R_{jb} (km)	Vs30 (m/s)	Scale Factor	PGA (g)	PGV (cm/s)	Sa_{T1} (g)	Arias Intensity (cm/s)	Housner Intensity (cm)
Tottori Japan	2000	TTRH02	H-1	6.61	0.83	310	1.535	1.443	187.4	2.309	283.00	577.33
Tottori Japan	2000	TTRH02	H-2	6.61	0.83	310	1.690	1.304	146.3	1.799	286.21	479.99
Parkfield-02 CA	2004	Parkfield - Fault Zone 14	H-1	6.0	8.45	246	1.739	2.277	145.0	2.933	236.42	436.65
El Mayor-Cucapah Mexico	2010	El Centro Array 11	H-2	7.2	15.36	196	2.132	1.250	134.8	2.672	256.73	474.92
Imperial Valley-06	1979	Bonds Corner	H-2	6.53	0.44	223	2.161	1.679	97.1	3.834	288.42	405.59
El Mayor-Cucapah Mexico	2010	El Centro Array 11	H-1	7.2	15.36	196	2.730	1.206	157.6	2.430	374.86	444.32
Parkfield-02 CA	2004	Parkfield - Fault Zone 14	H-2	6.0	8.45	246	2.926	1.685	123.8	5.537	241.68	425.14
Imperial Valley-06	1979	Bonds Corner	H-1	6.53	0.44	223	2.964	1.775	138.5	4.827	356.99	517.33
Chalfant Valley-02	1986	Zack Brothers Ranch	H-1	6.19	6.44	316	3.119	1.395	114.8	2.916	192.21	469.44
El Mayor-Cucapah Mexico	2010	El Centro Array 10	H-2	7.2	19.36	203	3.150	1.201	150.1	1.622	364.62	547.38
El Mayor-Cucapah Mexico	2010	MICHOACAN DE OCAMPO	H-1	7.2	13.21	242	3.237	1.740	199.2	3.158	650.91	705.04
Landers	1992	Coolwater	H-2	7.28	19.74	353	3.282	1.369	142.5	1.605	239.54	472.26
El Mayor-Cucapah Mexico	2010	RIITO	H-2	7.2	13.7	242	3.367	1.266	127.3	3.467	541.07	491.06
El Mayor-Cucapah Mexico	2010	El Centro - Imperial & Ross	H-1	7.2	19.39	229	3.391	1.304	160.6	2.923	438.56	506.33
Kocaeli Turkey	1999	Duzce	H-2	7.51	13.6	282	3.391	1.235	188.7	2.092	156.31	769.06
Chalfant Valley-02	1986	Zack Brothers Ranch	H-2	6.19	6.44	316	3.540	1.418	158.3	2.268	254.98	538.16
El Mayor-Cucapah Mexico	2010	RIITO	H-1	7.2	13.7	242	3.667	1.455	192.1	4.564	546.92	535.90
El Mayor-Cucapah Mexico	2010	El Centro Array 10	H-1	7.2	19.36	203	3.726	1.357	169.9	2.137	427.21	508.82
El Mayor-Cucapah Mexico	2010	El Centro - Imperial & Ross	H-2	7.2	19.39	229	3.749	1.387	178.4	4.407	469.84	627.58
Westmorland	1981	Westmorland Fire Sta	H-1	5.9	6.18	194	3.780	1.426	166.8	2.924	256.12	678.18

Table A.63: Ground Motion Suite for F8S3B Building with 1% Probability of Exceedence in 50 Years for NEHRP Class D Site

Earthquake Name	Year	Station Name	Component	M_w	R_{jb} (km)	Vs30 (m/s)	Scale Factor	PGA (g)	PGV (cm/s)	Sa_{T1} (g)	Arias Intensity (cm/s)	Housner Intensity (cm)
Tottori Japan	2000	TTRH02	H-1	6.61	0.83	310	1.471	1.383	179.6	2.213	259.83	553.20
Tottori Japan	2000	TTRH02	H-2	6.61	0.83	310	1.751	1.351	151.5	1.863	307.01	497.12
Parkfield-02 CA	2004	Parkfield - Fault Zone 14	H-1	6.0	8.45	246	1.779	2.330	148.3	3.002	247.55	446.82
El Mayor-Cucapah Mexico	2010	El Centro Array 11	H-2	7.2	15.36	196	2.127	1.247	134.4	2.666	255.46	473.74
Imperial Valley-06	1979	Bonds Corner	H-2	6.53	0.44	223	2.344	1.821	105.3	4.159	339.46	440.01
El Mayor-Cucapah Mexico	2010	El Centro Array 11	H-1	7.2	15.36	196	2.703	1.194	156.0	2.405	367.36	439.85
Imperial Valley-06	1979	Bonds Corner	H-1	6.53	0.44	223	2.933	1.756	137.1	4.776	349.52	511.89
Kocaeli Turkey	1999	Duzce	H-2	7.51	13.6	282	3.017	1.099	167.9	1.861	123.69	684.14
Kocaeli Turkey	1999	Duzce	H-2	7.51	13.6	282	3.017	1.099	167.9	1.861	123.69	684.14
El Mayor-Cucapah Mexico	2010	El Centro Array 10	H-2	7.2	19.36	203	3.073	1.172	146.5	1.583	347.21	534.15
El Mayor-Cucapah Mexico	2010	MICHOACAN DE OCAMPO	H-1	7.2	13.21	242	3.102	1.668	190.9	3.026	597.66	675.58
Chalfant Valley-02	1986	Zack Brothers Ranch	H-1	6.19	6.44	316	3.147	1.408	115.8	2.942	195.66	473.64
Parkfield-02 CA	2004	Parkfield - Fault Zone 14	H-2	6.0	8.45	246	3.220	1.854	136.3	6.092	292.61	467.80
Landers	1992	Coolwater	H-2	7.28	19.74	353	3.267	1.363	141.8	1.598	237.26	470.00
El Mayor-Cucapah Mexico	2010	El Centro - Imperial & Ross	H-1	7.2	19.39	229	3.335	1.282	157.9	2.874	424.16	497.95
El Mayor-Cucapah Mexico	2010	RIITO	H-2	7.2	13.7	242	3.366	1.266	127.3	3.467	540.83	490.95
Kobe Japan	1995	Amagasaki	H-2	6.9	11.34	256	3.458	1.130	155.0	2.308	238.10	762.54
Westmorland	1981	Westmorland Fire Sta	H-1	5.9	6.18	194	3.551	1.339	156.7	2.746	225.96	637.00
Chalfant Valley-02	1986	Zack Brothers Ranch	H-2	6.19	6.44	316	3.551	1.422	158.8	2.275	256.48	539.75
Imperial Valley-06	1979	El Centro Array 8	H-1	6.53	3.86	206	3.623	2.211	197.4	3.385	218.84	665.86

Table A.64: Ground Motion Suite for F2S2B Building with 1% Probability of Exceedence in 50 Years for NEHRP Class C Site

Earthquake Name	Year	Station Name	Component	M_w	R_{jb} (km)	Vs30 (m/s)	Scale Factor	PGA (g)	PGV (cm/s)	Sa_{T1} (g)	Arias Intensity (cm/s)	Housner Intensity (cm)
Tottori Japan	2000	TTRH02	H-2	6.61	0.83	310	1.225	0.945	106.0	1.304	150.32	347.85
Duzce Turkey	1999	IRIGM 496	H-2	7.14	4.21	760	1.536	1.153	60.9	2.581	156.69	149.23
Tottori Japan	2000	TTRH02	H-1	6.61	0.83	310	1.063	0.999	129.8	1.600	135.79	399.92
Tottori Japan	2000	TTR007	H-1	6.61	11.28	470	1.556	1.142	66.6	4.168	127.83	185.50
Baja California	1987	Cerro Prieto	H-2	5.5	3.43	472	1.575	1.425	86.9	3.261	81.75	301.79
Tottori Japan	2000	SMNH01	H-1	6.61	5.83	446	1.714	1.256	61.0	2.195	161.03	165.64
Duzce Turkey	1999	Lamont 375	H-1	7.14	3.93	454	1.721	1.532	64.0	3.216	300.67	134.51
Baja California	1987	Cerro Prieto	H-1	5.5	3.43	472	1.895	2.426	88.0	5.550	130.86	315.29
Kobe Japan	1995	Nishi-Akashi	H-1	6.9	7.08	609	1.952	0.943	91.4	1.426	130.11	288.23
Manjil Iran	1990	Abbar	H-1	7.37	12.55	724	2.038	1.049	86.5	3.011	196.50	275.28
Chalfant Valley-02	1986	Zack Brothers Ranch	H-1	6.19	6.44	316	2.061	0.922	75.8	1.927	83.89	310.14
Manjil Iran	1990	Abbar	H-2	7.37	12.55	724	2.107	1.047	106.6	4.027	339.93	464.33
Darfield New Zealand	2010	Heathcote Valley Primary School	H-1	7.0	24.36	422	2.234	1.288	94.5	3.568	194.94	196.24
Tottori Japan	2000	TTR009	H-2	6.61	8.82	420	2.253	1.357	58.7	3.745	149.84	168.02
Duzce Turkey	1999	IRIGM 496	H-1	7.14	4.21	760	2.266	2.336	91.1	3.704	699.60	221.65
Kobe Japan	1995	Nishi-Akashi	H-2	6.9	7.08	609	2.277	1.057	87.1	1.755	119.83	313.67
Big Bear-01	1992	Big Bear Lake - Civic Center	H-1	6.46	7.31	430	2.318	1.263	80.0	2.614	156.32	167.89
Managua Nicaragua-01	1972	Managua ESSO	H-2	6.24	3.51	289	2.373	0.782	72.9	1.656	115.27	262.86
Mammoth Lakes-06	1980	Long Valley Dam (Upr L Abut)	H-1	5.94	9.65	537	2.382	2.252	72.2	2.293	88.63	196.06
Tottori Japan	2000	OKY004	H-2	6.61	19.72	476	2.391	1.971	56.3	3.472	418.99	177.00

Table A.65: Ground Motion Suite for F5S4B Building with 1% Probability of Exceedence in 50 Years for NEHRP Class C Site

Earthquake Name	Year	Station Name	Component	M_w	R_{jb} (km)	Vs30 (m/s)	Scale Factor	PGA (g)	PGV (cm/s)	Sa_{T1} (g)	Arias Intensity (cm/s)	Housner Intensity (cm)
Baja California	1987	Cerro Prieto	H-2	5.5	3.43	472	1.464	1.324	80.7	3.031	70.59	280.44
Tottori Japan	2000	TTRH02	H-2	6.61	0.83	310	0.996	0.769	86.2	1.060	99.37	282.82
Tottori Japan	2000	TTRH02	H-1	6.61	0.83	310	0.901	0.847	110.1	1.356	97.60	339.04
Kobe Japan	1995	Nishi-Akashi	H-1	6.9	7.08	609	1.781	0.861	83.4	1.302	108.41	263.09
Chalfant Valley-02	1986	Zack Brothers Ranch	H-1	6.19	6.44	316	1.834	0.820	67.5	1.714	66.42	275.97
Tottori Japan	2000	TTR007	H-1	6.61	11.28	470	1.930	1.416	82.6	5.168	196.54	230.01
Tottori Japan	2000	TTR007	H-1	6.61	11.28	470	1.930	1.416	82.6	5.168	196.54	230.01
Landers	1992	Coolwater	H-2	7.28	19.74	353	1.932	0.806	83.9	0.945	83.00	277.99
Kocaeli Turkey	1999	Duzce	H-2	7.51	13.6	282	1.997	0.727	111.1	1.232	54.20	452.87
Duzce Turkey	1999	IRIGM 496	H-2	7.14	4.21	760	2.017	1.514	79.9	3.390	270.25	195.98
Baja California	1987	Cerro Prieto	H-1	5.5	3.43	472	2.045	2.619	94.9	5.990	152.43	340.28
Manjil Iran	1990	Abbar	H-2	7.37	12.55	724	2.070	1.029	104.7	3.956	328.18	456.24
Chalfant Valley-02	1986	Zack Brothers Ranch	H-2	6.19	6.44	316	2.084	0.835	93.2	1.335	88.35	316.78
Victoria Mexico	1980	Cerro Prieto	H-1	6.33	13.8	472	2.138	1.380	71.8	2.248	92.43	302.69
Kobe Japan	1995	Nishi-Akashi	H-2	6.9	7.08	609	2.192	1.018	83.9	1.690	111.13	302.07
Tottori Japan	2000	SMNH01	H-1	6.61	5.83	446	2.196	1.610	78.2	2.812	264.30	212.21
Duzce Turkey	1999	Lamont 375	H-1	7.14	3.93	454	2.241	1.995	83.3	4.189	510.01	175.18
Managua Nicaragua-01	1972	Managua ESSO	H-2	6.24	3.51	289	2.269	0.748	69.7	1.584	105.45	251.41
Joshua Tree CA	1992	Indio - Jackson Road	H-2	6.1	25.04	292	2.281	0.928	121.0	1.138	67.85	370.00
Manjil Iran	1990	Abbar	H-1	7.37	12.55	724	2.297	1.182	97.5	3.394	249.67	310.29

Table A.66: Ground Motion Suite for F8S3B Building with 1% Probability of Exceedence in 50 Years for NEHRP Class C Site

Earthquake Name	Year	Station Name	Component	M_w	R_{jb} (km)	Vs30 (m/s)	Scale Factor	PGA (g)	PGV (cm/s)	Sa_{T1} (g)	Arias Intensity (cm/s)	Housner Intensity (cm)
Baja California	1987	Cerro Prieto	H-2	5.5	3.43	472	1.451	1.313	80.0	3.005	69.38	278.04
Tottori Japan	2000	TTRH02	H-2	6.61	0.83	310	1.026	0.792	88.8	1.092	105.43	291.32
Tottori Japan	2000	TTRH02	H-1	6.61	0.83	310	0.859	0.807	104.8	1.292	88.56	322.97
Tottori Japan	2000	TTRH02	H-1	6.61	0.83	310	0.859	0.807	104.8	1.292	88.56	322.97
Kocaeli Turkey	1999	Duzce	H-2	7.51	13.6	282	1.768	0.644	98.4	1.090	42.47	400.88
Chalfant Valley-02	1986	Zack Brothers Ranch	H-1	6.19	6.44	316	1.844	0.825	67.8	1.724	67.16	277.49
Kobe Japan	1995	Nishi-Akashi	H-1	6.9	7.08	609	1.889	0.913	88.4	1.381	121.94	279.03
Landers	1992	Coolwater	H-2	7.28	19.74	353	1.912	0.797	83.0	0.935	81.24	275.02
Manjil Iran	1990	Abbar	H-2	7.37	12.55	724	1.915	0.952	96.9	3.660	280.85	422.06
Baja California	1987	Cerro Prieto	H-1	5.5	3.43	472	2.026	2.594	94.0	5.933	149.54	337.03
Chalfant Valley-02	1986	Zack Brothers Ranch	H-2	6.19	6.44	316	2.078	0.832	92.9	1.331	87.80	315.80
Tottori Japan	2000	TTR007	H-1	6.61	11.28	470	2.116	1.552	90.5	5.666	236.27	252.19
Joshua Tree CA	1992	Indio - Jackson Road	H-2	6.1	25.04	292	2.135	0.869	113.3	1.065	59.48	346.43
Kobe Japan	1995	Nishi-Akashi	H-2	6.9	7.08	609	2.151	0.999	82.3	1.659	107.02	296.43
Victoria Mexico	1980	Cerro Prieto	H-1	6.33	13.8	472	2.169	1.400	72.8	2.281	95.14	307.09
Hector Mine	1999	Hector	H-2	7.13	10.35	726	2.269	0.745	101.6	1.252	97.92	369.03
Managua Nicaragua-01	1972	Managua ESSO	H-2	6.24	3.51	289	2.272	0.749	69.8	1.585	105.68	251.68
Duzce Turkey	1999	IRIGM 496	H-2	7.14	4.21	760	2.347	1.762	93.0	3.945	365.99	228.06
Manjil Iran	1990	Abbar	H-1	7.37	12.55	724	2.384	1.227	101.2	3.522	268.94	322.04
Mammoth Lakes-06	1980	Long Valley Dam (Upr L Abut)	H-2	5.94	9.65	537	2.413	0.999	82.3	1.741	73.68	305.79

Table A.67: Ground Motion Suite for F2S2B Building with 1% Probability of Exceedence in 50 Years for Generic Rock Site

Earthquake Name	Year	Station Name	Component	M_w	R_{jb} (km)	Vs30 (m/s)	Scale Factor	PGA (g)	PGV (cm/s)	Sa_{T1} (g)	Arias Intensity (cm/s)	Housner Intensity (cm)
Baja California	1987	Cerro Prieto	H-2	5.5	3.43	472	1.487	1.345	82.0	3.077	72.78	284.75
Tottori Japan	2000	TTR007	H-1	6.61	11.28	470	1.469	1.077	62.8	3.934	113.87	175.08
Duzce Turkey	1999	IRIGM 496	H-2	7.14	4.21	760	1.448	1.087	57.4	2.434	139.32	140.71
Tottori Japan	2000	SMNH01	H-1	6.61	5.83	446	1.617	1.185	57.6	2.070	143.27	156.24
Duzce Turkey	1999	Lamont 375	H-1	7.14	3.93	454	1.623	1.445	60.3	3.033	267.46	126.86
Baja California	1987	Cerro Prieto	H-1	5.5	3.43	472	1.786	2.286	82.9	5.229	116.17	297.06
Kobe Japan	1995	Nishi-Akashi	H-1	6.9	7.08	609	1.842	0.890	86.2	1.346	115.89	272.01
Manjil Iran	1990	Abbar	H-1	7.37	12.55	724	1.922	0.989	81.6	2.840	174.79	259.62
Manjil Iran	1990	Abbar	H-2	7.37	12.55	724	1.987	0.987	100.5	3.797	302.30	437.88
Darfield New Zealand	2010	Heathcote Valley Primary School	H-1	7.0	24.36	422	2.102	1.212	89.0	3.358	172.64	184.68
Tottori Japan	2000	TTR009	H-2	6.61	8.82	420	2.125	1.280	55.3	3.531	133.21	158.42
Duzce Turkey	1999	IRIGM 496	H-1	7.14	4.21	760	2.138	2.203	86.0	3.494	622.66	209.11
Kobe Japan	1995	Nishi-Akashi	H-2	6.9	7.08	609	2.145	0.996	82.1	1.654	106.43	295.61
Big Bear-01	1992	Big Bear Lake - Civic Center	H-1	6.46	7.31	430	2.185	1.191	75.4	2.465	138.99	158.32
Mammoth Lakes-06	1980	Long Valley Dam (Upr L Abut)	H-1	5.94	9.65	537	2.248	2.125	68.1	2.164	78.93	185.01
Tottori Japan	2000	OKY004	H-2	6.61	19.72	476	2.256	1.861	53.2	3.277	373.23	167.06
Tottori Japan	2000	SMNH01	H-2	6.61	5.83	446	2.280	1.407	80.8	4.153	250.67	220.39
Victoria Mexico	1980	Cerro Prieto	H-1	6.33	13.8	472	2.335	1.507	78.4	2.456	110.29	330.64
Tottori Japan	2000	TTR009	H-1	6.61	8.82	420	2.410	1.519	95.8	5.137	144.59	214.45
Darfield New Zealand	2010	Heathcote Valley Primary School	H-2	7.0	24.36	422	2.458	1.552	55.8	3.299	253.66	135.98

Table A.68: Ground Motion Suite for F5S4B Building with 1% Probability of Exceedence in 50 Years for Generic Rock Site

Earthquake Name	Year	Station Name	Component	M_w	R_{jb} (km)	Vs30 (m/s)	Scale Factor	PGA (g)	PGV (cm/s)	Sa_{T1} (g)	Arias Intensity (cm/s)	Housner Intensity (cm)
Baja California	1987	Cerro Prieto	H-2	5.5	3.43	472	1.057	0.957	58.3	2.189	36.83	202.56
Kobe Japan	1995	Nishi-Akashi	H-1	6.9	7.08	609	1.286	0.622	60.2	0.940	56.51	189.94
Tottori Japan	2000	TTR007	H-1	6.61	11.28	470	1.393	1.022	59.6	3.731	102.43	166.05
Duzce Turkey	1999	IRIGM 496	H-2	7.14	4.21	760	1.457	1.094	57.8	2.450	141.13	141.62
Baja California	1987	Cerro Prieto	H-1	5.5	3.43	472	1.476	1.889	68.5	4.322	79.35	245.52
Manjil Iran	1990	Abbar	H-2	7.37	12.55	724	1.494	0.742	75.6	2.855	170.95	329.28
Victoria Mexico	1980	Cerro Prieto	H-1	6.33	13.8	472	1.541	0.995	51.8	1.621	48.06	218.26
Kobe Japan	1995	Nishi-Akashi	H-2	6.9	7.08	609	1.583	0.735	60.5	1.220	57.92	218.07
Tottori Japan	2000	SMNH01	H-1	6.61	5.83	446	1.586	1.163	56.5	2.031	137.88	153.27
Duzce Turkey	1999	Lamont 375	H-1	7.14	3.93	454	1.617	1.440	60.1	3.023	265.62	126.43
Manjil Iran	1990	Abbar	H-1	7.37	12.55	724	1.659	0.853	70.4	2.451	130.18	224.06
Mammoth Lakes-06	1980	Long Valley Dam (Upr L Abut)	H-2	5.94	9.65	537	1.765	0.730	60.2	1.274	39.43	223.70
Hector Mine	1999	Hector	H-2	7.13	10.35	726	1.772	0.582	79.3	0.978	59.72	288.19
Mammoth Lakes-06	1980	Long Valley Dam (Upr L Abut)	H-1	5.94	9.65	537	1.802	1.704	54.6	1.735	50.75	148.35
Big Bear-01	1992	Big Bear Lake - Civic Center	H-1	6.46	7.31	430	1.931	1.052	66.6	2.178	108.51	139.88
Duzce Turkey	1999	IRIGM 496	H-1	7.14	4.21	760	1.936	1.995	77.8	3.163	510.32	189.31
Morgan Hill	1984	Anderson Dam (Downstream)	H-2	6.19	3.22	489	1.959	0.567	54.4	0.976	33.15	206.27
Tottori Japan	2000	TTR009	H-2	6.61	8.82	420	1.999	1.204	52.0	3.322	117.89	149.03
Kobe Japan	1995	Kobe University	H-1	6.9	0.9	1043	2.023	0.558	111.8	1.424	50.99	432.11
Darfield New Zealand	2010	Heathcote Valley Primary School	H-1	7.0	24.36	422	2.048	1.181	86.7	3.271	163.84	179.91

Table A.69: Ground Motion Suite for F8S3B Building with 1% Probability of Exceedence in 50 Years for Generic Rock Site

Earthquake Name	Year	Station Name	Component	M_w	R_{jb} (km)	Vs30 (m/s)	Scale Factor	PGA (g)	PGV (cm/s)	Sa_{T1} (g)	Arias Intensity (cm/s)	Housner Intensity (cm)
Baja California	1987	Cerro Prieto	H-2	5.5	3.43	472	1.114	1.007	61.4	2.305	40.84	213.31
Kobe Japan	1995	Nishi-Akashi	H-1	6.9	7.08	609	1.450	0.701	67.9	1.060	71.83	214.15
Manjil Iran	1990	Abbar	H-2	7.37	12.55	724	1.468	0.730	74.3	2.806	165.10	323.60
Baja California	1987	Cerro Prieto	H-1	5.5	3.43	472	1.557	1.993	72.2	4.559	88.27	258.95
Tottori Japan	2000	TTR007	H-1	6.61	11.28	470	1.625	1.192	69.5	4.352	139.39	193.70
Kobe Japan	1995	Nishi-Akashi	H-2	6.9	7.08	609	1.652	0.767	63.2	1.274	63.10	227.62
Victoria Mexico	1980	Cerro Prieto	H-1	6.33	13.8	472	1.667	1.076	56.0	1.753	56.19	236.01
Hector Mine	1999	Hector	H-2	7.13	10.35	726	1.744	0.572	78.1	0.962	57.81	283.54
Duzce Turkey	1999	IRIGM 496	H-2	7.14	4.21	760	1.806	1.356	71.6	3.036	216.75	175.51
Manjil Iran	1990	Abbar	H-1	7.37	12.55	724	1.829	0.941	77.6	2.703	158.38	247.14
Mammoth Lakes-06	1980	Long Valley Dam (Upr L Abut)	H-2	5.94	9.65	537	1.854	0.767	63.3	1.338	43.48	234.90
Kobe Japan	1995	Kobe University	H-1	6.9	0.9	1043	1.904	0.525	105.3	1.340	45.17	406.72
Tottori Japan	2000	SMNH01	H-1	6.61	5.83	446	1.909	1.399	68.0	2.444	199.71	184.47
Morgan Hill	1984	Anderson Dam (Downstream)	H-2	6.19	3.22	489	2.081	0.602	57.9	1.037	37.44	219.22
Duzce Turkey	1999	Lamont 375	H-1	7.14	3.93	454	2.085	1.856	77.5	3.898	441.60	163.01
Kobe Japan	1995	Kobe University	H-2	6.9	0.9	1043	2.181	0.680	67.3	1.593	39.68	283.78
Mammoth Lakes-06	1980	Long Valley Dam (Upr L Abut)	H-1	5.94	9.65	537	2.195	2.075	66.5	2.114	75.30	180.71
Duzce Turkey	1999	IRIGM 496	H-1	7.14	4.21	760	2.217	2.285	89.2	3.624	669.71	216.87
Big Bear-01	1992	Big Bear Lake - Civic Center	H-1	6.46	7.31	430	2.313	1.260	79.8	2.608	155.66	167.54
Landers	1992	Morongo Valley Fire Station	H-1	7.28	17.36	396	2.325	0.519	69.6	0.753	66.29	276.55

Table A.70: Ground Motion Suite for F2S2B Building with 1% Probability of Exceedence in 50 Years for NEHRP Class B Site

Earthquake Name	Year	Station Name	Component	M_w	R_{jb} (km)	Vs30 (m/s)	Scale Factor	PGA (g)	PGV (cm/s)	Sa_{T1} (g)	Arias Intensity (cm/s)	Housner Intensity (cm)
Manjil Iran	1990	Abbar	H-1	7.37	12.55	724	1.164	0.599	49.4	1.721	64.17	157.31
Manjil Iran	1990	Abbar	H-2	7.37	12.55	724	1.204	0.598	60.9	2.302	111.07	265.42
Kobe Japan	1995	Nishi-Akashi	H-1	6.9	7.08	609	1.115	0.539	52.2	0.815	42.47	164.67
Duzce Turkey	1999	IRIGM 496	H-1	7.14	4.21	760	1.295	1.335	52.1	2.117	228.44	126.66
Kobe Japan	1995	Nishi-Akashi	H-2	6.9	7.08	609	1.302	0.605	49.8	1.004	39.20	179.40
Duzce Turkey	1999	IRIGM 496	H-2	7.14	4.21	760	0.880	0.660	34.9	1.479	51.43	85.49
Hector Mine	1999	Hector	H-2	7.13	10.35	726	1.830	0.601	81.9	1.010	63.68	297.60
Kobe Japan	1995	Kobe University	H-2	6.9	0.9	1043	2.205	0.688	68.1	1.611	40.59	287.00
Kobe Japan	1995	Kobe University	H-1	6.9	0.9	1043	2.329	0.642	128.7	1.640	67.58	497.47
Tottori Japan	2000	SMNH10	H-2	6.61	15.58	967	2.549	0.588	54.7	1.517	32.08	177.67
Parkfield-02 CA	2004	PARKFIELD - DONNA LEE	H-2	6.0	4.25	657	2.685	1.001	37.8	4.611	52.50	106.47
Hector Mine	1999	Hector	H-1	7.13	10.35	726	2.699	0.717	70.2	1.187	61.67	275.96
Tottori Japan	2000	SMN015	H-2	6.61	9.1	617	3.216	0.880	49.1	1.163	40.06	148.29
Tottori Japan	2000	OKYH14	H-2	6.61	26.51	710	3.395	1.537	78.8	8.290	144.69	148.90
Parkfield-02 CA	2004	PARKFIELD - DONNA LEE	H-1	6.0	4.25	657	3.426	1.009	52.1	1.973	42.84	131.60
Tottori Japan	2000	SMN015	H-1	6.61	9.1	617	3.427	0.520	65.7	1.316	41.80	244.77
Parkfield-02 CA	2004	PARKFIELD - TURKEY FLAT 1 (0M)	H-1	6.0	4.66	907	3.771	0.925	55.1	1.382	24.80	108.09
Duzce Turkey	1999	Lamont 531	H-2	7.14	8.03	638	3.876	0.479	52.0	0.906	63.23	168.33
Parkfield-02 CA	2004	PARKFIELD - TURKEY FLAT 1 (0M)	H-2	6.0	4.66	907	3.892	0.763	45.9	1.163	29.11	126.42
Duzce Turkey	1999	Lamont 531	H-1	7.14	8.03	638	3.917	0.628	42.6	0.932	69.88	114.76

Table A.71: Ground Motion Suite for F5S4B Building with 1% Probability of Exceedence in 50 Years for NEHRP Class B Site

Earthquake Name	Year	Station Name	Component	M_w	R_{jb} (km)	Vs30 (m/s)	Scale Factor	PGA (g)	PGV (cm/s)	Sa_{T1} (g)	Arias Intensity (cm/s)	Housner Intensity (cm)
Kobe Japan	1995	Nishi-Akashi	H-2	6.9	7.08	609	1.095	0.508	41.9	0.844	27.73	150.88
Manjil Iran	1990	Abbar	H-2	7.37	12.55	724	1.034	0.514	52.3	1.977	81.92	227.94
Manjil Iran	1990	Abbar	H-1	7.37	12.55	724	1.148	0.591	48.7	1.697	62.39	155.11
Duzce Turkey	1999	IRIGM 496	H-2	7.14	4.21	760	1.008	0.757	40.0	1.695	67.56	97.98
Hector Mine	1999	Hector	H-2	7.13	10.35	726	1.230	0.404	55.0	0.678	28.74	199.93
Kobe Japan	1995	Nishi-Akashi	H-1	6.9	7.08	609	0.889	0.430	41.6	0.650	27.00	131.30
Duzce Turkey	1999	IRIGM 496	H-1	7.14	4.21	760	1.340	1.381	53.9	2.190	244.63	131.07
Kobe Japan	1995	Kobe University	H-1	6.9	0.9	1043	1.401	0.386	77.4	0.986	24.45	299.23
Kobe Japan	1995	Kobe University	H-2	6.9	0.9	1043	1.548	0.483	47.8	1.131	20.00	201.49
Hector Mine	1999	Hector	H-1	7.13	10.35	726	1.961	0.521	51.0	0.862	32.56	200.51
Tottori Japan	2000	SMNH10	H-2	6.61	15.58	967	2.354	0.543	50.5	1.401	27.36	164.08
Tottori Japan	2000	SMN015	H-1	6.61	9.1	617	2.558	0.388	49.0	0.982	23.28	182.65
Chi-Chi Taiwan-04	1999	CHY035	H-2	6.2	25.01	573	2.726	0.364	40.5	0.526	21.87	161.34
Tottori Japan	2000	SMN015	H-2	6.61	9.1	617	2.848	0.779	43.5	1.030	31.43	131.34
Duzce Turkey	1999	Lamont 531	H-2	7.14	8.03	638	2.900	0.358	38.9	0.678	35.41	125.97
Parkfield-02 CA	2004	PARKFIELD - DONNA LEE	H-2	6.0	4.25	657	3.013	1.123	42.4	5.174	66.10	119.46
Chi-Chi Taiwan-04	1999	CHY035	H-1	6.2	25.01	573	3.284	0.383	56.2	0.652	21.72	171.62
Parkfield-02 CA	2004	PARKFIELD - DONNA LEE	H-1	6.0	4.25	657	3.328	0.980	50.6	1.916	40.40	127.81
Darfield New Zealand	2010	CSHS	H-2	7.0	43.6	638	3.451	0.399	41.3	0.593	46.68	204.01
Parkfield-02 CA	2004	PARKFIELD - TURKEY FLAT 1 (0M)	H-2	6.0	4.66	907	3.497	0.686	41.2	1.045	23.50	113.58

Table A.72: Ground Motion Suite for F8S3B Building with 1% Probability of Exceedence in 50 Years for NEHRP Class B Site

Earthquake Name	Year	Station Name	Component	M_w	R_{jb} (km)	Vs30 (m/s)	Scale Factor	PGA (g)	PGV (cm/s)	Sa_{T1} (g)	Arias Intensity (cm/s)	Housner Intensity (cm)
Kobe Japan	1995	Nishi-Akashi	H-2	6.9	7.08	609	1.054	0.490	40.3	0.813	25.70	145.26
Hector Mine	1999	Hector	H-2	7.13	10.35	726	1.112	0.365	49.8	0.614	23.51	180.84
Duzce Turkey	1999	IRIGM 496	H-2	7.14	4.21	760	1.154	0.866	45.7	1.940	88.47	112.13
Manjil Iran	1990	Abbar	H-1	7.37	12.55	724	1.170	0.602	49.7	1.729	64.78	158.06
Kobe Japan	1995	Kobe University	H-1	6.9	0.9	1043	1.215	0.335	67.2	0.855	18.39	259.53
Manjil Iran	1990	Abbar	H-2	7.37	12.55	724	0.939	0.466	47.5	1.794	67.45	206.84
Kobe Japan	1995	Nishi-Akashi	H-1	6.9	7.08	609	0.928	0.448	43.4	0.678	29.41	137.03
Kobe Japan	1995	Kobe University	H-2	6.9	0.9	1043	1.392	0.434	43.0	1.017	16.16	181.12
Duzce Turkey	1999	IRIGM 496	H-1	7.14	4.21	760	1.418	1.461	57.0	2.317	273.70	138.64
Hector Mine	1999	Hector	H-1	7.13	10.35	726	1.868	0.496	48.6	0.821	29.51	190.91
Tottori Japan	2000	SMNH10	H-2	6.61	15.58	967	2.300	0.530	49.4	1.369	26.13	160.35
Tottori Japan	2000	SMN015	H-1	6.61	9.1	617	2.429	0.368	46.5	0.932	20.99	173.46
Chi-Chi Taiwan-04	1999	CHY035	H-2	6.2	25.01	573	2.618	0.350	38.9	0.505	20.16	154.93
Duzce Turkey	1999	Lamont 531	H-2	7.14	8.03	638	2.929	0.362	39.3	0.685	36.12	127.23
Tottori Japan	2000	SMN015	H-2	6.61	9.1	617	2.973	0.813	45.4	1.075	34.24	137.10
Darfield New Zealand	2010	CSHS	H-2	7.0	43.6	638	3.010	0.348	36.0	0.517	35.50	177.91
Chi-Chi Taiwan-04	1999	CHY035	H-1	6.2	25.01	573	3.158	0.369	54.0	0.627	20.08	165.00
Parkfield-02 CA	2004	PARKFIELD - DONNA LEE	H-2	6.0	4.25	657	3.235	1.206	45.5	5.555	76.17	128.25
Chi-Chi Taiwan-04	1999	CHY086	H-2	6.2	33.63	665	3.369	0.369	37.2	0.493	20.76	143.70
Parkfield-02 CA	2004	PARKFIELD - DONNA LEE	H-1	6.0	4.25	657	3.534	1.040	53.7	2.035	45.56	135.72

Appendix B

GROUND MOTION SUITE SPECTRA

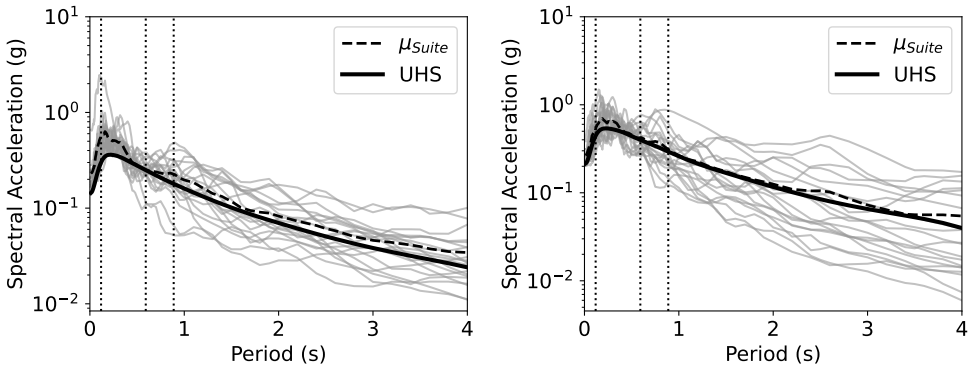

(a) 68% poe in 50 years

(b) 50% poe in 50 years

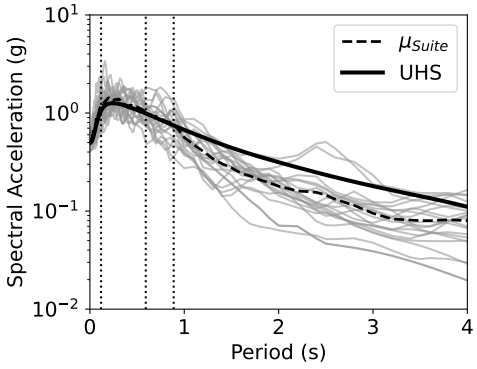

(c) 10% poe in 50 years

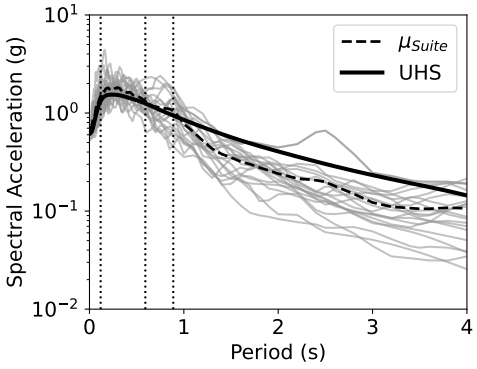

(d) 5% poe in 50 years

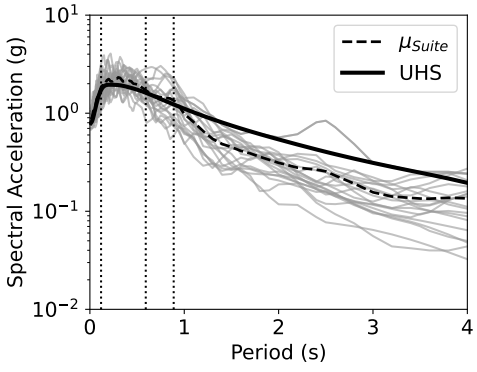

(e) 2% poe in 50 years

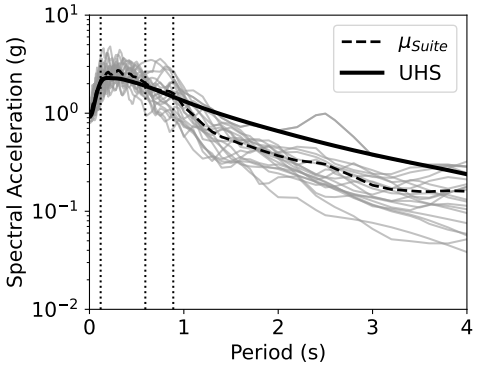

(f) 1% poe in 50 years

Figure B.1: GM Suite Spectra for NEHRP Class D Site F2S2B Building

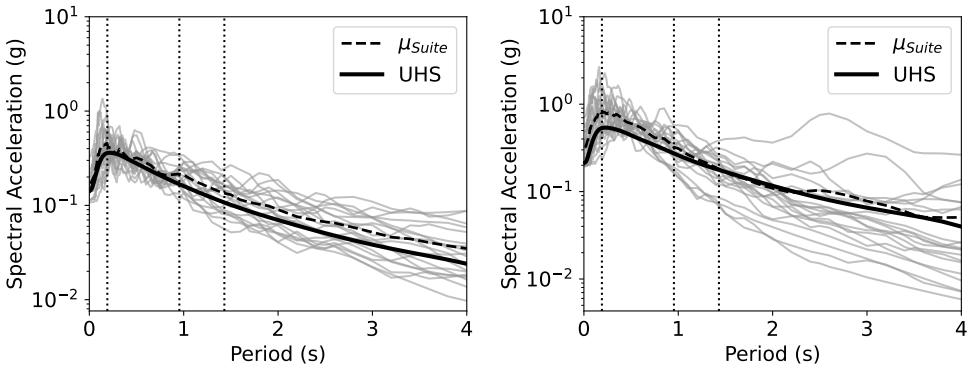

(a) 68% poe in 50 years

(b) 50% poe in 50 years

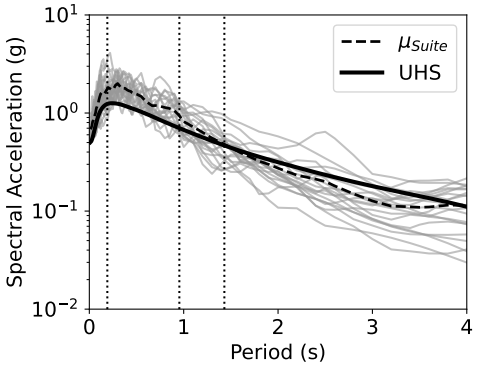

(c) 10% poe in 50 years

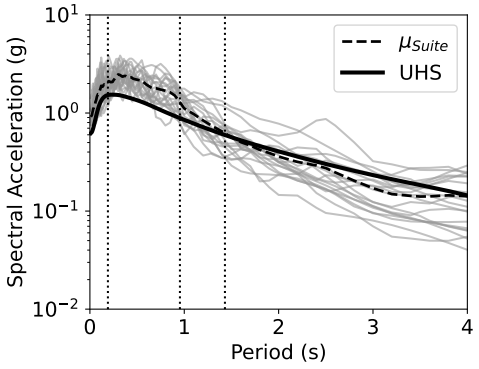

(d) 5% poe in 50 years

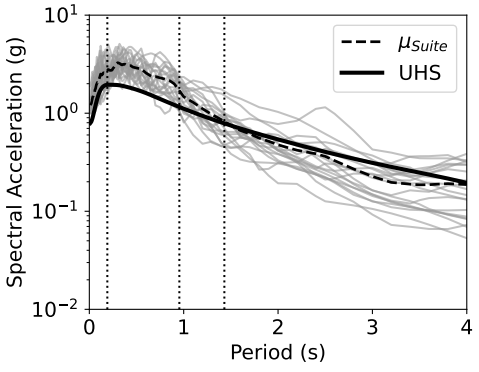

(e) 2% poe in 50 years

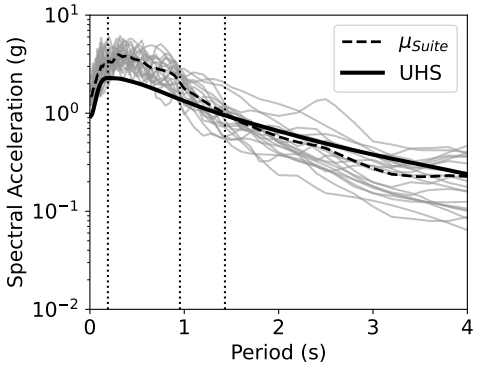

(f) 1% poe in 50 years

Figure B.2: GM Suite Spectra for NEHRP Class D Site F5S4B Building

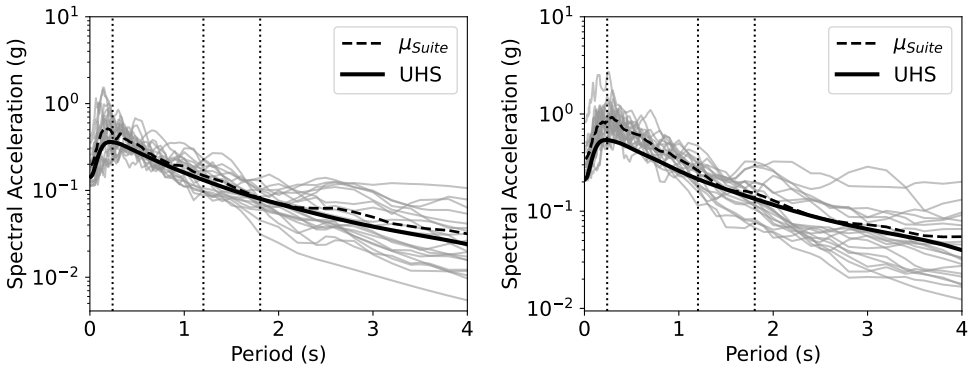

(a) 68% poe in 50 years

(b) 50% poe in 50 years

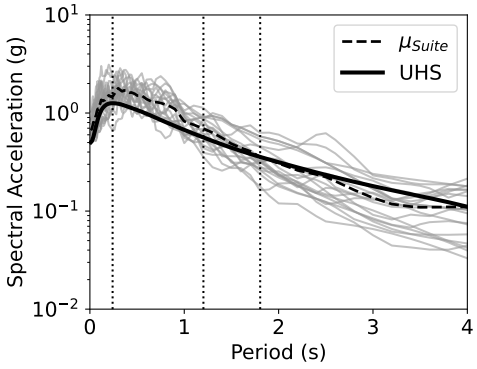

(c) 10% poe in 50 years

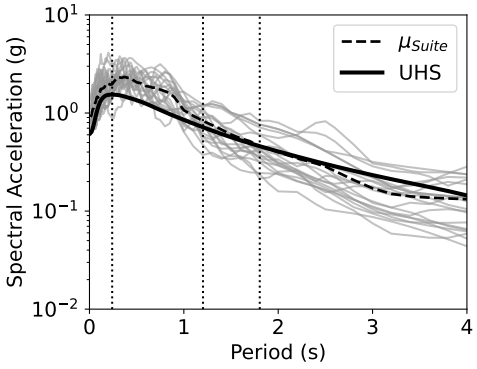

(d) 5% poe in 50 years

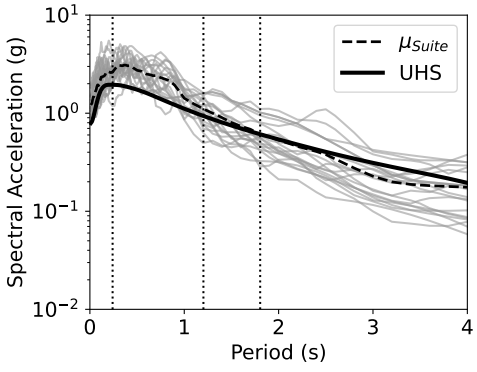

(e) 2% poe in 50 years

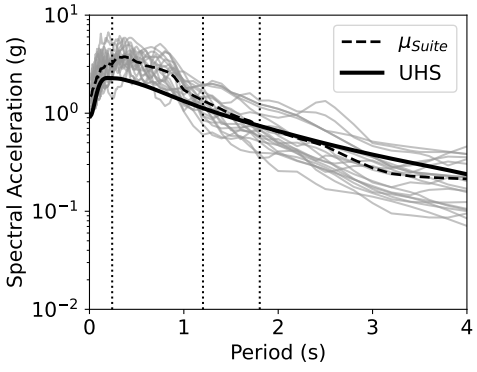

(f) 1% poe in 50 years

Figure B.3: GM Suite Spectra for NEHRP Class D Site F8S3B Building

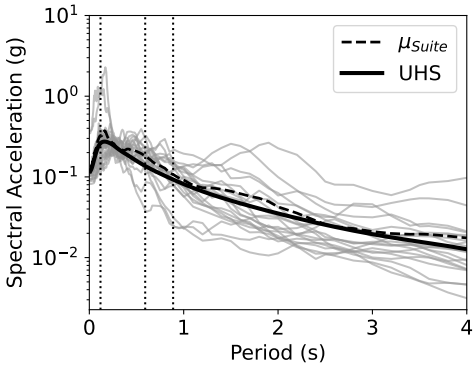

(a) 68% poe in 50 years

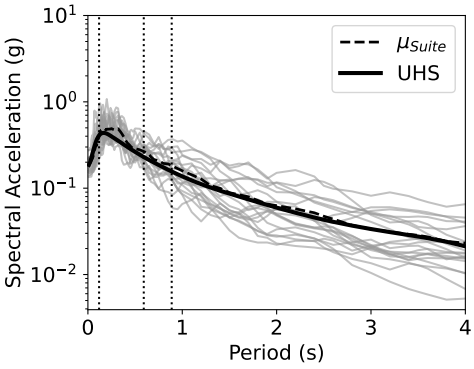

(b) 50% poe in 50 years

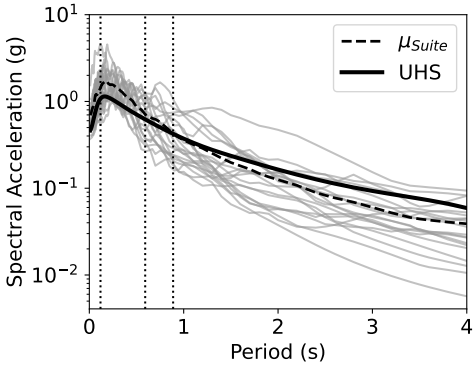

(c) 10% poe in 50 years

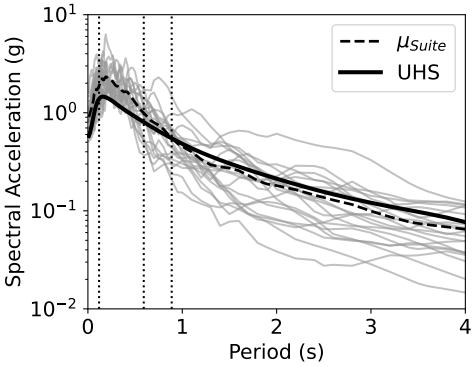

(d) 5% poe in 50 years

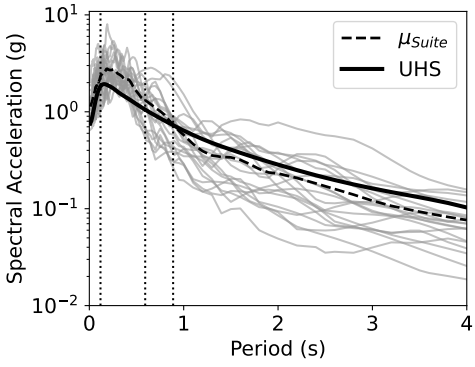

(e) 2% poe in 50 years

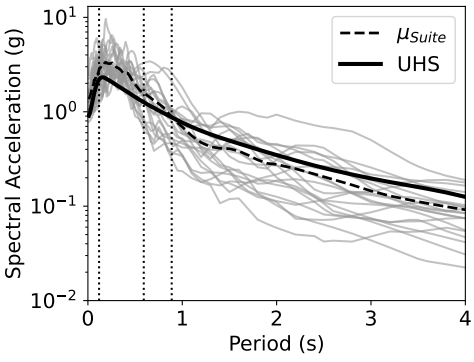

(f) 1% poe in 50 years

Figure B.4: GM Suite Spectra for NEHRP Class C Site F2S2B Building

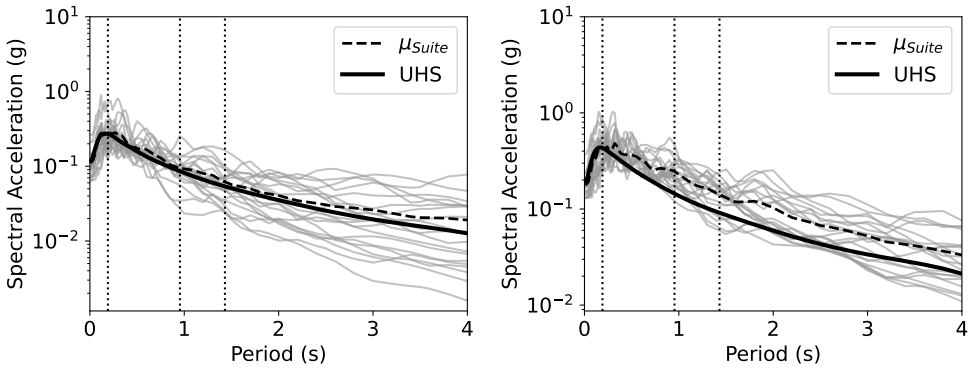

(a) 68% poe in 50 years

(b) 50% poe in 50 years

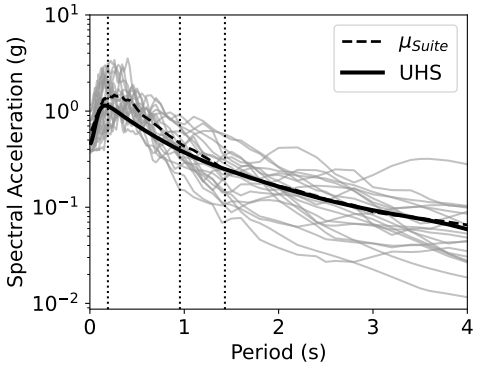

(c) 10% poe in 50 years

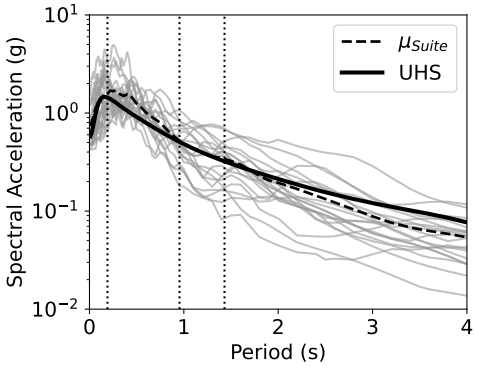

(d) 5% poe in 50 years

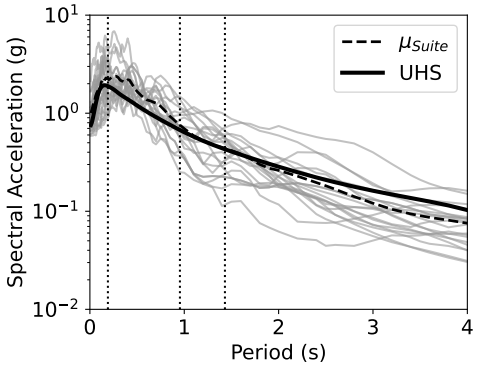

(e) 2% poe in 50 years

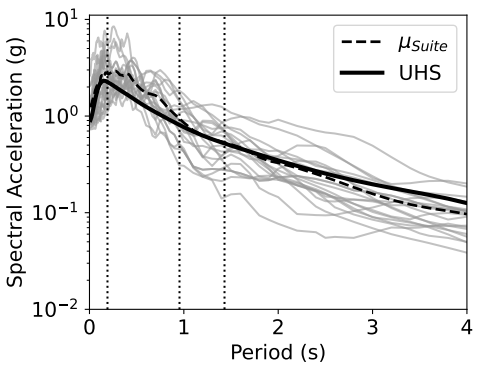

(f) 1% poe in 50 years

Figure B.5: GM Suite Spectra for NEHRP Class C Site F5S4B Building

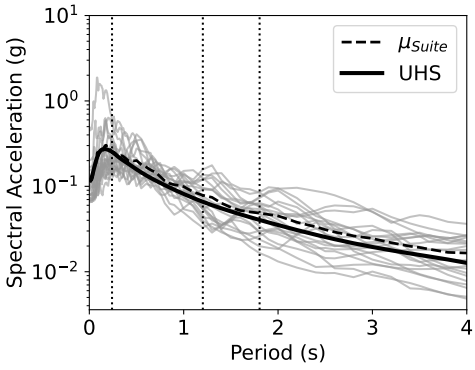

(a) 68% poe in 50 years

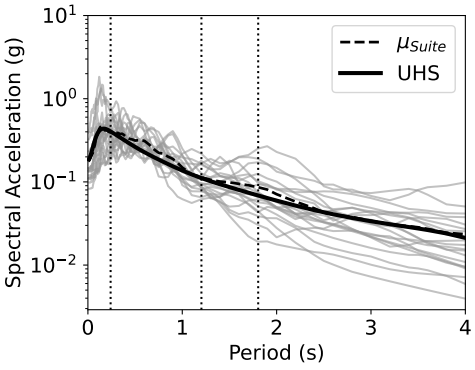

(b) 50% poe in 50 years

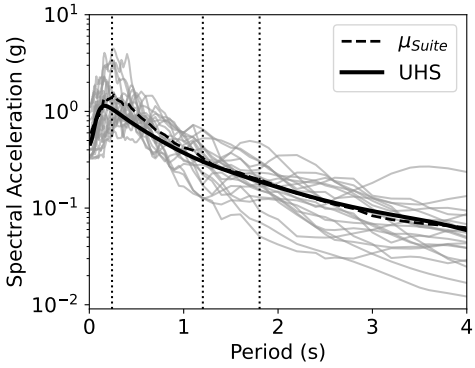

(c) 10% poe in 50 years

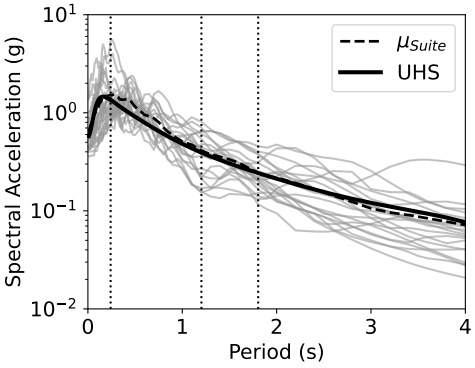

(d) 5% poe in 50 years

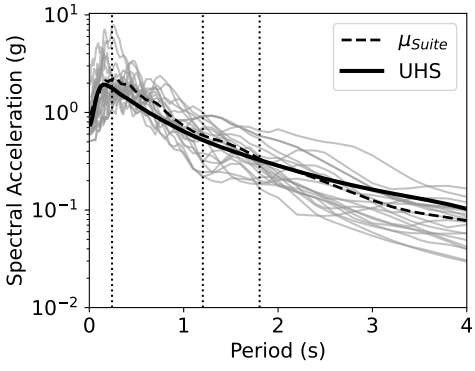

(e) 2% poe in 50 years

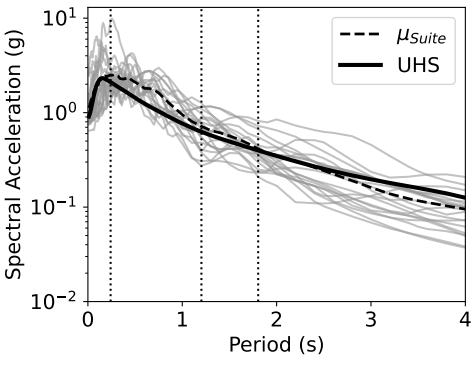

(f) 1% poe in 50 years

Figure B.6: GM Suite Spectra for NEHRP Class C Site F8S3B Building

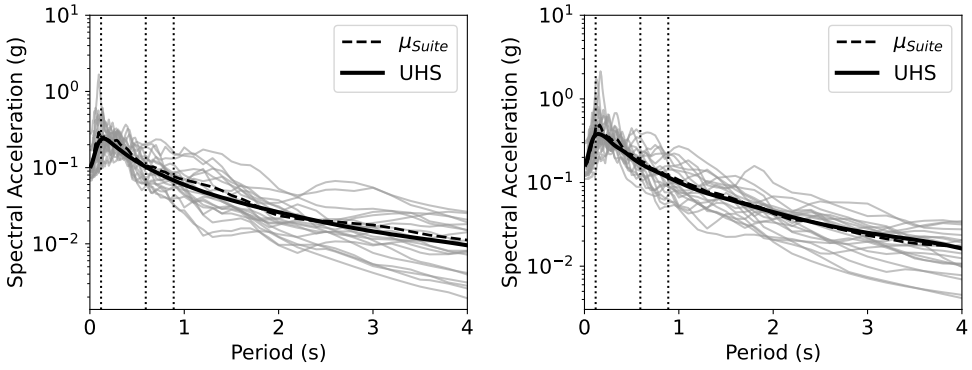

(a) 68% poe in 50 years

(b) 50% poe in 50 years

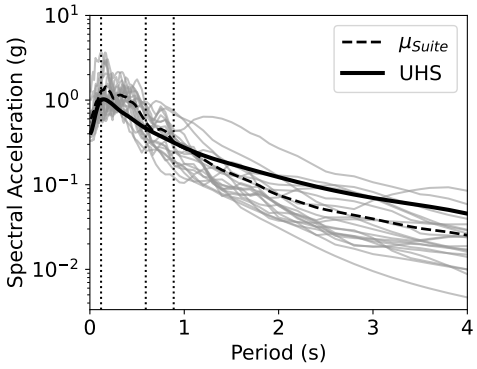

(c) 10% poe in 50 years

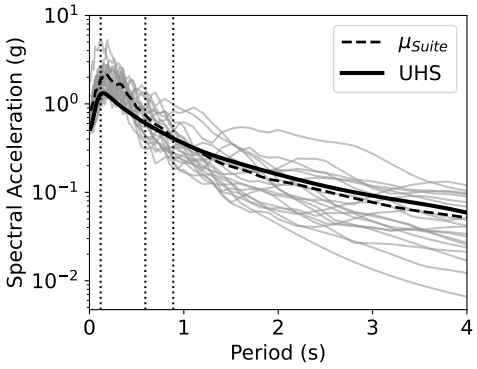

(d) 5% poe in 50 years

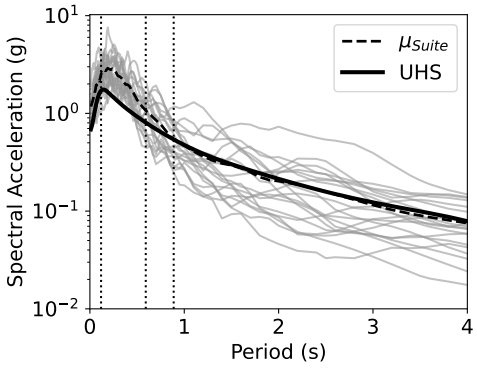

(e) 2% poe in 50 years

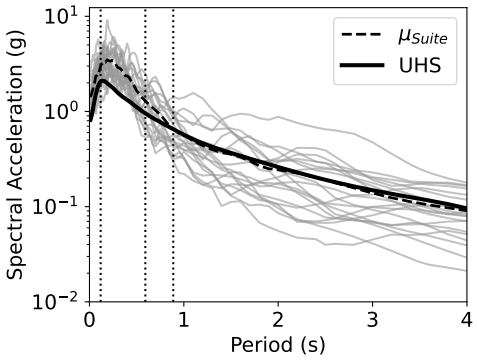

(f) 1% poe in 50 years

Figure B.7: GM Suite Spectra for Generic Rock Site F2S2B Building

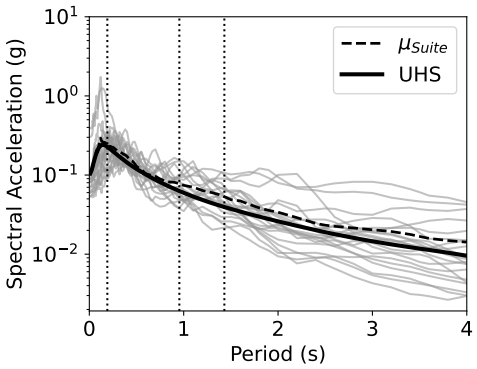

(a) 68% poe in 50 years

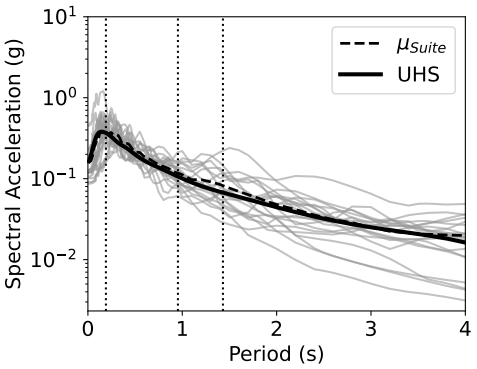

(b) 50% poe in 50 years

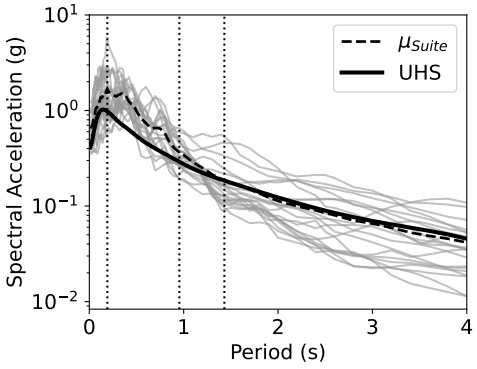

(c) 10% poe in 50 years

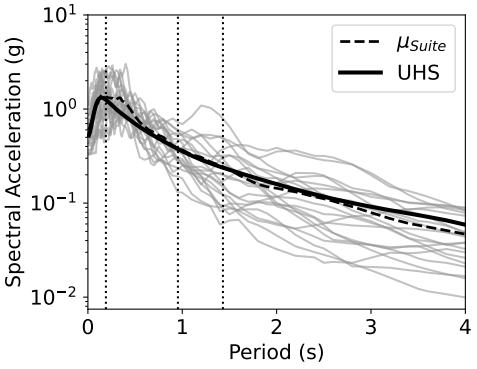

(d) 5% poe in 50 years

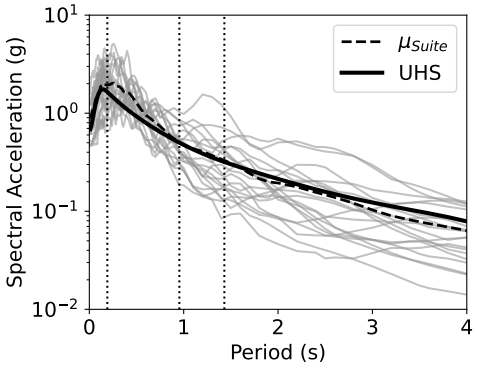

(e) 2% poe in 50 years

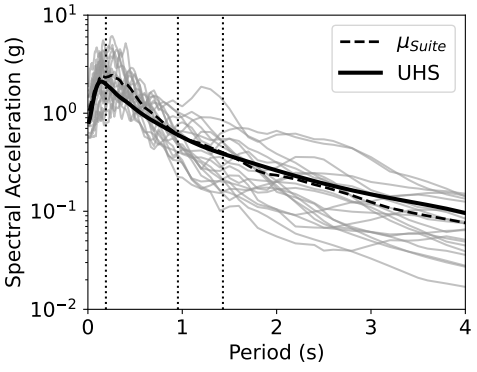

(f) 1% poe in 50 years

Figure B.8: GM Suite Spectra for Generic Rock Site F5S4B Building

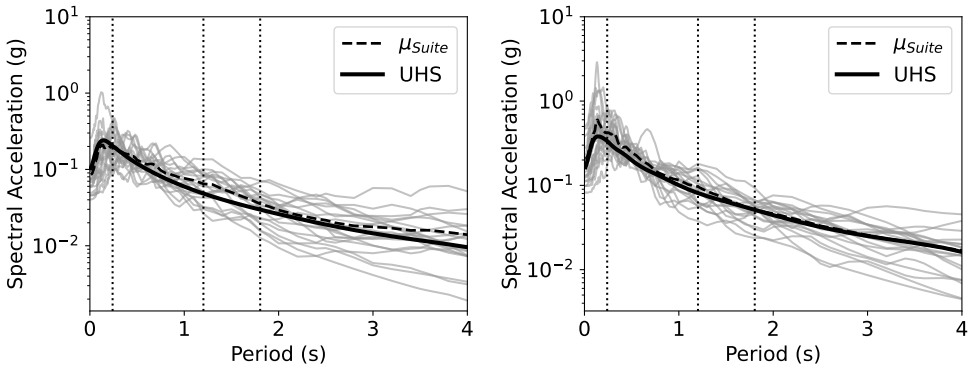

(a) 68% poe in 50 years

(b) 50% poe in 50 years

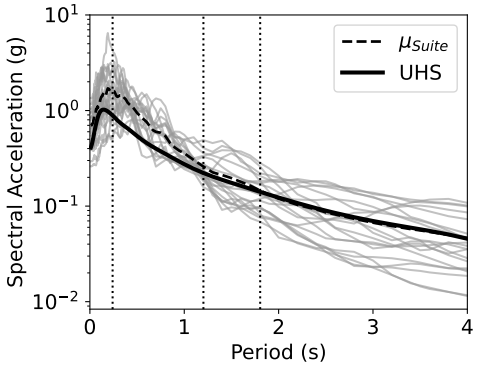

(c) 10% poe in 50 years

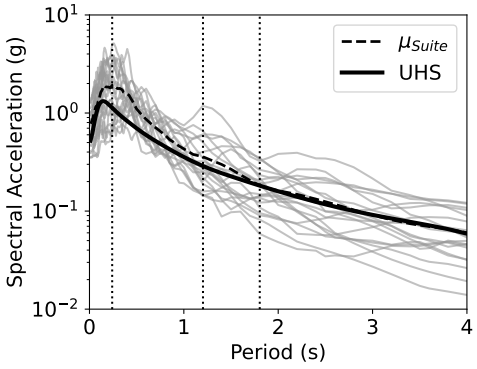

(d) 5% poe in 50 years

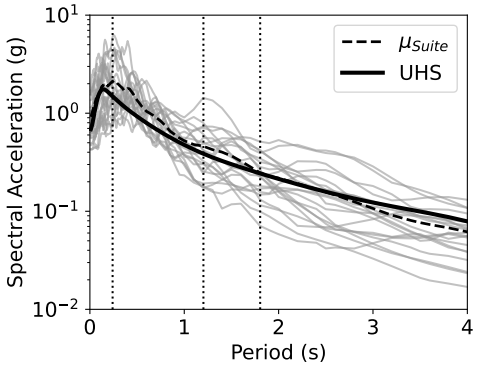

(e) 2% poe in 50 years

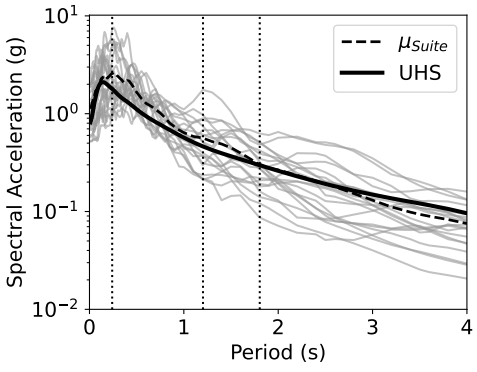

(f) 1% poe in 50 years

Figure B.9: GM Suite Spectra for Generic Rock Site F8S3B Building

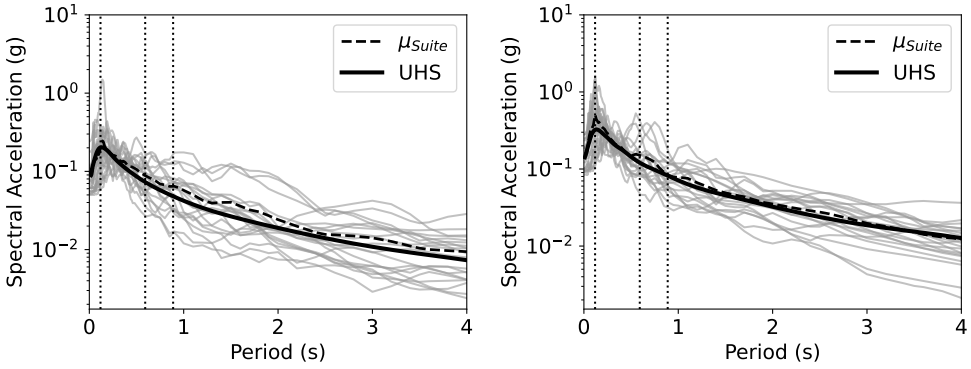

(a) 68% poe in 50 years

(b) 50% poe in 50 years

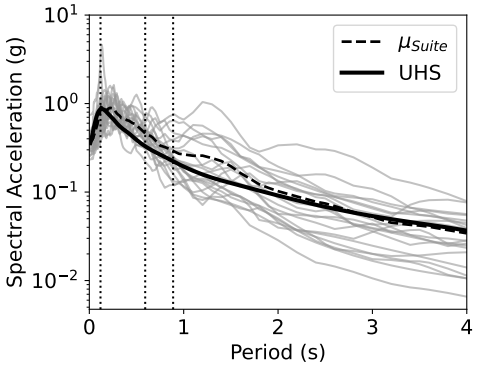

(c) 10% poe in 50 years

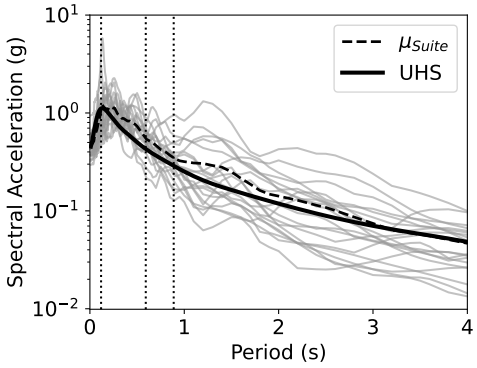

(d) 5% poe in 50 years

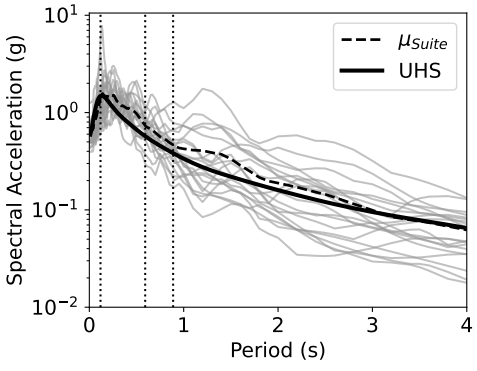

(e) 2% poe in 50 years

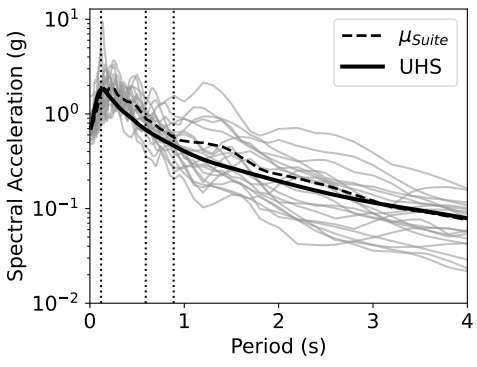

(f) 1% poe in 50 years

Figure B.10: GM Suite Spectra for NEHRP Class B Site F2S2B Building

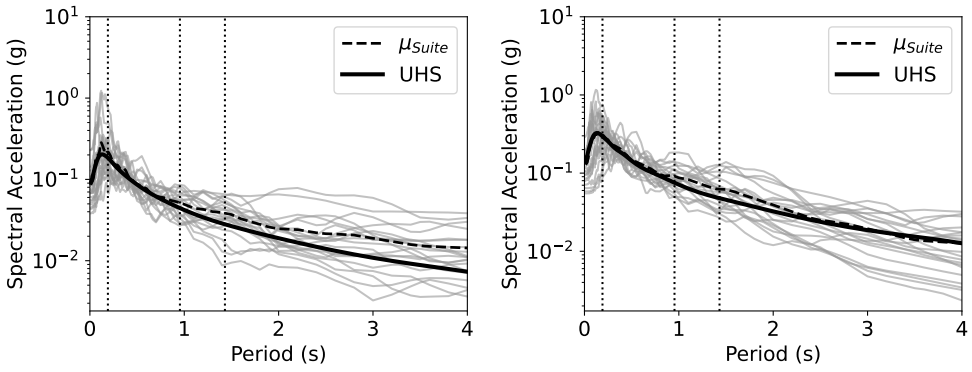

(a) 68% poe in 50 years

(b) 50% poe in 50 years

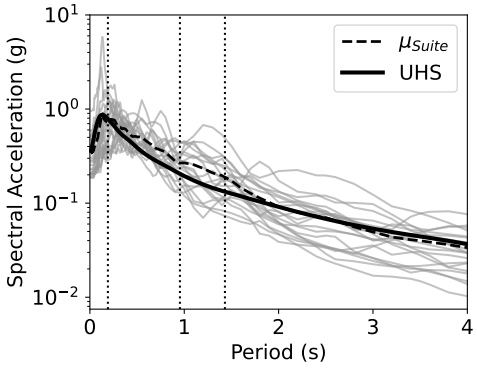

(c) 10% poe in 50 years

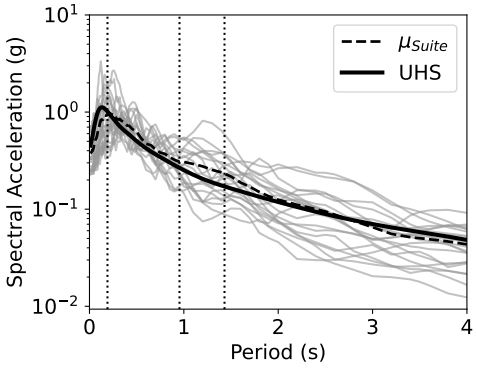

(d) 5% poe in 50 years

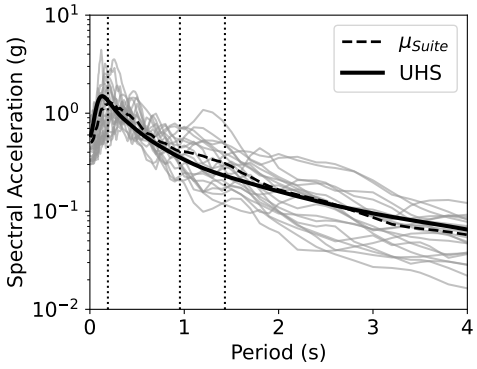

(e) 2% poe in 50 years

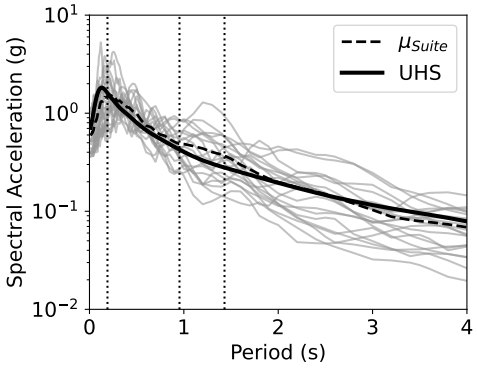

(f) 1% poe in 50 years

Figure B.11: GM Suite Spectra for NEHRP Class B Site F5S4B Building

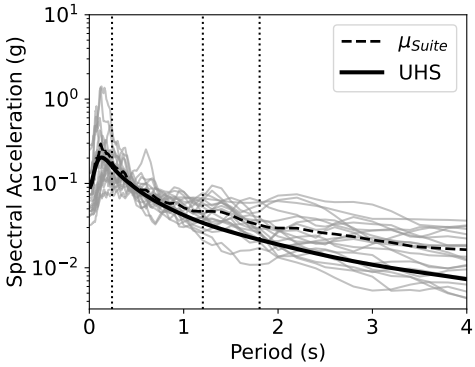

(a) 68% poe in 50 years

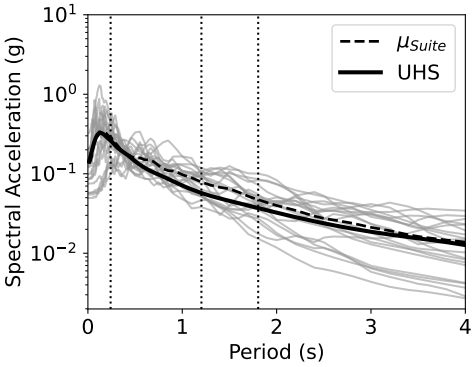

(b) 50% poe in 50 years

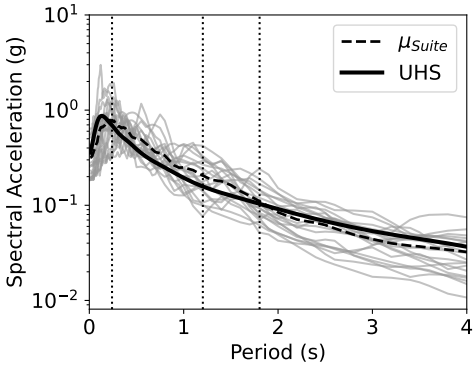

(c) 10% poe in 50 years

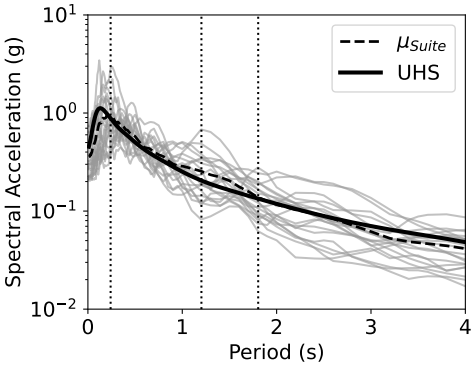

(d) 5% poe in 50 years

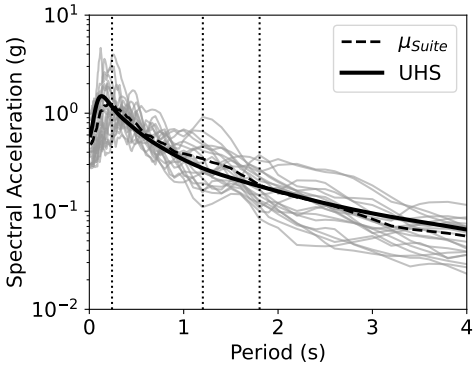

(e) 2% poe in 50 years

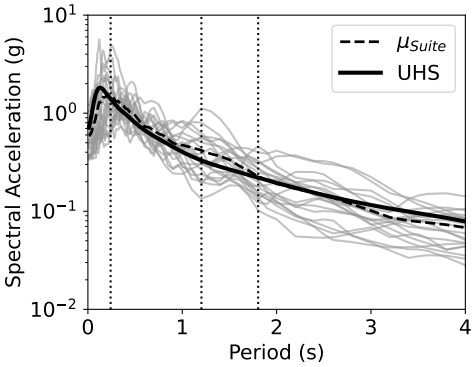

(f) 1% poe in 50 years

Figure B.12: GM Suite Spectra for NEHRP Class B Site F8S3B Building

Appendix C

ANALYSIS INPUT PARAMETERS

Table C.1: Tornado Analysis Input Parameters of F2S2B

Structure	ξ (%)	$f_c^{'}$ **(MPa)**	f_y **(MPa)**	**Mass (tons)**	b_{C1} **(mm)**	cc_{C1} **(mm)**	h_{B1} **(mm)**	cc_{B1} **(mm)**	h_{B2} **(mm)**	cc_{B2} **(mm)**	s **(mm)**
Reference	2.51	26.000	492.689	275	610	61	556	56	508	51	100
1	1.16	26.000	492.689	275	610	61	556	56	508	51	100
2	5.41	26.000	492.689	275	610	61	556	56	508	51	100
3	2.51	21.002	492.689	275	610	61	556	56	508	51	100
4	2.51	30.998	492.689	275	610	61	556	56	508	51	100
5	2.51	26.000	448.742	275	610	61	556	56	508	51	100
6	2.51	26.000	540.939	275	610	61	556	56	508	51	100
7	2.51	26.000	492.689	240	610	61	556	56	508	51	100
8	2.51	26.000	492.689	311	610	61	556	56	508	51	100
9	2.51	26.000	492.689	275	589	61	556	56	508	51	100
10	2.51	26.000	492.689	275	630	61	556	56	508	51	100
11	2.51	26.000	492.689	275	610	61	541	56	494	51	100
12	2.51	26.000	492.689	275	610	61	571	56	522	51	100
13	2.51	26.000	492.689	275	610	45	556	42	508	38	100
14	2.51	26.000	492.689	275	610	77	556	70	508	64	100

Table C.1: Tornado Analysis Input Parameters of F2S2B, Continued

Structure	ξ (%)	$f_c^{'}$ **(MPa)**	f_y **(MPa)**	**Mass (tons)**	b_{C1} **(mm)**	cc_{C1} **(mm)**	h_{B1} **(mm)**	cc_{B1} **(mm)**	h_{B2} **(mm)**	cc_{B2} **(mm)**	s **(mm)**
15	2.51	26.000	492.689	275	610	61	556	56	508	51	87
16	2.51	26.000	492.689	275	610	61	556	56	508	51	113

Table C.2: Tornado Analysis Input Parameters of F5S4B

Structure	ξ (%)	$f_c^{'}$ **(MPa)**	f_y **(MPa)**	**Mass (tons)**	b_{C1} **(mm)**	cc_{C1} **(mm)**	h_{B1} **(mm)**	cc_{B1} **(mm)**	h_{B2} **(mm)**	cc_{B2} **(mm)**	s **(mm)**
Reference	2.51	28.000	457.782	1007	711	46	660	66	508	51	100
1	1.16	28.000	457.782	1007	711	46	660	66	508	51	100
2	5.41	28.000	457.782	1007	711	46	660	66	508	51	100
3	2.51	22.617	457.782	1007	711	46	660	66	508	51	100
4	2.51	33.383	457.782	1007	711	46	660	66	508	51	100
5	2.51	28.000	416.949	1007	711	46	660	66	508	51	100
6	2.51	28.000	502.614	1007	711	46	660	66	508	51	100
7	2.51	28.000	457.782	878	711	46	660	66	508	51	100

Table C.2: Tornado Analysis Input Parameters of F5S4B, Continued

Structure	ξ (%)	$f_c^{'}$ **(MPa)**	f_y **(MPa)**	**Mass (tons)**	b_{C1} **(mm)**	cc_{C1} **(mm)**	h_{B1} **(mm)**	cc_{B1} **(mm)**	h_{B2} **(mm)**	cc_{B2} **(mm)**	s **(mm)**
8	2.51	28.000	457.782	1136	711	46	660	66	508	51	100
9	2.51	28.000	457.782	1007	687	46	660	66	508	51	100
10	2.51	28.000	457.782	1007	735	46	660	66	508	51	100
11	2.51	28.000	457.782	1007	711	46	642	66	494	51	100
12	2.51	28.000	457.782	1007	711	46	678	66	522	51	100
13	2.51	28.000	457.782	1007	711	34	660	49	508	38	100
14	2.51	28.000	457.782	1007	711	58	660	83	508	64	100
15	2.51	28.000	457.782	1007	711	46	660	66	508	51	87
16	2.51	28.000	457.782	1007	711	46	660	66	508	51	113

Table C.3: Tornado Analysis Input Parameters of F8S3B

Structure	ξ (%)	$f_c^{'}$ **(MPa)**	f_y **(MPa)**	**Mass (tons)**	b_{C1} **(mm)**	cc **(mm)**	b_{C2} **(mm)**	b_{C3} **(mm)**	h_{B1} **(mm)**	h_{B2} **(mm)**	h_{B3} **(mm)**	s **(mm)**
Reference	2.51	28.000	457.782	1816	1100	50	1000	920	900	750	600	100

Table C.3: Tornado Analysis Input Parameters of F8S3B, Continued

Structure	ξ (%)	$f_c^{'}$ **(MPa)**	f_y **(MPa)**	**Mass (tons)**	b_{C1} **(mm)**	cc **(mm)**	b_{C2} **(mm)**	b_{C3} **(mm)**	h_{B1} **(mm)**	h_{B2} **(mm)**	h_{B3} **(mm)**	s **(mm)**
1	1.16	28.000	457.782	1816	1100	50	1000	920	900	750	600	100
2	5.41	28.000	457.782	1816	1100	50	1000	920	900	750	600	100
3	2.51	22.617	457.782	1816	1100	50	1000	920	900	750	600	100
4	2.51	33.383	457.782	1816	1100	50	1000	920	900	750	600	100
5	2.51	28.000	416.949	1816	1100	50	1000	920	900	750	600	100
6	2.51	28.000	502.614	1816	1100	50	1000	920	900	750	600	100
7	2.51	28.000	457.782	1583	1100	50	1000	920	900	750	600	100
8	2.51	28.000	457.782	2049	1100	50	1000	920	900	750	600	100
9	2.51	28.000	457.782	1816	1063	50	966	889	900	750	600	100
10	2.51	28.000	457.782	1816	1137	50	1034	951	900	750	600	100
11	2.51	28.000	457.782	1816	1100	50	1000	920	876	730	584	100
12	2.51	28.000	457.782	1816	1100	50	1000	920	924	770	616	100
13	2.51	28.000	457.782	1816	1100	37	1000	920	900	750	600	100
14	2.51	28.000	457.782	1816	1100	63	1000	920	900	750	600	100
15	2.51	28.000	457.782	1816	1100	50	1000	920	900	750	600	87

Table C.3: Tornado Analysis Input Parameters of F8S3B, Continued

Structure	ξ (%)	$f_c^{'}$ **(MPa)**	f_y **(MPa)**	**Mass (tons)**	b_{C1} **(mm)**	cc **(mm)**	b_{C2} **(mm)**	b_{C3} **(mm)**	h_{B1} **(mm)**	h_{B2} **(mm)**	h_{B3} **(mm)**	s **(mm)**
16	2.51	28.000	457.782	1816	1100	50	1000	920	900	750	600	113

Table C.4: NLTHA Analysis Input Parameters of F2S2B

Structure	ξ (%)	$f_c^{'}$ **(MPa)**	f_y **(MPa)**	**Mass (tons)**	b_{C1} **(mm)**	cc_{C1} **(mm)**	h_{B1} **(mm)**	cc_{B1} **(mm)**	h_{B2} **(mm)**	cc_{B2} **(mm)**	s **(mm)**
Reference	2.51	26.000	492.689	275	610	61	556	56	508	51	100
1	2.20	23.821	467.581	289	637	59	563	54	514	49	97
2	2.80	30.445	501.500	249	628	62	575	57	525	52	110
3	0.96	26.472	460.200	265	615	75	560	68	512	62	108
4	6.93	25.724	455.615	292	610	61	580	56	530	51	105
5	5.45	23.397	400.503	285	624	64	564	59	515	54	91
6	4.93	26.970	522.763	302	602	55	553	50	505	46	99
7	10.33	31.694	471.314	293	585	72	534	66	488	60	102
8	4.72	24.408	504.576	255	606	51	558	47	510	43	99

Table C.4: NLTHA Analysis Input Parameters of F2S2B, Continued

Structure	ξ (%)	$f_c^{'}$ **(MPa)**	f_y **(MPa)**	**Mass (tons)**	b_{C1} **(mm)**	cc_{C1} **(mm)**	h_{B1} **(mm)**	cc_{B1} **(mm)**	h_{B2} **(mm)**	cc_{B2} **(mm)**	s **(mm)**
9	2.74	24.767	465.073	277	590	84	569	77	519	70	82
10	3.64	27.769	479.390	259	613	69	536	64	490	58	107
11	2.30	29.614	510.955	235	627	67	553	62	505	56	96
12	3.94	22.669	559.536	305	596	56	562	51	513	47	113
13	1.73	21.717	569.120	252	621	37	554	34	506	31	113
14	1.61	21.426	543.448	282	597	49	541	45	494	41	88
15	3.36	24.055	524.914	297	594	45	555	41	507	38	119
16	0.74	25.602	484.213	246	606	57	573	53	524	48	97
17	4.43	26.213	492.531	272	615	77	545	71	498	64	109
18	1.38	25.304	481.691	284	640	83	550	77	503	70	77
19	2.98	30.037	453.289	310	634	66	565	61	516	55	93
20	2.42	29.278	515.474	311	607	52	556	48	508	44	86
21	1.95	16.366	528.900	268	588	63	545	58	498	53	89
22	3.80	19.812	487.297	222	622	48	558	44	510	40	117
23	1.41	32.097	535.474	269	619	47	551	43	504	39	95

Table C.4: NLTHA Analysis Input Parameters of F2S2B, Continued

Structure	ξ (%)	$f_c^{'}$ **(MPa)**	f_y **(MPa)**	**Mass (tons)**	b_{C1} **(mm)**	cc_{C1} **(mm)**	h_{B1} **(mm)**	cc_{B1} **(mm)**	h_{B2} **(mm)**	cc_{B2} **(mm)**	s **(mm)**
24	1.23	35.358	442.640	274	604	70	559	64	511	58	105
25	1.91	27.560	494.059	278	601	42	566	39	517	35	103
26	3.23	22.859	434.040	234	609	75	543	69	496	63	92
27	1.07	28.678	506.155	317	617	60	549	55	501	51	102
28	1.65	20.797	474.863	242	599	56	570	52	521	47	100
29	2.60	27.208	496.945	335	612	58	546	54	499	49	104
30	2.14	28.355	519.098	261	577	68	549	62	502	57	94

Table C.5: NLTHA Analysis Input Parameters of F5S4B

Structure	ξ (%)	$f_c^{'}$ **(MPa)**	f_y **(MPa)**	**Mass (tons)**	b_{C1} **(mm)**	cc_{C1} **(mm)**	h_{B1} **(mm)**	cc_{B1} **(mm)**	h_{B2} **(mm)**	cc_{B2} **(mm)**	s **(mm)**
Reference	2.51	28.000	457.782	1007	711	46	660	66	508	51	100
1	2.20	25.654	434.453	1059	743	45	668	64	514	49	97
2	2.80	32.787	465.969	910	733	47	682	67	525	52	110

Table C.5: NLTHA Analysis Input Parameters of F5S4B, Continued

Structure	ξ (%)	$f_c^{'}$ **(MPa)**	f_y **(MPa)**	**Mass (tons)**	b_{C1} **(mm)**	cc_{C1} **(mm)**	h_{B1} **(mm)**	cc_{B1} **(mm)**	h_{B2} **(mm)**	cc_{B2} **(mm)**	s **(mm)**
3	0.96	28.508	427.595	969	717	56	665	81	512	62	108
4	6.93	27.703	423.335	1068	712	46	688	66	530	51	105
5	5.45	25.197	372.127	1042	728	48	669	69	515	54	91
6	4.93	29.045	485.726	1104	702	41	656	59	505	46	99
7	10.33	34.131	437.922	1072	682	54	634	78	488	60	102
8	4.72	26.286	468.827	934	706	38	663	55	510	43	99
9	2.74	26.672	432.123	1013	688	63	675	91	519	70	82
10	3.64	29.906	445.425	946	714	52	637	75	490	58	107
11	2.30	31.892	474.754	861	731	51	657	72	505	56	96
12	3.94	24.413	519.893	1115	695	42	667	60	513	47	113
13	1.73	23.388	528.798	923	724	28	658	40	506	31	113
14	1.61	23.074	504.945	1031	696	37	642	53	494	41	88
15	3.36	25.905	487.724	1085	693	34	659	49	507	38	119
16	0.74	27.571	449.906	900	706	43	680	62	524	48	97
17	4.43	28.230	457.636	994	717	58	647	83	498	64	109

Table C.5: NLTHA Analysis Input Parameters of F5S4B, Continued

Structure	ξ (%)	$f_c^{'}$ **(MPa)**	f_y **(MPa)**	**Mass (tons)**	b_{C1} **(mm)**	cc_{C1} **(mm)**	h_{B1} **(mm)**	cc_{B1} **(mm)**	h_{B2} **(mm)**	cc_{B2} **(mm)**	s **(mm)**
18	1.38	27.250	447.563	1040	746	63	653	90	503	70	77
19	2.98	32.348	421.173	1134	739	50	670	71	516	55	93
20	2.42	31.530	478.953	1139	708	39	661	57	508	44	86
21	1.95	17.625	491.428	980	685	48	647	68	498	53	89
22	3.80	21.336	452.772	813	726	36	662	52	510	40	117
23	1.41	34.566	497.536	983	722	35	655	51	504	39	95
24	1.23	38.078	411.279	1002	704	53	664	76	511	58	105
25	1.91	29.680	459.055	1016	701	32	672	46	517	35	103
26	3.23	24.618	403.288	855	710	57	644	82	496	63	92
27	1.07	30.884	470.293	1159	720	46	651	65	501	51	102
28	1.65	22.396	441.219	885	699	43	676	61	521	47	100
29	2.60	29.300	461.736	1227	713	44	648	63	499	49	104
30	2.14	30.536	482.320	955	673	51	652	74	502	57	94

Table C.6: NLTHA Analysis Input Parameters of F8S3B

Structure	ξ (%)	$f_c^{'}$ **(MPa)**	f_y **(MPa)**	**Mass (tons)**	b_{C1} **(mm)**	cc **(mm)**	b_{C2} **(mm)**	b_{C3} **(mm)**	h_{B1} **(mm)**	h_{B2} **(mm)**	h_{B3} **(mm)**	s **(mm)**
Reference	2.51	28.000	457.782	1816	1100	50	1000	920	900	750	600	100
1	2.20	25.654	434.453	1910	1150	48	1046	962	911	759	607	97
2	2.80	32.787	465.969	1642	1134	51	1031	948	930	775	620	110
3	0.96	28.508	427.595	1747	1110	61	1009	928	906	755	604	108
4	6.93	27.703	423.335	1925	1101	50	1001	921	938	782	625	105
5	5.45	25.197	372.127	1879	1126	53	1024	942	913	761	609	91
6	4.93	29.045	485.726	1990	1086	45	987	908	894	745	596	99
7	10.33	34.131	437.922	1934	1055	59	959	883	864	720	576	102
8	4.72	26.286	468.827	1684	1093	42	994	914	904	753	603	99
9	2.74	26.672	432.123	1827	1065	69	968	891	920	767	614	82
10	3.64	29.906	445.425	1706	1105	57	1005	924	868	724	579	107
11	2.30	31.892	474.754	1552	1131	55	1028	946	895	746	597	96
12	3.94	24.413	519.893	2011	1075	46	977	899	909	758	606	113
13	1.73	23.388	528.798	1664	1120	30	1018	937	897	747	598	113
14	1.61	23.074	504.945	1858	1077	41	979	901	875	729	583	88

Table C.6: NLTHA Analysis Input Parameters of F8S3B, Continued

Structure	ξ (%)	$f_c^{'}$ **(MPa)**	f_y **(MPa)**	**Mass (tons)**	b_{C1} **(mm)**	cc **(mm)**	b_{C2} **(mm)**	b_{C3} **(mm)**	h_{B1} **(mm)**	h_{B2} **(mm)**	h_{B3} **(mm)**	s **(mm)**
15	3.36	25.905	487.724	1957	1072	37	974	896	899	749	599	119
16	0.74	27.571	449.906	1622	1093	47	993	914	928	773	619	97
17	4.43	28.230	457.636	1793	1109	63	1008	928	882	735	588	109
18	1.38	27.250	447.563	1876	1154	68	1049	965	890	742	594	77
19	2.98	32.348	421.173	2046	1143	54	1039	956	914	762	610	93
20	2.42	31.530	478.953	2053	1096	43	996	916	901	751	600	86
21	1.95	17.625	491.428	1766	1060	52	964	887	882	735	588	89
22	3.80	21.336	452.772	1466	1123	39	1021	939	903	752	602	117
23	1.41	34.566	497.536	1773	1118	38	1016	935	893	744	595	95
24	1.23	38.078	411.279	1808	1089	57	990	911	905	754	603	105
25	1.91	29.680	459.055	1832	1084	35	986	907	916	764	611	103
26	3.23	24.618	403.288	1541	1098	62	999	919	878	732	586	92
27	1.07	30.884	470.293	2090	1114	50	1012	931	888	740	592	102
28	1.65	22.396	441.219	1597	1081	46	983	904	922	769	615	100
29	2.60	29.300	461.736	2212	1104	48	1003	923	884	737	589	104

Table C.6: NLTHA Analysis Input Parameters of F8S3B, Continued

Structure	ξ (%)	$f_c^{'}$ **(MPa)**	f_y **(MPa)**	**Mass (tons)**	b_{C1} **(mm)**	cc **(mm)**	b_{C2} **(mm)**	b_{C3} **(mm)**	h_{B1} **(mm)**	h_{B2} **(mm)**	h_{B3} **(mm)**	s **(mm)**
30	2.14	30.536	482.320	1722	1042	56	947	871	889	741	593	94

VITA

BARIŞ ÜNAL

EDUCATION

Middle East Technical University	*2012 - 2015*
MSc in Earthquake Studies (Earthquake Engineering)	GPA: 3.75
Middle East Technical University	*2007 - 2012*
BS in Civil Engineering	GPA: 2.76

PROFESSIONAL EXPERIENCE

Technical Manager, MATRiSEB	*2019-*
Structural Engineering Analyst, MATRiSEB	*2016-2019*
Research Assistant, METU, Earthquake Studies	*2013-2015*

SKILLS

Programming Languages: Python, R, MATLAB
MS Office : Word, Excel, PowerPoint, Project
Languages: Turkish (Native), English (Advanced)

PUBLICATIONS

Ünal, B., Askan, A., & Selcuk-Kestel, A. S. (2017). Simulation of large earthquakes and its implications on earthquake insurance rates: a case study in Bursa region (Turkey). Natural Hazards, 85(1), 215-236.